Antimicrobial Peptide Gene Expression in Human Tonsils

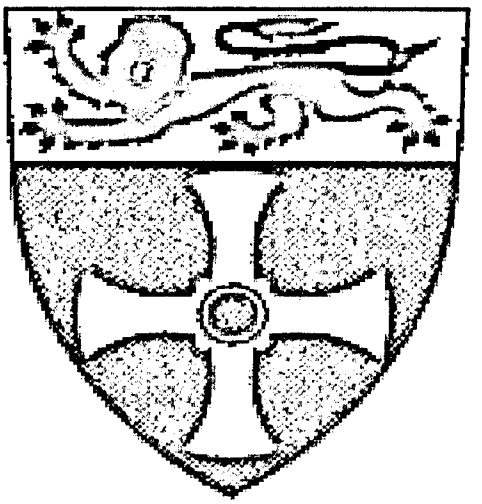

Stephanie Bell BSc (Hons)

Submitted for the degree of Doctor of Philosophy

Institute for Cell and Molecular Biosciences
Medical School
Newcastle University
Catherine Cookson Building
Framlington Place
NE2 4HH

September 2008

Acknowledgements

Firstly I would like to thank Dr Alison Howard and Dr Judith Hall for all of their tireless support and advice throughout the duration of this project. I would also like to thank my supervisory team Prof. Barry Hirst, Prof Mike Kehoe and Prof. Janet Wilson, post-docs Emily Abbot, Wendy Smith for their guidance and Maxine Geggie for tissue culture advice. Thanks to all members of the BHH lab and Epithelial Research Group including Georgina Carr and Susan Harrison for advice and friendship.

I'd also like to acknowledge the staff in the ENT department at the Freeman Hospital, Newcastle upon Tyne for their help with tissue collection and to thank the volunteers for their valuable contribution to this study.

A big thanks to my friends and family for their continued friendship throughout this project. Finally, I'd like to thank my parents for their love and encouragement (and everything else!).

This project was funded by the MRC, the ENT department at the Freeman Hosptal, Newcastle upon Tyne and the North of England Otolaryngological Society.

Abstract

Antimicrobial Peptide Gene Expression in Human Tonsils

The human palatine tonsils play important roles in host immunity and provide a barrier against invading pathogens. However the Gram-positive bacterium, *Streptococcus pyogenes* often penetrates their defences. This results in tonsillitis, in which sufferers present with swollen and painful palatine tonsils. Moreover tonsillitis is often recurrent. Despite tonsillitis being relatively common, the immunological factors that allow this infection to perpetuate remain obscure. Antimicrobial peptides (AMPs), expressed at epithelial and mucosal surfaces, provide a first-line of defence against potential pathogens. Moreover these molecules have also been reported to be up-regulated in response to infection, but their roles in the defence of the human palatine tonsils are not well known. Studies were therefore initiated to test the hypothesis that a defect in the innate immune response involving host AMPs, is a cause or contributory factor to recurrent acute tonsillitis (RAT).

The first study investigated and compared AMP gene expression patterns in palatine tonsils excised from patients undergoing tonsillectomy for RAT to those of control subjects whose tonsils were excised for conditions such as snoring. To date it was the largest investigation of its kind using over ninety tonsils. The levels of LL-37, HBD1, HBD2 and LEAP-2 AMP mRNA expression were quantified by real-time PCR assays developed and optimised specifically for the study. The data indicated that all AMP genes examined were expressed, that considerable variability was detected between the AMP expression levels of individual subjects but that the mean AMP expression levels between the RAT and control groups were not statistically different. This study was conducted using tonsils excised from RAT patients at the time of their surgery when they were probably not suffering a streptococcal infection. To answer the question of whether RAT was due to a failure of the AMPs to up-regulate in response to infection, an *in vitro* model was adopted.

HaCaT cells were used as the *in vitro* model of the tonsil and challenged with Group A streptococci. Quantitative real-time expression data suggested that in response to the *S. pyogenes* M1 serotype, HBD1 gene expression was decreased, suggesting that GAS down regulates the expression of this gene, whereas that of LEAP-2 was induced. The results of challenge experiments performed using pili-defective mutants also suggested that such changes in the host response occurred in the absence of streptococcal binding. The HaCaT cells were not however derived from tonsil. Thus to further investigate streptococcal–tonsil AMP responses an *ex vivo* tonsil model was used.

Following challenge of the control (non-RAT) and RAT tonsil sections with *S. pyogenes*, a statistically significant increase in HBD1 gene expression and a decrease in HBD2 gene expression were observed in the control (non-RAT) tonsils. No comparable statistically significant changes were identified in the RAT tonsils. These data therefore highlighted differences between the AMP expression profiles of the control (non-RAT) and RAT tonsils in response to a *S. pyogenes* M1 challenge. Although speculative these data indicate that the RAT tonsils were less able to respond to the *S. pyogenes* challenge, which in part may help to explain the susceptibility of RAT patients to infection.

Abbreviations

A260	Absorbance 260
AMP	Antimicrobial Peptide
ANOVA	Analysis of Variance
ATCC	American Type Culture Collection
AU	Arbitrary unit
BLAST	Basic Local Alignment Search Tool
bp	Base pair
BSA	Bovine Serum Albumin
cDNA	Copy or Complementary Deoxyribronucleic Acid
CE	Control Epithelium
Cfu	Colony forming unit
Cfu/ml	Colony forming unit per millilitre
CL	Control Lymphoid
COREC	Central Office for Ethics Committees
Cp	Crossing Point
CRAMP	Cathelicidin related AMP
Cys	Cysteine
D3	1,25 dihydroxyvitamin-D3
DRS	Distantly Related to SIC
FCS	Foetal Calf Serum
FITC	Fluorescein isothiocyanate
FRET	Fluorescence Resonance Energy Transfer
G	Group A *Streptococcus*
GAPDH	Glyceraldehyde-3-Phosphate Dehydrogenase
GFP	Green Fluorescent Protein
GRAB	G- related α-2 macroglobulin binding protein
GTC	Guanidium isothiocyanate
h	Hour
H	Hour
HAMP	Hepcidin Antimicrobial Peptide
HBD	Human beta-defensin
HBD1	Human beta-defensins 1
HBD2	Human beta-defensin 2
HBD3	Human beta-defensin 3
hCAP18	Human cathelicidin protein
HD5	Human alpha defensin 5
HEp-2	Human Epithelial Cell Line-2
HNP	Human Neutrophil Peptide
Ig	Immunoglobulin
IL	Interleukin
IPTG	Isopropyl β-D-1 Thioglactopyranoside
Kb	Kilobase
Kr-Ar	Krypton-Argon

LB	Luria- Bertani
LC480	LightCycler 480
LEAP-1	Liver Expressed Antimicrobial Peptide 1
LEAP-2	Liver Expressed Antimicrobial Peptide 2
LPS	Lipopolysaccharide
LREC	Local and Regional Ethics Committee
LTA	Lipoteichoic Acid
LUX	Light Upon Extension
M	Size Marker
MAPK	Mitogen Activated Kinase
MHC	Major Histocompatability Complex
Min	Minutes
MMLV	Murine Molony Leukemia Virus
mRNA	Messenger RNA
NCBI	National Centre For Biotechnology Information
NOD	Nucleotide binding oligomerisation domain
OD	Optical density
OSA	Obstructive Sleep Aponea
PAMPs	Pathogen Associated Molecular Patterns
PBS	Phosphate Buffered Saline
PCR	Polymerase Chain Reaction
PFA	Paraformaldehyde
PMA	Phorbol 12-myristate 13-acetate
RAT	Recurrent Acute Tonsillitis
RE	RAT Epithelium
RL	RAT Lymphoid
rRNA	Ribosomal Ribonucleic Acid
RT	Reverse Transcription
RT-PCR	Reverse transcription-Polymerase Chain Reaction
s	Seconds
S. pyogenes	*Streptococcus pyogenes*
Sbjct	Subject
SD	Standard Deviation
SEM	Standard Error or the Mean
SIC	Streptococcal Inhibitor of Complement
SIgA	Secretory Immunoglobulin
SLO	Streptolysis O
SLPI	Secretory Leukocyte Protease Inhibitor
SLS	Streptolysin S
Spe	Streptococcal Pyrogenic Endotoxin
SpeB	Streptococcal Cysteine Protease Endotoxin B
Strep	Streptococci
THB	Todd Hewitt Broth
THYB	Todd Hewitt Yeast Broth
TLR	Toll-Like Receptor
Tm	Melting Temperature
TNF-α	Tumour Necrosis Factor Alpha
TRITC	Tetramethyl rhodamine isothiocyanate

UPL	Universal Probe Library
UV	Ultra Violet
VDRE	Vitamin D Response Element
Vitamin D3	1,25 dihydroxyvitamin-D3
VITD3	1, 25-dihydroxyvitamin-D3
α-helical	Alpha-helical

Table of Contents

List of Figures

List of Tables

Chapter 1

Introduction

1.1 Tonsils

1.1.1 Morphology and Function

Human palatine tonsils are lymphoepithelial organs ovoid in shape and situated in the pharynx at the opening of the gastrointestinal and respiratory tracts (Perry and Whyte 1998) (Figure 1.1). They sit within the tonsillar fossa between the palatoglossal and the palapharyngeal arches (Nave, Gebert et al. 2001), and being secondary lymphoid organs function in the body's immune responses. Indeed in this position they encounter large numbers of respiratory and gastrointestinal antigens, and through activation of immune pathways help protect the body from infection.

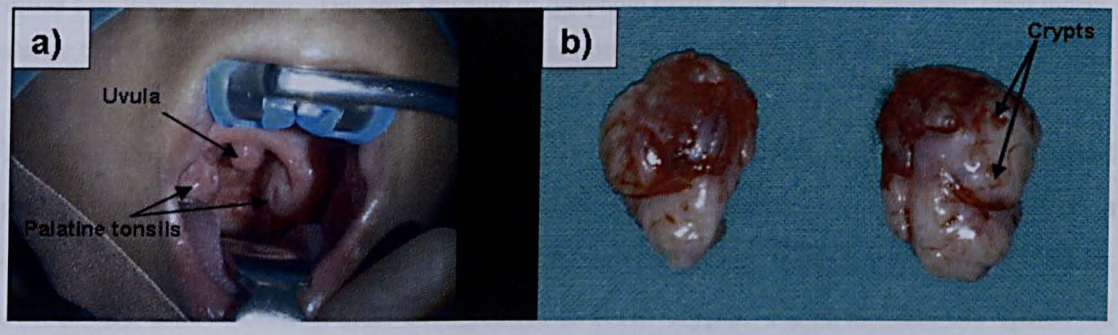

Figure 1.1a&b: Human palatine tonsils: a) *in-situ* in the airways. The palatine tonsils can be observed at each side of the throat. **b)** A pair of human palatine tonsils immediately after excision.

The tonsils are components of a ring structure consisting of lymphoid tissues, first described by, and subsequently named after Waldeyer in 1884 (cited by (Perry and Whyte 1998). Waldeyer's ring (Figure 1.2), comprises the palatine tonsils, paired tubal tonsils, nasopharyngeal tonsils (adenoids) and the lingual tonsil, all joined by smaller lymphoid tissues (Perry and Whyte 1998). This lymphoid ring is organised in a similar way to the lymphoid tissue in the gut and lung (Cebra, Periwal et al. 1998; Tschernig and Pabst 2000).

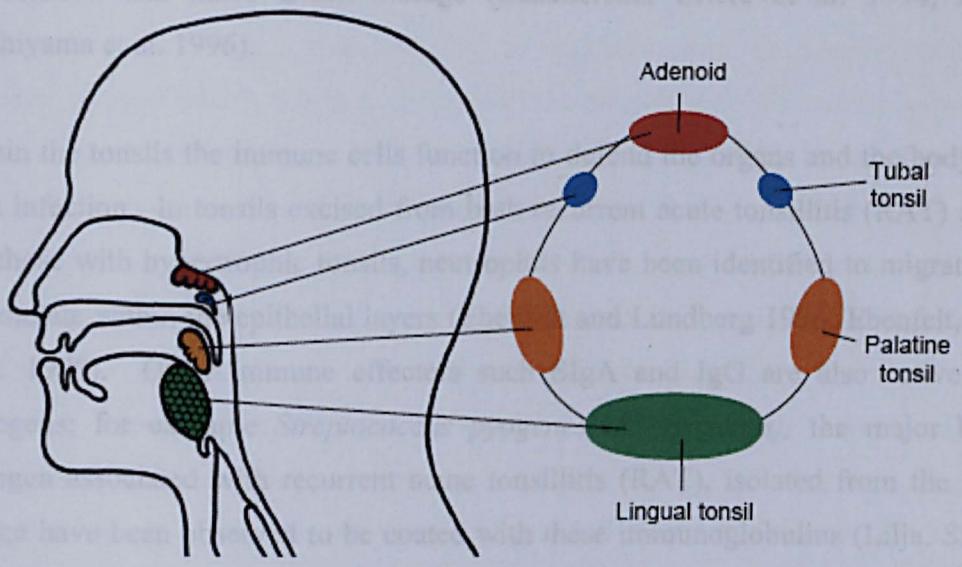

Figure 1.2: Waldeyer's ring: This ring structure of lymphoid tissue comprises the adenoids, tubal tonsils, palatine tonsils and the lingual tonsil. This diagram is from (Perry and Whyte 1998).

The surface of each tonsil is covered by a stratified squamous non-keratinised epithelium. This epithelium contains a thick band of connective tissue containing a network of blood vessels, nerves and lymphatics (Perry and Whyte 1998; Nave, Gebert et al. 2001), and at certain sites invaginates to form crypts. At such sites the epithelial cells are reshaped and there is no connective tissue, which allows motile, non-epithelial cells to be incorporated. Indeed, this reticulated epithelium contains, primarily, cells of the immune system including T-cells, Immunoglobulin (Ig) - IgA, IgG, IgM- producing B-cells, macrophages, dendritic and Langerhan cells. Some of these cells have been observed to infiltrate the tonsillar crypts from as early as the 16th week of gestation (von Gaudecker and Muller-Hermelink 1982; Perry and Whyte 1998). It has been determined that the surface area of the oropharyngeal surface of the tonsils is 45cm^2, however, when the surface area of the 10-30 crypts per tonsil is taken into account this is increased considerably to 295cm^2 (Perry 1994; Perry and Whyte 1998).

Below the surface epithelium are a number of primary and secondary lymphoid follicles. Lymphoid follicles are round or elliptical in shape and here T-lymphocytes are activated and B-cells mature (Nave, Gebert et al. 2001). The secondary lymphoid follicles contain germinal centres and mantle zones. These are the sites of centroblast

proliferation and naïve B-cell storage (Banchereau, Briere et al. 1994; Brachtel, Washiyama et al. 1996).

Within the tonsils the immune cells function to defend the organs and the body *per se*, from infection. In tonsils excised from both recurrent acute tonsillitis (RAT) sufferers and those with hypertrophic tonsils, neutrophils have been identified to migrate to and accumulate within the epithelial layers (Ebenfelt and Lundberg 1996; Ebenfelt, Ericson et al. 1998). Other immune effecters such SIgA and IgG are also active against pathogens; for example *Streptococcus pyogenes* (*S. pyogenes),* the major bacterial pathogen associated with recurrent acute tonsillitis (RAT), isolated from the tonsillar surface have been observed to be coated with these immunoglobulins (Lilja, Silvola et al. 1999). However, it is not surprising that the tonsils have a large number of active immune cells and molecules, as they have been identified as a reservoir for a number of potential pathogenic bacteria. Indeed the microbiota of the pharynx has been shown to include α-hemolytic and non-hemolytic streptococci, coagulase negative staphylococci, *Neisseria flavesceus, Corynebacterium diphtheriae* and *Neisseria gonorrhoea* (Kielmovitch, Keleti et al. 1989). Recently the estimated probabilities of typical bacterial types being found on the tonsillar surface, as determined from tonsillar swabs, were *Haemophilus Influenza* (27%), *Staphylococcus aureus* (38%), *S. pneumoniae* 66% and Group A *Streptococcus* (GAS) (62%) (Gul, Okur et al. 2007).

1.2 Tonsillitis

1.2.1 Clinical Implications

Infection of the palatine tonsils usually presents as a sore throat. Although often dismissed as trivial complaints, such infections are painful with the victims requiring periods of absence from their employment or school. Moreover tonsillitis is often recurrent, occurring in some patients at least once per month.

Diseased tonsils appear swollen and often accumulate debris within the crypts and pits (Caldas, Neves et al. 2007). Although in most cases the disease can be treated successfully with antibiotics, a tonsillectomy is recommended for severe cases of

recurrent acute tonsillitis (RAT) (Rosenfeld and Green 1990; Discolo, Darrow et al. 2003). To qualify for a tonsillectomy the sufferer must have experienced seven episodes of tonsillitis in the year preceding tonsillectomy, five episodes over the two years, or three episodes over the two preceding years (SIGN 1999). The fact that tonsillectomy is the single most common operation in ENT units world-wide and costs the NHS >£60 million annually emphasises the seriousness of the infection (Little and Williamson 1996). Tonsillectomy is also often recommended for obstructive sleep apnoea (OSA) and sufferers of peritonsillar abscess, also know as quincy (Galioto 2008). The procedure itself takes between 15 and 30 minutes to perform under a general anaesthetic, and involves removing the palatine tonsils. This procedure can be performed relatively easily with little risk to the patient and causes no deleterious effects on the immune system.

1.2.2 Pathology

Tonsillitis can be caused by viruses and/or bacteria (Putto 1987). Viral tonsillitis is common, with approximately 40% of all tonsillitis infections being caused by respiratory viruses, with adenovirus being the most common agent (Putto 1987). However Epstein-Barr, Influenza and Respiratory Syncytial Viruses have all been reported to be involved in the pathology of the infection (Putto 1987; Nokso-Koivisto, Hovi et al. 2006). As mentioned previously a number of bacteria including *S. pneumoniae* and *S. aureus* (Gul, Okur et al. 2007), inhabit the tonsillar surface asymptomatically. However *S. pyogenes*, a Gram-positive, facultative anaerobe is the major bacterium found in bacterial tonsillitis infections.

It is of interest that tonsillar size has also been perceived to be a causal factor in the susceptibility to tonsillitis, and a connection between tonsillar hypertrophy and recurrent acute tonsillitis has long been held by those in the medical field, although never really proven. Some support for this link was provided in the late 1980s when a report was published that identified tonsillar size as being proportional to the mean bacterial colony forming units/g tonsil in both RAT and hypertrophic tonsils (Brodsky, Moore et al. 1988). However further investigation of a potential link between tonsillar size and disease status has since determined that the number of follicles in the lymphoid centres

are equal in hypertrophic tonsils and those susceptible to bacterial tonsillitis, but that the follicles of the former are significantly enlarged. This in turn indicates that the immune mechanisms associated with the two conditions, hypertrophy and RAT, are probably different (Zhang, Pang et al. 2003).

1.3 Group A *Streptococcus*

1.3.1 Introduction

Streptococcus pyogenes is a coccus shaped bacterium that forms chains and can colonise epithelial and mucosal tissues (Cunningham 2000). As mentioned previously Group A *Streptococcus* (GAS), a major causal factor in RAT, is not part of the normal flora of the human body, but can be carried asymptomatically (Cunningham 2000; Tyrrell, Lovgren et al. 2002). Moreover this opportunistic pathogen can, if unchecked, cause necrotizing lesions in skin (Taviloglu, Cabioglu et al. 2005), and pyrogenic infections (Cunningham 2000), both of which can be life-threatening.

1.3.2 Identification and classification

Classical microbiological techniques have been used routinely to identify GAS. The most common method is to grow the bacteria on 5% sheep blood agar. The GAS can be identified like most beta-haemolytic streptococci by halos around the cocci shaped colonies which are indicative of haemolysis. Other streptococci including alpha-haemolytic streptococci and members of the normal flora will grow, but will cause partial or no halos i.e. they cause lysis few the red blood cells (Cunningham 2000).

During the 20th century Rebecca Lancefield, working in the Rockefeller Institute in New York, investigated the cell wall composition of streptococci and classified them according to the carbohydrate composition of their bacterial cell wall. Classification of the streptococci in this manner requires the bacteria to be grown in Todd Hewitt broth and treated with boiling 0.1M hydrochloric acid, which allows the bacterial wall

polysaccharides and M proteins (protein projections extending from the cell surface) to be extracted. Further analyses of the cell wall components by the Lancefield capillary precipitation technique and the slide agglutination procedure allows the streptococci to be typed into groups A, B, C, D, F and G respectively (Cunningham 2000). Each group is typified by a different cell wall polysaccharide composition, for example the major carbohydrate moieties of the GAS cell wall are N-acetylglucosamine and rhamnose. In addition the bacteria can also be typed through their T-proteins, which are protein markers on the bacterial cell surface, and identified via an agglutination test (Cunningham 2000). Indeed T proteins are often used as epidemiological markers.

Today a molecular biological approach is usually taken to classify streptococci. One such method uses PCR and focuses on the *emm* gene sequence that encodes the variable region within the M protein. This approach has elucidated more than 95 M serotypes of streptococci (Beall, Facklam et al. 1996), and recently the genomes of some GAS strains have been published in their entirety, such as M1 (SF370) (Ferretti, McShan et al. 2001), M3 (MGAS315) (Beres, Sylva et al. 2002) and M18 (MGAS8232) (Smoot, Barbian et al. 2002).

The *S. pyogenes* M1 and M2 serotypes were used in the studies described in this thesis as they have been previously isolated from the area of focus i.e. the throat, although GAS have been isolated from other sites including the blood, the brain and the Cerebral Spinal Fluid (Tyrrell, Lovgren et al. 2002). However as discussed by Cunningham et al (2000), in their work reviewing Group A *Streptococcus* infections, certain *S. pyogenes* serotypes are more likely to cause a particular type of infection. For example *S. pyogenes* serotypes M1, M3, M5, M6, M14, M18, M19 and M24 are more likely to be associated with throat infections, whereas the *S. pyogenes* M serotypes M2, M49, M57, M59, M60 and M61 are more likely to be associated with pyodema skin infection and glomerulonephritis.

1.3.3 Pathogenesis

Streptococcus pyogenes M1 infection is the most common cause of bacterial tonsillitis (Stenfors, Bye et al. 2003), and it has been demonstrated that individuals retain GAS

intracellularly in their pharyngeal epithelial cells following an episode of tonsillitis (Osterlund and Engstrand 1997). Streptococci also specifically colonise epithelium such as keratinocytes and the pharynx (Osterlund and Engstrand 1997; Cunningham 2000; Dorschner, Pestonjamasp et al. 2001), in the first instance causing erysipelas, cellulitis and impetigo in skin, and pharynxgitis or tonsillitis in the airways (Cunningham 2000). A GAS infection can also have severe consequences such as rheumatic fever, rheumatic heart disease, reactive arthritis and glomerulonephritis, and invasive diseases such as toxic shock syndrome, necrotising fasciitis sepsis and scarlet fever (Cunningham 2000). GAS are also implicated in stress induced psoriasis that interestingly, often follows a bacterial tonsillitis infection (England, Strachan et al. 1997).

Streptococci exert their deleterious effects and defend themselves via a number of virulence factors which can be broadly classified into two groups, cell surface factors and secreted exoproteins (Russell and Sriskandan 2008). The cell surface factors protein molecules which are anchored or attached to the cell surface, for example the M-protein, fibronectin binding proteins, the G-related α-2-macroglobulin binding protein (GRAB) and C5a peptidase. As well as cell wall components peptidoglycan, LTA, the hyaluronic acid capsule and carbohydrates (Russell and Sriskandan 2008). The secreted exoproteins are toxins such as streptolysin O (SLO) and streptolysin S (SLS) and superantigens (Russell and Sriskandan 2008).

The M-protein, as mentioned previously in 1.3.2 are dimeric, coiled-coil fibrils, approximately 50-60nm in length, which confer the ability to resist phagocytosis by polymorphonuclear leukocytes in the absence of type specific antibodies (Fischetti 1989). In a review by Fischetti et al (1989) it described the M-proteins to be highly variable in the N-terminal region, this area of the protein was the extracellular part which extended outside of the bacterial cell wall and is also the part of the molecule which is used for emm typing. The C-terminal of the protein is highly conserved and remains internalised within the bacterium. These M-proteins have been shown to facilitate adhere to cells (Cue, Lam et al. 2001) and bind through a variety of proteins on the host cell surface such as fibronectin (Schmidt and Wadstrom 1990; Courtney, Li et

al. 1994; Cue, Lam et al. 2001), sialic acid (Ryan, Pancholi et al. 2001), complement (Horstmann, Sievertsen et al. 1988), IgG and albumin (Schmidt and Wadstrom 1990).

Fibronectin binding proteins are also cell surface virulence factors. Fibronectin is an extracellular glycoprotein which is a large component of the connective tissue matrix and laminae (Hedman, Vaheri et al. 1978) and is common throughout many tissues in the human body, thus being a readily available target molecule for binding (Navarre and Schneewind 1999). These protein have been reviewed in the thesis by W.D. Smith (2004) and have found to be M-proteins, streptococcal surface GAPDH and surface endolase, SfbI, FBP54, SfbII, protein F2, PFBP, FBa/FbaA, FbaB and sfbX.

GRAB is a protein which is found in most strains of *S. pyogenes* (Toppel, Rasmussen et al. 2003). It protects the bacterium and causes utilised a cysteine proteinase in order to exert deleterious effects on host cell immune defences, as described in 1.4.10.

C5a peptidase is a bacterial cell wall associated protein which was analysed by sodium dodecyl-sulphate polyacrylamide electrophoresis to determine that this molecule is approximately 140 kDa in size (Cleary, Handley et al. 1992). This enzyme cleaves a chemotaxin C5a (involved in the complement cascade) in the polymorphonuclear leukocyte binding domain, thus affecting the immune response of the host cell (Cleary, Handley et al. 1992).

A number of bacterial cell wall components have been observed to act as bacterial cell virulence factor such as LTA, which was first reported to be a molecule associated with bacterial cell adhesion to the host cell in 1976 (Beachey and Ofek 1976). It is presented in Ofek, Beachey et al (1982) that LTA is associated with the M-protein on the surface of *S. pyogenes* and can bind to fibronectin (Nealon, Beachey et al. 1986), thus acting as an adhesion and therefore encouraging colonization. The hyaluronic acid capsule is encoded by a three gene operon, containing the locus for *hasA, hasB* and *hasC* (DeAngelis, Papaconstantinou et al. 1993). This capsule causes extracellular matrix proteins to undergo paracellular translocation by binding CD44, thus indicating host defences are affected by hyaluronic acid binding (Fanning, Volkov et al. 2005).

The secreted exoproteins are toxins such as streptolysin O (SLO) and streptolysin S (SLS) (Fontaine, Lee et al. 2003). SLO is a thiol activated 571 amino acid secreted protein toxin which exerts cytolytic effects via pore formation in the cell membrane. SLO has a conserved core, with the variation seen at the N-terminal. This toxin has a cysteine 41 amino acid residues up-stream of the C-terminus which can be converted to disulphide structures with thiol compounds which can prevent the binding of the toxin to membranes (Palmer 2001). This molecule which targets cholesterol in eukaryotic cell membranes binds as a monomer via a conserved region close to the C-terminal. Proliferation of arc and ring structures can be observed surrounding the pores (Palmer, Vulicevic et al. 1998). SLS is also an extracellular, cytolytic toxin which is only active when bound to a carrier molecule (Theodore and Calandra 1981). This toxin was cloned and sequenced a research group in 2002 and it was discovered that the operon in which this toxin was encoded contained 9 genes *sagA-I.*

S. pyogenes has been seen to be a large producer of the superantigenic toxins (Proft and Fraser 2007), for instance the streptococcal pyrogenic exotoxin (Spe A, C, G-J, L, M); streptococcal superantigens (SSA) which are exotoxins that have interactions with antigen presenting cells, specifically with major histocompatibility complex class II molecules which leads to activation of T-cells (Russell and Sriskandan 2008) and streptococcal mitogenic exotoxin Z cause severe invasive infections and are the most powerful T-cell antigens found to-date (Proft and Fraser 2007). Since the completion of GAS genomes more superantigens have been discovered as database mining has elucidated these molecules (Proft and Fraser 2007). GAS has been seen to express the following superantigen genes *speA, spec, speG, speH, speI, speJ, speK, speM, ssa* and *smeZ* (Russell and Sriskandan 2008). These molecules approximately 25kDa in size, characteristically soluble and non-glycosylated (Russell and Sriskandan 2008). The molecules are secreted from the bacterium and the signal N-terminal is cleaved at the bacterial surface (Russell and Sriskandan 2008).

The function of these molecules is reviewed in (Russell and Sriskandan 2008) and the main ways they use of interfering with the host immune responses and protective mechanisms are to inhibit the production of specific antibodies, to disrupt T-cell responses and to cause proliferation of proimflammatory cytokines such as TNF-α.

They act on host antigen presenting cells, inducing an immune response via MHC class II molecules (Russell and Sriskandan 2008) which cause massive, non-antigen specific T-cell activation (Llewelyn and Cohen 2002). As reviewed in Russell and Sriskandan, (2008), this action has also been observed to be closely related to the structure of the molecule as crystallography studies have shown a common structure between all of the superantigens which have been crystallised and studied, these molecules are SPEA, SPEC, SPEH, SPEJ and SMEZ, which have all been identified as having two globular domains, the N-terminal domain is a β-barrel and a C-terminal domain which is a β-grasp domain. These domains have an alpha-helix between the two domains.

It is known that superantigens and some other toxins can cause their virulent effects by the non-specific activation of T-cells resulting in cytokine release, through mechanisms involving major histocompatibility complex (MHC) class II molecules and some Vβ-regions of the T-lymphocyte receptor (Fast, Schlievert et al. 1989; Hackett and Stevens 1992; Norrby-Teglund, Norgren et al. 1994). Specifically with superantigens the conserved superantigenic structure interacts with specific regions of the major histocompatibility complex (MHC) class II molecules to elicit this response (Russell and Sriskandan 2008).

Streptococcus pyogenes also secretes other exotoxins such as endoglycosidase (Collin and Olsen 2001), Immunoglobulin G degrading enzyme of *S. pyogenes* (von Pawel-Rammingen, Johansson et al. 2002), DNases (Wannamaker 1958), as well as the cysteine protease (speB) further described in 1.4.10i and SIC (streptococcal inhibitor of complement) and DRS (distantly related to SIC) which are described in 1.4.10ii.

Streptococcal virulence factors can often be identified post-infection, for example mice infected with *S. pyogenes* present with raised levels of antibody against the streptococcal extracellular cysteine protease, exotoxin B (Guzman, Talay et al. 1999; Cunningham 2000).

1.3.4 Adhesion

Streptococci are known to adhere to host epithelial cells. Moreover, adherence is a two-way relationship where adhesins from both bacterial and host cells are monopolised. Originally M-proteins, projections extending from the streptococcal surface and discovered by electron microscopy, were thought to be the primary adhesins used by the bacteria (Ellen and Gibbons 1972). To date however at least eleven GAS adhesins have been identified including the aforementioned M-protein and LTA, as well as number of binding proteins that specifically target host cell proteins including collagen, vitronectin, galactose and serum opacity factor. Other proteins targeted on the host cell surface include fibronectin, fibrinogen, fucosylated glycoprotein and membrane proteins e.g. CD46 on keratinocytes (Cunningham 2000).

Pili, which are typically found on the surface of Gram-negative bacteria, also function as adhesins and actually play a major role in adherence of the bacteria to the host cell (Wu and Fives-Taylor 2001). As discussed in Wu and Fives-Taylor (2001) many types of pili have been discovered and are grouped based in their modes of assembly and expression, for example Type I fimbria, Type 4 pili and Curli fimbriae.

Until relatively recently (2003), pili were not identified in Gram-positive bacteria. They were discovered in *Cornebacterium diptheria* using electron microscopy and further investigations using deletions in the genome of this bacterium determined that the pili were made of three subunits encoded by there genes, *SpaA, SpaB* and *SpaC* (Ton-That and Schneewind 2003). Later more Gram-positive bacteria were shown to have pili, and these included *S. agalacticae*, a Group B streptococci which was discovered by screening multiple genomes of GAS, after the discovery of high molecular weight polymers. After this discovery immunogold electron microscopy was used to deduce that the polymers produced a pilus structure (Lauer, Rinaudo et al. 2005) and *S. pyogenes,* which were discovered in a similar manner, using a bioinformatic approach of genome scanning by comparing the DNA sequences of GAS strains using GcG Wisconsin 10.0 software. This yielded the genes encoding pili in this organism.

Electron microscopy was then conducted to confirm the presence of pili (Mora, Bensi et al. 2005).

Recently there has been extensive work conducted in Newcastle by Abbot, Smith et al (2007), looking at invasion and adhesion of GAS to both tonsils and skin. This study showed that after 5mins of incubation with a tissue sample *S. pyogenes* had already begun to bind to the tonsil. The study showed binding rate continued rapidly between 30min and 2 hours of incubation and after this time continued at a slower rate. Abbot, Smith et al (2007) was also able to show using plate counts that after 2 hours of incubation with tonsil tissue 10-20% ($>10^6$ cfu) *S. pyogenes* had adhered to the tissue; this adhesion also appeared to be the same in control (excised for apnoea or snoring) and RAT tonsils. Pili-defective mutants did not adhere to tonsil, even after an extended incubation time of 18 hours (Abbot Smith et al 2007). Using the pili-defective mutant *S. pyogenes* in adhesion experiments with all three genes encoding the pili subunits (*Δspy125 Δspy128 and Δspy130)* and the gene for pili assembly (*Δspy129)* all required for pili formation Abbot, Smith et al (2007) had established emphatically that pili are necessary to cause a GAS infection in human tonsils and keratinocytes. Two pili-defective mutants have been used in the studies reported in this thesis. These are *Δspy129* that lacks pili and *Δspy1154* that lacks pili and surface proteins such as adhesins.

1.4 Host Defense Peptides: Cationic Antimicrobial peptides

1.4.1 Introduction

Antimicrobial peptides (AMPs) are small, between 11 and 50 amino acids in length, hydrophobic, cationic peptides, with a positive net charge due to the presence of lysine and arginine amino acids (Hancock 1997; Hancock and Scott 2000). These peptides are host encoded and can kill a broad range of microorganisms such as Gram-positive and Gram-negative bacteria, fungi and enveloped viruses (Izadpanah and Gallo 2005). These peptides, being a fundamental part of the innate immune system are synthesised in both the plant and animal kingdoms and in the latter are found in mammals, amphibians, avian, fish and insects (Hancock and Chapple 1999; Wong, Xia et al. 2007; van Dijk, Veldhuizen et al. 2008). In mammals they are localised at epithelial and mucosal surfaces, and within antigen presenting cells including neutrophils and macrophages (Huttner and Bevins 1999).

Historically, the first AMPS were reported in 1962 by Kiss and Michl et al (cited by Hancock, Chapple et al. 1999), who reported the presence of these natural antibiotics in the skin of the frog *Bombina Variegata*. These host defence peptides were aptly named Bombinins. Later, in 1972, Melittin, an AMP derived from bee venom was reported (Habermann 1972). Mammalian AMPs were first reported in the mid 1960s in two papers, which described the antibacterial and enzymatic activities of cationic proteins isolated from the polymorphonuclear leukocyte lysosomes of guinea pigs (Zeya and Spitznagel 1966 (a); Zeya and Spitznagel 1966 (b); Habermann 1972). Since then many more AMPs have been documented and characterised. Moreover to facilitate studies involving AMPs, the peptides have been classified into families, usually on the basis of their structure and amino acid content. Currently there are well over 1000 AMPs documented in a number of databases, the largest of which can be accessed at http://www.bbcm.univ.trieste.it/~tossi/search.htm.

There are at least four different families of AMPs: the alpha-helical (α-helical) AMPs without cysteine amino acids, of which the cathelicidin LL-37 is a member; AMPs with cysteines linked by disulphide bridges e.g. the α-defensin, Human Neutrophil Peptide 1 (HNP-1); AMPs with an unusually high proportion of specific amino acid residues, e.g.

Histatins including His 1 and His 2; and AMPs with loop structures such as Bactenecin (Bals 2000; Koczulla and Bals 2003). The work presented in this study is focussed on two major families, the cathelicidins and the human beta-defensins (HBDs).

The term host defence peptides has been used to describe small, cationic peptides often referred to in the literature as antimicrobial peptides as these biological molecules have been seen to have immunomodulatory properties e.g. acting as an inducer of chemokines or other immune effectors, as well as having antimicrobial functions. Recently, some research groups have begun to favour the term host defence peptides, rather than antimicrobial peptides as it fully describes their multiplicity of function (Devine and Hancock 2004; Devine and Cosseau 2008). This shift in terminology was proposed by Hancock and Devine in their 2004 editorial 'Antimicrobial or Host defence peptides' this proposal has also been included in the recent review by (Devine and Hancock 2004; Devine and Cosseau 2008). This proposal states that the physiological concentrations at which these peptides are found in some biological tissues are not high enough to exhibit an antimicrobial effect and therefore their immunomodulatory role is the primary function. It is considered in the editorial that while some of these peptides do have an antimicrobial role at a particular site in the body they may have other host defence functions at many others. The Hancock and Devine (2004) editorial also suggested that antimicrobial ability of many AMPs has been measured in a 10mM phosphate buffer or growth medium which are not physiologically relevant and that salt concentration, cell surface factors and serum factors may affect antimicrobial activity *in vivo*. In particular salt concentration is considered and it is discussed that at physiological salt concentrations in blood (1mM Mg^{2+} and 2mM Ca^{2+}) the antimicrobial activity of most host defence peptides would be removed.

The within the mouth a vast number of bacteria can be found, more than 700 types have been isolated (Devine and Cosseau 2008). As reviewed in Devine and Cosseau (2008), this number comprises both oral commensals e.g. Streptococcus *mitis*, Streptococcus *oralis*, some species of Prevotella and Fusobacterium *nucleatum* and some organisms associated with disease e.g Streptotoccus *mutans*, Streptococcus sobrinus and lactobacilli. As this environment is bacteria rich the mouth has developed complex defence mechanisms, including many molecules such as AMPs, lysozyme, lactoferrin,

lactoperoxidase, myeloperoxidase, Secretory IgA, Chitinase and von ebnerglands proteins (Devine and Cosseau 2008).

Within the mouth AMP expression has seen to be within saliva, the gingival crevicular fluid, oral epithelial cells and neutrophils (Devine and Cosseau 2008). The AMPs expressed here are the Histatins (Oppenheim, Xu et al. 1988), alpha defensins (Dale and Fredericks 2005), beta defensins (Bonass, High et al. 1999) and the cathelicidins (Putsep, Carlsson et al. 2002). Within the mouth AMPs have been seen to be expressed at concentration which would be antimicrobial (Tao, Jurevic et al. 2005), the AMPs reported here were extracted from saliva samples from subjects, of which 92% were healthy, they were 0.31μg/ml, 3.07μg/ml and 0.8μg/ml for HBD3, LL-37 and HNP1-3 respectively (Tao, Jurevic et al. 2005). The physiological concentration of HBD2 was reported as being 0.04μg/ml in oral epithelial tissue (Sawaki, Mizukawa et al. 2002). Tao, Jurevic et al (2005), also reported that HNP1-3 and LL-37 concentrations were higher in the groups of subjects without caries, suggesting a protective role of AMPs in the mouth.

1.4.2 Cathelicidins

The cathelicidin family of AMPs was discovered in the 1990s as a consequence of studies focussed originally on Bac 5, an AMP derived from bovine neutrophils (Zanetti, Del Sal et al. 1993; Gennaro and Zanetti 2000). In fact cathelicidin molecules were found to be synthesised at the myeloid and metamyeloid stages of maturation of the neutrophil cells, and packaged into azurophil granules for storage (Gabay, Heiple et al. 1986; Sorensen, Arnljots et al. 1997).

Cathelicidins, are not specific to mammals as they are also found in birds (Xiao, Cai et al. 2006; van Dijk, Veldhuizen et al. 2008) and fish (Chang, Zhang et al. 2006; Maier, Dorn et al. 2008). In humans there is one cathelicidin called hCAP18 (Gudmundsson, Magnusson et al. 1995; Nizet, Ohtake et al. 2001). Although the human genome contains only one cathelicidin gene (Durr, Sudheendra et al. 2006), multiple genes have been found in other species such as horse, pig and cow (Lee, Ohtake et al. 2005). It is

hypothesized that evolution of multiple cathelicidin genes provides these species with enhanced resistance to infection (Lee, Ohtake et al. 2005). The human cathelicidin gene (Figure 1.3), positioned on chromosome 3p21, is composed of four exons and three introns (Agerberth, Gunne et al. 1995; Gennaro and Zanetti 2000; Elloumi and Holland 2008); (Sorensen, Follin et al. 2001). The encoded protein is synthesised as an 18 kDa precursor molecule, with a conserved N-terminal domain and a variable C-terminal sequence (Figure 1.3). The prepropeptide, known originally as either Profall-39, hCAP18 or cathelin-LL-37, was discovered by three different groups simultaneously, (Agerberth, Gunne et al. 1995; Cowland, Johnsen et al. 1995; Larrick, Hirata et al. 1995), although it is now routinely referred to as hCAP18. The precursor protein is cleaved enzymatically to release the mature C-terminus (4.5kDa), which has antimicrobial activity (Putsep, Carlsson et al. 2002). *In vitro* three serine proteinases, cathepsin G, elastase and proteinase 3 have all been shown to cleave hCAP-18, although proteinase 3 is believed to function *in vivo* (Zanetti, Gennaro et al. 1995).

The mature antimicrobial peptide is called LL-37. This name is based on the structure of the peptide that contains 37-amino acids with the amino acid leucine at positions 1 and 2 respectively (Putsep, Carlsson et al. 2002). The peptide sequence is: LLGDFFRKSK EKIGKEFKRI VQRIKDFLRN LVPRTES (Tjabringa, Aarbiou et al. 2003).

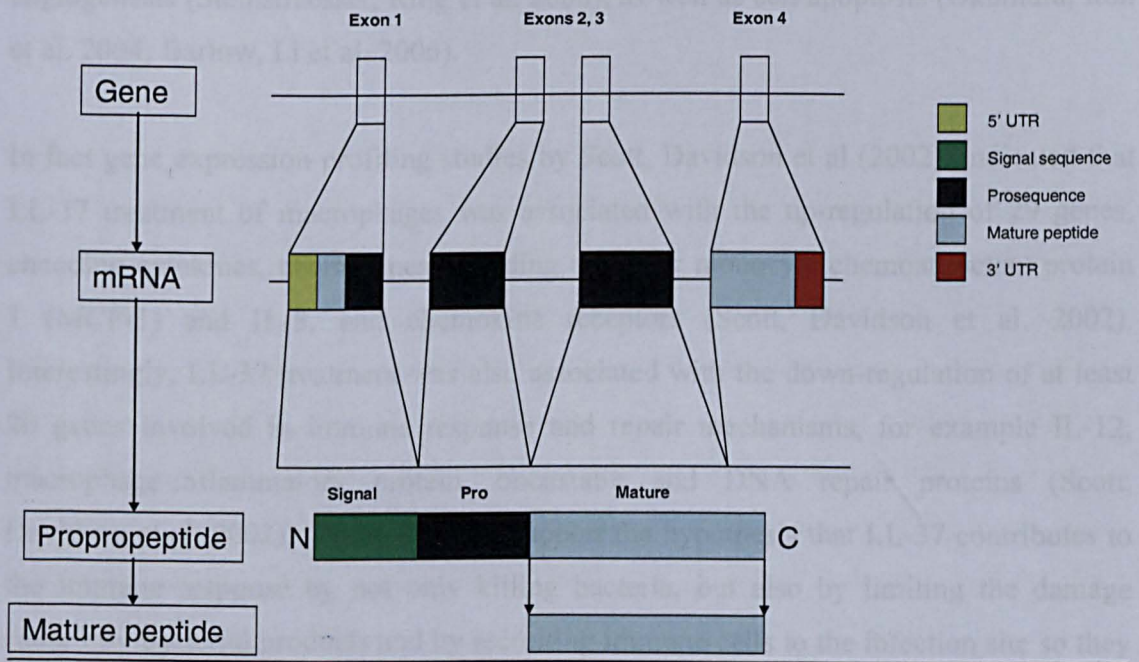

Figure 1.3: LL-37 Structure: Gene to mature peptide. Schematic representation. Adapted from (Koczulla and Bals 2003).

Expression of LL-37 has been reported in a number of tissues in humans including the tonsils (Song, Hwang et al. 2006; Ball, Siou et al. 2007), sweat glands (Murakami, Ohtake et al. 2002), the lungs and airway epithelium (Bals, Wang et al. 1998), keratinocytes (Frohm, Agerberth et al. 1997) and breast tissue (Heilborn, Nilsson et al. 2005). In body fluids such as serum and airway surface fluid a LL-37 concentration of 0.2 - 1μM has been reported (Sorensen, Cowland et al. 1997; Schaller-Bals, Schulze et al. 2002).

LL-37 has both killing and signalling roles in the protection of the host from infection (Dorschner, Pestonjamasp et al. 2001; Nizet, Ohtake et al. 2001). As regards signalling the molecule has been shown to have chemotactic effects on monocytes, neutrophils, T-lymphocytes and mast cells (Yang, Chertov et al. 2001; Niyonsaba, Iwabuchi et al. 2002), and to stimulate the differentiation of dendritic cells (Davidson, Currie et al. 2004). Moreover in relation to mast cells, which are among the first inflammatory cells to encounter invading pathogens, LL-37 has been shown to induce intracellular calcium mobilisation and histamine release (Niyonsaba, Someya et al. 2001). The peptide, through mitogen activated kinase (MAPK) signalling pathways also induces IL-8, IL-18 and IL-20 production in primary keratinocytes (Niyonsaba, Ushio et al. 2005). Other non-microbial roles for this peptide have been reported, and include wound healing and angiogenesis (Steinstraesser, Ring et al. 2006), as well as cell apoptosis (Okumura, Itoh et al. 2004; Barlow, Li et al. 2006).

In fact gene expression profiling studies by Scott, Davidson et al (2002), indicated that LL-37 treatment of macrophages was associated with the up-regulation of 29 genes, encoding cytokines, chemokines including those for monocyte chemoattractant protein 1 (MCP-1) and IL-8, and chemokine receptors (Scott, Davidson et al. 2002). Interestingly, LL-37 treatment was also associated with the down-regulation of at least 20 genes involved in immune response and repair mechanisms, for example IL-12, macrophage-inflammatory protein, oncostatin and DNA repair proteins (Scott, Davidson et al. 2002). These findings support the hypothesis that LL-37 contributes to the immune response by not only killing bacteria, but also by limiting the damage caused by bacterial products and by recruiting immune cells to the infection site so they can clear the infection.

1.4.3 Defensins

The defensins, like cathelicidin, function to protect the host from a microbial assault. In humans there is more than one defensin gene, and defensin genes are expressed and peptides synthesised in a broad range of tissues and cells. Defensins are subdivided into three main classes in vertebrate, the α-defensins, the β-defensins and the θ-defensins. They are classified according to the arrangement of the disulphide bridges between the six conserved cysteine residues (Hollox, Armour et al. 2003).

The α-defensins are a major constituent of granulocytes and neutrophils (Lehrer and Ganz 2002), and the genes are expressed in a limited number of epithelial tissues that include the gut epithelium, the endocervix and the vagina (Hollox, Armour et al. 2003). They are between 29-35 amino acid residues in length, and characterised by three disulphide bonds with the following pairing Cys1-Cys6, Cys2-Cys4 and Cys3-Cys5 (Lehrer and Ganz 2002). There are six known α-defensins; these include four human neutrophil peptides that are primarily expressed by granulocytes and neutrophils, and HD5 and HD6 that are expressed by the Paneth cells in the intestine (Lehrer and Ganz 2002). The alpha-defensins can kill a wide range of Gram-positive and Gram-negative bacteria including both intracellular and extracellular organisms. For example the gut α-defensin HD5, displays activity against *Escherichia coli*, *Listeria monocytogenes*, *Salmonella typhimurium* as well as *Candida albicans*, with minimal inhibitory concentrations in the nanomolar range (Porter, van Dam et al. 1997).

The main human β-defensin locus is 8p22-p23 (Semple, Rolfe et al. 2003), and the genes are characterised by two exons flanking one intron (Figure 1.4) (Koczulla and Bals 2003). Through *in silico* analyses over 40 open reading frames with DNA sequences, potentially encoding β-defensins, have been identified in the human genome although many appear to encode transcripts with premature stop codons, and are thought to be pseudogenes (Pazgier, Hoover et al. 2006). The activities of HBD1-4 have however been well characterised and mRNA expression of the HBD1-4 genes has been shown in numerous tissues including skin (Harder, Meyer-Hoffert et al. 2004), intestine (Fahlgren, Hammarstrom et al. 2004), tonsil (Harder, Bartels et al. 2001; Ball, Siou et al. 2007) and cartilage (Varoga, Pufe et al. 2005).

The β-defensin family peptides are 38-42 amino acid residues long and structurally, are similar to the α-defensins, except for the different pairing of the six cysteines. In β-defensins the pairing is Cys1-Cys5, Cys2-Cys4, Cys3-Cys6 (Yang, Chertov et al. 2001). The human β-defensins exhibit antimicrobial activity against numerous pathogens including Gram-negatives e.g. *E. coli* and *P. aeruginosa* (Harder, Bartels et al. 1997) and Gram-positives e.g. *S. pyogenes* (Fernie-King, Seilly et al. 2004; Fernie-King, Seilly et al. 2006).

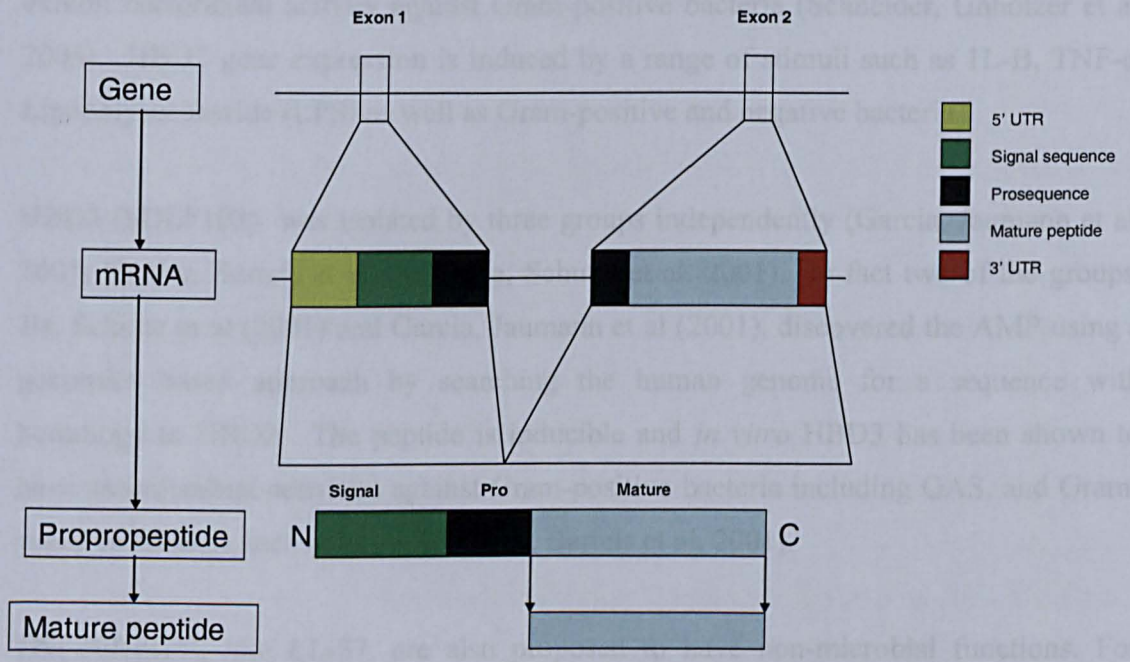

Figure 1.4: HBD Structure: Gene to mature peptide. Schematic representation. Adapted from (Koczulla and Bals 2003).

The work in this thesis is focussed particularly on the human β-defensins 1-3. There are, in the public domain, many excellent reviews describing the defensins, including those by (Schneider, Unholzer et al. 2005; Pazgier, Hoover et al. 2006; Menendez and Finlay 2007) and (Devine and Cosseau 2008). Because of this information in this thesis relating to HBD1-3 will be summarised in a few paragraphs.

HBD1 (also referred to as hDEFB1), was first identified in the mid 1990s in plasma (Bensch, Raida et al. 1995). The gene is classically recognised as being constitutively expressed in most cells including those derived from the trachea, bronchi, gingiva (Zhao, Wang et al. 1996; Krisanaprakornkit, Weinberg et al. 1998; Mathews, Jia et al.

1999; Proud, Sanders et al. 2004), although it has been shown to be up-regulated in Acne Vulgaris, a potentially microbial infection (Chronnell, Ghali et al. 2001). Gram-negative bacteria are particularly susceptible to the antimicrobial effects of HBD1.

HBD2 (hDEFB4), was isolated originally from psoriatic skin lesions where it is found in high concentrations (Harder, Bartels et al. 1997). *In vitro* this AMP is known to exhibit antimicrobial activities against Gram-negative bacteria including *E. coli* and *P. aeruginosa* (Harder, Bartels et al. 2001), but at high concentrations 100μg/ml can also exhibit bactericidal activity against Gram-positive bacteria (Schneider, Unholzer et al. 2005). HBD2 gene expression is induced by a range of stimuli such as 1L-B, TNF-α, Lipopolysaccharide (LPS) as well as Gram-positive and negative bacteria.

HBD3 (hDEF103) was isolated by three groups independently (Garcia, Jaumann et al. 2001; Harder, Bartels et al. 2001; Jia, Schutte et al. 2001). In fact two of the groups, Jia, Schutte et al (2001) and Garcia, Jaumann et al (2001), discovered the AMP using a genomics based approach by searching the human genome for a sequence with homology to HBD2. The peptide is inducible and *in vitro* HBD3 has been shown to have antimicrobial activities against Gram-positive bacteria including GAS, and Gram-negative bacteria such as *E. coli* (Harder, Bartels et al. 2001).

The defensins, like LL-37, are also proposed to have non-microbial functions. For example in keratinocytes, HBD2 and HBD3 have been shown to promote the production and release of inflammatory mediators such as cytokines (Niyonsaba, Ushio et al. 2007). HBD2 has been reported to induce histamine release in mast cells (Niyonsaba, Someya et al. 2001), while HBD3 has been suggested to play a role in wound healing (Varoga, Pufe et al. 2005). There is also evidence to show that the HBDs influence cell differentiation (Shiba, Mouri et al. 2003), as well as acting as chemoattractant agents (Yang, Chertov et al. 1999).

1.4.4 Hepcidin

Hepcidin is found in mammals and insects (Park, Valore et al. 2001), and the mammalian peptide has been shown to have antimicrobial activity against *Bacillus sp.*,

Micrococcus luteus and Staphylococcus carnosus (Krause, Neitz et al. 2000). Like the human β-defensins hepcidin is cysteine rich, but the peptide has eight, rather than six, cysteine amino acids which form four disulphide bonds (Park, Valore et al. 2001).
The primary amino acid structure of the active form of hepcidin is DTHFPICIFCCGCCHRSKCGMCCKT, and the secondary structure as determined by two-dimensional ^{H}NMR spectroscopy comprises a beta-sheet structure with a hairpin loop (Hunter, Fulton et al. 2002). The active peptide is 2-3 kDa in size with a positive charge of 3 at neutral pH. It is synthesised as a 84 amino acid prepropeptide and like other AMPS, mature hepcidin is cleaved in this case by propeptide convertases.

Hepcidin was discovered almost simultaneously by two research groups. In 2001, Park and colleagues, reported a peptide with antimicrobial activity in human urine (Park, Valore et al. 2001), while Krause and co-workers, identified the same peptide (also known as LEAP-1) in a human plasma ultrafiltrate (Krause, Neitz et al. 2000). Interestingly in the study by Park, Valore et al (2001), three Hepcidin molecules were reported, Hepc20, Hepc22 and Hepc25, the former two being processed forms. In fact *in silico* analysis has revealed that more than one active peptide is possible from the single precursor protein due to various possible cleavage sites (Park, Valore et al. 2001).

Park and colleagues demonstrated elevated hepcidin expression in fetal and adult livers, although they were unable to detect gene expression in tissues such as the prostate, testes, ovary, small intestine or colon (Park, Valore et al. 2001). This result was supported by the studies of Krause, Neitz et al (2000), who using real-time PCR indicated that the liver expression of hepcidin, was comparable to that of the house-keeping gene, GAPDH.

Although the hepcidin, or LEAP-1 molecule, was identified originally as an AMP it actually plays a key role in iron homeostasis. Indeed injection of synthetic hepcidin into mice induces hypoferremia within one hour (Rivera, Nemeth et al. 2005). The roles of hepcidin in iron homeostasis were actually established through transgenic mice models and investigation of genetic defects that result in iron deficiency (Nicolas, Bennoun et al. 2001; Roetto, Papanikolaou et al. 2003; Viatte, Lesbordes-Brion et al. 2005) or extreme peptide production (Nicolas, Bennoun et al. 2002) in humans. The induction of

hepcidin expression by inflammatory stimuli and the resulting hypoferraemia is proposed to play a role in host defences against microbial infection (Ganz 2007).

1.4.5 Liver Expressed Antimicrobial Peptide-2 (LEAP-2)

Liver Expressed Antimicrobial Peptide-2 (LEAP-2) was, like hepcidin, isolated from human blood ultrafiltrate. This LEAP-2 peptide was characterised by Krause, Sillard et al (2003), and is known to be synthesised as a 77-residue precursor molecule, which is processed, probably by furin, to release the mature peptide. LEAP-2 is again cysteine rich with four cysteine residues forming two disulphide bonds binding in the conformation Cys1-Cys3 and Cys2-Cys4. Studies carried out by this group identified LEAP-2 gene expression in many epithelial tissues including the liver, kidney, colon, lung, trachea and heart (Krause, Sillard et al. 2003). The mature LEAP-2 peptide has been shown to have antimicrobial activity against Gram-positive and Gram-negative bacteria (Krause et al. 2003; Townes, Michailidis et al. 2004).

1.4.6 AMP killing mechanisms

It is widely recognised that cationic AMPs neutralize and kill both Gram-negative and Gram-positive bacteria as well as fungi, parasites, cancer cells and enveloped viruses, e.g. Herpes simplex virus and HIV; however the usual targets of the AMPs microbial rather than eukaryotic (Hancock and Scott 2000). Some of the exact mechanisms by which this killing occurs are debated but it is widely agreed that killing is linked to the charge and hydrophobicity of the peptides, and the formation of pores in the microbial membranes.

A good general explanation of actions of AMPs on membrane can be found in a review by Brogden et al (2005). This review outlines how attraction between the peptide and the cell membrane through electrostatic bonding allows the AMP to attach to the membrane. Generally AMPs are cationic and are attracted to the negatively charged outer membrane of bacteria, in Gram-negative bacteria the net negative charge is generated by anionic phosholipids and phosphate groups. In Gram-positive bacteria this is generated by the teichoic acids. The AMPs then attach to the membrane by adsorbing and embedding into it, the lipid head groups then stretch the membrane. This review

also details that in a low peptide:lipid situation peptide molecules will bind to the membrane and in a high peptide:lipid situation pores will be formed.

The mode of action against Gram-negative bacteria is widely accepted basically as 1) interaction with cell membranes, 2) crossing of the cell membrane and 3) killing of cells (Hancock and Scott 2000). Initially, the AMPs interact with the membrane surface, specifically the polyanionic surface LPS, next the divalent cations which bridge and partly neutralise LPS. This disruption of the outer bacterial cell membrane allows the AMP to pass through the membrane (Hancock and Scott 2000). In a review on killing mechanism of this type this entrance to the membrane by electrostatic interactions with itself has been termed 'self promotion of their own uptake', this review by Hancock and Scott (2000) suggests this term which they once used to described the uptake of polycationic antibiotics across the outer membrane (Hancock and Chapple 1999). The next stage of AMP action on Gram-negative bacteria is to integrate into the membrane via associating with negatively charged phospholipids so that the AMPs become orientated parallel to the membrane (Hancock and Scott 2000). At this stage of membrane disruption it is understood that at a particular concentration the peptide molecules form transmembrane channels in the membrane, these are also know as aggregate channels, supramolecular peptide/lipid complexes or toroidal channels (Hancock and Scott 2000). There is debate around mechanisms of cell death at this stage, as to whether the depolarisation of the membrane by disruption of the proton motive force is enough to cause leakage of the contents of the cell, therefore the departure of molecules essential for the live of the cell, or as to whether this pore formation is just an 'intermediate step' in the process of cell death and that the inhibition of a vital function of the cell such as DNA synthesis causes the death of the cell (Hancock and Scott 2000).

The mode of action of AMPs on Gram-positive is not agreed on in literature and the method of action is still not resolved to-date. It is proposed in some studies that interactions with cytoplasmic membranes are voltage dependant (Falla, Karunaratne et al. 1996) but in other studies transmembrane potential for AMP interactions have been seen to vary between peptides (Koo, Yeaman et al. 1997; Yeaman, Bayer et al. 1998). In the study by Koo, Yeaman et al (1997), when defensin transmembrane potential was compared to thrombin-induced platelet microbicidal protein 1, the defensins appeared to

have potentially independent or very low membrane potential in comparison. This variation in membrane potential and permeablisation was also observed after analysis with flow cytometry by Yeaman, Bayer et al (1998) as here as HNP-1 was observed to depolarise and permeablise the membrane, whereas thrombin-induced platelet microbicidal protein 1 permeabilised but did not depolarise (Yeaman, Bayer et al. 1998). These articles suggest that membrane perturbation is required for killing but is not essential; leading to the suggestion that killing may be due to the inhibition of an intracellular target.

The membrane disrupting properties of AMPs have been analysed using model systems involving the lipid bilayers of artificial liposomes (Jelinek and Kolusheva 2005), and three main models of pore formation have been proposed: the barrel-stave mechanism (Rapaport and Shai 1992), the carpet mechanism or the Shai-Matsuzakul method (Matsuzaki 1999; Zasloff 2002), and the toroidal pore mechanism (Brogden 2005). It has also been observed that the AMPs differentiate between the membranes of higher eukaryotes and prokaryotes including bacteria, through the different compositions of the membranes, including the absence or presence of cholesterol (Schroder 1999).

1.4.6i Barrel-stave mechanism

A representation of this killing mechanism is shown in Figure 1.5. Essentially, α-helical cationic peptides form bundle-like structures, which target the bacterial membrane via the alignment of their hydrophobic regions with the lipid core of the membrane. This results in a membrane pore and further AMP monomers, recruited to the site, enlarge the pore (Oren and Shai 1998; Brogden 2005).

1.4.6ii Carpet mechanism

In the carpet mechanism the cationic AMPs bind to the negatively charged surface membrane of the bacteria and 'carpet it' i.e. the bacterial membrane is covered with a layer of AMPs. The peptides then permeate the membrane causing the negatively charged membrane lipid heads to rotate and make contact with the positively charged

cationic peptides, which subsequently results in the formation of micelles and membrane disruption (Oren and Shai 1998; Brogden 2005).

1.4.6iii The 'toroidal-pore' mechanism

The AMPs LL-37 and magainin are proposed to function through a toroidal pore or 'aggregate channel' killing mechanism (Huang, Chen et al. 2004). This involves AMP helices inserting into the lipid bilayer leading to the dynamic formation of pores. The peptides are believed to induce bending of the lipid monolayers continuously through the pore, resulting in the pore being lined with both the AMP and the lipid head groups of the bilayer. The toroidal-pore model differs from the barrel-stave model in that the AMPs are always associated with the lipid head groups.

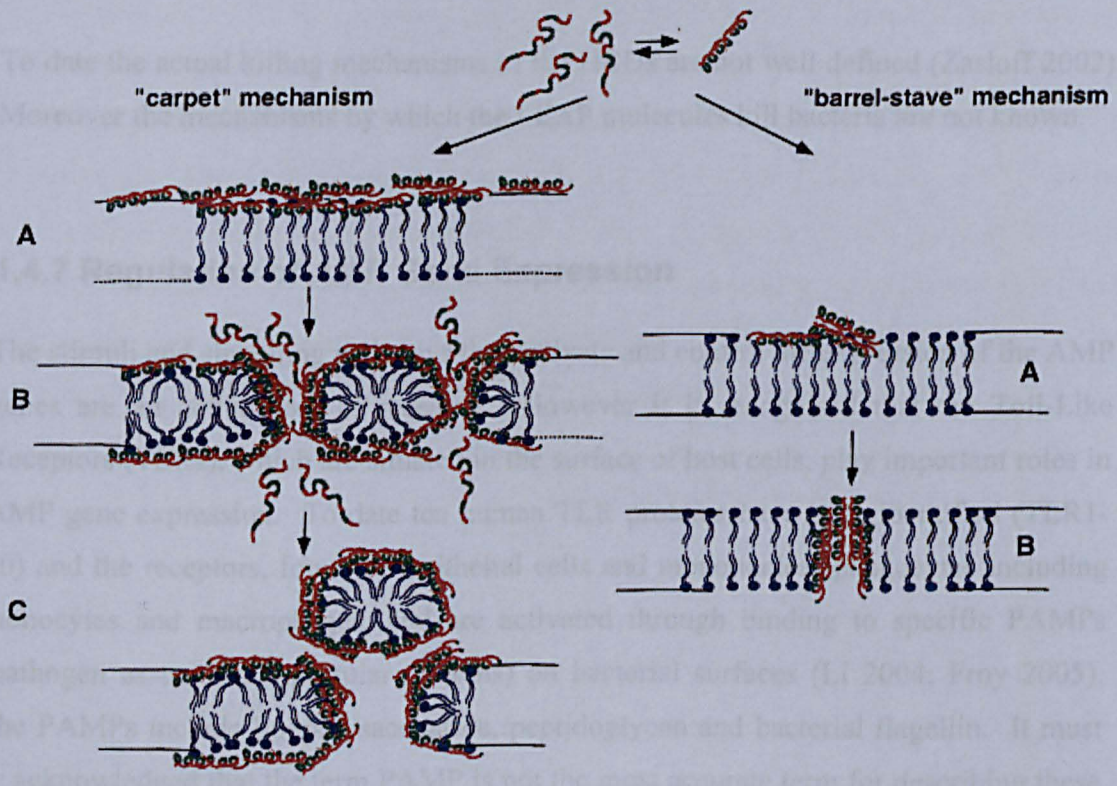

Figure 1.5: Barrel-stave and carpet mechanisms are represented as above. This schematic representation was adapted from (Oren and Shai 1998). The orientation of AMP molecules and their ability to form pores in the bacterial membranes is shown. The cationic AMPs initiate contact with the lipid bilayer of cell membranes in **A** for both mechanisms. In the carpet mechanism **B** the membrane is disrupted by the movement of the negatively charged lipid heads to be in contact with the cationic peptides, forming micelles and thus breaking down the membrane **C**. The α-helical cationic peptides depicted in the barrel stave mechanism form a bundle and permeate the lipid bilayer using their charges to align the hydrophobic core regions with the hydrophilic peptides **B** allowing pore formation and further internalisation of AMPs.

In each case these interactions lead to a loss of membrane function including breakdown of membrane potential, loss of cell metabolites and ions, and alteration of membrane permeability, all of which result in bacterial cell killing. The ability of a peptide to cause bacterial cell death through a number of different mechanisms is termed the 'multi-hit process' and may be responsible for the success, in evolutionary terms, of AMPs in host defence (Zhang, Dhillon et al. 2000). Many AMPs have intracellular targets once they are inside the membrane. Some have been seen to inhibit vital cellular processes such as cell wall synthesis, nucleic acid synthesis, protein synthesis and enzymatic activity (Brogden 2005).

Interestingly PR-39, a proline rich AMP identified in the pig intestine is also reported to inhibit DNA synthesis in *E. coli* (Boman, Agerberth et al. 1993; Schroder 1999).

To date the actual killing mechanisms of the HBDs are not well defined (Zasloff 2002). Moreover the mechanisms by which the LEAP molecules kill bacteria are not known.

1.4.7 Regulation of AMP Gene Expression

The stimuli and signalling pathways that activate and control the expression of the AMP genes are an active area of research. However it is recognised that the Toll-Like Receptors (TLRs), which are situated in the surface of host cells, play important roles in AMP gene expression. To date ten human TLR proteins have been identified (TLR1-10) and the receptors, found on epithelial cells and mononuclear phagocytes including monocytes and macrophages, and are activated through binding to specific PAMPs (pathogen associated molecular patterns) on bacterial surfaces (Li 2004; Froy 2005). The PAMPs include lipopolysaccharide, peptidoglycan and bacterial flagellin. It must be acknowledged that the term PAMP is not the most accurate term for describing these molecular patterns which activate TLRs, as often they are not derived from pathogens in source, whereas PAMP implies only pathogen associated molecular patterns would active TLRs.

Activation of a TLR, following the binding of an appropriate ligand, generates a signalling cascade, which ultimately results in the nuclear translocation of NF-κB

(Figure 1.6). This transcription factor then binds to the promoters of genes encoding a number of pro-inflammatory molecules, including the cytokines, TNFα, IL-1, IL-6 and IL-8 (Cook, Pisetsky et al. 2004) as well as AMPs (Lu, Kurago et al. 2006). In addition TLRs can also activate pathways involving mitogen activated protein kinase (MAPK) leading to the nuclear translocation of the AP-1 transcription factor (Froy 2005).

The TLRs 2-6 and 9 have been shown to mediate an increase in defensin gene expression. For example HBD2 gene expression is mediated through TLR4 signalling in gut epithelia, but TLR2 and TLR6 signalling in airway epithelia (Froy 2005). HBD2 gene expression has also been shown to be up-regulated by *Salmonella* flagellin (FliC) via TLR5 in the immortalised Caco-2 cell line (Ogushi, Wada et al. 2001).

In addition to the TLRs, mammals are typified by a family of intracellular receptors known as NOD (nucleotide binding oligomerisation domain) proteins. Binding of NOD proteins to intracellular bacterial components via a C terminal LRR (leucine–rich repeat) domain leads to activation of both NF-κB and MAPK pathways. NOD is found in intestinal cells and has been implicated in the regulation of HBD2 gene expression (Voss, Wehkamp et al. 2006). Recently it has been shown, at least in oral epithelial cells, that the combination of signalling through TLRs and NODs leads to the synergistic activation of antibacterial responses (Uehara and Takada 2008).

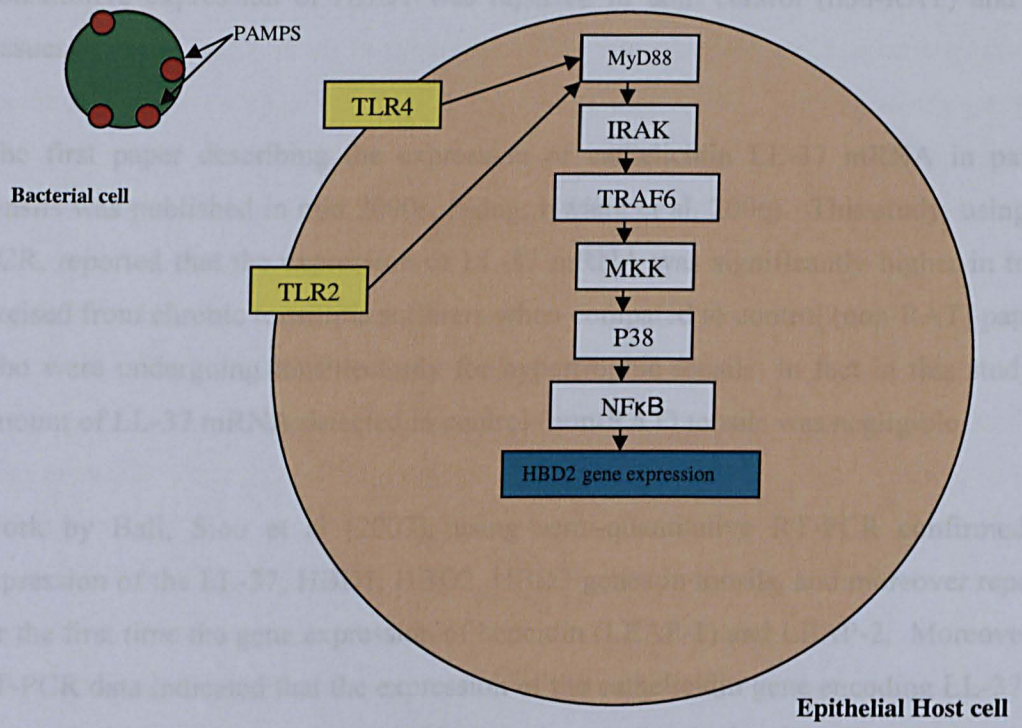

Figure 1.6: A representative TLR signalling pathway.

1.4.8 AMPs and tonsil

Compared to the literature relating to host defence peptides, in particular, the number of articles focussed on AMPs and tonsils is limited.

The first references relating to defensin gene expression in tonsil were published seven years ago by Chae, Lee et al (2001), and Harder, Bartels et al (2001), and these studies used RT-PCR analyses to identify the expression of HBD1 and HBD3 mRNA transcripts in tonsil. The groups of Weise, Meyer et al (2002), and Wang, Dong et al (2004), then published research papers in which the authors used RT-PCR analyses, to investigate and compare AMP gene expression profiles in control (non-RAT) and RAT tonsils. In the study by Weise, Meyer et al (2002), a cohort of 49 hyperplastic tonsils and RAT tonsils were analysed and compared for HBD1, HBD2, HNP1 and HNP4 mRNA expression and the results indicated constitutive expression of HBD1 mRNA, but an up-regulation of HBD2 mRNA in the chronically diseased groups. Similarly in the study conducted by Wang, Dong et al (2004), involving a sample cohort of 18,

constitutive expression of HBD1 was reported in both control (non-RAT) and RAT tissues.

The first paper describing the expression of cathelicidin LL-37 mRNA in palatine tonsils was published in mid 2000s, (Song, Hwang et al. 2006). This study, using RT-PCR, reported that the expression of LL-37 mRNA was significantly higher in tonsils excised from chronic tonsillitis sufferers when compared to control (non-RAT) patients, who were undergoing tonsillectomy for hypertrophic tonsils. In fact in this study the amount of LL-37 mRNA detected in control (non-RAT) tonsils was negligible.

Work by Ball, Siou et al (2007), using semi-quantitative RT-PCR confirmed the expression of the LL-37, HBD1, HBD2, HBD3 genes in tonsils, and moreover reported for the first time the gene expression of hepcidin (LEAP-1) and LEAP-2. Moreover the RT-PCR data indicated that the expression of the cathelicidin gene encoding LL-37 was detectable in tonsils from control subjects and moreover the levels appeared comparable in control and RAT patient tonsils, although it was acknowledged that the control (non-RAT) data was from two subjects only.

1.4.9 Antimicrobial peptide- streptococcal interactions

In comparison to the wealth of literature focussed on host defence peptides and cationic antimicrobial peptides in particular, there are again relatively few papers documenting the interactions between AMPs and streptococci. Moreover of those published the majority are focused on the interactions between streptococci and the cathelicidins.

1.4.9i AMPs prevent GAS infections in the skin

Studies conducted *in vitro* and *in vivo* have shown the importance of the cathelicidins in protecting the mammalian host against streptococcal infections. For example an *in vivo* study carried out in a murine model (Dorschner, Pestonjamasp et al. 2001), showed the protective effects of CRAMP, the murine analogue of LL-37. In normal skin the levels of CRAMP were not able to be detected, whereas after wounding and inoculation with

GAS, the expression of this gene was up-regulated and an increase in peptide synthesis was recorded. Indeed it was estimated that the wounds in the mice, resulting from 1cm incisions, contained up to 0.1μg CRAMP (cathelicidin related antimicrobial peptide) per mg total protein (Dorschner, Pestonjamasp et al. 2001). Moreover CRAMP knock-out mice were observed to experience greater necrotising skin lesions than their wild-type siblings when challenged with GAS (Nizet, Ohtake et al. 2001). Recently, the up-regulation of LL-37 in response to GAS has also been documented in human skin (Johansson, Thulin et al. 2008), and a unique murine 28 amino acid cathelicidin peptide, which protects against Gram-positive infection of the mouse skin has been identified in mast cells (Di Nardo, Yamasaki et al. 2008).

As stated previously it has been proposed that multiple cathelicidin genes provide an organism with an increased resistance to infection. This has been shown quite elegantly in studies using transgenic mice (Lee, Ohtake et al. 2005). In these studies transgenic mice, engineered to express either the porcine cathelicidin gene PR-39 or over express the endogenous cathelicidin CRAMP, were challenged with GAS. The mice expressing PR-39 and endogenous CRAMP, showed increased resistance to GAS skin infections when compared to those expressing CRAMP alone. Indeed up to 50% fewer necrotic ulcers and 60% fewer surviving bacteria were observed in the mice synthesising the two different cathelicidins. Whether the added protection was due to direct killing activities of the peptides or to the PR-39 inducing cytokines, chemokines and potentially other AMPs is not however known.

1.4.9ii Interaction with *Streptococcus salivarius*

While the host innate responses function to eliminate potential pathogens there is a paradigm in that some bacterial species evade these systems and actually function as probiotic commensals. *Streptococcus salivarius* is one such organism. It colonises epithelial surfaces in the human mouth and naso-pharynx and is reported to be protective against pathogens such as *S. pyogenes.* It has been proposed recently that *S. salivarius* achieves this by modulating genes associated with adhesion to the epithelial layer and by inhibiting host inflammatory responses through down-regulation of the NFκB pathway. Indeed *S. salivarius* was shown to suppress IL-8 secretion in bronchial

cells stimulated with LL-37 (Cosseau, Devine et al. 2008). This suggests that the organism not only functions directly against pathogens, *S. salivarius* synthesises its own antimicrobial peptides, but protects the host tissues from potential damage caused by immunostimulatory cells and products.

1.4.10 GAS Defence mechanisms

In order to be successful, as *S. pyogenes* obviously is, micro-organisms must evolve mechanisms to protect themselves from host innate defences, including AMPs. The mechanisms employed are numerous and many have been discussed in a number of review articles including one by Peschel, (2002). One common bacterial mechanism employed by bacteria to avoid killing by AMPs is the binding and/or neutralisation of the AMP. Examples of this includes the staphylokinase of *S. aureus* that binds α-defensins (Jin, Bokarewa et al. 2004), and proteases synthesised by many human pathogens which are able to degrade LL-37 (Schmidtchen, Frick et al. 2002), and thus inactivate the peptide before it reaches the bacterial membrane. Bacteria may also undergo cell surface modifications to reduce their charge and hence reduce the electrostatic interactions between the AMPs and the bacterial surface. Indeed the incorporation of D-alanine into the Gram-positive cell wall generates a more positive charged microbial surface (Peschel 2002).

Many streptococcal proteins including GRAB, streptococcal cysteine protease, streptococcal endotoxin B (SpeB), streptococcal inhibitor of complement (SIC) and Distantly related to SIC (DRS) have been identified as factors which protect GAS from the effects of AMPs. Of these SpeB and SIC are particularly protective against LL-37.

1.4.10i SpeB – Cysteine proteinase

S. pyogenes secretes the extracellular cysteine protease SpeB as a 40kDa zymogen that is cleaved to the mature 28kDa active proteinase (Hauser and Schlievert 1990). The proteinase has broad proteolytic activity and cleaves a large number of human proteins including fibrin and fibronectin (Kapur, Topouzis et al. 1993). Proteoglycan is also

degraded by SpeB, which leads to the release of dermatan sulphate, which in turn inactivates α-defensins and LL-37 (Schmidtchen, Frick et al. 2002).

A link between the GAS surface protein GRAB and SpeB in bacterial resistance to AMPs has been proposed following experiments in which different concentrations and combinations of α-2-macroglobulin, SpeB, an Spe inhibitor and LL-37 were added to GAS (Nyberg, Rasmussen et al. 2004). It was shown *in vitro* that SpeB is actually trapped by GRAB and while in this complex SpeB cannot degrade large proteins, the small LL-37 peptides can permeate the complex, where they are degraded. It is assumed therefore that *in vivo* GRAB secures SpeB at the bacterial surface and hence protects GAS from killing by LL-37.

1.4.10ii SIC and DRS

SIC, a 31kDa extracellular protein synthesised by GAS, particularly the M1 and M57 serotypes was so named because it was first identified as a protein that inactivates complement (Akesson, Sjoholm et al. 1996). It is essential for GAS virulence as Δ*sic* mutants were shown not to colonise the mouse throat (Lukomski, Hoe et al. 2000). SIC protein has been shown to inhibit lysozyme and SLPI, (Secretory Leukocyte Protease Inhibitor), two major components of the innate immune system. Indeed binding to the latter protects GAS from killing by SLPI (Fernie-King, Seilly et al. 2004). In addition SIC and a related molecule, DRS, exert their protective effects by also binding to LL-37, and physically inhibiting its action. Binding is in a ratio of one molecule of SIC to two molecules of LL-37 while DRS binds LL-37 in a 1:1 ratio (Fernie-King, Seilly et al. 2006).

1.5 Hypothesis and Aims

Although the human palatine tonsils play important roles in host immunity and provide a barrier against invading pathogens, the Gram-positive bacterium, *S. pyogenes* often penetrates their defences. This results in tonsillitis, in which sufferers present with swollen and painful palatine tonsils. However despite tonsillitis being relatively common, the physiological and immunological factors that allow this infection to perpetuate remain obscure. AMPs, expressed at epithelial and mucosal surfaces, provide a first-line of defence against potential pathogens. Moreover these molecules have also been reported to be up-regulated in response to infection. However the roles of AMPs in the defence of the human palatine tonsils are not well known.

The hypothesis was therefore proposed that a defect in the innate immune response involving host AMPs, such as a deficiency in AMP expression at the epithelial surface and/or a failure of the AMPs to up-regulate in response to infection, is a cause or contributory factor to recurrent acute tonsillitis.

The aims of this study were:

(i) To investigate and compare the AMP gene expression patterns of palatine tonsils excised from patients undergoing tonsillectomy for RAT to those of control subjects whose tonsils were excised for conditions such as snoring or sleep apnoea.

(ii) To identify an immortalised cell line that modelled the tonsil epithelium *in vitro*, to describe its AMP expression profile, and to challenge the cells *in vitro* with *S. pyogenes*, and determine the effects of binding and infection on AMP gene expression.

(iii) To use the *ex vivo* tonsil model, to investigate and compare the effects of *S. pyogenes* challenges on the AMP expression patterns in human tonsils excised from control (non-RAT) subjects and RAT patients.

Chapter 2

Materials and Methods

2.1 Bacterial Strains

2.1.1 *Streptococcus pyogenes* strains

Streptococcus pyogenes M1 and M2 serotypes and mutants thereof were used. These are detailed in Table 2.1

Table 2.1: *Streptococcus pyogenes* wild-type and recombinant strains.

M Serotype	Strain	Source/ Reference
S. pyogenes M1 wild-type	SF370	ATCC 700294/ (Suvorov and Ferretti 1996).
S. pyogenes M1 Δ*spy129* (pilus mutant)	SF370	Engineered from *S. pyogenes* M1 wild-type, (Abbot, Smith et al. 2007).
S. pyogenes M1 Δ*spy1154* (surface protein mutant)	SF370	Engineered from *S. pyogenes* M1 wild-type, (Abbot, Smith et al. 2007).
S. pyogenes M2 wild-type	*Ncl75245*	Clinical Isolate, Newcastle upon Tyne.

The wild-type and recombinant strains where appropriate were transfected with the pCM18 plasmid expressing green fluorescent protein (GFP) as described in Section 2.2.4. Transfections were performed by Dr Wendy D. Smith (ICaMB).

2.1.1i Culture and maintenance of *Streptococcus pyogenes* strains

Streptococcus pyogenes were grown without shaking in either Todd-Hewitt Broth (THB, Difco) supplemented with 0.5% (w/v) Bacto-yeast extract (Difco), or on blood agar plates (Todd-Hewitt Yeast Broth (THYB) with 1.5% (w/v) Bacto-agar (Difco)), at 37°C and 5% CO_2. Where selection for plasmids was required,

erythromycin dissolved in 100% ethanol was added to a final concentration of 1.0μg/ml. Glycerol stocks of *S. pyogenes* were produced by adding one bacterial colony to 5ml THYB, culturing the bacteria overnight at 37°C in a static incubator in the presence of 5% CO_2, and then adding sterile glycerol to 1ml of the culture to give a final concentration of 20% (v/v). Glycerol stocks were stored at -80°C.

2.1.2 *Escherichia coli*

JM109 competent cells were purchased as part of the p-GEM-T Easy Vector System kit (Promega). Genotype: *end*A1, *rec*A1, *gyr*A96, *thi, hsd*R17 (r_k^-, m_k^+), *rel*A1, *sup*E44, Δ(*lac-pro*AB), [F′ *tra*D36, *pro*AB, *laq*I^qZΔM15]. *E. coli* were cultured as described in 2.7.5.

2.2 Human Tonsils

2.2.1 Ethical approval

The Local and Regional Ethics Committee (LREC), Newcastle upon Tyne was consulted prior to the study and ethical approval was granted to allow collection of human tonsil tissue. The information sheets and consent forms distributed to potential volunteers (Appendix A and Appendix B respectively), were designed to comply with current Central Office for Ethics Committees (COREC) regulations. Patients were informed of the study at their pre-admissions appointment, which provided a 'cooling off period' to allow them time to decide whether or not they wished to take part in the study.

2.2.2 Tonsil collection and processing

Human tonsils were collected from patients undergoing tonsillectomy at the Freeman Hospital, Newcastle upon Tyne. Before excision patients were asked to complete a short questionnaire detailing their gender, age and last sore throat (Appendix C). Tonsils were excised for conditions including recurrent acute tonsillitis (RAT), obstructive sleep apnoea, enlarged tonsils and tonsillar crypts, and snoring. In most cases both tonsils were obtained from the patient. Tissues from patients with exceptionally scarred tonsils or those which had undergone trauma during surgery, and in which the epithelia could not be differentiated from the lymphoid interior, were not used. Scarred tonsils from which epithelium and lymphoid tissues could be differentiated were used as many of the tonsils from RAT sufferers had this appearance.

Tonsils collected for RNA extraction were dissected immediately after excision. Whole tonsil dissection involved the intact epithelial surface being separated from the lymphoid interior of the tonsils and samples of both being taken. The samples were either snap frozen in liquid nitrogen or preserved in RNA Later (Ambion). For

the *ex vivo* challenge experiments the tonsils were transported to the laboratory in sterile polypropylene tubes.

2.2.3 Tonsil: *ex vivo* model

Within an hour of excision intact tonsil epithelium was dissected from the whole tonsils and divided into segments approximately 3mm x 3mm in size. Each segment was placed apical side up in a 12mm diameter well (Corning), and incubated at 37°C and 5% CO_2 for three hours in RPMI-1640 (Sigma) culture medium supplemented with 2% (v/v) non-essential amino acids (NEAA, Sigma) and 200ng/ml gentamycin (Sigma), the latter to kill surface bacteria from the pharyngeal cavity. After washing three times in phosphate buffered saline (PBS) the samples were transferred to the upper chamber of a Transwell (0.4μM pore size, CoStar) containing antibiotic free culture medium in the lower chamber. Tissue samples were submerged in either 200μl of culture medium (control) or culture medium containing appropriate challenge reagents (test) before incubation for a pre-determined time period. For investigations involving a bacterial challenge, binding controls, described in Section 2.2.5 were included. Following incubation the tissue samples were washed three times in PBS and analysed as appropriate.

2.2.4 *Streptococcus pyogenes* bacterial challenge experiments

Streptococcus pyogenes contained pCM18, a low copy number plasmid which is 8.2 kb in size including a 1.8kb cloned *gfp*mut3* gene from a constitutive lactococcal promoter CP25 which it expressed (Hansen, Palmer et al. 2001). The plasmid also includes an erythromycin resistance gene. *S. pyogenes* was grown to an optical density$_{600}$ (OD_{600}) of 0.5 (10^8 cfu/ml; (Abbot, Smith et al. 2007), washed three times in distilled water and re-suspended in the antibiotic free RPMI-1640 culture medium. An aliquot of the bacterial suspension (200μl) was added directly to each tissue (equivalent to a multiplicity of infection of approximately 200:1; (Abbot, Smith et al. 2007) and the tissues incubated at 37°C and 5% CO_2 for pre-determined time periods.

Following the bacterial challenge weakly adhering bacteria were removed by washing three times with PBS, and the tissues fixed as described in Section 2.2.5 (binding controls) or the RNA extracted as described in Sections 2.5.1 or 2.5.2 for use in the gene expression analyses.

2.2.5 Binding controls

To check for the binding of the streptococci during the tonsil infections binding controls were employed. For such controls tissue samples were challenged as above with bacteria, but after the appropriate incubation periods the samples were fixed in 100% (v/v) ice-cold methanol for 15min, blocked at room temperature for 30min in 3% (v/v) goat serum (Sigma) and stained with a murine anti-cytokeratin-14 monoclonal antibody (Sigma) diluted 1:200 in PBS with 3% (v/v) goat serum for 1h at room temperature. After washing in PBS the tonsil samples were incubated with goat anti-mouse Alexa-fluor 568, diluted 1:100 in PBS with 3% (v/v) goat serum, for 1h at room temperature. Tissue samples were again washed in PBS before being mounted and imaged by confocal laser scanning microscopy (TCS-NT Leica with Kr-Ar laser). Using appropriate excitation and emission filter sets, Z-series images were collected.

2.2.6 Immunohistochemical analysis of tonsil

Frozen human tonsil sections were fixed in 2% Paraformaldehyde (PFA, Sigma) in PBS for 30min on ice. After PFA fixation tonsil sections were permeablised with 0.1% Triton X-100 for 30min at room temperature. All tissue sections were blocked in 10% goat serum in PBS (Sigma) for 1h on ice before incubation with anti-human LEAP-2 purified IgG (1:100 in PBS) over night at 4°C. The sections were then incubated with goat anti-rabbit antibody-FITC (Chemicon), 1 : 50 in PBS for 3h before being mounted on slides with Vectashield. LEAP-2 expression was shown in bright green after visualisation with a confocal laser scanning microscope. Control sections were performed alongside test sections; these were prepared without primary antibody.

2.3 HaCaT cells

2.3.1 Origin

The HaCaT cells are an immortalised keratinocyte cell line, originally derived from human skin (Boukamp, Petrussevska et al. 1988) and were obtained from Dr Carol Todd (Dermatological Sciences, Newcastle University).

2.3.2 Tissue culture

To establish the HaCaTs from frozen a vial of cells (10^6/ml) was thawed gently at 37°C in a water bath before being added to a 25cm^3 flask (Corning) containing 10ml of cell culture medium (Dulbecco's Modified Eagle's Medium (Sigma) including glucose 4.5g/l and L-glutamine 584mg/ml supplemented with sodium pyruvate 110µg/ml (Sigma), 10% (v/v) FCS (Sigma) and 1% (v/v) penicillin/streptomycin (Sigma 100u/µl penicillin/100µg/ml streptomycin in 0.9% sodium chloride)).

To passage the HaCaT cells, the culture medium was decanted off, the cells washed in PBS and 5ml Trypsin-EDTA (Sigma) was added to the cells. After approximately 10min at 37°C and 5% CO_2 the detached cells were resuspended in 25ml of fresh medium, dispersed by passing through a large gauge needle, and cell numbers determined using a cell counter (Coulter). For maintenance of the cell line the HaCaT cells were split at a ratio of 1:10 and cells were passaged every seven days.

2.3.3 HaCaT: cell challenge assays

The cultured HaCaT cells were subjected to either bacterial and/or environmental challenges. For such experiments the cells were counted, seeded into 12 well plates (12mm diameter), at a density of 10^6 cells per well and cultured in 1ml growth medium at 37°C and 5% CO_2 until confluent. Prior to challenge, the HaCaT cells were incubated for 3h at 37°C and 5% CO_2 in cell culture medium lacking FCS and antibiotics. This medium was removed and replaced by either 1ml control medium or

medium containing the appropriate challenge (bacterial and/or environmental) reagents. These reagents were Lipoteichoic acid (LTA, from *S. pyogenes*, Sigma, final concentration 2μg/ml), Lipopolysaccharide (LPS, Sigma, final concentration 0.2μg/ml), Phorbol 12-myristate 13-acetate (PMA, Sigma, final concentration 20μM) and 1,25 dihydroxyvitamin-D3 (D3, Fluka, final concentration 200nM). After a pre-determined incubation period the medium was removed, the cells washed three times with PBS and RNA extracted from the cells as described in Section 2.5.2.

2.3.4 HaCaT cells: bacterial challenge

For the bacterial challenge of HaCaT cells *S. pyogenes* was grown to an OD_{600} of 0.5 (10^8 cfu/ml) and prepared as described in Section 2.2.4. 1.5ml of bacterial suspension was added per well; cells and bacteria were incubated at 37°C with 5% CO_2 for an appropriate pre-determined incubation period.

2.3.5 HaCaT cell binding controls

To check for the binding of the streptococci to HaCaT cells binding controls were performed. For such controls the HaCaT cells were seeded and cultured to confluence on pre-sterilised (ethanol) 10mm coverslips (VWR) placed in the wells of a 12 well plate. Following bacterial challenge the HaCaT cells were fixed in 2% paraformaldehyde for 15min on ice, washed three times with PBS, permeabilised with 0.1% Triton-X100 (Sigma) at room temperature and incubated with Phalloidin-Rhodamine (Sigma), a stain of filamentous actin, diluted 1:200 in PBS for 1h at room temperature before mounting and imaging as described in Section 2.2.5.

2.4 HEp-2 Cells

2.4.1 Origin

The HEp-2 (Human Epithelial Cell line 2) immortalised cell line was purchased from ATCC (CCL-23). This cell line was derived originally from an epidermoid carcinoma of the larynx but has since been found to have been contaminated with HeLa cells derived from a cervical cancer cell line (www.lgcpromochem-atcc.com).

2.4.2 Tissue culture

HEp-2 cell monolayers were established from frozen using the same procedures as described for HaCaT cells (Section 2.3.2) and maintained in cell culture medium containing Dulbecco's Modified Eagle's Medium, supplemented with 2mM L-glutamine, 10% (v/v) FCS, 2% (v/v) NEAA and 1% (v/v) penicillin/streptomycin (Sigma 100u/µl penicillin/100µg/ml streptomycin in 0.9% sodium chloride).

HEp-2 cells were maintained routinely in 175cm^3 flasks. To passage the cells, the culture medium was decanted off, the cells washed in PBS and 5ml Trypsin-EDTA (Sigma) added. After approximately 10min at 37°C and 5% CO_2 the detached cells were transferred to a 30ml universal, dispersed by passing through a large gauge needle, centrifuged at 5,000g for 3min at room temperature, resuspended in 10ml of medium and cell numbers determined using a cell counter (Coulter). For maintenance of the cell line 2x10^6 HEp-2 cells were seeded per 175cm^3 flask with the addition of 30ml cell growth medium. Cells were passaged every seven days.

2.4.3 Immunocytochemical staining of HEp-2 cells

For immunocytochemical staining 10^5 cells were seeded onto 10mm sterile coverslips positioned in each well of a 24 well plate (Corning). 1ml of HEp-2

culture medium was added per well and cells were cultured at 37°C and 5% CO_2. Once confluent the cells were washed three times in PBS, fixed and permeabilised as described in Section 2.3.5. The cells were incubated with Phalloidin (Sigma) diluted 1:4 for 1h at 4°C before washing three times with PBS. The coverslips were removed from the wells mounted on slides (VWR) with Vectashield and visualised at x100 magnification using a confocal microscope and TRITC filters as described in Section 2.2.5.

2.5 RNA Extraction

2.5.1 RNA extraction from tonsil

Extraction of RNA from human tonsil was performed using a 'Pure Link Micro-to-Midi Total RNA Purification System' (Invitrogen). Essentially, the tissue samples were weighed and the appropriate amount of lysis solution, supplied with the kit and containing guanidinium isothiocyanate (GTC) and 1% (v/v) 2-mercaptoethanol, required for the extraction was calculated according to the manufacturer's instructions (Table 2.2).

Table 2.2: Determining volume of RNA lysis solution required per sample

Amount of tissue (mg)	RNA lysis solution (ml)
≤10	0.5
10-60	0.6
60-100	1.2
100-200	2.4

(Table adapted from Invitrogen Pure Link Micro-Midi RNA Purification System manual p12)

Fresh tonsil tissue or tissue preserved in 'RNA Later' (Ambion) was dissected into small pieces; frozen tissue was crushed to a fine powder using a pestle and mortar. The tissue was added to a pre-cooled polypropylene tube containing the appropriate amount of lysis solution and homogenised on medium setting for approximately 45s until a smooth suspension was observed. Homogenisation was performed using a rotor-stator style homogeniser, a TissueRupter (Qiagen), with disposable probes. Between samples the rotor-stator probe was rinsed in 100% ethanol and PBS to prevent cross contamination of the samples. Following homogenisation, the tissue samples were centrifuged at 2600g for 5min and room temperature, to remove any remaining cellular debris. The supernatants containing the nucleic acids were transferred to sterile 15ml polypropylene tubes and one volume 100% ethanol was added to each. Any precipitate formed was dispersed by vortexing and each sample was added in 700µl aliquots to a fresh spin cartridge. After centrifugation at 12,000g for 15s a series of wash steps were performed using wash buffers I and II from the kit

(constituents not provided by manufacturer), which removed any impurities from the RNA preparations. The RNA was finally eluted in 2 x 30µl volumes of nuclease-free water and stored at -80°C.

2.5.2 RNA extraction from cultured cells

To isolate RNA from HaCaT cells and HEp-2 cells the SV Total RNA Isolation System (Promega) was used. As recommended by the manufacturer, 175µl of lysis solution (4M guanidinium isothiocyanate, 0.01M Tris, 0.97% β-mercaptoethanol) was added directly to cells cultured in a 12mm diameter well. A sterile pipette tip was used to scrape the cells from the plastic and the cells were sheared by passing through a 20-gauge needle. Following centrifugation of the cell lysate at 12000g for 10min, the supernatant was collected and the nucleic acid precipitated by the addition of 250µl of 95% ethanol. For purification of the RNA the nucleic acid was bound to silica contained within a column provided with the kit, washed to remove proteins with buffer containing 60mM potassium acetate, 10mM Tris-HCl and 60% ethanol (using a vacuum manifold fitted with spin column adapters (Promega)), DNase 1 treated as recommended by the manufacturer and the RNA eluted in 100µl of nuclease-free water. The purified RNA was stored at -80°C.

2.5.3 Analyses of RNA concentration and purity

The concentrations of RNA extracted from the tissue samples and cells were determined spectrophotometrically. Essentially, RNA samples were diluted 1:10 or 1:100 in nuclease-free water and the absorption of RNA measured at 260nm. The conversion factor 40µg/ml per 1 unit OD_{260nm} was used to calculate RNA concentration. For initial calibration of the spectrophotometer nuclease-free water was used. Absorbance was also measured at 280nm and 230nm to check for contamination of the sample with protein (A_{260}/A_{280}) and guanidine isothiocyanate (A_{260}/A_{230}). In both cases ratios of 1.8-2.2 indicated that the sample was within an acceptable purity range and was free from protein and /or chemical contamination.

2.5.4 RNA integrity: denaturing RNA gel electrophoresis

The RNA quality of the samples was also investigated by gel electrophoresis. This provided separation and visualisation of the 18S and 28S ribosomal RNA (rRNA) subunits and allowed an assessment of the integrity of the nucleic acid.

For such analyses, a 1% (w/v) denaturing RNA gel was used. This was prepared by gently dissolving molecular biology grade agarose (Sigma) in a solution of 86% (v/v) distilled water, 5% (v/v) 20x MOPS buffer (400mM MOPS (Sigma), 100mM sodium acetate (NaAc, BDH), 20mM EDTA (Sigma)) and 7.5% (v/v) formaldehyde (BDH). The molten gel was poured into a gel casting tray in a fume hood, left to set and then positioned in a gel electrophoresis tank. 1μg of each RNA sample diluted in nuclease-free water to a volume of 10μl was incubated for 5min at 45°C with 14μl formamide (Sigma). To each sample formaldehyde (38% concentrated), MOPS buffer, ethidium bromide and bromophenol blue loading dye (Sigma) was added in the ratio 4.3:1.4:1:4 to give a final total sample volume of 20.7μl. The samples were incubated for 5min at 65°C and loaded onto the denaturing RNA gel submerged in a 1x MOPS running buffer containing 75ml formaldehyde per litre. Electrophoresis was performed at 110V for 90min. The molecular weight markers were RNA Millenium Markers (Ambion). For good quality RNA both the 28S and 18S rRNA bands were visible and the 28S rRNA band was twice as bright as the 18S rRNA band.

2.6 Reverse Transcription - Polymerase Chain Reaction (RT-PCR)

2.6.1 DNase treatment of RNA

To eliminate any genomic DNA contamination of the RNA samples DNAse treatments were performed. The HaCaT RNA, as described in Section 2.5.2, was DNAse treated on the column as part of the RNA extraction process. All human tonsil RNA samples were subjected to DNAse treatment using a DNase treatment kit (Promega), containing DNAse (1u/µl).

For DNAse treatment, 3.5µg RNA was diluted with nuclease-free water to a final volume of 24.5µl. DNAse prepared in reaction buffer (400mM Tris-HCl, 100mM $MgSO_4$ and 10mM $CaCl_2$) was added at 1u per µg RNA and the solution incubated for 30min at 37°C. The DNAse treatment was halted by the addition of stop solution (200mM EGTA, $1/10^{th}$ of the final reaction volume) and heat inactivated for 10min at 65°C.

2.6.2 Reverse transcription (RT)

Total RNA was reverse transcribed into complementary or copy DNA (cDNA) for use in end-point and real-time PCR analyses. For such reactions 1µg of total RNA was resuspended in 25.5µl nuclease-free water, 1µl of random hexamers (stock 0.5mg/ml: GE Healthcare UK Ltd), was added and the solution incubated at 65°C for 5min before being rapidly cooled on ice. This denatured any secondary structure and allowed the hexamers to anneal to the single-stranded RNA. Following the incubation step, 12.5µl of 5x reaction buffer (stock 50mM Tris-HCl, 75mM KCl, 3mM $MgCl_2$ and 10mM DTT), 10µl of dNTPs (stock 2mM), 0.1µl Human Placental RNAse inhibitor (stock RNasin (40u/µl), Promega) and 1µl of M-MLV RNaseH reverse transcriptase (stock 200u/µl) (Promega) were added. This was mixed and the solution incubated for 2h at 42°C in a Thermo Px2 thermal cycler followed by a

final 70°C step to inactivate the enzyme prior to polymerase chain reaction. Sample incubations included no template and no reverse transcriptase enzyme controls.

2.6.3 End-point polymerase chain reaction

Polymerase chain reaction (PCR) was used to replicate cDNA exponentially by an enzymatic reaction using DNA polymerase. The DNA polymerase used was *Taq* polymerase, a "hot start" enzyme requiring an initial period of high temperature for activation. Typical PCR reactions were set-up as shown in Table 2.3 in a final volume of 25µl.

Table 2.3: A typical end-point PCR reaction

Reagent	Amount Added
Template cDNA	2µl
Nuclease-free water	To a final volume of 25µl
Reaction buffer (200mM Tris-HCL, 500mM KCl),	2.5µl
dNTP (Invitrogen) (dATP, dGTP, dTTP, dCTP each at 2mM)	2.5 µl
$MgCl^{2+}$ (50µM)	1µl
Target specific primers (10µM) (Forward and Reverse)	0.5 µl of each
Platinum *Taq* DNA Polymerase (Invitrogen) 5u/µl	0.25µl

Each PCR was performed in a Thermo Px2 thermal cycler as follows:

1 cycle at 95°C for 15min to activate the *Taq* DNA polymerase
40 cycles of :
95°C for 30s, 55 or 58°C (dependent on gene of interest) for 30s, 72°C for 45s
Followed by 1 cycle of 72°C for 10min and a holding stage at 4°C.

No template controls, with nuclease-free water as a substitute for cDNA, were performed with each PCR reaction to ensure the specificity of PCR product.

2.6.4 Agarose gel electrophoresis

cDNA products from end-point PCR were separated based on their size and visualised on an agarose electrophoresis gel (1.2%). An agarose gel was prepared by melting the appropriate amount of electrophoresis grade agarose (1.2g of agarose in a 100ml gel) in 1x TBE buffer (54g Tris, 27.5g Boric Acid, 20ml 0.5M EDTA per litre) containing a final concentration of $2.5x10^{-3}$µg/ml ethidium bromide. This was allowed to set in a gel-casting tray of the appropriate size, transferred to a gel tank (Thistle Scientific Ltd) and submerged in x1 TBE electrophoresis buffer. The samples containing loading dye (0.25% bromophenol blue / 50% glycerol) added in a 1:5 dye to sample ratio were loaded into the wells of the gel and electrophoresed at 110V for 90min. Visualisation of the DNA was performed using a UV transilluminator (302nm, AlphaImager 1200 gel documentation and analysis system, Flowgen). Various DNA ladders including a 100 base pair (bp) DNA ladder and a 1Kb DNA ladder (All from NEB) were used as appropriate.

2.6.5 Densitometry

Densitometry was performed using software provided as part of the AlphaImager 1200 gel documentation system.

2.7 DNA Cloning

2.7.1 DNA extraction

To extract DNA from agarose gels for further analyses including DNA cloning, the gels were first visualised under UV light and the required DNA bands excised using a scalpel blade. The bands were weighed and the DNA recovered using a GenElute Gel Extraction kit (Sigma).

For this procedure a volume of gel solubilisation solution was added to each sample according to the weight of the agarose gel (3µl/mg). This was incubated at 50-60°C for 10min with regular vortexing to dissolve the gel slice, and then 100% isopropanol (1µl/ml) was added. During this period, a spin column was inserted into a collection tube and primed by the addition of 500µl of column preparation solution followed by centrifugation at 13000g for 1min. The flow-through was discarded from the collection tube and the solution containing the melted agarose gel was passed through the column in 700µl aliquots to allow the DNA to bind to the membrane. Sample impurities were removed by treating the column with an ethanol-based wash solution and the purified DNA was eluted from the column in 50µl of 10mM Tris-HCl.

2.7.2 PCR product clean-up and purification

PCR products contain impurities such as primers and unincorporated dNTPs that have been carried over from the amplification reaction. Purification of these products was undertaken by either gel purification, as described in Section 2.7.1, or by using an Amicon Microcon-PCR Centrifugal Filter Device (Millipore). This device was used according to manufacturer's instructions.

Essentially, the PCR product to be purified was diluted to a final volume of 500µl with nuclease-free water and forced through a 'clean-up' filtration column by centrifugation in a microfuge at 1500g for 10min. 20µl of nuclease-free water was

then added to the column, which was inverted, placed into a second collection tube and subjected to a second centrifugation at 1500g for 2min. The eluate containing the concentrated, purified PCR product was collected.

2.7.3 DNA cloning in pGEM-T-Easy Vector System

Recombinant DNA clones were engineered by ligation of the appropriate PCR products into the pGEM-T-Easy vector.

2.7.4 DNA ligation

Initially, a PCR reaction was performed as described in Section 2.6.3. A characteristic of the *Taq* polymerase enzyme is that following amplification adenosine triphosphate residues are added to the 3' ends of the double-stranded PCR product. This property can be exploited by cloning the product into a linearised vector, such as the pGEM-T Easy vector, with complementary 3' T overhangs. The amount of insert required per reaction was determined using the equation:

$$\text{ng of insert to be used} = \frac{\text{ng of vector x Kb size of insert}}{\text{Kb size of the vector}} \text{ x insert to vector molar ratio (3:1)}$$

For cloning ligation reactions were set-up as follows in a final volume of 10µl:
3µl PCR product (purified by column or gel)
5µl 1x rapid ligation buffer (Promega)
1µl pGEM-T Easy Vector (50ng/µl)
1µl T4 DNA ligase (Promega) (3u/µl)

Positive control inserts were provided with the kit and for negative controls the PCR product was replaced with 3µl nuclease-free water. Ligations were performed overnight at 4°C to yield the maximum number of transformants.

2.7.5 Transformation and plasmid selection

To produce recombinant clones the ligated DNA was transformed into JM109 competent cells. These high efficiency competent cells were provided with the pGEM-T Easy system.

Essentially, 50µl of competent cells were added to 2µl of the ligation reaction and incubated on ice for 20min. This was 'shocked' at 42°C for 45-50s and 950µl of SOC medium (2% (w/v) Bacto-tryptone (BD Biosciences), 0.5% (w/v) Bacto-yeast extract (BD Biosciences), 1% (v/v) 1M NaCl (Sigma), 0.25% (v/v) 1M KCl (Sigma), 1% (v/v) $MgCl_2$ (filter sterilised, Sigma), 1% (v/v) 2M glucose (filter sterilised, Sigma)), was added and the culture incubated for 1.5h at 37°C in a shaking incubator. The culture was plated on Luria-Bertani (LB, 10% (w/v) Bacto-tryptone, 5% (w/v) Bacto-yeast extract, 5% NaCl (Sigma) in nuclease-free water) agar plates containing a final concentration of 100 µg/ml ampicillin and spread with 40µl Isopropyl β-D-1-thiogalactopyranoside (IPTG, stock: 24mg/ml) and 40µl 5-Bromo-3-indolyl-β-D-Galactopyranoside (Stock: 25mg/ml in dimethylformamide, Sigma) and grown overnight at 37°C. Blue-white selection was used to indicate which transformants had incorporated the pGEM-T Easy vector. Bacteria containing vectors and insert were white colonies and bacteria containing only the vector were blue.

Propagation of the bacteria with the insert was achieved by selecting white colonies and culturing each for approximately 12-16 hours in 5ml LB broth containing 100 µg/ml ampicillin (Sigma) in a shaking incubator at 37°C.

2.7.6 Plasmid preparation

For plasmid preparation a Wizard Plus SV Miniprep DNA Purification System (Promega) was used.

Essentially, cells were pelleted from the 5ml culture by centrifugation at 10,000g for 5min. The pellet was resuspended in 250µl cell resuspension solution (50mM Tris-

HCl, 10mM EDTA, 100μg/ml RNase A) by vortexing, the cells lysed with 250μl cell lysis solution (0.2M NaOH, 1% SDS) and 10μl of an alkaline protease solution added to digest unwanted proteins from the bacterial cells. This was followed by 350μl of a neutralisation solution (4.09M guanidine hydrochloride, 0.759M potassium acetate, 2.12M glacial acetic acid). The cellular suspension was centrifuged at 13,000g for 10min to separate unwanted bacterial chromosomal DNA from the plasmid DNA. Plasmid DNA was isolated and purified using a spin column; essentially 750μl of column wash solution (60% ethanol, 60mM potassium acetate, 8.3mM Tris-HCl, 0.04mM EDTA) was forced through the column by centrifugation at 13,000g for 1min, this was repeated using 250μl of column wash solution before a 2min spin at 13,000g to dry the column. The plasmid DNA was eluted in 100μl of nuclease-free water.

2.7.7 DNA restriction enzyme analyses

Restriction enzyme digests were used to excise and identify potential inserts in the recombinant plasmids. The restriction enzyme used was EcoR1.
For restriction analysis reactions were set-up as follows in a final volume of 20μl:

8μl of plasmid DNA (250ng/μl)
2μl 10x reaction buffer 'H' (provided with enzyme)
0.8μl BSA (Bovine Serum Albumin) (provided with enzyme 10mg/ml)
1μl EcoR1 (Promega, 12u/μl)

The reaction was incubated for 1-3h at 37°C before electrophoresis on a 1.2% agarose gel. DNA samples that were seen to contain an insert of the correct size were sequenced to confirm identity as described in Section 2.7.8.

2.7.8 DNA sequencing

DNA sequencing of the recombinant clones was performed at the Pinnacle Laboratory based in Newcastle University using M13 forward (5'-tgtaaaacgaccggccagt-3') and reverse primers (5'-caggaaacagctatgacc-3') using an Applied Biosystems Sequencer. Sequences returned were compared to GENBANK sequences and identified using BLAST (Basic Local Alignment Search Tool) available on the NCBI (National Centre for Biotechnology Information) website (http://www.ncbi.nlm.nih.gov/).

2.8 Real-Time PCR

Real-time PCR methods were developed to quantify the expression of genes encoding LL-37, HBD1, HBD2 and LEAP-2. The development and optimisation of these methods is described in detail in Chapter 3 and the final method for each assay can be found in Table 3.15 (LL-37 assay), Table 3.25 (HBD1 assay), Table 3.30 (HBD2 assay), Table 3.36 (LEAP-2 assay) and Table 3.40 (GAPDH assay).

2.9 Statistical Analyses

Analyses were performed using Graph Pad Prism 4. T-tests and ANOVA statistical tests were performed and suitable post-tests applied when appropriate. Dunnett's post-tests were applied when treatments compared to control were being considered. Bonferroni post-tests were used when more than one group of data were being compared. For the patient studies Dr Tom Chadwick (School of Population and Health Sciences, Newcastle University) advised on the power calculations and samples size; these are described further in Chapter 4.

Chapter 3

Optimisation and Development of Quantitative Real-Time PCR Assays for the Antimicrobial Peptides LL-37, HBD1, HBD2, HBD3, Hepcidin and LEAP-2 and the Housekeeping Gene GAPDH

3.1 Introduction

In previous studies semi-quantitative end-point PCR assays were developed and used to investigate the expression of the AMPs LL-37, HBD1, HBD2, HBD3, hepcidin and LEAP-2 in human palatine tonsil and HEp-2 cells (Ball, Siou et al. 2007). These assays have limited sensitivity, are time consuming and expensive and thus not suited to the larger scale study of AMP gene regulation required for the current work. This chapter describes the development of assays to quantify these AMPs using a more sensitive technique with a large dynamic range: real-time PCR. Optimisation of RNA extraction from cells and human palatine tonsils and reverse transcription of the RNA to cDNA is also described. In subsequent chapters the assays are used to compare expression of AMPs in the cDNA samples extracted from human tonsil samples and the immortalised keratinocyte cell line, HaCaT following manipulation or challenge.

3.1.1 Real-time PCR

Real-time PCR uses fluorescent reporter molecules to quantify the amount of product generated throughout the reaction. The fluorescence generated is proportional to the quantity of the specific mRNA, determined by the choice of oligonucleotide primers, in the starting sample. Fluorescence is detected and measured by a fluorimeter incorporated into the thermal cycler; a measurement is taken in each cycle of amplification and the data obtained manipulated through the relevant software to allow determination of mRNA quantity. This requires determination of the background level of fluorescence, a threshold level of fluorescence and cycle number, known as the crossing point (Cp), for each sample at which its fluorescence surpasses the threshold. In the case of the Roche LightCycler 1.2 or 480, the two real-time PCR instruments used in this study, background fluorescence is determined for each sample during the early cycles of PCR when fluorescence from reaction products is negligible. The software provided with the instrument uses this in an algorithm to determine the respective threshold value and reports the Cp for each sample. Additionally if concentration standards are included in the assay, the concentration of the specific mRNA in the starting sample is also reported.

The Cp of a particular sample can be used to determine the efficiency of a PCR and also gives an indication of the relative expression level of a particular mRNA in a sample. An efficient, exponential PCR reaction is defined by a one cycle increase in Cp when template concentration is reduced by 50%. A high Cp indicates either a low level of gene expression or inefficient amplification. When optimising an assay, a reduction in Cp of a specific sample is taken to indicate an increase in the efficiency of the PCR and therefore to result from a beneficial alteration.

3.2 Assay development: an overview

The main stages of assay development are outlined in Figure 3.1.

3.2.1 Template preparation

RNA extracted from tissues or cultured cell lines was reverse transcribed into cDNA for PCR. The quality of the template added to the PCR reaction can affect the quantification of the gene of interest, therefore optimisation of the RNA extraction and the reverse transcription (RT) method was undertaken. An important aspect in the selection of RT reagents is the carry over of factors into the PCR which can result in inhibition of the DNA polymerase. One example is dithiothreitol (DTT), used as a stabilising reagent in the buffer. Products of RT were required to be used directly in the PCR reactions without any purification, so it was necessary to determine if this was the case and also to investigate the effect of dilution of RT products on PCR efficiency; dilution of the cDNA can dilute out such impurities, reducing their effect and resulting in increased PCR efficiency. Therefore a dilution series of RT products was tested in each PCR.

3.2.2 Selection of detection format

The selection of detection format depends on many factors such as PCR instrumentation, template concentration, level of expression of the gene of interest and specific assay design

choices, for example, multiplexing. Both specific (oligonucleotide probe based detection) and non-specific (intercalating DNA dyes) detection formats are available for use. The suitability of these for each AMP assay was assessed in this investigation and the preferable set of conditions chosen.

3.2.2i Non-specific detection formats

These are methods based on the use of intercalating dyes such as Sybr-green 1 that bind to double-stranded nucleic acids and on excitation with a laser, fluoresce. The proportion of double-stranded product in a PCR reaction is directly proportional to fluorescence.

Non-specific detection formats have been used longer than other methods; which is advantageous as procedures for assay development are readily available. These detection formats may also be more sensitive than probes as multiple reporter molecules are intercalated per product, and therefore generate higher fluorescence levels. However, the non-specific nature of the intercalating dyes can be problematic as any double-stranded nucleic acids, including primer-dimer, PCR artefacts or misprimed products will be detected and may affect quantification of the target gene. To overcome this, melting temperature analysis of the PCR products is performed. Different products or artefacts melt at different temperatures and are detected as changes in fluorescence, plotted as either a melt curve (fluorescence vs. temperature) or the rate of change of fluorescence (first derivative) vs. temperature (commonly called melt peaks). Melt curve analysis was performed for all assays using Sybr-green in this work. Only data showing a single major peak, i.e. representative of the single correct product, was used in analysis.

3.2.2ii Specific detection formats

Specific detection formats usually involve primers and an oligonucleotide probe which hybridises to a specific complementary sequence within the amplicon giving a second level of specificity to the assay. The use of multiple probes each labelled with a different

fluorophore also gives the ability to quantify more than one gene in a sample, known as multiplexing. Specific detection formats are usually based on fluorescence resonance energy transfer (FRET) or donor and quencher based mechanisms such as the Universal Probe Library (UPL, Roche) assays which were attempted here. In these assays, design software provided by Roche is used to determine the primer and probe combinations required for each gene (http://www.exiqon.com/uploads/Universal_ProbeLibrary.pdf).

In contrast, LUX or Light Upon Extension assays, use labelled primers (Kusser 2006). Each gene specific primer pair has one labelled primer holding a quenched fluorophore within a hairpin conformation and one unlabelled primer. Fluorescence is generated when the labelled primer anneals to a complementary sequence releasing the fluorophore from the hairpin structure surrounding it. When the primer is extended the fluorophore is unquenched and emits fluorescence of a specific wavelength. LUX assays require only a single fluorescent label per assay thus are generally cheaper than probe based methods and retain the simplicity of design of Sybr-green type assays. As with probe based detection methods, they also allow multiplex reactions to be performed. For multiplexing, each set of primers is labelled with a different fluorophore, emitting fluorescence at discrete wavelengths. Compared to Sybr-green type assays, the LUX system is also advantageous as only double-stranded cDNA structures containing the labelled primer are detected and quantified. However, primer-dimer and mis-primed products containing the labelled primer would also fluoresce; therefore melt curve analysis was used in all LUX assays.

3.2.3 Primer design and confirmation of specificity

Primers were designed following general PCR requirements, i.e. approximately 20-25 bases long with 50-60% GC content and no obvious secondary structure or GC runs at the 3' terminus, with some further specialisation for real-time PCR. As PCR works more efficiently with shorter products, primers were designed to generate products of between 100-200bp, to minimise the effect of any genomic DNA contamination of samples, primers were designed either to cross exon-exon boundaries or with the hybridisation sites for each primer in a pair located on separate exons.

To confirm the specificity of the primers and determine that they amplified the required region of the target gene, PCR products were purified by agarose gel electrophoresis (Section 2.6.4) and characterised either by direct sequencing (Section 2.7.8); cloning in pGem-T-easy and sequencing of multiple clones (Section 2.7) or determination of the melting temperature of the PCR product (Section 3.2.2i).

3.2.4 Optimisation of PCR conditions

After an initial trial of a basic PCR reaction with each gene, optimisation of PCR conditions such as cycle number, incubation times and temperatures, primer and magnesium chloride concentration, and annealing temperature was performed to improve the reaction.

3.2.5 Standard curve formation

The usual methods of cDNA quantification by real-time PCR are either use of a standard concentration curve or PCR based efficiency calculations (Gentle, Anastasopoulos et al. 2001; Livak and Schmittgen 2001; Pfaffl 2001; Liu and Saint 2002; Muller, Janovjak et al. 2002; Peirson, Butler et al. 2003; Huggett, Dheda et al. 2005; Larionov, Krause et al. 2005). Most commonly the PCR efficiency method is used. However, the use of standard curves has some advantages, including simplicity and reliability, when compared to efficiency calculations. Inclusion of a standard curve in each PCR also allows the assay to be validated each time it is run (Larionov, Krause et al. 2005). This method was chosen for the current study. Standard curves were obtained by serial dilutions of a concentrated stock of the PCR target, in most cases a 'miniprep' of the cloned PCR product or cDNA.

3.3 Optimisation of template preparation

3.3.1 Storage and handling of human tonsil samples

3.3.1i Comparison of tissue storage in liquid nitrogen vs. chemical preservative

Tonsil samples were collected fresh at surgery, transported to the laboratory and stored prior to RNA extraction. As RNA is susceptible to degradation it was necessary to determine the preferred method of tissue storage between collection and extraction. Two preservation methods, liquid nitrogen and a chemical preservative, RNA Later (Ambion) were compared. The RNA extraction method described in Section 2.5.1 was used and the isolated RNA compared using denaturing gel electrophoresis. Results (Figure 3.2) showed that tissue stored in either RNA Later or in liquid nitrogen was good quality, indicated by the presence of strong bands for both 28S and 18S rRNA, therefore allowing the use of both tissue preservation methods throughout the study.

3.3.1ii Homogenisation of human tonsil samples

In the first step of processing, tonsils were mechanically disrupted to allow efficient lysis of cells and release of nucleic acids during subsequent extraction steps. The use of manual and rotor-stator style homogenisers was compared. Prior to homogenisation, frozen tonsil was ground into a fine powder using a pestle and mortar under liquid nitrogen and samples stored in RNA Later were finely dissected.

3.3.1iia Manual homogenisation

A plastic homogeniser (Schütterlabor) was used to grind (approximately 30mg) tissue in (175µl) lysis buffer in a 1.5ml microfuge tube. Subsequent processing resulted in low yield of poor quality RNA. It was observed that during homogenisation tough, connective tissue could not be dispersed and remained in the sample. This may have clogged the column based down-stream steps resulting in poor RNA purification and this method was therefore deemed unsuitable for further use.

3.3.1iib Rotor-stator homogeniser

The Tissue Rupter (Qiagen), a rotor-stator style homogeniser was used with a disposable probe to mechanically disrupt tissue (Section 2.5.1). Tissue (approximately 100mg) in (0.5ml) lysis solution was dispersed into a thick suspension with no obvious clumps of connective tissue. It was concluded that mechanical disruption of tissue with the rotor-stator was preferred for homogenate production. This method required greater starting amounts of tonsil tissue, but the amount of tissue was not a limiting factor and allowed use of this method in all cases.

3.3.2 Extraction of RNA from human tonsil homogenates

RNA extracted from human tonsil homogenates using the SV RNA Isolation kit (Promega), the Micro-Midi Pure-Link RNA Purification System (Invitrogen) and Side-Step reagent (Stratagene) was compared.

RNA extracted using either the SV total RNA kit was found to be of low quality (Figure 3.3a) although purity and yield were good (Table 3.1a). Similar results were obtained with Side-Step reagent (results not shown). In contrast, that obtained using the Micro-Midi

Pure-Link RNA Purification System was of high quality (Figure 3.3b), purity and yield (Table 3.1b).

In conclusion, RNA extraction using the Invitrogen Micro-Midi Pure-Link RNA Purification System resulted in the best quality RNA. Therefore this was used for all subsequent RNA extractions from human tonsil.

3.3.3 Extraction of RNA from HEp-2 cells

HEp-2 cells (5 x 10^5 cells seeded) were grown on 12-well plates until confluent, before RNA extraction using the Promega SV Total RNA extraction kit. The resulting RNA was eluted in a 100µl volume and yield and concentration was assessed as described in Sections 2.5.3 and 2.5.4 respectively. Using this method, the concentration of RNA in the final eluate was within the concentration range of 100-400ng/µl. Representative results from a single experiment with 11 samples are shown in Table 3.2. An assessment of RNA purity was made by examining absorbance at 230, 260 and 280nm and absorbance ratios calculated; a value of 2 for A_{260}/A_{230} and A_{260}/A_{280} indicated pure RNA. As ratios for A_{260}/A_{230} were obtained in the range 2.05 to 2.44 and A_{260}/A_{280} in the range 2.04 to 2.14 (Table 3.2), RNA was deemed to be free from any substantial contamination.

The integrity of RNA was investigated using denaturing gel electrophoresis as described in Section 2.5.4. 18S and 28S rRNA subunits were clearly visible (Figure 3.4a). The 28S rRNA subunit was seen to be twice as bright as the 18S rRNA subunit indicating RNA was intact and suitable for use in PCR analysis. As the concentration, purity and integrity of RNA extracted from HEp-2 cells was sufficient, no further optimisation of this extraction protocol was required.

3.3.4 Extraction of RNA from HaCaT cells

HaCaT cell RNA was extracted and analysed as described for HEp-2 cells. Usually RNA concentration was in the range of 30-310ng/µl. This was a suitable concentration range for reverse transcription and PCR. RNA purity was also found to be suitable (usually 1.5-2 for A_{260}/A_{280} ratios and a lower but still suitable range of values for A_{260}/A_{230} ratios). Results from a representative experiment with 11 samples are shown in Table 3.3.

Integrity of RNA was investigated by subjecting samples to electrophoresis on a denaturing gel, as described in Section 2.5.4. 28S and 18S rRNA bands could be clearly seen and the 28S band was twice as bright as the 18S band, indicating intact RNA of good quality (Figure 3.4b).

3.3.5 Optimisation of reverse transcription

Reverse transcription (RT) using either MMLV RNaseH$^+$ Reverse Transcriptase (Promega) or Transcriptor (Roche), an enzyme engineered specifically for real-time PCR applications from Roche, was compared. The use of a reverse transcriptase with RNAseH$^+$ is advantageous for real-time PCR as the RNAseH$^+$ activity destroys the RNA template, which can interfere with PCR efficiency, when it is formed into a DNA:RNA hybrid with the nascent cDNA (Gerard and Grandgenett 1975). Transcriptor, which is a modified MMLV Reverse Transcriptase, also has endogenous RNaseH$^+$ activity.

1µg of human tonsil RNA from the same sample was reverse transcribed with each enzyme using the recommended conditions (Section 2.6.2) and a 1:2 dilution series in nuclease-free water (from 1:4 to 1:64) was made and amplified in real-time PCR with LL-37 primers. Data showed that dilution had less of an effect on reverse transcriptase products generated with the Promega MMLV RNAseH$^+$ (Cp range 32.98-35.21) than those synthesised with the Roche enzyme (32.56-36.66). Using Transcriptor, lower Cp values were found with the more dilute cDNA, indicating dilution of inhibitors present in the RT product. As there

may be slight variation in the amount of RT buffer and RNA present between samples, a reverse transcriptase that has less effect on PCR was most suitable, indicating use of the Promega reagents.

3.4 LL-37 Assay Development

Assay development for quantification of LL-37 mRNA involved the testing of oligonucleotide probe, Sybr-green and LUX detection and two real-time PCR instruments: the LightCyclers 1.2 and 480.

3.4.1 Oligonucleotide primer and probe design

Four sets of primers were used in the development of the LL-37 assay. These are listed in Table 3.4. Primers were tested by amplifying human tonsil, HEp-2 cell or HaCaT cell cDNA.

3.4.2 Test of probe based assays for LL-37 mRNA quantification

Two oligonucleotide primer and probe combinations were tested. The Universal Probe Library (UPL; Roche) consists of ninety oligonucleotide probes which together are able to detect all human genes. Primers specific to the sequence of interest are selected to amplify a small region which contains the hybridisation site for one of the 9 bp probes.

The UPL online design software (Section 3.2.2ii) was used to design probe and primer combinations for human LL-37. From these, the combinations identified as best and second best, probe no. 85 with Primer Set 1 and probe no. 79 with Primer Set 2 (Table 3.4), were selected for testing. Reactions were set-up as directed in the UPL guide (Roche). However, neither probe and primer combination worked; each resulted in very low fluorescence and no products were detected. Despite attempts to optimise the assays by varying annealing temperature and time, they remained unsuccessful and use of this system was not investigated further.

3.4.3 Assay development with Primer Set 3 and Sybr-green detection on the LightCycler 1.2

Primer Set 3 was used in semi-quantitative RT-PCR assays as described in Chapter 2. It had been previously shown to amplify a single product of 518bp from human tonsil cDNA which was confirmed to be LL-37 by direct sequencing (Ball, Siou et al. 2007). In the current work, amplification of HEp-2 cell and HaCaT cell cDNA by end-point PCR with these primers gave a single product of approximately 500bp (Figure 3.5). Sequencing of HEp-2 products showed them to be >99% identical to the human LL-37 sequence (Genbank accession number NM_004345) between bases 140 – 657 (Figure 3.6). The mismatched bases were located towards the 3' end of the sequence, most likely indicating errors introduced during the sequencing reaction and caused by factors such as reduced enzyme stringency, shortage of dNTPs or the accumulation of inhibitory by-products. Other possible causes of these errors are mis-incorporation of bases during PCR and allelic differences between individuals. The polymerase used for the amplification was a *Taq* DNA polymerase which has an error rate of no more than 4% (U.S Patent no. 7384739, issued 10th June 2008). The individuals from which the tonsil was obtained and from which HEp-2 and HaCaT cells were originally transformed may have a genomic sequence that differs by one or two bases, e.g. single nucleotide polymorphisms, from that used to derive the Genbank sequence.

An initial attempt to amplify two human tonsil cDNA samples in real-time PCR using Primer Set 3, x1 Sybr-green *Taq* Ready Mix (Sigma) and 1μM of each primer following the manufacturers protocols resulted in low levels of product with a T_m of ~89°C for each sample. The amount of product was below the level required to generate a reliable Cp value. To optimise the assay, PCRs were performed in which the concentration of primers and $MgCl_2$, and the amount of RT product added to the reaction were varied. Increasing primer concentration from 0.5μM to 2μM reduced Cp from 33.52 cycles to 27.61 cycles (Table 3.5), whereas increasing $MgCl_2$ concentration above that contained in the ready-mix (7mM) had no effect on Cp (Table 3.6). Reducing the volume of RT product added also improved PCR performance; using 1μl of RT product (added as 2μl of a 1:2 dilution in

ultra-pure water) resulted in a Cp of 36.41 whereas 0.5 µl of RT product (2µl of a 1:4 dilution) resulted in a Cp of 33.52 (Table 3.7).

Primer Set 3 was designed to measure LL-37 expression in a semi-quantitative PCR assay and generated a product of 518bp, which is greater than the preferred amplicon size for real-time PCR (100-200bp). Despite the improvements obtained by altering primer concentration and reducing the amount of RT product added, the Cp values recorded for tonsil samples remained high (~30 cycles), therefore it was decided not to proceed further with this primer pair and to design new primers which better fitted the requirements of real-time PCR.

3.4.4 Assay development with Primer Set 4

3.4.4i PCR optimisation

Primer Set 4 was designed to amplify a 104bp product, suitable for real-time PCR, and included a fluorescently labelled primer allowing product detection by the LUX mechanism (Invitrogen, Section 3.2.2ii). Initially these reactions were performed in Platinum *TAq* Supermix (Invitrogen) following the manufacturer's protocols. The primers were designed to lie within the region of the human LL-37 cDNA delineated by Primer Set 3 and, when used to amplify that cloned sequence, generated a product of approximately 100bp (Figure 3.7) with a T_m of 86°C (Figure 3.8).

When used to amplify human tonsil cDNA these primers also produced a product with T_m of 86°C, confirming amplification of LL-37 from these samples. However, the Cps for each of a series of six samples were all high, >30 cycles (Table 3.8), indicating either inefficient amplification or low expression of this AMP in human tonsil. Despite attempts to improve the PCR, the Cp was not reduced by altering primer or $MgCl_2$ concentration (Tables 3.9 and 3.10, respectively) or the annealing temperature of the reaction (Table 3.11). At this time, a new instrument for real-time PCR, the LightCycler 480 (Roche), became available. This uses a 96-well plate format instead of the 36-glass capillary format

of the LightCycler 1.2. Advantages of this instrument include higher throughput and increased ease of reaction set-up. Therefore it was decided to perform further optimisation on the LightCycler 480. Initial observation showed that Platinum *TAq* SuperMix was not suitable for use on the LightCycler 480 as it resulted in considerable well-to-well variation; therefore further assays were performed in LC480 Probes Master Mix (Roche) following the manufacturer's instructions.

To test the effect of RT product concentration on real-time PCR a sample of human tonsil cDNA was serially diluted and a fixed volume (5µl) of each dilution included in a series of real-time PCRs. This showed that the Cp of the sample was lower when the cDNA was more concentrated, therefore a 1:2 dilution of RT product was selected for future assays (Table 3.12).

3.4.4ii Development of concentration standards and standard curve optimisation

Human tonsil cDNAs amplified with Primer Set 4 produced a Cp range of 32-37 cycles (Section 3.4.4); therefore, a standard curve was developed to cover this range. Starting with the master stock of cloned LL-37 PCR product (Figure 3.6), a 1 in 10^7 dilution was made and from this a 1:5 dilution series generated (Table 3.13). These were amplified following the protocols determined during optimisation (Table 3.13). Melt curve analysis (Figure 3.9) of the reaction products showed that while standards 1-4 generated single products with T_m of ~88°C, standard 5 produced two products, the major with T_m of ~82°C and likely representative of primer-dimer, and standard 6 did not generate any products, suggesting that the concentration of target sequence in standards 5 and 6 is so low that amplification does not result in detectable quantities of product. The Cps for standards 1-4 ranged from 30-39 cycles (Table 3.13), which was appropriate for the predicted Cp of human tonsil samples. Arbitrary concentration values were assigned to standards 1-4 and plotted against measured Cp (Figure 3.10). This generated a standard curve with a calculated efficiency for the reaction of 1.85 (for an ideal exponential reaction the

efficiency, which is determined from the slope of the curve, is 2) and an error of 0.0491. Serial dilutions were prepared, assayed alongside the cDNA samples and a standard curve was plotted each time the assay was used.

3.4.4iii Reliability and reproducibility determination of coefficient of variation

A comparison of Cp values of standards 1-4 from six PCRs performed at different times was conducted. The coefficient of variation was calculated by:

$$\frac{\text{Average Cp value of the six experiments}}{\text{Standard deviation of the six experiments}} \times 100 = \text{Coefficient of variation (\%)}$$

Calculations were performed in Microsoft Excel. The coefficient of variation was in the range 5-15% (Table 3.14). Due to the high level of variation between PCR runs, it was decided to include a series of standards and generate a standard curve each time a PCR was performed. This would validate the assay on each occasion. It was also decided that each sample should be assayed in quadruplicate to ensure the greatest possible accuracy.

3.4.5 Summary of LL-37 Assay

Optimisation of real-time PCR assays for LL-37 used a variety of instruments and chemistries. Compared to the LightCycler 1.2 the LightCycler 480 offered the advantage of high throughput, therefore it was chosen for sample analyses. Data described in subsequent chapters were all obtained from the LightCycler 480 using the LUX assay. The final preparation and conditions required for the analysis of the LL-37 expression in human tonsil and HaCaT cells are described in Table 3.15.

3.5 HBD1 Assay Development

Assay development for the quantification of HBD1 mRNA included the testing of different detection formats (SYBR green and LUX), use of the LightCyclers 1.2 and 480 and optimisation of PCR conditions.

3.5.1 Oligonucleotide primer design

Two sets of primers were used in the development of the HBD1 assay. These are listed in Table 3.16. Primers were tested by amplifying human tonsil or HaCaT cell cDNA and sequencing of the products.

3.5.2 Primer Set 1

As with LL-37 Primer Set 1, these primers were available from a previous study. In that study a product of 221bp amplified from human tonsil was confirmed to be HBD1 by direct sequencing (Ball, Siou et al. 2007). In this study, products of similar size were generated from both HEp-2 and HaCaT cell cDNA using Primer Set 1 (Figure 3.11). In real-time PCR using 1 x Sybr-green *Taq* Ready Mix (Sigma) and 1μM of each primer on the LightCycler 1.2 and following the manufacturer's protocol, a single human tonsil sample gave a Cp of 25.02 with a Tm of ~85 °C (Figure 3.12). Although these results indicated that this primer set would be suitable for the development of a real-time assay for HBD1 using Sybr-green detection, at this time a problem beyond my control was encountered; due to production problems the manufacturers withdrew Sybr-green *Taq* Ready Mix from sale. A few alternatives were tested but did not give similar signal strength therefore, because of the success of LUX assay development with LL-37, it was decided to develop a LUX assay for HBD1. However, having shown the suitability of these primers for detection of HBD1, they were used for the semi-quantitative PCR assays described in Chapter 2.

3.5.3 Primer Set 2

This primer set was specifically designed to generate short amplicons of 87bp suitable for real-time PCR and used LUX detection. Products from amplification of human tonsil and HaCaT cells were cloned using the p-GEM-T-Easy vector system and sequenced. The sequence of clones from both templates was 100% identical to the HBD1 sequence in Genbank (Accession No. NM_005218.3) (Figure 3.13).

Initially the LightCycler 1.2 was used for assay optimisation. Using standard conditions (20µl reaction containing 1x Platinum *Taq* Supermix (Invitrogen) and 1µM each primer), a series of six tonsil samples gave a Cp range of 27.78-33.68 cycles (Table 3.17). This was not improved by altering primer or $MgCl_2$ concentration (Tables 3.18 and 3.19). The optimal annealing temperature was determined to be 60°C (Table 3.20).

The assay was then transferred to the LightCycler 480 and, because of similar problems in well-to-well variation as encountered during LL-37 assay optimisation when using Platinum *Taq* Supermix, to LC480 Probes Master Mix (Roche). Using these reagents, a series of four tonsil samples gave a Cp range of 27.35-28.17 cycles (Table 3.21). However, when a series of HaCaT cell cDNA samples were amplified these were found to give a much higher Cp range (33.01- 35.05 cycles; Table 3.22). Therefore to cover the full range of samples included in this study, a standard curve for the assay was constructed which covered the Cp range 22-37 cycles. The starting point for the standard curve was a DNA miniprep of the cloned PCR product generated with Primer Set 2. This was diluted as shown in Table 3.23 and resulted in a standard curve with efficiency of 1.581 and error of 0.0669 (Figure 3.14). Each standard was assayed in duplicate. Melt peak analysis of the PCR products showed that all, except one replicate of the weakest standard, six, generated a single product with Tm of ~86°C. The small peak at ~81°C in standard 6, replicate 1 most likely represents primer-dimer (Figure 3.15).

To determine the reproducibility of the assay, standard number 3 was assayed on six separate occasions. Analysis of the obtained Cps gave a coefficient of variation of 4%

(Table 3.24). It was also noted that intra-assay variation between replicates of a single sample was very low (data not shown), therefore it was determined that assaying each sample and standard in duplicate gave sufficient accuracy.

3.5.4 Summary of HBD1 Assay

The optimised assay for HBD1 mRNA is a LUX assay and uses LC480 Probes Master mix on the Light Cycler 480. The final preparation and conditions required for the analysis of the HBD1 mRNA expression in human tonsil and HaCaT cells are described in Table 3.25.

3.6 HBD2 assay development

3.6.1 Oligonucleotide primer and probe design

Two sets of primers were used in the development of the HBD2 assay. These are listed in Table 3.26. Primers were tested by amplifying human tonsil, or HaCaT cell cDNA.

3.6.2 Assay optimisation

Assay development for HBD2 followed the same path as described for LL-37 and HBD1 assays. Two styles of assay, Sybr-green and LUX, were tested. In contrast to LL-37 and HBD1, reactions using Sybr-green detection and the appropriate master mix gave better results for HBD2 quantification than did the LUX assay. Primer Set 1, the LUX assay, consistently generated a significant amount of primer-dimer despite attempts at optimisation (Figure 3.16) and so was abandoned. Primer Set 2 was originally designed for use in the semi-quantitative PCR assays described in Chapter 2. It was confirmed that the product of amplification with these primers from HaCaT cells and tonsil was ~320bp long and identical to the HBD1 mRNA sequence (Genbank accession no. NM_004942) (Figure 3.17). Initially, these primers gave very poor amplification in real-time PCR and resulted in a low yield of a product with Tm of ~87°C (Figure 3.18). This was significantly improved by purchasing primers which were HPLC purified; salts and other reaction components carried over from oligonucleotide synthesis can have severe adverse effects on real-time PCR, removing these improves reaction efficiency and product yield (Figure 3.18). Further optimisation showed that required conditions in 1 x LC480 Sybr Green Master mix (Roche) were annealing temperature of 58°C and primer concentration of 1μM. No adjustments to the $MgCl_2$ concentration were required. For the standard curve, a DNA miniprep of the cloned HBD2 fragment shown in Figure 3.17 was diluted as shown in Table 3.27 and the Cp of each standard determined. Each was measured in duplicate. Of the six standards, only 1-5 generated useable Cp values. Following melt curve analysis it was found that the product of amplification of standard six differed from that of all other

standards (Tm of 80°C compared to 87°C) and was most likely primer-dimer rather than the required HBD1 product. Melt curve analysis of standards 1-5 were as of Standard 1 at 87°C (Figure 3.18). Thus only standards 1-5 were included in the plotted standard curve (Figure 3.19), which has an efficiency of 1.963, error of 0.0408 and covers the Cp range 24.68-34.09 cycles. Human tonsil samples ranged in Cp from ~29-34 cycles, thus this was an appropriate standard range (Table 3.28).

To determine the reproducibility of the assay, standards 1-4 were assayed on six separate occasions. Analysis of the obtained Cps showed that the coefficient of variation ranged from 3-6 (Table 3.29). These standards were included in each PCR carried out and a standard curve plotted for each run. It was also noted that intra-assay variation between replicates of a single sample was low (data not shown), therefore it was determined that assaying each sample and standard in duplicate gave sufficient accuracy.

3.6.3 Summary of HBD2 Assay

The optimised assay for HBD2 mRNA measurement is a Sybr-green assay and uses LC480 Sybr-green Master Mix on the Light Cycler 480. The final preparation and conditions required for the analysis of the HBD2 mRNA expression in human tonsil and HaCaT cells are described in Table 3.30. It was essential for this assay that primers were HPLC-purified.

3.7 HBD3 Assay Development

3.7.1 Oligonucleotide primer and probe design

Two sets of primers were used in attempts to develop a HBD3 assay. These are listed in Table 3.31. Primers were tested by amplifying human tonsil or HaCaT cell cDNA and confirmed to generate products of the correct size or sequence in end-point PCR (Figure 3.20).

3.7.2 Assay optimisation

Despite confirming that the two primers sets used to amplify HBD3 generated the expected product from both tonsil and HaCaT cells (Figure 3.20) it was not possible to develop an accurate or reproducible real-time PCR assay for this AMP using either. Melting temperature analysis of products generated during real-time PCR showed multiple melt peaks, indicative of the formation of primer-dimer and other non-specific products (Figure 3.21). Repeat analysis of a series of samples of tonsil and HaCaT samples showed significant intra- and inter-assay variation that was not abolished by any optimisation procedure. It is possible that HBD3 is expressed at very low levels within the samples tested and thus was not reliably detected. A semi-quantitative assay for HBD3 using Primer Set 1 was developed as described in Chapter 2. Results from this are reported in Chapter 5. As real-time PCR is generally expected to be more sensitive and reliable than end-point PCR for the quantification of nucleic acid abundance it is possible that an alternative approach, such as using a specific oligonucleotide probe, may be successful.

3.8 Hepcidin Assay Development

3.8.1 Oligonucleotide primer and probe design

A single set of primers were used in the development of the hepcidin assay. These are shown in Table 3.32. These primers had previously been shown to specifically amplify hepcidin sequence fragment from human tonsil (Ball, Siou et al. 2007). Further investigations in this study, they also amplified a product of ~190bp from HaCaT cell cDNA (Figure 3.22). This was cloned in p-GEM-T-Easy and sequenced; analysis showed it to have 91% identity to human hepcidin (Genbank Accession No. NM_021175). Although this was a poor match, this was the best match identified by BLAST and the result of poor sequence data (Figure 3.22).

3.8.2 Assay development

As with HBD3, it was not possible to develop an assay suitable for the measurement of hepcidin mRNA abundance. Similar strategies to those used in the development of assays for LL-37 and HBD1 and HBD2 were employed, including the testing of HPLC purified primers in a Sybr-green assay mix. However, the Cps recorded for a series of HaCaT cell samples were high, ranging from 36.11-39.93 cycles. When it was attempted to produce a standard series appropriate to this range, it was found that only the most concentrated standard produced a product with the predicted Tm, all others had a lower Tm indicative of primer-dimer formation (Figure 3.23). At the lower dilutions, the HBD3 clone was no longer sufficiently concentrated to form a product; thus the primers preferentially bind to each other and produce primer-dimer. The same results were seen in repeats of the assay and when PCR products were subjected to electrophoresis it was seen that only in standard 1 were products of the predicted size, approximately 200bp, generated; in all other dilutions only primer-dimer, represented by bands at approximately 25bp, was visible (Figure 3.23). As this assay was problematic and because the fundamental role of hepcidin is in iron transport and metabolism rather than its antimicrobial activity (Yamaji, Sharp et al. 2004;

Verga Falzacappa and Muckenthaler 2005; Vyoral and Petrak 2005; Shinzato, Abe et al. 2008), this assay was not developed further. The primers were, however, found to be suitable for semi-quantitative PCR and were used to generate the data in Chapter 5.

3.9 LEAP-2 Assay Development

3.9.1 Oligonucleotide primer and probe design

Primers used in the development of the LEAP-2 assay are listed in Table 3.33. Primers were tested by amplifying human tonsil and HaCaT cell cDNA. This primer set was designed to have short amplicons of 161bp suitable for real-time PCR, however, they were also used in semi-quantitative RT-PCR assays described in Chapter 2. PCR products of this size were amplified from both human tonsil and HaCaT cell cDNA (Figure 3.24) and, when cloned into p-GEM-T-Easy, sequence analysis confirmed them to be derived from human LEAP-2 (Genbank Accession No. NM_052971) (Figure 3.24).

3.9.2 Assay optimisation

The LEAP-2 real-time PCR assay was developed using Sybr-green detection, LC480 Sybr-green master mix and was run exclusively on the LightCycler 480. Initial observations showed that prior to optimisation, the Cp of HaCaT cell samples was ~32 cycles whereas that of tonsil samples was ~ 34-35 cycles. The first step in optimisation was to introduce HPLC purified primers. This reduced the CP of HaCaT samples to ~28-29 cycles and that of tonsil samples to ~30-31 cycles. Melt curve analysis of products from HaCaT cell cDNA amplification showed that the specific LEAP-2 product had a Tm of ~85°C (Figure 3.25). A standard curve was developed, focused around the Cp range 23-34 cycles (Table 3.34 and Figure 3.26). At lower concentrations the standards (4 and 5) showed poor reproducibility between replicates, however melt curve analysis showed the products to be LEAP-2 specific, therefore all points were used to plot the concentration curve (Figure 3.26). This had an efficiency of 1.945 and error of 0.0806.

To determine the reproducibility of the assay, standards 1-4 were assayed in six PCRs performed on different days and times. The coefficient of variation was calculated and was

in a range of 6-8% (Table 3.35). These standards were included in each PCR performed and a standard curve plotted on each occasion. It was also noted that intra-assay variation between sample replicates was low (data not shown) and therefore it was determined that assaying each sample in duplicate would produce reliable results.

3.9.3 Summary of LEAP-2 assay

The optimised assay for LEAP-2 mRNA measurement is a Sybr-green assay and uses LC480 Sybr-green Master Mix on the Light Cycler 480. The sample preparation and conditions required for the analysis of LEAP-2 mRNA expression in human tonsil and HaCaT cells are described in Table 3.36.

3.10 GAPDH Assay Development

3.10.1 Oligonucleotide primer and probe design

The set of primers used in the development of the GAPDH assay are listed in Table 3.37. The primers used in the semi-quantitative RT-PCR assays (5', TGAAGGTCGGAGTCCACGGATTTG; 3',CATGTAAACCATGTAGGTTGAGGTC) had large amplicons of 983bp, therefore GAPDH Primer Set 1 were specifically designed to produce a short amplicon of 177bp suitable for real-time PCR and were HPLC purified. Primers were tested by amplifying human tonsil, or HaCaT cell cDNA. The specificity of this primer pair was confirmed by amplifying human tonsil and HaCaT cDNA and subsequent sequencing of the PCR products, which were shown to be 100% identical to human GAPDH cDNA (Genbank Accession No. NM_002046) (Figure 3.27).

3.10.2 Assay optimisation

The Cps of GAPDH PCR products from experimental samples was required to be measured. PCR reactions using three HaCaT cell cDNA samples (1:2 dilution of each) were performed using 1 x LC480 Sybr-green master mix and 1μM of each primer on the LC 480. These samples gave Cps of 17.09, 15.97 and 17.99 cycles. Melt curve analysis of the products showed peaks representing GAPDH at 85°C (Figure 3.28). It was determined from this that sample cDNA being used as template in this assay should be diluted 1:100 with nuclease-free water; this would reduce the amount of the sample required for the assay and still give a Cp of ~ 22-25 cycles.

To generate a standard curve a dilution series of a single HaCaT cDNA sample was made. This stock was diluted so that standards with Cps ranging from 20 - 30 cycles were produced (Table 3.38). It was possible to use this means of generating the standard series because GAPDH mRNA is of high abundance. Each standard in the series was assigned an arbitrary concentration value (Table 3.38) which was plotted against its Cp to produce the

standard curve for GAPDH shown in Figure 3.29. The efficiency of the curve is 1.552 and the error 0.0111. Melt peak analysis, shown in Figure 3.30, showed all standards had a peak at 84.5°C.

To determine the reproducibility of the assay, a comparison of Cp values of standard four from six PCRs performed on different days was conducted. The coefficient of variation was 0.5% (Table 3.39). Due to the low levels of variation observed between reactions it was decided to import the standard curve shown in Figure 3.29 to each run and use an internal calibrator method to allow comparisons between PCRs. The data for the curve are stored in the LightCycler software and then in subsequent runs only a single standard is assayed, thus saving reagents and time. Standard number four was chosen as the calibrator sample. It was also determined that assaying each sample in duplicate was sufficient to produce an accurate reading.

3.10.3 Summary of GAPDH assay

The optimised assay for GAPDH uses the LightCycler 480, LC 480 Sybr-green Master Mix, and HPLC purified primers. The final sample preparation and conditions required for the analysis of GAPDH expression in human tonsil, and HaCaT cells are described in Table 3.40.

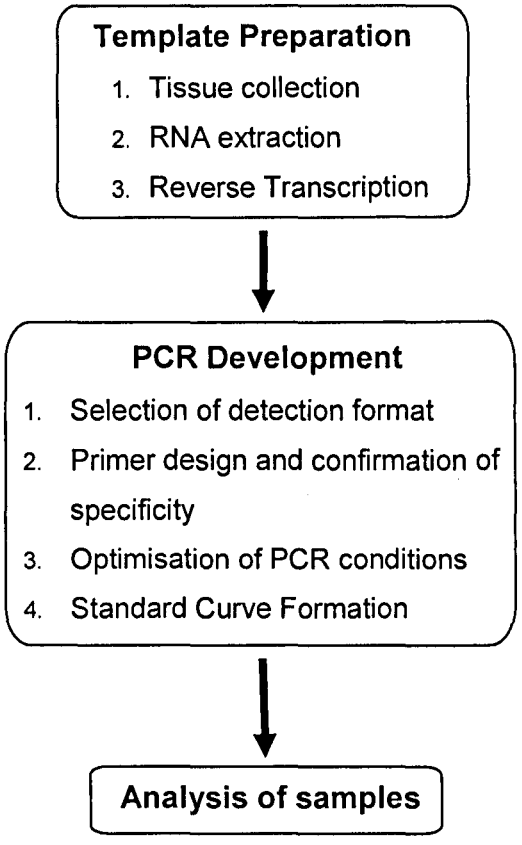

Figure 3.1: Steps in real-time PCR assay development.

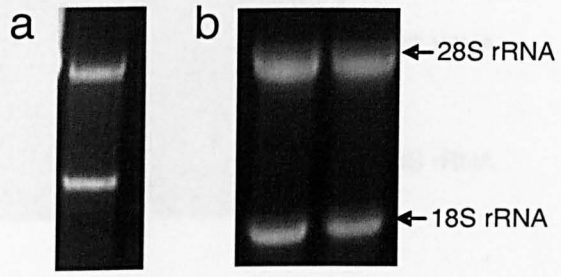

Figure 3.2: Denaturing gel electrophoresis of RNA extracted from human tonsil tissue preserved and stored in **a)** liquid nitrogen or **b)** RNA Later. All samples show strong bands indicating the presence of 28S and 18S rRNA (labelled).

a)

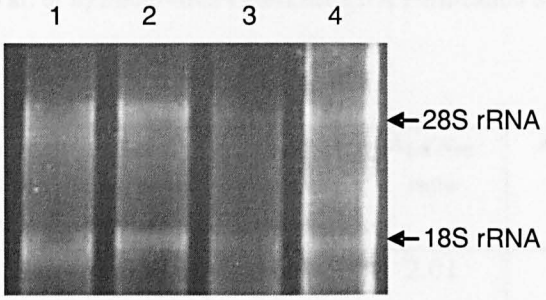

b)

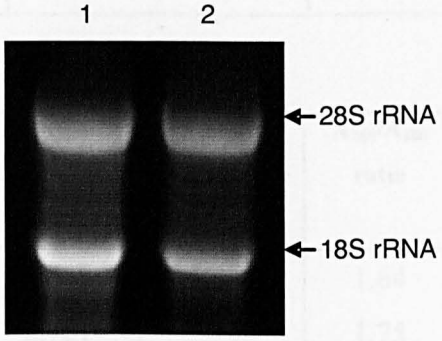

Figure 3.3: Representative denaturing gel electrophoresis of human tonsil RNA extracted using **a)** the SV Total RNA Extraction kit rotor-stator homogenisation and **b)** the Micro-Midi Pure-Link RNA Purification System. In **a)** 0.5µg RNA from four independent samples (lanes 1-4) was loaded. In **b)** 1µg RNA from two independent samples was loaded (lanes 1-2). On each gel bands representing 28S and 18S rRNA are visible, however the samples on gel **a)** are clearly degraded.

Table 3.1: Representative spectroscopy results from RNA extracted from human tonsil samples with either **a)** SV Total RNA Isolation kit or **b)** Micro-Midi Pure-Link RNA Purification System.

a)

Sample	A_{230} (absorbance units)	A_{260} (absorbance units)	A_{280} (absorbance units)	A_{260}/A_{280} ratio	A_{260}/A_{230} ratio	Calculated concentration (µg/µl)
1	0.745	1.330	0.644	2.01	1.79	0.532
2	1.029	2.011	0.988	2.04	1.96	0.804
3	0.512	0.955	0.463	2.06	1.87	0.382
4	1.585	3.065	1.567	1.96	1.93	1.226

b)

Sample	A_{230} (absorbance units)	A_{260} (absorbance units)	A_{280} (absorbance units)	A_{260}/A_{280} ratio	A_{260}/A_{230} ratio	Calculated concentration (µg/µl)
1	0.792	1.648	1.006	1.64	2.08	0.66
2	1.464	2.981	1.706	1.75	2.04	1.19
3	0.218	0.406	0.282	1.44	1.87	0.162
4	0.776	1.484	0.830	1.79	1.91	0.59
5	0.962	1.949	1.072	1.82	2.1	0.78
6	0.338	0.563	0.432	1.3	1.66	0.23
7	0.614	0.981	0.554	1.77	1.6	0.39
8	1.161	0.731	0.411	1.78	0.63	0.29
9	0.732	1.355	0.804	1.69	1.85	0.54

Table 3.2: Spectroscopy results from a representative set of eleven HEp-2 cell RNA samples.

Sample	A_{230} (absorbance units)	A_{260} (absorbance units)	A_{280} (absorbance units)	A_{260}/A_{280} ratio	A_{260}/A_{230} ratio	Calculated concentration (µg/µl)
1	0.390	0.83	0.406	2.04	2.13	0.332
2	0.389	0.840	0.406	2.07	2.16	0.336
3	0.259	0.609	0.292	2.09	2.35	0.244
4	0.209	0.511	0.246	2.07	2.44	0.204
5	0.254	0.58	0.280	2.09	2.3	0.234
6	0.369	0.755	0.363	2.08	2.05	0.302
7	0.299	0.684	0.325	2.1	2.29	0.273
8	0.212	0.445	0.212	2.1	2.1	0.178
9	0.218	0.509	0.244	2.09	2.34	0.204
10	0.107	0.288	0.135	2.14	2.7	0.115
11	0.165	0.374	0.178	2.11	2.26	0.150

Table 3.3: Spectroscopy results from a representative set of eleven HaCaT cell RNA samples.

Sample	A_{230} (absorbance units)	A_{260} (absorbance units)	A_{280} (absorbance units)	A_{260}/A_{280} ratio	A_{260}/A_{230} ratio	Calculated concentration (µg/µl)
1	0.184	0.322	0.164	1.96	1.75	0.130
2	0.158	0.297	0.150	1.99	1.88	0.120
3	0.345	0.439	0.218	2.01	1.27	0.180
4	0.427	0.334	0.167	2.01	0.78	0.130
5	0.311	0.239	0.121	1.97	0.77	0.100
6	0.803	0.467	0.232	2.02	0.58	0.190
7	0.223	0.186	0.1	1.87	0.84	0.070
8	0.934	0.461	0.259	1.78	0.49	0.180
9	0.339	0.511	0.251	2.04	1.51	0.200
10	0.146	0.068	0.038	1.79	0.47	0.030
11	0.303	0.099	0.070	1.41	0.33	0.040

a)

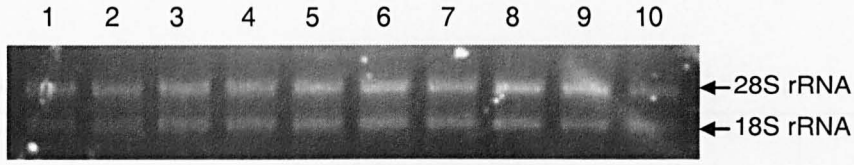

b)

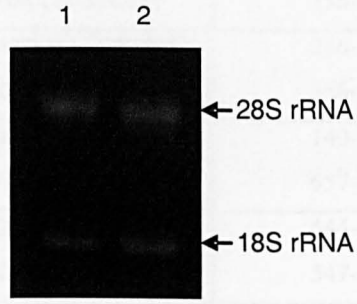

Figure 3.4: a) Representative HEp-2 cell RNA from 10 individual samples separated by denaturing gel electrophoresis. 0.5µg of RNA was loaded per lane. Samples 1-10 correspond to 1-10 shown in Table 3.2. **b)** HaCaT cell RNA from two samples (1 and 2, corresponding to samples 1 and 2 in Table 3.3) separated by denaturing gel electrophoresis. Sample 1 = 364ng, sample 2 = 336ng.

Table 3.4: List of primer sets designed to amplify regions of the mRNA sequence encoding human LL-37.

Primer set	Primer sequences (5'-3')	Position in cDNA/ base numbers in NM_004345	Predicted product size (bp)
1	Forward: TCGGATGCTAACCTCTACCG [1] Reverse: GTCTGGGACCCCATCCAT	291-310 356-339	65
2	Forward: GTCCTCGGATGCTAACCTCTAC[2] Reverse: GTCTGGGACCCCATCCAT	286-308 356-339	70
3	Forward: CATGAAGACCCAAAGGGATG Reverse: CACACTAGGACTCTGTC	140-160 657-638	518
4	Forward: cgctGACGGGCTGGTGAAGcG[3] Reverse: CCCAGCAGGGCAAATCTCTT	444-460 547-528	104

[1] This primer set required the FAM labelled oligonucleotide probe no. 85 from the Universal Probe Library to quantify LL-37 gene expression.
[2] This primer set required the FAM labelled oligonucleotide probe no. 79 from the Universal Probe Library to quantify LL-37 gene expression.
[3] This primer was labelled with the fluorescent probe FAM, which excites at 488nM and emits at 518nM, at position 'c' and had a 4bp 5' extension (shown underlined) to enable hairpin formation for LUX assays.

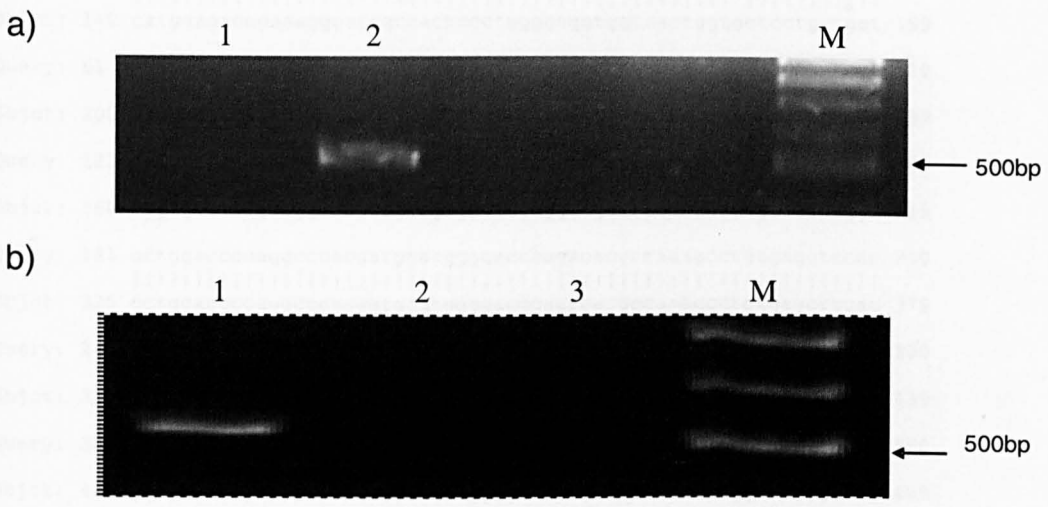

Figure 3.5: Agarose gel electrophoresis of PCR products amplified from a) HEp-2 and b) HaCaT cell cDNA with LL-37 Primer Set 3. In **a)** lane 1 is no template control, lane 2 shows products from HEp2 cell cDNA and M is the DNA size marker. In **b)** lane 1 shows products from HaCaT cells treated with 1,25 dihydroxyvitamin D3, lanes 2 and 3 show products from untreated HaCaT cells and M is DNA size marker. LL-37 was not detectable in untreated HaCaT cells. On both gels the position of the 500bp DNA marker is shown.

```
Query: 1   catgaagacccaaagggatggccactccctggggcggtggtcactggtgctcctgctgct 60
           ||||||||||||||||||||||||||||||||||||||||||||||||||||||||||||
Sbjct: 140 catgaagacccaaagggatggccactccctggggcggtggtcactggtgctcctgctgct 199

Query: 61  gggcctggtgatgcctctggccatcattgcccaggtcctcagctacaaggaagctgtgct 120
           ||||||||||||||||||||||||||||||||||||||||||||||||||||||||||||
Sbjct: 200 gggcctggtgatgcctctggccatcattgcccaggtcctcagctacaaggaagctgtgct 259

Query: 121 tcgtgctatagatggcatcaaccagcggtcctcggatgctaacctctaccgcctcctgga 180
           ||||||||||||||||||||||||||||||||||||||||||||||||||||||||||||
Sbjct: 260 tcgtgctatagatggcatcaaccagcggtcctcggatgctaacctctaccgcctcctgga 319

Query: 181 cctggaccccaggcccacgatggatggggacccagacacgccaaagcctgtgagcttcac 240
           ||||||||||||||||||||||||||||||||||||||||||||||||||||||||||||
Sbjct: 320 cctggaccccaggcccacgatggatggggacccagacacgccaaagcctgtgagcttcac 379

Query: 241 agtgaaggagacagtgtgccccaggacgacacagcagtcaccagaggattgtgacttcaa 300
           ||||||||||||||||||||||||||||||||||||||||||||||||||||||||||||
Sbjct: 380 agtgaaggagacagtgtgccccaggacgacacagcagtcaccagaggattgtgacttcaa 439

Query: 301 gaaggacgggctggtgaagcggtgtatggggacagtgaccctcaaccaggccaggggctc 360
           ||||||||||||||||||||||||||||||||||||||||||||||||||||||||||||
Sbjct: 440 gaaggacgggctggtgaagcggtgtatggggacagtgaccctcaaccaggccaggggctc 499

Query: 361 ctttgacatcagttgtgataaggataacaagagatttgccctgctgggtgatttcttccg 420
           ||||||||||||||||||||||||||||||||||||||||||||||||||||||||||||
Sbjct: 500 ctttgacatcagttgtgataaggataacaagagatttgccctgctgggtgatttcttccg 559

Query: 421 gaaatctaaagaaaagattggcaaagagtttaaaagaattgtccagagaatcaaagggat 480
           |||||||||||| ||||||||||||||||||||||||||||||||||||||  ||||
Sbjct: 560 gaaatctaaagagaagattggcaaagagtttaaaagaattgtccagagaatcaa--ggat 617

Query: 481 tttttgcggaatctttgtacccaggacaga 510
           |||||||||||| ||||||||||||||||
Sbjct: 618 tttttgcggaatc-ttgtacccaggacaga 646
```

Figure 3.6: Sequence of the PCR product amplified from HEp-2 cell cDNA with LL-37 Primer Set 3 aligned to the LL-37 cDNA sequence. Sequence analysis performed by BLAST (http://www.ncbi.nlm.nih.gov/blast/Blast.cgi) matched the cloned PCR product ('Query') to the Genbank sequence ('Sbjct') for LL-37 (NM_004345) with 99.2% identity.

Table 3.5: Cp values from primer titration in an LL-37 specific PCR using Primer Set 3 and Sybr-green detection on the LightCycler 1.2. The same tonsil cDNA sample was used in all reactions.

Primer concentration (μM)	Cp (cycle number)
0.5	33.52
1.25	29.00
2	27.61

Table 3.6: Cp values from $MgCl_2$ titration in an LL-37 specific PCR using Primer Set 3 and Sybr-green detection on the LightCycler 1.2. The same tonsil cDNA sample was used in all reactions.

Concentration of $MgCl_2$ (mM)	Cp (cycle number)
7.00	33.52
8.25	33.52
10.13	33.55
12.00	>38*

* (an accurate Cp value was not registered as the product was not detected at significant strength)

Table 3.7: Cp values from cDNA titration in an LL-37 specific PCR using Primer Set 3 and Sybr-green detection on the LightCycler 1.2. The same tonsil cDNA sample was used in all reactions.

Amount of cDNA (μl)	Cp (cycle number)
2	36.41
4	33.52

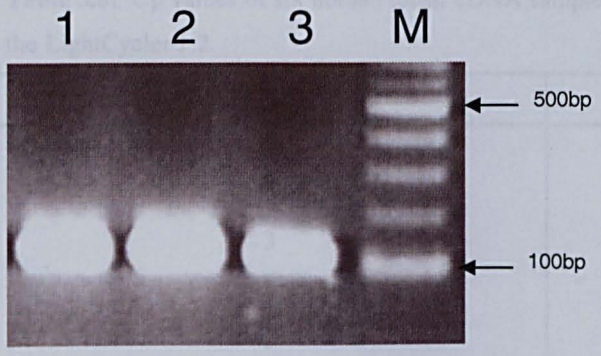

Figure 3.7: Agarose gel electrophoresis of PCR products amplified from the cloned sequence of LL-37 with Primer Set 4. These PCR products correspond to melt peaks of 86°C (Figure 3.8), representing LL-37 PCR products melting temperature.

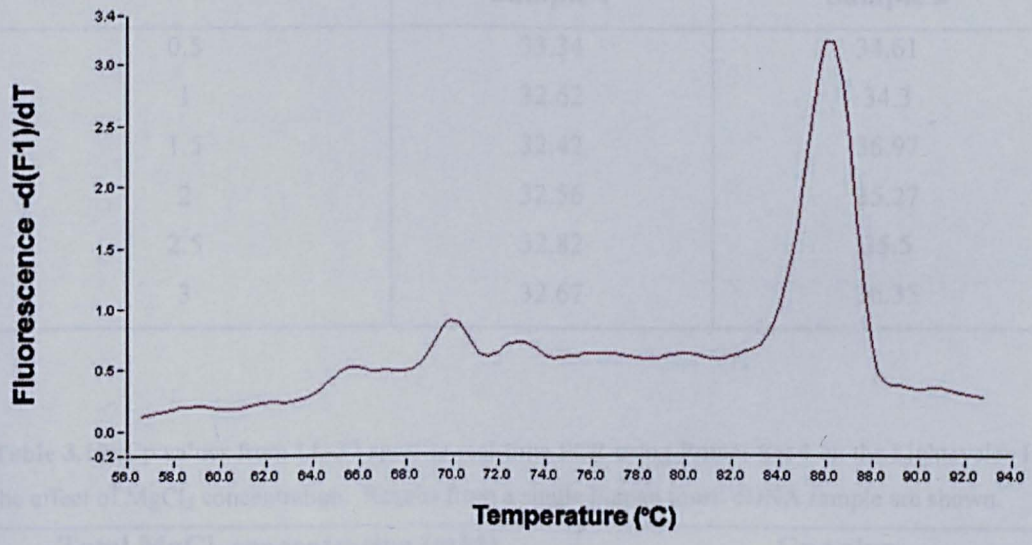

Figure 3.8: Melt peak analysis of products generated in real-time PCR using Primer Set 4 with cloned LL-37 PCR product as template on the LightCycler 1.2. The major peak shows that the product of this amplification has a T_m of 86°C.

Table 3.8: Cp values of six human tonsil cDNA samples from an LL-37 specific PCR using Primer Set 4 on the LightCycler 1.2.

Sample number	Cp
1	31.76
2	31.65
3	36.92
4	36.68
5	31.83
6	33.11

Table 3.9: Cps from LL-37 specific real-time PCR using Primer Set 4 on the Lightcycler 1.2 showing the effect of primer concentration. Results from two human tonsil cDNA samples are shown

Primer concentration (μM)	Cp value	
	Sample 1	Sample 2
0.5	33.34	34.61
1	32.62	34.3
1.5	32.42	36.97
2	32.56	35.27
2.5	32.82	35.5
3	32.67	36.35

Table 3.10: Cp values from LL-37 specific real-time PCR using Primer Set 4 on the Lightcycler 1.2 showing the effect of $MgCl_2$ concentration. Results from a single human tonsil cDNA sample are shown.

Total $MgCl_2$ concentration (mM)	Cp value
6	31.76
7	31.81
8	31.64
9	31.75
10	31.55
11	31.70
12	31.57

Table 3.11: Cp values from LL-37 specific PCRs using Primer Set 4, conducted at annealing temperatures of 55, 56, 58 and 60°C on the LightCycler 1.2. Results from a single human tonsil cDNA sample are shown.

Annealing temperature (°C)	Cp value
55	32.84
56	32.87
58	32.47
60	32.93

Table 3.12: Cp values from LL-37 specific PCRs using Primer Set 4 with varying amounts (2µl each of a 1:2 dilution series) of human tonsil RT product added. Performed on the LightCycler 480.

Dilution of cDNA in nuclease-free water	Cp (cycle number)
1:2	32.29
1:4	32.98
1:8	35.21
1:16	33.99
1:32	34.29
1:64	33.08

Table 3.13: Cp values from a dilution series of cloned LL-37 sequence fragment, amplified with Primer Set 4 on the LightCycler 480. Dilution of miniprep and arbitrary concentration values are shown.

Standard	Mean Cp (2 replicates)	Dilution of master stock	Concentration (arbitrary values)
1	29.70	1 in $1x10^7$	3125
2	32.47	1 in $5x10^7$	625
3	34.93	1 in $2.5x10^8$	125
4	38.33	1 in $1.25x10^9$	25
5	38.05*	1 in $6.25x10^9$	5
6	>40*	1 in $3.125x10^{10}$	1

*the amplification product in the samples is probably primer-dimer as indicated by T_m, therefore these values are not included in the final standard curve used for analysis.

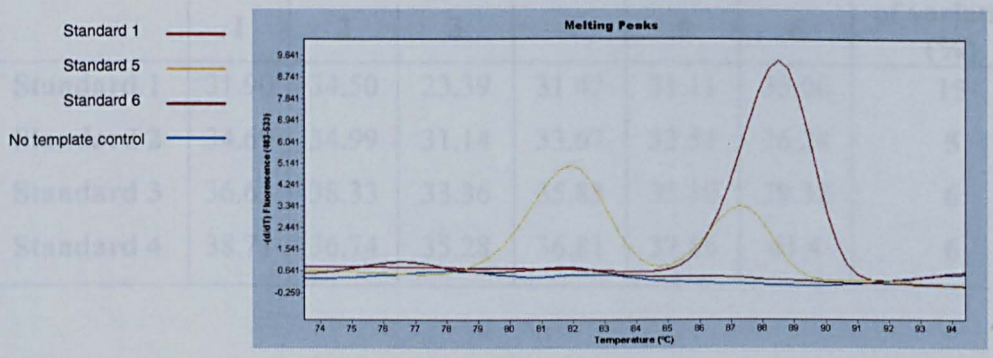

Figure 3.9: Melt peak analysis of LL-37 PCR products:

Melt peak analysis for LL-37 standards. The peak for standard 1, shown in red, at 88°C represents the LL-37 product. For standard 5, yellow trace, peaks at 82 and 87°C represent the PCR product peak and primer-dimer. Standard 6 (brown) does not display a peak, indicating no PCR products were formed. The no template control is shown in blue.

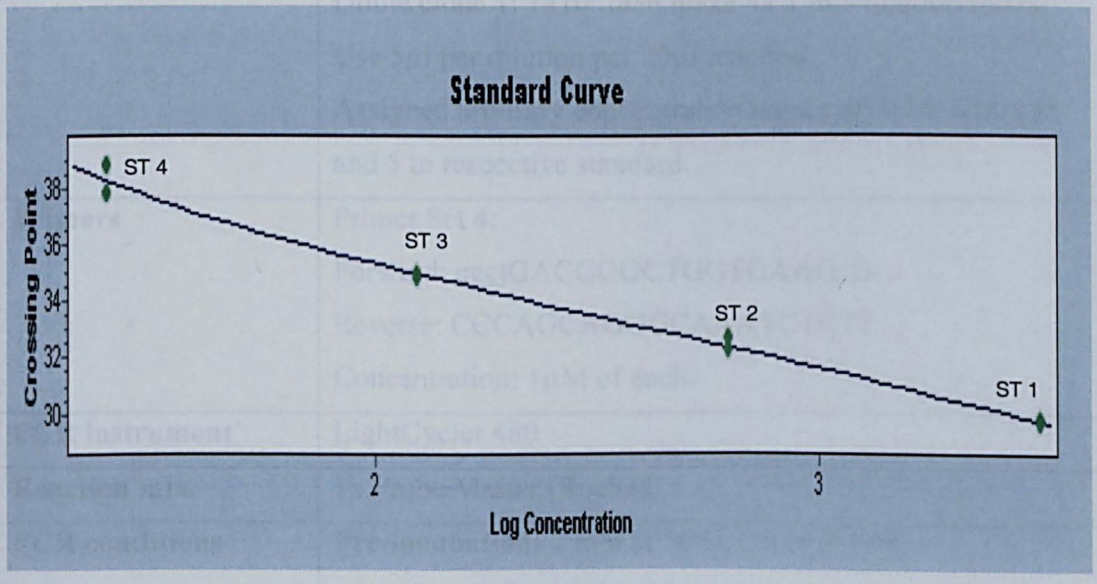

Figure 3.10: A representative LL-37 standard curve using standards 1-4 shown in Table 3.13. ST 1: Standard 1, ST 2: Standard 2, ST 3: Standard 3, ST 4: Standard 4. Plot of log standard concentration vs. crossing point.

Table 3.14: Cp values of standards 1-4 from six independent PCRs from which the coefficient of variation of the assay was calculated.

	Experiment						Coefficient of variation (%)
	1	2	3	4	5	6	
Standard 1	31.90	34.50	23.39	31.42	31.11	35.06	**15**
Standard 2	34.69	34.99	31.14	33.67	33.51	36.24	**5**
Standard 3	36.63	38.33	33.36	35.83	35.10	39.32	**6**
Standard 4	38.71	36.74	35.28	36.81	37.56	41.4	**6**

Table 3.15: Summary of LL-37 assay.

Step	Process
Sample preparation	Reverse transcribe 1µg of RNA in a 50µl reaction using MMLV RNAseH$^+$ RT. Dilute product 1:2 with nuclease-free water. Use 5µl in a 20µl PCR reaction.
Standard curve	Using 'miniprep' of cloned LL-37 PCR product. Dilute clone 1: 1x10^7 then make 4x 1 in 5 dilution series. Use 5µl per dilution per 20µl reaction. Assigned arbitrary concentration values of 3125, 625, 125 and 5 to respective standard.
Primers	Primer Set 4: Forward: cgctGACGGGCTGGTGAAGcG Reverse: CCCAGCAGGGCAAATCTCTT Concentration: 1µM of each.
PCR instrument	LightCycler 480
Reaction mix	1x Probe Master (Roche).
PCR conditions	**Pre-incubation:** 2 min at 50°C, 2 min at 95°C. **45 cycles of:** 5s at 94°C, 10s at 55°C and 10s at 72°C. **Melt curve:** Performed over 60-95°C **Cooling:** 40°C

Table 3.16: List of primer sets designed to amplify regions of the mRNA sequence encoding HBD1.

Primer set	Primer sequences (5'-3')	Position in cDNA/ base numbers in NM_005218	Predicted product size (bp)
1	Forward: CCATGAGAACTTCCTACCTTC	149-169	221
	Reverse: GTCACTCCCAGCTCACTTG	369-351	
2	Forward: GTCAGCTCAGCCTCCAAAGGA	100-80	87
	Reverse: cgccGGTAGGAAGTTCTCATGGcG[1]	147-166	

[1] This primer was labelled with the fluorescent probe ALX 568 at position 'c' and had a 4bp 5' extension (shown underlined) to enable hairpin formation for LUX assays.

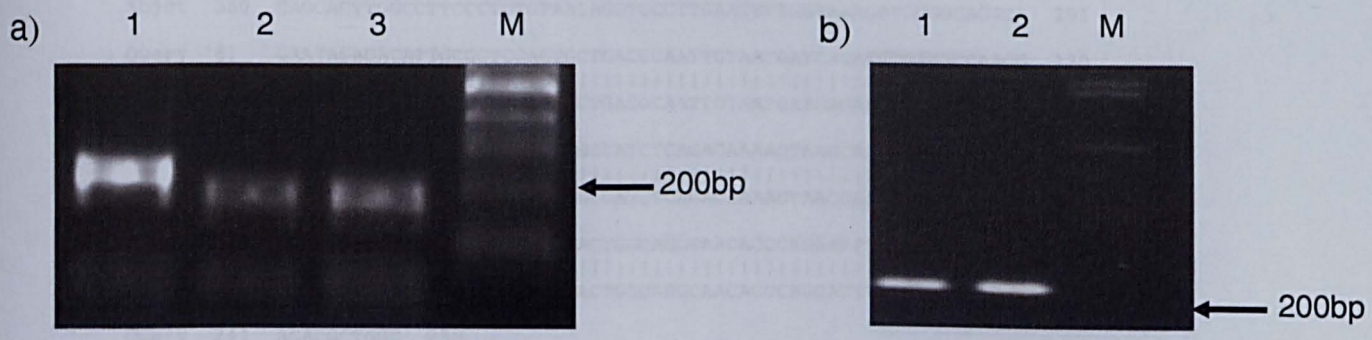

Figure 3.11: Agarose gel electrophoresis of **a)** HEp-2 cell and **b)** HaCaT cell PCR products amplified using HBD1 Primer Set 1. **a)** Lanes 1, HBD1 amplification product; lanes 2 and 3 HBD3 amplification products (see Section 3.7); lane M, DNA size ladder. **b)** Lanes 1 and 2, HBD1 products; Lane M, DNA size ladder. The position of the 200bp size marker is given for each gel

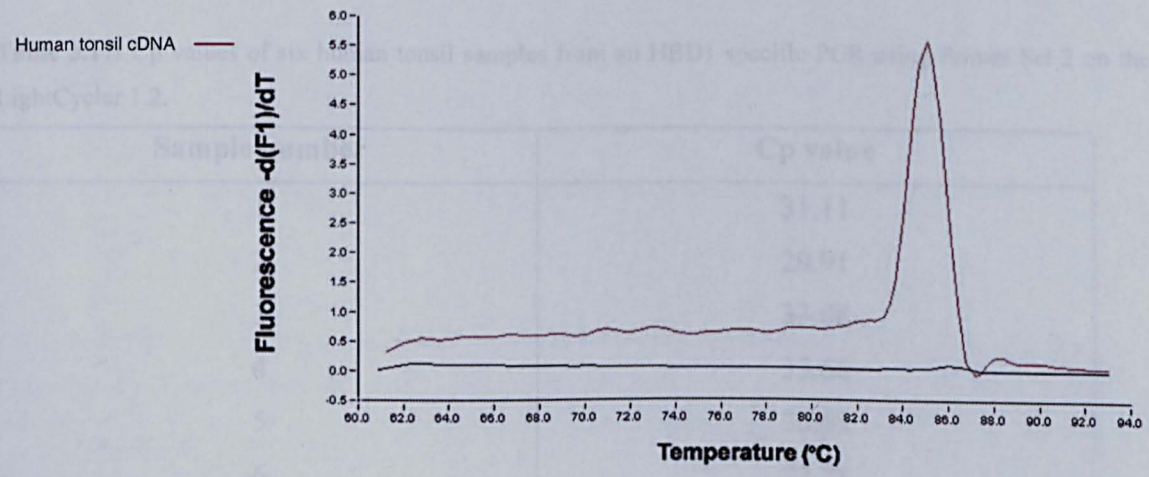

Figure 3.12: Melt peak analysis from real-time PCR generated from human tonsil cDNA using HBD1 Primer Set 1 and human tonsil cDNA. A single peak representing HBD1 can be seen at approximately 85°C. No product was detected in the no template control.

```
Query  1    CAGCACTTGGCCTTCCCTCTGTAACAGGTGCCTTGAATTTTGGTAAAGATCGGGCAGGCA  60
            ||||||||||||||||||||||||||||||||||||||||||||||||||||||||||||
Sbjct  350  CAGCACTTGGCCTTCCCTCTGTAACAGGTGCCTTGAATTTTGGTAAAGATCGGGCAGGCA  291

Query  61   GAATAGAGACATTGCCCTCCACTGCTGACGCAATTGTAATGATCAGATCTGTGGCCAAGG  120
            ||||||||||||||||||||||||||||||||||||||||||||||||||||||||||||
Sbjct  290  GAATAGAGACATTGCCCTCCACTGCTGACGCAATTGTAATGATCAGATCTGTGGCCAAGG  231

Query  121  CCTGTGAGAAAGTTACCACCTGAGGCCATCTCAGACAAAAGTAAGCAGAGAGTAAACAGC  180
            ||||||||||||||||||||||||||||||||||||||||||||||||||||||||||||
Sbjct  230  CCTGTGAGAAAGTTACCACCTGAGGCCATCTCAGACAAAAGTAAGCAGAGAGTAAACAGC  171

Query  181  AGAAGGTAGGAAGTTCTCATGGCGACTGGCAGGCAACACCCAGGATTTCAGGAACTGGGG  240
            ||||||||||||||||||||||||||||||||||||||||||||||||||||||||||||
Sbjct  170  AGAAGGTAGGAAGTTCTCATGGCGACTGGCAGGCAACACCCAGGATTTCAGGAACTGGGG  111

Query  241  AGACGCTGGC  250
            ||||||||||
Sbjct  110  AGACGCTGGC  101
```

Figure 3.13: Sequence of PCR product from human tonsil amplified using HBD1 Primer Set 2. Sequence analysis performed by BLAST (http://www.ncbi.nlm.nih.gov/blast/Blast.cgi) matched the cloned PCR product ('Query') to the Genbank sequence ('Sbjct') for HBD1 (NM_005218.3) with 100% identity.

Table 3.17: Cp values of six human tonsil samples from an HBD1 specific PCR using Primer Set 2 on the LightCycler 1.2.

Sample number	Cp value
1	31.11
2	29.91
3	33.68
4	33.66
5	30.05
6	27.78

Table 3.18: Cp values from a single human tonsil sample amplified with HBD1 Primer Set 2 on the LightCycler 1.2 in reactions with varying primer concentration.

Primer concentration (μM)	Cp value
1	31.92
1.5	33.36
2	34.00
2.5	34.14
3	34.09

Table 3.19: Cp values from a single human tonsil sample amplified with HBD1 Primer Set 2 on the LightCycler 1.2 in reactions with varying $MgCl_2$ concentration.

Total $MgCl_2$ concentration (mM)	Cp value
6	29.82
7	29.82
8	29.76
9	29.72
10	29.38
11	29.66
12	29.77
13	29.02

Table 3.20: Cp values from a single human tonsil sample amplified with HBD1 Primer Set 2 on the LightCycler 1.2 in reactions with varying annealing temperature.

Annealing temperature (°C)	Cp value
55	25.09
56	25.14
58	23.25
60	23.08

Table 3.21: Cp values of four tonsil samples from an HBD1 specific PCR using Primer Set 2 on the LightCycler 480.

Sample number	Cp value
1	27.35
2	28.00
3	27.77
4	28.17

Table 3.22: Cp values of four HaCaT cell samples from an HBD1 specific PCR using Primer Set 2 on the LightCycler 480.

Sample number	Cp value
1	33.20
2	35.05
3	33.01
4	33.46

Table 3.23: Cp values from a dilution series of cloned HBD1 PCR product, amplified with Primer Set 2 on the LightCycler 480. Dilution of miniprep and assigned arbitrary concentrations are shown. Used to plot the standard curve shown in Figure 3.14

Standard	Cp value	Dilution	Concentration (arbitrary value)
1	22.18	1 in $1.25x10^7$	15625
2	25.87	1 in $6.25x10^7$	3125
3	27.37	1 in $3.125x10^8$	625
4	32.85	1 in $1.5625x10^9$	125
5	34.84	1 in $7.8125x10^9$	25
6	37.09	1 in $3.90625x10^{10}$	5

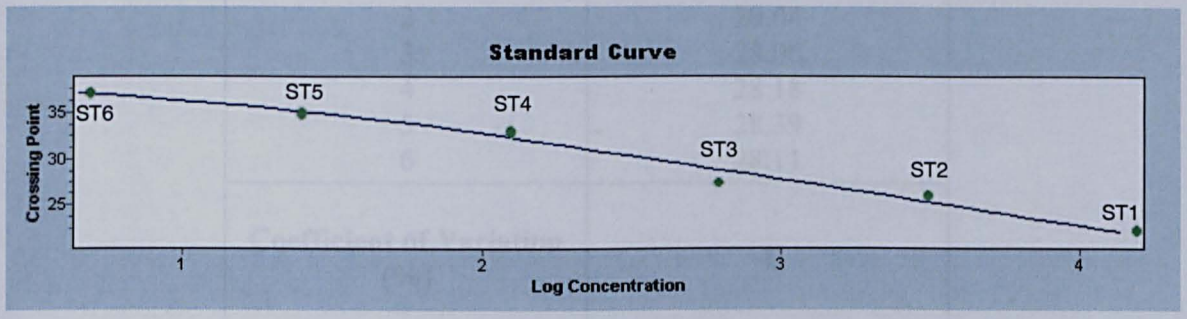

Figure 3.14: HBD1 standard curve plotted from dilution series shown in Table 3.23. Plot of log standard concentration vs. Cp (Cycle No.).

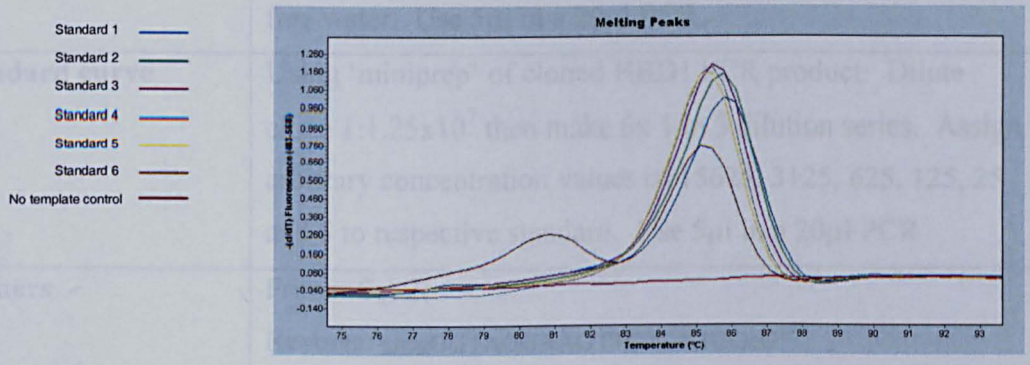

Figure 3.15: Melt peak analysis of HBD1 standards. A major peak representing HBD1 is seen at 86°C for all standards. Peaks are not generated in negative control reactions (ntc). A smaller peak at 81°C in standard 6 probably represents primer-dimer.

Table 3.24: Cp values from six independent PCR reactions from which the coefficient of variation of the assay was calculated.

Experiment	Cp
1	25.51
2	29.04
3	28.06
4	28.18
5	28.39
6	28.11
Coefficient of Variation (%)	**4**

Table 3.25: Summary of HBD1 assay.

Step	Process
Sample preparation	Reverse transcribe 1µg of RNA in a 50µl reaction using MMLV RNAseH$^+$ RT. Dilute product 1:2 with nuclease-free water. Use 5µl in a 20µl PCR.
Standard curve	Using 'miniprep' of cloned HBD1 PCR product: Dilute clone 1:1.25x10^7 then make 6x 1 in 5 dilution series. Assign arbitrary concentration values of 15625, 3125, 625, 125, 25 and 5 to respective standard. Use 5µl in a 20µl PCR
Primers	Primer Set 2: Reverse: cgccGGTAGGAAGTTCTCATGGcG[1] Forward: GTCAGCTCAGCCTCCAAAGGA Concentration: 1µM of each.
PCR instrument	LightCycler 480
Reaction mix	1x Probe Master (Roche).
PCR conditions	**Pre-incubation:** 2 min at 50°C, 2 min at 95°C. **45 cycles of:** 5s at 94°C, 10s at 60°C and 10s at 72°C. **Melt curve:** Performed over 60-95°C. Tm of product = 85°C **Cooling:** 40°C

Table 3.26: List of primer sets designed to amplify regions of the mRNA sequence encoding HBD2.

Primer set	Primer sequences (5'-3')	Position in cDNA/ base numbers in NM_004942	Predicted product size (bp)
1	Forward: CATCAGCCATGAGGGTCTTG	29-48	102
	Reverse: cgatcAAGGCAGGTAACAGGATcG[1]	132-113	
2	Forward: GTGAAGCTCCCAGCCATCAG	15-34	324
	Reverse: GATTGCGTATCTTTGGACACC	339-318	

[1] This primer was labelled with the fluorescent probe FAM, which excites at 488nM and emits at 518nM, at position 'c' and had a 5bp 5' extension (shown underlined) to enable hairpin formation for LUX assays.

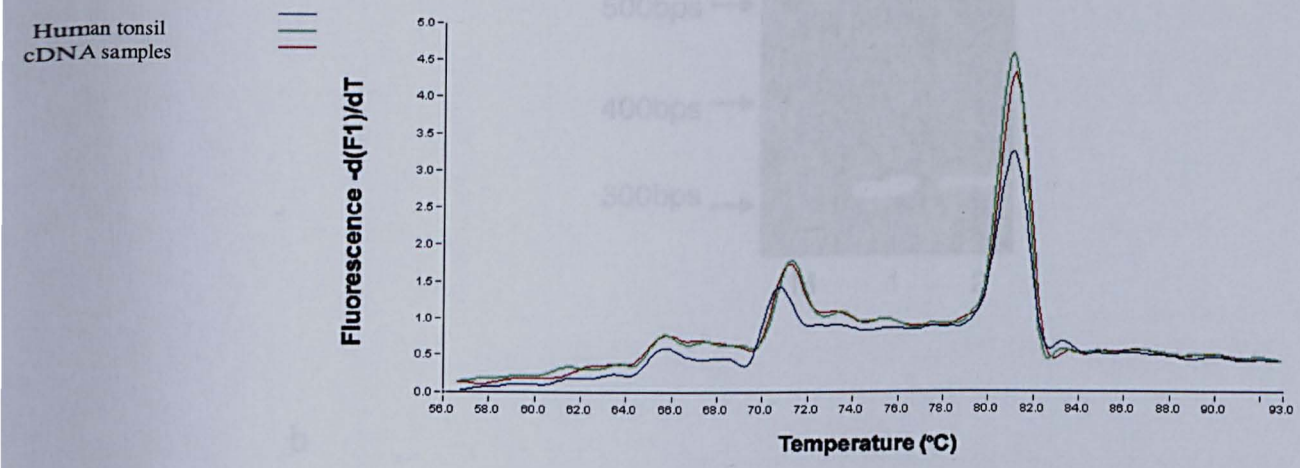

Figure 3.16: Melt peak analysis of PCR products generated from human tonsil cDNA with HBD2 Primer Set 1. A large peak representing HBD2 is seen at 81°C, a smaller peak representing primer-dimer is also seen at approximately 71°C.

a

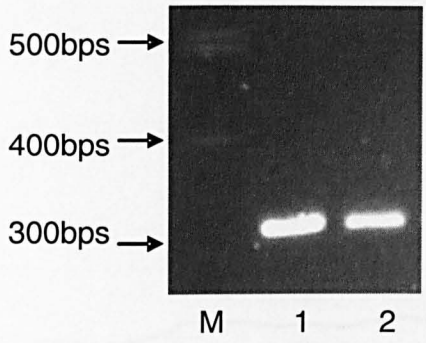

b

```
Query: 1   ccatgagggtcttgtatctcctcttctcgttcctcttcatattcctgatgcctcttccag 60
           ||||||||||||||||||||||||||||||||||||||||||||||||||||||||||||
Sbjct: 35  ccatgagggtcttgtatctcctcttctcgttcctcttcatattcctgatgcctcttccag 94

Query: 61  gtgtttttggtggtataggcgatcctgttacctgccttaagagtggagccatatgtcatc 120
           ||||||||||||||||||||||||||||||||||||||||||||||||||||||||||||
Sbjct: 95  gtgtttttggtggtataggcgatcctgttacctgccttaagagtggagccatatgtcatc 154

Query: 121 cagtcttttgcccctagaaggtataaacaaattggcacctgtggtctccctggaacaaaat 180
           ||||||||||||||||||||||||||||||||||||||||||||||||||||||||||||
Sbjct: 155 cagtcttttgcccctagaaggtataaacaaattggcacctgtggtctccctggaacaaaat 214

Query: 181 gctgcaaaaagccatgaggaggccaagaagctgctgtggctgatgcggattcagaaaggg 240
           ||||||||||||||||||||||||||||||||||||||||||||||||||||||||||||
Sbjct: 215 gctgcaaaaagccatgaggaggccaagaagctgctgtggctgatgcggattcagaaaggg 274

Query: 241 ctccctcatcagagacgtgcgacatgtaaaccaaattaaactatggtgtccaaagatacg 300
           ||||||||||||||||||||||||||||||||||||||||||||||||||||||||||||
Sbjct: 275 ctccctcatcagagacgtgcgacatgtaaaccaaattaaactatggtgtccaaagatacg 334

Query: 301 ca 302
           ||
Sbjct: 335 ca 336
```

Figure 3.17: a) Agarose gel electrophoresis of PCR products amplified using HBD2 Primer Set 2 from HaCaT cell (lane 1) and tonsil (lane 2) cDNA. The position of 300, 400 and 500bp size markers are shown. **b)** Sequence of the PCR product shown in lane 2, aligned to the HBD2 cDNA sequence. Sequence analysis performed by BLAST (http://www.ncbi.nlm.nih.gov/blast/Blast.cgi) matched the cloned PCR product ('Query') to the Genbank sequence ('Sbjct') for HBD2 (NM_004942) with 100% identity.

a)

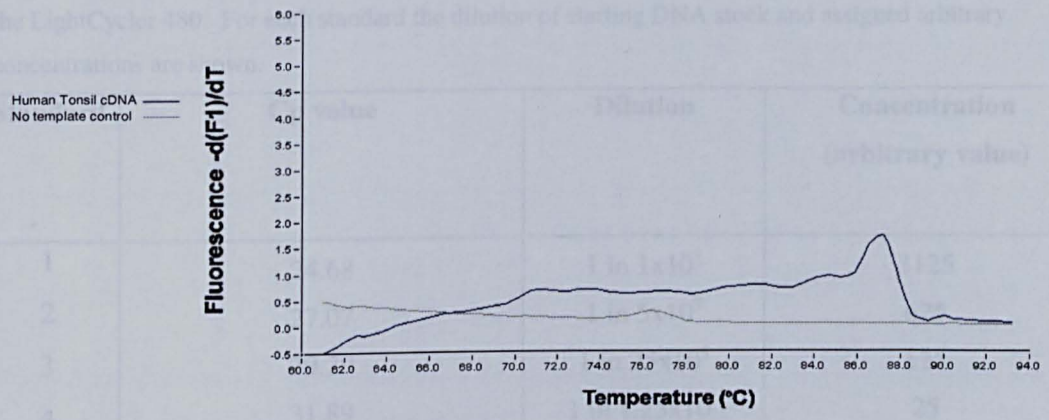

b)

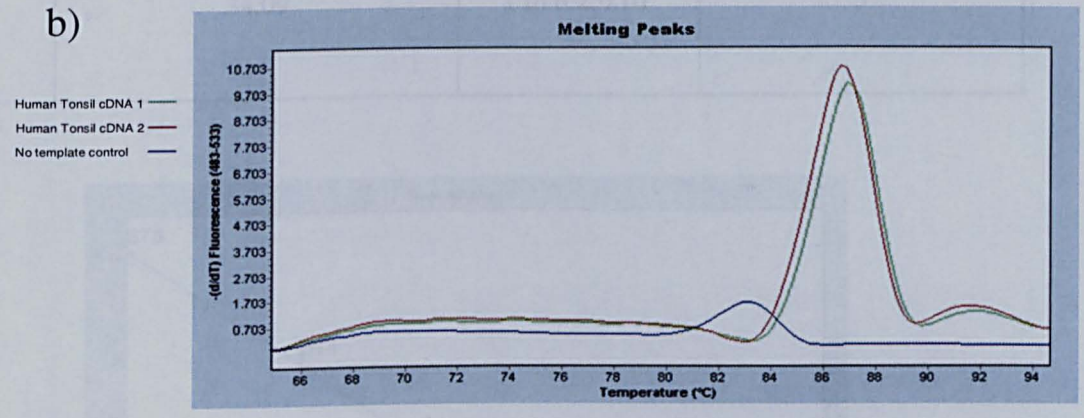

c)

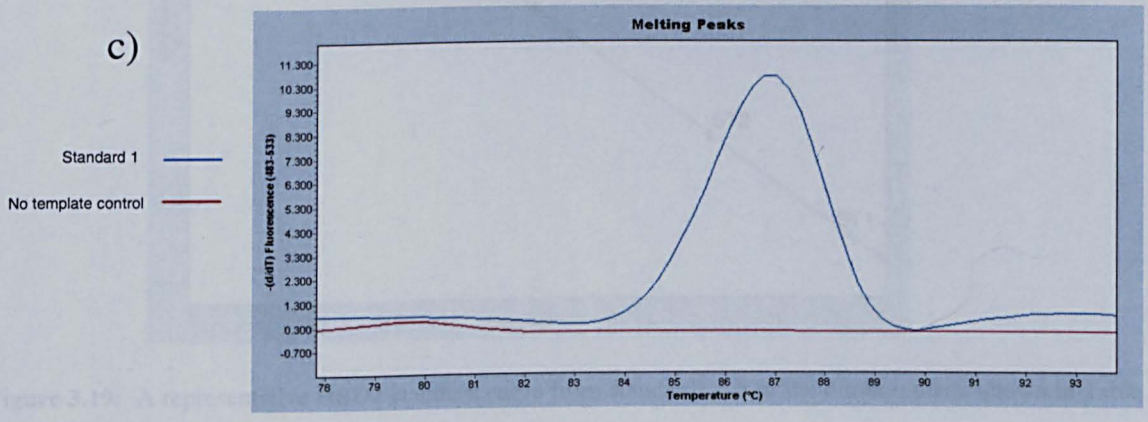

Figure 3.18: Melt peak analysis of PCR products generated from human tonsil cDNA with HBD2 specific primers. In **a)** a human tonsil sample was amplified using reverse-phase cartridge purified primers, **b)** shows the same sample amplified using HPLC-purified primers and in **c)** the HBD2 standard sample representative of all in standard curve (Figure 3.19) from the dilutions shown in Table 3.27. The standard was amplified using HPLC-purified primers.

Table 3.27: Cp values from a dilution series of cloned HBD2 PCR product, amplified with Primer Set 2 on the LightCycler 480. For each standard the dilution of starting DNA stock and assigned arbitrary concentrations are shown.

Standard	Cp value	Dilution	Concentration (arbitrary value)
1	24.68	1 in $1x10^7$	3125
2	27.07	1 in $5x10^7$	625
3	29.29	1 in $25x10^8$	125
4	31.89	1 in $1.25x10^9$	25
5	34.09	1 in $6.25x10^9$	5

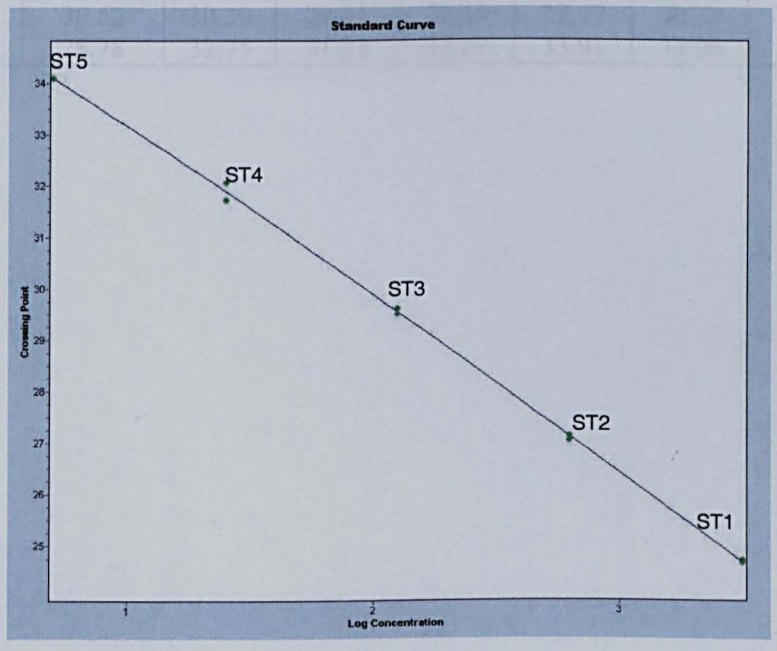

Figure 3.19: A representative HBD2 standard curve from standards 1-5 of the dilution series shown in Table 3.27. Plot of log standard concentration vs. Cp (Cycle No.).

Table 3.28: Cp values of three human tonsil samples from an HBD2 specific PCR using Primer Set 2.

Sample number	Cp (mean of 2 replicates)
1	34.04
2	29.53
3	30.94

Table 3.29: Cp values of HBD2 standards 1-4 from six independent PCR reactions from which the coefficient of variation for each was calculated.

	Experiment						Coefficient of variation (%)
	1	2	3	4	5	6	
Standard 1	24.99	24.80	23.69	24.11	24.66	25.8	3
Standard 2	27.26	27.75	25.45	26.82	27.59	28.31	4
Standard 3	30.52	30.30	28.41	29.49	29.97	30.77	3
Standard 4	28.78	32.75	31.33	32.27	33.91	33.06	6

Table 3.30: Summary of HBD2 assay.

Step	Process
Sample preparation	Reverse transcribe 1µg of RNA in a 50µl reaction using MMLV RNAseH$^+$ RT. Dilute product 1:2 with nuclease-free water. Use 5µl in a 20µl PCR reaction.
Standard curve	Dilute cloned HBD2 PCR product 1:1x10^7 then make 5x 1 in 5 dilution series. Assign concentrations of 3125, 625, 125, 25 and 5 to respective standards.
Primers	Primer Set 2 – HPLC purified Forward: GTGAAGCTCCCAGCCATCAG Reverse: GATTGCGTATCTTTGGACACC Concentration: 1µM of each
PCR instrument	LightCycler 480
Reaction mix	Sybr Green Master Mix (Roche).
PCR conditions	**Pre-incubation:** 2 min at 50°C, 2 min at 95°C. **45 cycles of:** 5s at 94°C, 10s at 58°C and 10s at 72°C. **Melt curve:** Performed over 60-95°C **Cooling:** 40°C

Table 3.31: List of primer sets designed to amplify regions of the mRNA sequence encoding HBD3.

Primer set	Primer sequences (5'-3')	Position in cDNA/ base numbers in NM_001081551	Predicted product size (bp)
1	Forward: gttccaggtcatggaggaatc Reverse: ccacactctcgtcatgtttcag	270-290 450-428	180
2	Forward: cgctgCCTTTTCATCCAGCTTCAGcG[1] Reverse: CCTGCCGATCTGTTCCTCCTTT	178-196 380-358	203

[1] This primer was labelled with the fluorescent probe FAM, which excites at 488nM and emits at 518nM, at position 'c' and had a 5bp 5' extension (shown underlined) to enable hairpin formation for LUX assays.

a)

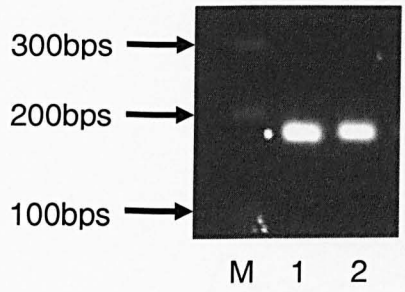

b)

```
Score =  390 bits (203),  Expect = 1e-105
Identities = 203/203 (100%), Gaps = 0/203 (0%)
Strand=Plus/Plus

Query  10   CCTTTTCATCCAGTCTCAGCGTGGGGTGAAGCCTAGCAGCTATGAGGATCCATTATCTTC  69
            ||||||||||||||||||||||||||||||||||||||||||||||||||||||||||||
Sbjct  178  CCTTTTCATCCAGTCTCAGCGTGGGGTGAAGCCTAGCAGCTATGAGGATCCATTATCTTC  237

Query  70   TGTTTGCTTTGCTCTTCCTGTTTTTGGTGCCTGTTCCAGGTCATGGAGGAATCATAAACA  129
            ||||||||||||||||||||||||||||||||||||||||||||||||||||||||||||
Sbjct  238  TGTTTGCTTTGCTCTTCCTGTTTTTGGTGCCTGTTCCAGGTCATGGAGGAATCATAAACA  297

Query  130  CATTACAGAAATATTATTGCAGAGTCAGAGGCGGCCGGTGTGCTGTGCTCAGCTGCCTTC  189
            ||||||||||||||||||||||||||||||||||||||||||||||||||||||||||||
Sbjct  298  CATTACAGAAATATTATTGCAGAGTCAGAGGCGGCCGGTGTGCTGTGCTCAGCTGCCTTC  357

Query  190  CAAAGGAGGAACAG  213
            ||||||||||||||
Sbjct  358  CAAAGGAGGAACAG  371
```

Figure 3.20. Analysis of HBD3 PCR products. **a)** Agarose gel electrophoresis of products from two HaCaT cell samples amplified using HBD3 Primer Set 1. Both samples generated a single band of approximately 180bp. **b)** Sequence of PCR product amplified from human tonsil cDNA with HBD3 Primer Set 2. Sequence analysis performed by BLAST matched the cloned PCR product ('Query') to the HBD3 cDNA sequence ('Sbjct'; Genbank Accession no. NM_001081551) with 100% identity

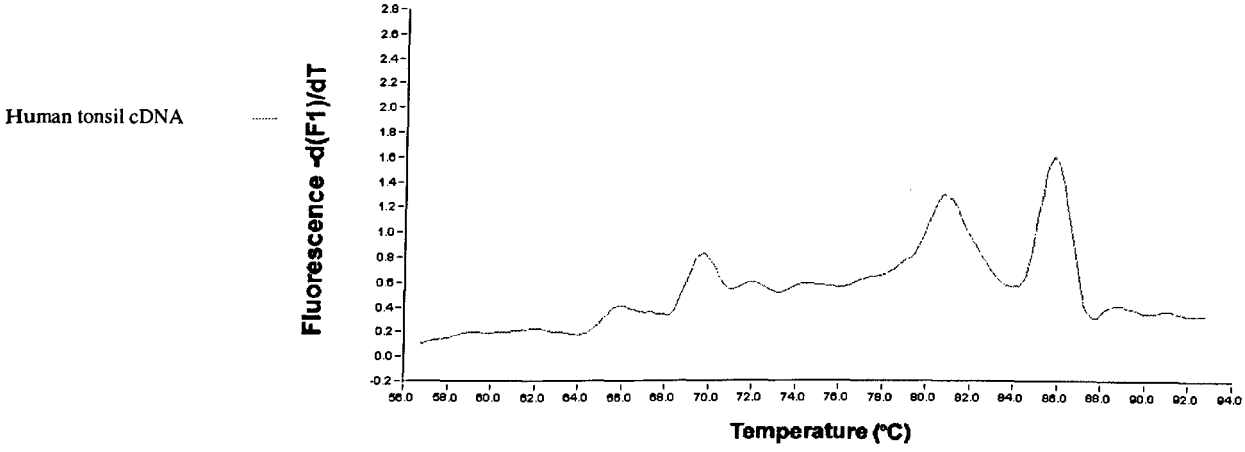

Figure 3.21: Melt peak analysis of PCR products generated from human tonsil cDNA with HBD3 Primer Set 2. A large peak representing HBD3 is seen at 85°C. Other smaller peaks, including one representing primer-dimer at 81°C, are representative of non-specific reaction products.

Table 3.32: Sequence of oligonucleotide primers used to amplify a region of the mRNA sequence encoding human hepcidin.

Primer set	Primer sequences (5'-3')	Position in cDNA (base numbers in NM_021175)	Predicted product size (bps)
1	Forward: CAGTGGCTCTGTTTTC Reverse: GTCTTGCAGCACATCCCACAC	104-119 289-268	186

a)

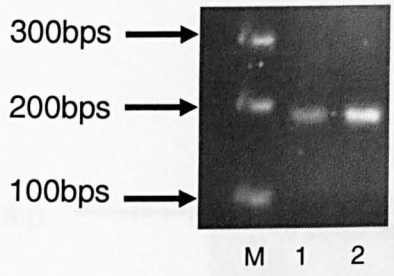

b)

```
Query: 12  agtggctctgttttcccacaactagacanggacaacttgcntaagctgcaaccccagnac 71
           ||||||||||||||||||||||| ||||  ||||||||||  | ||||||||||||| ||
Sbjct: 117 agtggctctgttttcccacaac-agac-gggacaacttgcaga-gctgcaaccccaggac 173

Query: 72  agagctggagccagggccaactggatgcccatgttncagangcgaangaggcgangacac 131
           |||||||||||||||||| |||||||||||||| |||| ||||| ||||||| |||||
Sbjct: 174 agagctggagccagggccagctggatgcccatgttccagaggcgaaggaggcga-gacac 232

Query: 132 ccacttccccatctgcattttcttgcctgcaggctgcttgtcatcgatcaaagtgtggg 190
           ||||||||||||||||||||||| || |||| ||||| ||||||||||||||||||||
Sbjct: 233 ccacttccccatctgcattttct-gc-tgc-ggctgc-tgtcatcgatcaaagtgtggg 287
```

Figure 3.22. Analysis of hepcidin PCR products. **a)** Agarose gel electrophoresis of PCR products from two HaCaT cell samples amplified using hepcidin primers. Both samples generated a single band of approximately 190bp. **b)** Sequence of PCR product amplified from human tonsil cDNA with hepcidin Primer Set 1. Sequence analysis performed by BLAST matched the cloned PCR product ('Query') to the hepcidin cDNA sequence ('Sbjct'; Genbank Accession no. NM_021175) with 91% identity.

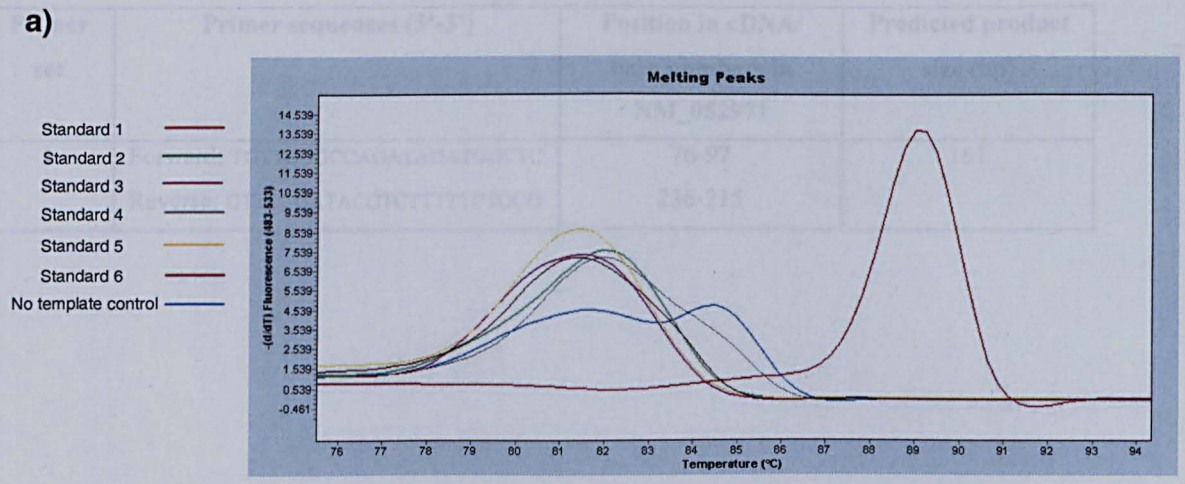

Figure 3.23: Analysis of real-time PCR products generated form the cloned hepcidin target sequence amplified with hepcidin specific primers. **a)** Melt curve analysis. For standard 1 a peak representing hepcidin was seen at 89°C. For all other standards peaks representing primer-dimer were seen at approximately 82°C. PCR products were not formed in the no template control; **b)** Agarose gel electrophoresis of products from standards 1, 2 and 6 shown in **a)**. Only for standard 1 is a band of the predicted size (~190bp) visible. Lane M, DNA size ladder; lanes 1 and 2, standard 1 products; lane 3, standard 2 product; lanes 4 and 5, standard 6 product. The position of the 200bp and 25 bp markers are indicated.

Table 3.33: Sequence of oligonucleotide primers designed to amplify regions of the mRNA sequence encoding human LEAP-2.

Primer set	Primer sequences (5'-3')	Position in cDNA/ base numbers in NM_052971	Predicted product size (bp)
1	Forward: TGTTGGGCCAGATAGATGGCTC Reverse: GTTCCGATACGTCTTTTTCTGCG	76-97 236-215	161

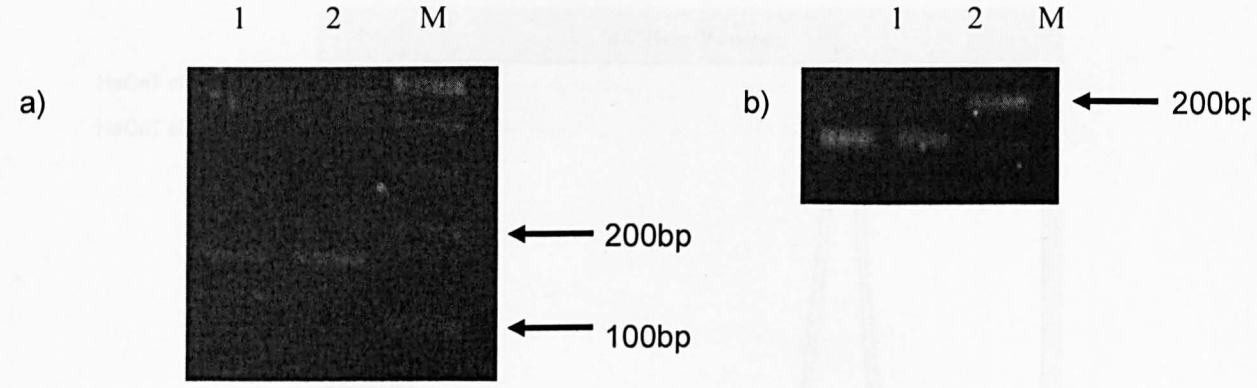

(c)

```
Query  1    TGTTGGGCCAGATAGATGGCTCCCCAATACCAGAAGTGAGTTCGGCAAAGAGAAGGCCAC  60
            ||||||||||||||||||||||||||||||||||||||||||||||||||||||||||||
Sbjct  76   TGTTGGGCCAGATAGATGGCTCCCCAATACCAGAAGTGAGTTCGGCAAAGAGAAGGCCAC  135

Query  61   GGAGAATGACCCCATTTTGGAGAGGGGTTTCCCTCAGGCCTATTGGAGCCTCCTGCCGGG  120
            ||||||||||||||||||||||||||||||||||||||||||||||||||||||||||||
Sbjct  136  GGAGAATGACCCCATTTTGGAGAGGGGTTTCCCTCAGGCCTATTGGAGCCTCCTGCCGGG  195

Query  121  ATGATTCTGAGTGTATCACAAGGCTATGCAGAAAAAGACGC  161
             |||||||||||||||||||||||||||||||||||||||
Sbjct  196  ATGATTCTGAGTGTATCACAAGGCTATGCAGAAAAAGACGC  236
```

Figure 3.24: Analysis of PCR products amplified with LEAP-2 specific primers. **a)** Agarose gel electrophoresis of human tonsil PCR. Lanes 1 and 2, human tonsil samples; lane M, DNA size marker. LEAP-2 PCR products can be seen at approximately 160bp. **b)** Agarose gel electrophoresis of HaCaT cell PCR products. Lanes 1 and 2, HaCaT samples; lane M, DNA size marker. LEAP-2 PCR products can be seen at approximately 160bp. **c)** Sequence of PCR product. Sequence analysis performed by BLAST (http://www.ncbi.nlm.nih.gov/blast/Blast.cgi) matched the cloned PCR product ('Query') to the Genbank sequence ('Sbjct') for LEAP-2 (NM_052971) with 100% identity.

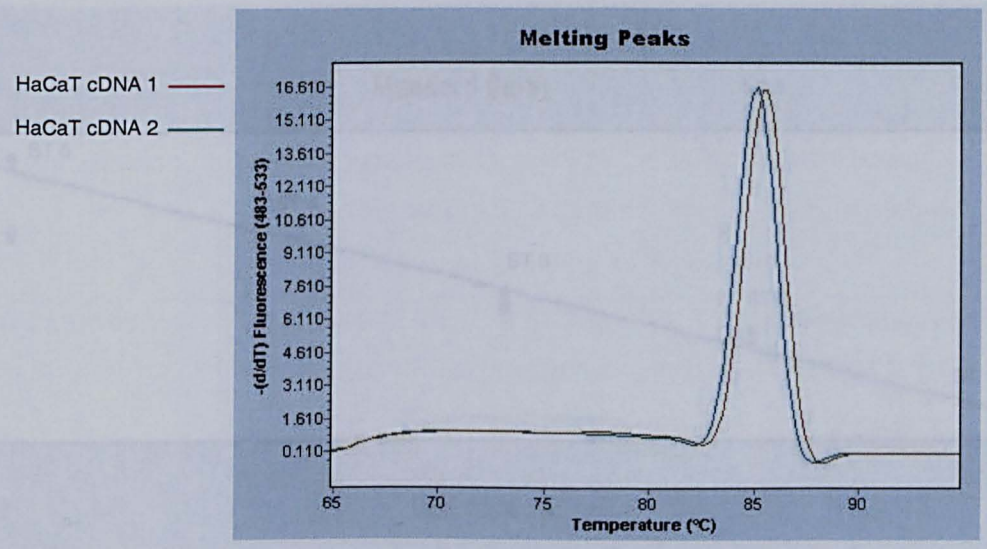

Figure 3.25: Melt peak analysis of PCR products generated from HaCaT cDNA with LEAP-2 Primer Set 1. Peaks representing LEAP-2 amplification products were seen at 85°C.

Table 3.34: Cp values from a dilution series of cloned LEAP-2 PCR product, amplified with Primer Set 1 on the LightCycler 480. For each standard the dilution of starting DNA stock and assigned arbitrary concentrations are shown.

Standard	Cp value	Dilution	Concentration (arbitrary value)
1	23.53	1 in $1x10^6$	3125
2	26.42	1 in $5x10^6$	625
3	27.75	1 in $25x10^7$	125
4	33.98	1 in $1.25x10^8$	25
5	32.08	1 in $6.25x10^8$	5

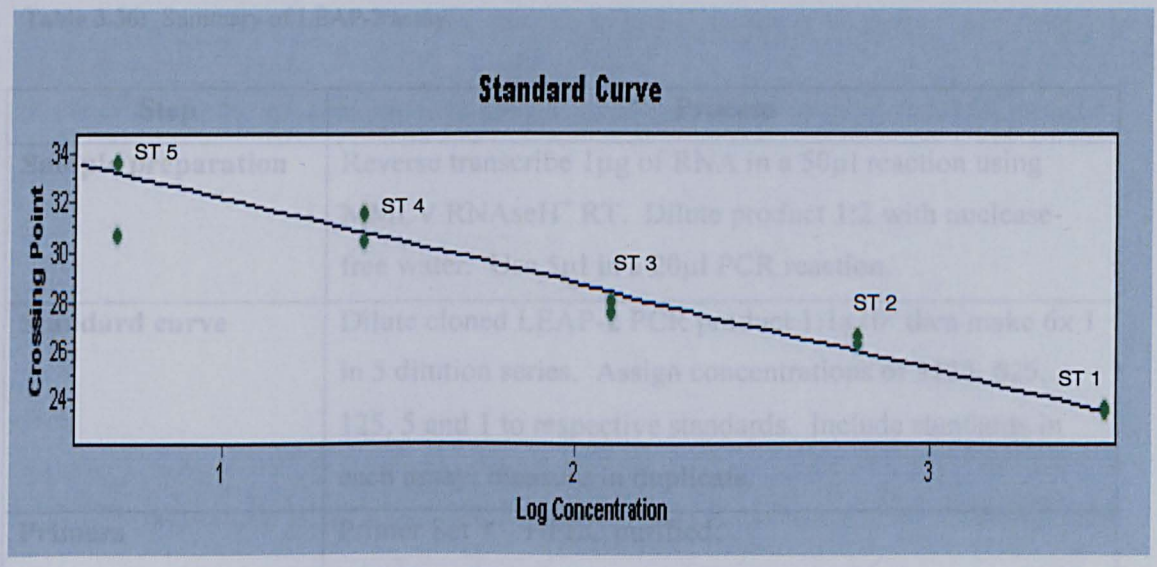

Figure 3.26: A representative LEAP-2 standard curve from standards 1-5 of the dilution series shown in Table 3.34. Plot of log standard concentration vs. Cp (Cycle No.).

Table 3.35: Cp values of LEAP-2 standards 1-4 from six independent PCR reactions from which the coefficient of variation for each was calculated.

Standard	Experiment						Coefficient of variation (%)
	1	2	3	4	5	6	
1	33.39	27.69	27.68	30.93	27.79	27.75	**8**
2	34.50	30.05	30.05	35.04	29.88	29.89	**8**
3	35.18	32.26	32.26	39.05	32.88	32.05	**8**
4	37.00	33.88	33.88	38.41	34.10	33.90	**6**

Table 3.36: Summary of LEAP-2 assay.

Step	Process
Sample preparation	Reverse transcribe 1µg of RNA in a 50µl reaction using MMLV RNAseH$^+$ RT. Dilute product 1:2 with nuclease-free water. Use 5µl in a 20µl PCR reaction.
Standard curve	Dilute cloned LEAP-2 PCR product 1:1x10^6 then make 6x 1 in 5 dilution series. Assign concentrations of 3125, 625, 125, 5 and 1 to respective standards. Include standards in each assay; measure in duplicate.
Primers	Primer Set 1 – HPLC purified: Forward: TGTTGGGCCAGATAGATGGCTC Reverse: GTTCCGATACGTCTTTTTCTGCG Concentration: 1µM of each.
PCR instrument	LightCycler 480
Reaction mix	1x Sybr Green Master Mix (Roche).
PCR conditions	**Pre-incubation:** 2 min at 50°C, 2 min at 95°C. **45 cycles of:** 5s at 94°C, 10s at 58°C and 10s at 72°C. **Melt curve:** Performed over 60-95°C **Cooling:** 40°C

Table 3.37: Sequence of oligonucleotide primers designed to amplify a fragment of the mRNA sequence encoding human GAPDH.

Primer set	Primer sequences (5'-3')	Position in cDNA (base numbers in NM_002046)	Predicted product size (bp)
1	Forward: CGGAGTCAACGGATTTGGTC Reverse: CCGTTCTCAGCCTTGA	120-139 279-296	177

```
Query  15   GGGCTGCTTTTAACTCTGGTAAAGTGGATATTGTTGCCATCAATGACCCCTTCATTGACC  74
            ||||||||||||||||||||||||||||||||||||||||||||||||||||||||||||
Sbjct  161  GGGCTGCTTTTAACTCTGGTAAAGTGGATATTGTTGCCATCAATGACCCCTTCATTGACC  220

Query  75   TCAACTACATGGTTTACATGTTCCAATATGATTCCACCCATGGCAAATTCCATGGCAC  132
            ||||||||||||||||||||||||||||||||||||||||||||||||||||||||||
Sbjct  221  TCAACTACATGGTTTACATGTTCCAATATGATTCCACCCATGGCAAATTCCATGGCAC  278
```

Figure 3.27: GAPDH sequence. Sequence analysis performed by BLAST (http://www.ncbi.nlm.nih.gov/blast/Blast.cgi) matched the PCR product ('Query') to the Genbank sequence ('Sbjct') for GAPDH (NM_002046) with 100% identity.

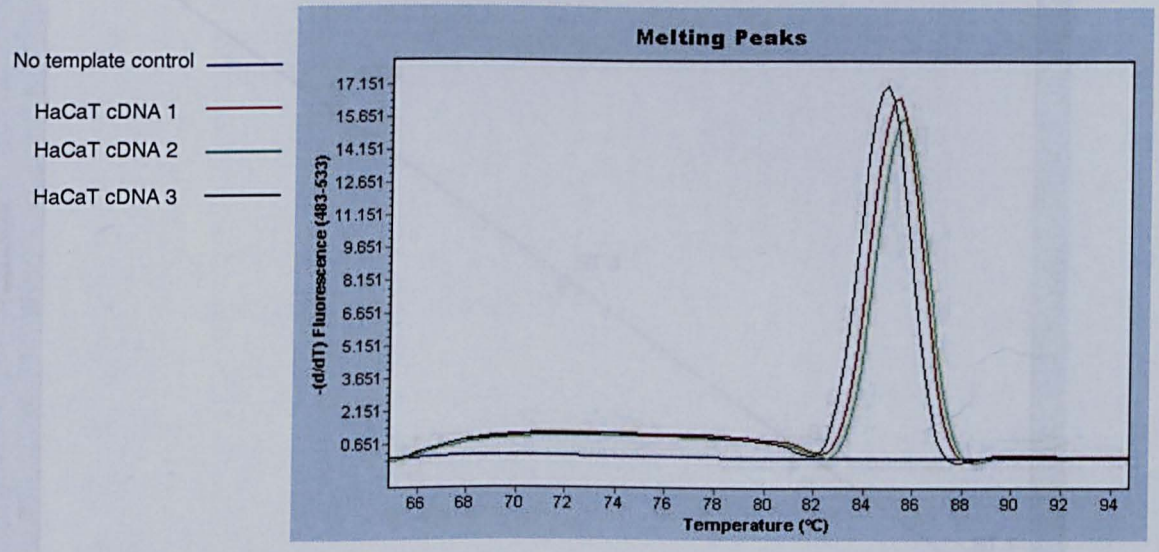

Figure 3.28: Melt peak analysis of PCR products generated from three HaCaT cDNA samples 1-3 with GAPDH Primer Set 1. Peaks representing GAPDH were seen at 85°C for all three samples. The negative control (ntc) did not have a melt peak.

Table 3.38: Cp values from a dilution of GAPDH cDNA, amplified with Primer Set 1 on the LightCycler 480). Dilution of cDNA and arbitrary values are shown.

Standard	Mean Cp value (2 replicates)	Dilution	Concentration (arbitrary value)
1	22.58	1 x $1x10^2$	16
2	23.63	0.5 x $1x10^2$	8
3	24.75	0.25 x $1x10^2$	4
4	25.73	0.125 x $1x10^2$	2
5	26.90	0.0625 x $1x10^2$	1

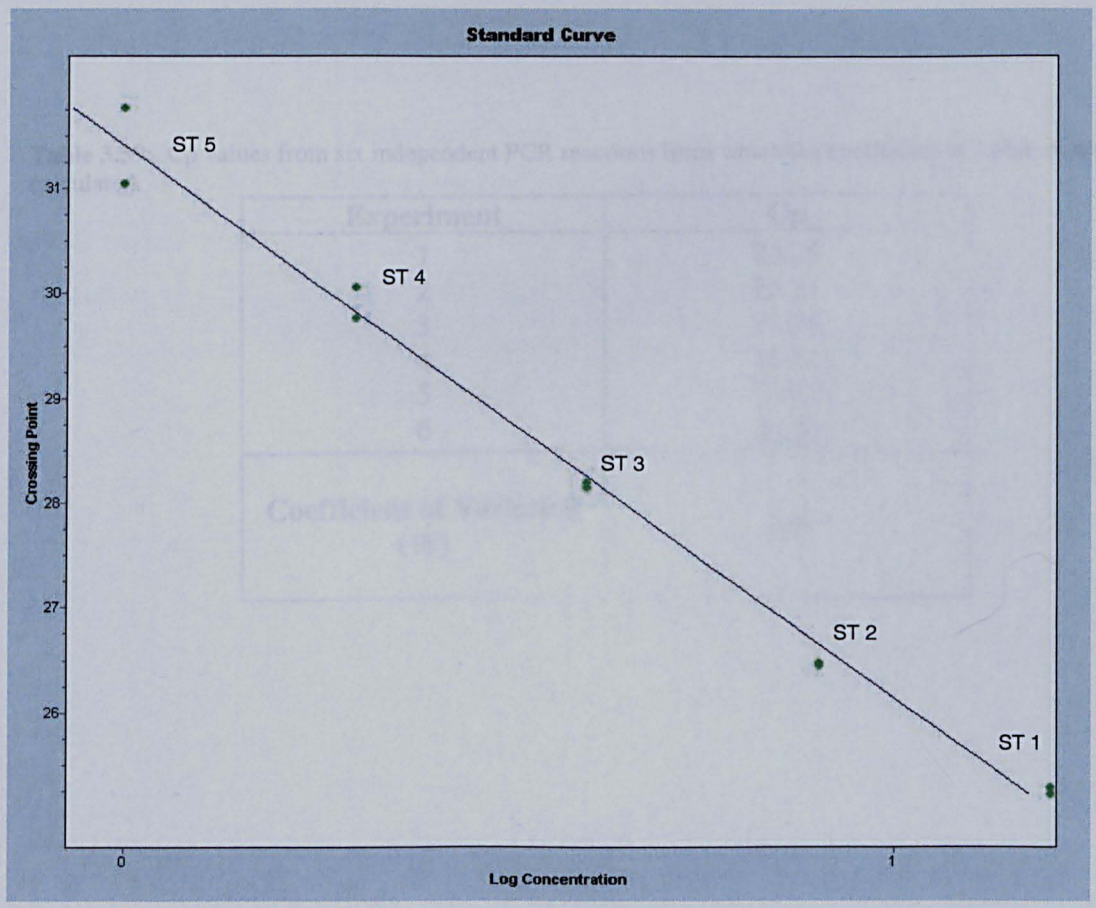

Figure 3.29: GAPDH standard curve from dilution series shown in Table 3.38. Plot of log standard concentration vs. Cp value (Cycle No.).

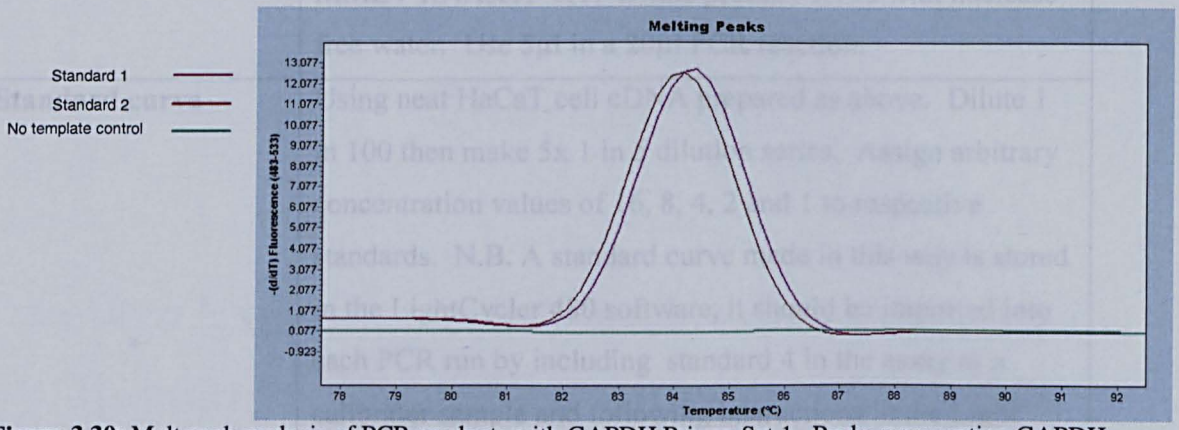

Figure 3.30: Melt peak analysis of PCR products with GAPDH Primer Set 1. Peaks representing GAPDH were seen at 84.5°C

Table 3.39: Cp values from six independent PCR reactions from which the coefficient of variation was calculated.

Experiment	Cp
1	25.25
2	25.21
3	25.14
4	25.21
5	25.52
6	28.30
Coefficient of Variation (%)	**0.5**

Table 3.40: Summary of GAPDH assay.

Step	Process
Sample preparation	Reverse transcribe 1µg of RNA in a 50µl reaction using MMLV RNAseH$^+$ RT. Dilute product 1:100 with nuclease-free water. Use 5µl in a 20µl PCR reaction.
Standard curve	Using neat HaCaT cell cDNA prepared as above. Dilute 1 in 100 then make 5x 1 in 5 dilution series. Assign arbitrary concentration values of 16, 8, 4, 2 and 1 to respective standards. N.B. A standard curve made in this way is stored in the LightCycler 480 software, it should be imported into each PCR run by including standard 4 in the assay as a calibrator sample and following instructions in the Light Cycler software.
Primers	Primer Set 1 -HPLC purified: Forward: CGGAGTCAACGGATTTGGTC Reverse: CCGTTCTCAGCCTTGA Concentration: 1µM of each.
PCR instrument	LightCycler 480
Reaction mix	1x Sybr Green Master Mix (Roche).
PCR conditions	**Pre-incubation:** 2 min at 50°C, 2 min at 95°C. **45 cycles of:** 5s at 94°C, 10s at 58°C and 10s at 72°C. **Melt curve:** Performed over 60-95°C **Cooling:** 40°C

Chapter 4

In Vivo Expression of Antimicrobial Peptides in Human Tonsils from Control and Tonsillitis Patients

4.1 Introduction

Human palatine tonsils play important roles in host immunity at both local and systemic levels. Their localisation at the openings of both the gastrointestinal and respiratory tracts make them ideal antigen sampling organs that function to alert the primary and secondary immune responses of the host. As described previously each palatine tonsil has a lymphoid core, encapsulated by a stratified, non-keratinising epithelium. This protective epithelial layer provides not only a physical barrier but also through the synthesis of antimicrobial peptides (AMP) an effective innate defence mechanism (Bals 2000). Although tonsils provide a shield against invading pathogens, the Gram-positive bacterium, *S. pyogenes* often breaches these defences and causes tonsillitis. This infection is often recurrent and sufferers present with swollen and painful palatine tonsils. Treatment is, in the first instance, with antibiotics such as erythromycin or penicillin which are prescribed to stop the infection and to reduce swelling in the tonsils. Often, when the infection is severe or recurrent, a tonsillectomy may be undertaken and in fact approximately 65 out of every 10,000 British children undergo this procedure each year (Van Den Akker, Hoes et al. 2004). However despite tonsillitis being relatively common, the physiological and immunological factors that allow this infection to perpetuate remain elusive.

Expressed at epithelial and mucosal surfaces, AMPs provide a first-line of defence against potential pathogens (Bals 2000). Moreover these molecules have also been reported to be up-regulated in response to infection (Schaller-Bals, Schulze et al. 2002). Globally, many studies have investigated the roles of AMPs in different disease states (Bajaj-Elliott, Fedeli et al. 2002; Chen, Schaller-Bals et al. 2004; Fahlgren, Hammarstrom et al. 2004; Heilborn, Nilsson et al. 2005; Voss, Wehkamp et al. 2006; Warnke, Springer et al. 2006), yet one area that is not well researched is the role of AMPs in the defence of the human palatine tonsils.

Prior to this study, Ball, working in Newcastle examined the expression and synthesis of LL-37, HBD1, HBD2, HBD3, hepcidin and LEAP-2 in tonsil samples using end-point PCR and immunohistochemical analyses (Ball, Siou et al. 2007). The molecular results suggested that the LL-37, HBD1, HBD2, HBD3 and hepcidin and LEAP-2 genes were

expressed in whole tonsils removed from control subjects for sleep apnoea and snoring (n=2), and in tonsils excised from patients suffering RAT (n=13). However the sample size of the study was small and the levels of expression of each AMP were not determined.

The hypothesis was therefore proposed that a defect in the innate immune response involving host AMPs, such as a deficiency in AMP expression at the epithelial surface and/or a failure of the AMPs to up-regulate in response to infection, is a cause or contributory factor to recurrent acute tonsillitis. To investigate this further a total of 93 tonsil samples excised from control and RAT patients respectively were analysed to determine and compare AMP mRNA expression profiles using the more accurate quantitative real-time PCR assays described in Chapter 3.

4.2 Subjects and Methods

Tonsils were collected with informed consent from patients undergoing tonsillectomy for recurrent acute tonsillitis (RAT) or for reasons other than bacterial tonsillitis, such as obstructive sleep apnoea, snoring or enlarged tonsillar crypts (control non-RAT).

4.2i Sample size

Prior to the study, power calculations were completed to ascertain the patient sample size required to show statistically significant trends or differences within the data. These were performed in conjunction with Dr Tom Chadwick (School of Population and Health Sciences). The number of patient samples required for the study was based on power calculations performed on preliminary data in Mini-Tab 14.

The sample size calculation was based on the use of the 2-sample T-test to compare the mean value of epithelial LL-37 mRNA expression between the control (non-RAT) and RAT groups. The standard deviation (SD) of this measure was estimated as 1000 from

preliminary data and the detectable (clinically significant) difference was chosen to be 1000. We use a significance level of 0.05 and 80% power. For these choices a sample size of 17 per group would be required.

A similar calculation was made for lymphoid samples. Here, the SD of this measure was estimated as 1100 from preliminary data and the detectable (clinically significant) difference was chosen to be 1000. We use a significance level of 0.05 and 80% power. For these choices a sample size of 21 per group would be required.

Additionally, the differences observed between different tonsils from one individual, determined that each excised tonsil could be analysed as one sample.

4.3 Quantitative Real-Time PCR Analysis of Control Subjects and Tonsillitis Patients, Measuring LL-37, HBD1, HBD2 and LEAP-2 mRNA

Quantitative real-time PCR data measuring LL-37, LEAP-2, HBD1 and HBD2 mRNA expression in a total of 93 tonsil samples was analysed. A total of 37 samples were collected from control subjects and 56 samples were collected from patients undergoing tonsillectomy for RAT (the majority of which were not suffering from infection at the time of surgery). This sample size exceeded the number of samples predicted by power calculations to show significant differences. Tonsils are usually removed from tonsillitis sufferers when the patient is not experiencing an episode of tonsillitis, therefore it can be presumed that the majority of tonsils used in this study were excised when the patient was not suffering an active infection. The decision as to when the patient is in a suitable condition for tonsillectomy was taken by the clinician. Upon removal tonsils from chronic tonsillitis sufferers often showed signs of necrosis or scarring. Heavily scarred areas of epithelium were difficult to dissect from the lymphoid core but were still used in experiments when possible. Tonsils excised from control patients tended to be large and relatively unscarred. All data were adjusted to GAPDH mRNA and data analyses were performed.

As variation between samples was seen to be large, any samples which were outside of ± two standard deviations of the mean were not included in analyses. If the inclusion of these samples made a statistically significant difference to the data sets and therefore the final graphs and conclusions they were included in the data set. The inclusion or exclusion of the samples lying outside the normal range is stated in the Figure legend of each graph.

For data analysis involving two groups of data an unpaired T-test was performed. This test was chosen following guidelines in the Prism statistical guide which is included with the software, (Motulsky 2003) as the two groups of data for analysis were not matched i.e. the data were not before/after data, or samples from twins or parent child pairs etc. For data analysis involving more than three groups of data a one way ANOVA was used followed by a Bonferroni post-test as appropriate as each data set was required to be compared to each other set. Prism guidelines were once again followed to determine choice of test.

4.3.1 All patient samples

The quantitative real-time PCR data collected from all the subjects were analysed initially to investigate AMP gene expression in the whole sample population in terms of tissue type (epithelial or lymphoid).

4.3.1i Epithelial and lymphoid tissues

Patient samples were classified based on tissue type. Data from epithelial samples, dissected from the undulating outer surface of the tonsils were compared to data from samples from the lymphoid tissue core which was encapsulated by the epithelium.

The results for LL-37 mRNA expression are shown in Figure 4.1a. A total of 83 samples were analysed (49 epithelial and 34 lymphoid). The means ± the standard error of the mean (± SEM) of epithelial and lymphoid groups were similar, 16±7 and 10±1 arbitrary units (AU) respectively and no statistically significant differences were identified. The majority of samples from both groups were observed to express between 1 and 63AU of LL-37 mRNA. Two samples were recorded outside of this range.

A total of 88 tonsil samples were analysed for LEAP-2 mRNA expression, of which 55 were epithelial and 37 were lymphoid samples (Figure 4.1b). No statistically significant differences were recorded between the groups. As observed with LL-37 mRNA expression in Figure 4.1a, a number of out-lying points were observed within the epithelial group. These values related to samples from both control and RAT patients. Immunohistochemical analysis of RAT tonsil using an antibody to LEAP-2 (anti-human-LEAP-2 purified IgG (Phoenix Pharmaceuticals, G-075-40)), identified LEAP-2 immunoreactivity in both epithelial and lymphoid tissues (Figure 4.2).

HBD1 mRNA expression of 53 epithelial and 35 lymphoid samples is shown in Figure 4.1c. No statistically significant differences were observed between the groups. The values relating to HBD1 mRNA expression were however widespread (5-572AU). The samples with elevated HBD1 mRNA levels were identified and investigated further, but there was no correlation between the two groups i.e. no single subject or groups of subjects were high expressers in both epithelial and lymphoid groups respectively.

Figure 4.1d shows data relating to HBD2 gene expression from 92 tonsil samples (52 epithelial and 40 lymphoid). The epithelial samples expressed HBD2 mRNA at a statistically significantly higher level than the lymphoid samples ($P<0.05$). The mean (± SEM) values of the groups were 42±10 and 2±0AU for epithelial and lymphoid groups respectively.

4.3.2 Tissue type and disease state

To investigate the effects of recurrent acute tonsillitis (RAT) on AMP gene expression patterns the data from the control and diseased tonsils was compared (Figure 4.3).

The data from 84 tonsil samples analysed for LL-37 expression were considered in terms of disease state and tissue type (Figure 4.3a). The values recorded in the majority of the samples were between 0.1 - 43AU of LL-37 mRNA, although the measured values of two control epithelial samples, 63 and 127AU respectively, were elevated in comparison (Figure 4.3ai). The mean (± SEM) expression of LL-37 mRNA was not statistically different between groups.

The LEAP-2 mRNA expression data (Figure 4.3b) no statistically significant differences were seen between the mean values of the epithelial groups (means (± SEM) 13±5 and 10±3AU) respectively and the lymphoid groups (means (± SEM) 2±0 and 3±0AU respectively). However, it was observed that LEAP-2 mRNA expression was more variable in the epithelial compared to the lymphoid groups; LEAP-2 values in the epithelial groups ranged from 0.4 - 40AU whereas the values in the lymphoid tissues were focussed between 0.1-10AU. Two out-lying values shown in Figure 4.3bi, and recorded as 96 and 111AU respectively, were both epithelial derived; one was from the tonsil of a control (non-RAT) subject and the other from a RAT patient. A further sample, also of epithelial origin, with value of 201AU (Figure 4.1b) was not included in these analyses as all data was standardised to within ± two standard deviations of the mean of the group and any samples that fell outside of this limit, including this one was removed from the data set.

Analyses of the HBD1 mRNA expression results according to tonsil disease state are shown in Figure 4.3c. No statistically significant differences were observed. However, interestingly, a large range of HBD1 mRNA expression was observed in the epithelial tissues of the control and RAT tonsils (ranging between 5-516AU) and in the RAT lymphoid tissues not the control lymphoid tissues.

The HBD2 mRNA expression data of the control and RAT subject groups were similarly analysed (Figure 4.3d), once again no statistically significant differences were observed. As noted with HBD1, considerable variations in the epithelial HBD2 mRNA values were observed (0.1-955AU).

4.3.3 Gender

The HBD1 analyses indicated that gender may influence AMP expression profiles. To investigate this further all the AMP expression data was re-analysed according to the gender of the subjects.

4.3.3i Intra-gender differences

Analyses of the LL-37 and LEAP-2 mRNA expression data relating to the male subjects only (Figure 4.4a & b) revealed no statistically significant differences between the groups. No statistically significant differences were also seen in HBD1 and HBD2 mRNA expression levels between disease state and tissue type groups in males (Figure 4.4c & d).

Analyses of the data relating to tonsils excised from females was compromised by the reduced sample numbers (n=5 maximum in the control epithelial group). Analyses of the LL-37, LEAP-2, HBD1 and HBD2 mRNA expression data relating to the female subjects only (Figure 4.5a, d, c & d) revealed no statistically significant differences between the control or RAT groups from either tissue type.

4.3.3ii Gender and disease state

Presentation of all the tonsil AMP expression data in terms of gender is provided in Figures 4.6a-d. Despite the low sample numbers in some of the groups the patterns of LL-37 and LEAP-2 expression detected in males and females were comparable and no statistically significant differences between groups were recorded. After HBD1 and HBD2 mRNA expression analysis no statistically significant differences were seen. Interestingly, a large range of HBD1 mRNA expression was recorded, as seen previously in Figure 4.1 & 4.3.

4.3.4 Age of subject and disease state

Children between the ages of six and ten years present most frequently with tonsillitis (Batra, Safaya et al. 2004). Thus the tonsil AMP expression profiles of a group of children suffering recurrent acute tonsillitis were investigated and compared to those of similarly aged control children.

4.3.4i Expression of AMP mRNA in children <10 years old

Epithelial AMP expression data from patients who were <10 years old at the time of tonsillectomy is presented in Figure 4.7. The age range was three to nine years, and the median ages of the control and RAT groups were four years six months and five years respectively.

Comparison of the LL-37 mRNA expression data from 12 control and 15 RAT epithelial samples (22±11 compared to 8±2AU respectively) indicated no statistically significant difference in the mean values (Figure 4.7a). It was noted that two of the values determined in the control group (127 and 63AU respectively) were at least six to twelve times higher than the other values. However re-calculation of the data with these sample values excluded resulted in mean values of 7±2 and 8±2AU respectively and

only re-affirmed that tonsil LL-37 expression did not appear to be significantly altered in the young tonsillitis sufferers.

Similarly no statistical difference was observed between the mean LEAP-2 mRNA expression values of the two groups (Figure 4.7b). Indeed the values detected in each of the groups were comparable and in the range 0-40AU, with a sample indicative of very high expression detected in the control group (96AU respectively) and one in the RAT group (111AU).

Comparison of the mean values relating to the HBD1 mRNA expression (Figure 4.7c) determined that no statistically significant differences were present in the data. The values were however very variable, with expression values ranging from 0.1 to >500AU in both groups.

A similar pattern was observed in relation to HBD2 expression with no statistically significant difference recorded between the means of the control 75±28 AU and RAT 56±20 AU groups (Figure 4.7d). As observed with HBD1 mRNA, the expression values varied greatly, ranging from 0.1 to >200AU in both the control and RAT groups.

4.3.4ii Expression of AMP mRNA in under 45s compared to the over 45s.

It has also been reported in the literature that the proportion of asymptomatic carriers of *S. pyogenes,* known to be a causal factor in RAT, differs between those under and over 45 years of age (Hoffmann 1985). Thus the tonsil data was analysed to investigate whether AMP expression profiles of the control and RAT groups, further divided according to age i.e. >45 years or < 45 years respectively, differed. Unfortunately no data from samples excised from RAT patients >45 years were collected. These analyses included the AMP expression data relating to the children <10 years age.

The tonsil epithelial samples were analysed for LL-37 mRNA expression in relation to age and the results are presented Figure 4.8a. No statistically significant differences were seen between age groups in the control patients.

Analyses of the tonsil LEAP-2 gene expression data in relation to age are presented in Figure 4.8b. Again, as with the LL-37 data, no statistically significant differences were detected between the mean values of the three other groups.

The mean expression values of the HBD1 and HBD2 genes followed similar profiles (Figure 4.8c & d) and no statistical significant differences were detected between the groups.

4.3.5 Previous or current infections

As part of the study information was collected from the subjects regarding the time of their last sore throat or bout of tonsillitis. Although not confirmed clinically these data were used to investigate potential links between the levels of AMP mRNA expression and the time since each subject's last sore throat. For these analyses the AMP expression data was plotted according to the period of time since each subject's last sore throat i.e. currently, 1-4 weeks, 1-6 months, 6-12 months, 2-5 years or 'never'.

The complete data are presented in Figure 4.9. The LL-37 expression data is shown in Figure 4.9a. Each group, apart from the 6-12 month group, is characterised by the diverse spread of the LL-37 expression values and statistical analyses of the data revealed no significant differences between the groups.

Similar AMP expression profiles were observed in relation to LEAP-2, HBD1 and HBD2 expression (Figure 4.9b-d). In all cases statistical analyses of the data revealed no significant differences between the groups although again it should be noted that the 6 -12 months, 2-5 years or 'never' groups had small numbers of subjects.

4.4 Discussion

A pilot study by our group in Newcastle using end-point PCR investigated the expression of the genes encoding AMPs in tonsils excised from 13 RAT patients and two control (non-RAT) subjects. The molecular analyses suggested that the LL-37, HBD1, HBD2, HBD3 hepcidin and LEAP-2 genes were expressed in both sets of tonsils and, using semi-quantitative analyses, the results indicated that the tonsil epithelium expressed AMP mRNAs at increased levels compared to the lymphoid tissues (Ball, Siou et al. 2007). However the sample size of the study was small and the actual levels of expression of each AMP were not determined. Thus to address the hypothesis that a defect in the host innate immune response involving AMPs, such as a deficiency in AMP expression at the tonsil epithelial surface and/or a failure of the tonsil AMPs to up-regulate in response to infection, is a cause or contributory factor to recurrent acute tonsillitis a much larger study was conducted. In this study, the largest recorded to date, the levels of LL-37, HBD1, HBD2 and LEAP-2 AMP gene expression were quantified and compared in over ninety tonsils removed from control subjects and RAT patients.

Power calculations indicated that the data from groups of 21 control and RAT tonsils respectively was required to have an 80% chance of detecting differences at the 5% significance level, in the AMP expression levels of the epithelial and lymphoid tissues. A total of 93 tonsil samples (37 from control subjects and 56 from RAT patients) were analysed. Moreover the tonsils removed from the control subjects were considered as healthy organs as the controls comprised those individuals referred to surgery to address problems such as sleep apnoea and snoring caused, in the main, by enlarged but functionally 'normal' tonsils. As such the reduced numbers of control tonsils reflected the smaller numbers of patients referred to surgery to address such problems.

Initial analyses of the AMP data compared the levels of AMP expression in the epithelial and lymphoid layers of all tonsils. The mean data indicated that the levels of HBD2 mRNA expression were significantly higher, by approximately twenty-fold, in the epithelium compared to the lymphoid tissues. In contrast no significant differences were observed in relation to the LL-37, HBD1 and HBD2 expression patterns. These

results conflicted with those observed previously (Ball, Siou et al. 2007), but can probably be explained by the more sensitive real-time analyses used in this study and the increased sample size. However in some respects the LL-37, HBD1 and HBD2 results were unexpected. The tonsil epithelium functions in part as a physical barrier against potential pathogens and the AMPs can be considered as an 'antiseptic layer' on its surface. Thus from an initial defence point of view it would be more efficient if the AMP levels were higher in the outer epithelial layers than the inner lymphoid tissues. However this study investigated only AMP gene expression and it is feasible that the encoded peptide concentrations were higher in the epithelial layers. Indeed previous work reported by our group using frozen sections of tonsil and antibodies to the AMPs showed HBD1, HBD2, HBD3 and LL-37 peptides to be localised specifically to the surface epithelium rather than the lymphoid tissues, and to be reduced in the surface epithelia of tonsils from RAT patients (Ball, Siou et al. 2007).

Furthermore comparison of the mean epithelial LL-37, HBD1, HBD2, LEAP-2 data in relation to the control and RAT tonsils did not support any differences in the levels of AMP gene expression. A similar picture was evident for the lymphoid tissues. These data therefore countered our original hypothesis that a deficiency in AMP expression at the tonsil epithelial surface contributes to recurrent acute tonsillitis (RAT). It was also proposed that RAT is caused by a failure of the AMPs to up-regulate in response to infection. AMPs are induced in host cells in response to microbes (Dorschner, Pestonjamasp et al. 2001; Chromek, Slamova et al. 2006; Rivas-Santiago, Hernandez-Pando et al. 2008) and as the RAT patients recruited to the study were about to undergo a tonsillectomy and thus presumably infection free it was perhaps not surprising that elevated levels were not observed.

Reports have been published which show that the cathelicidin LL-37 is particularly active against *S. pyogenes* (Nizet, Ohtake et al. 2001; Lee, Ohtake et al. 2005) the major bacterial cause of tonsillitis. Some patients recruited to the study indicated recent bouts of sore throat or tonsillitis prior to their surgery and it was perhaps unexpected therefore that there were no significant clusters of elevated LL-37 values in either the epithelial or lymphoid RAT samples. However the data may have reflected the reliability of patient self-diagnosis. Conversely, the commensal *Streptococcus salivarius* K12 has been shown to promote down-regulation of innate immune responses in epithelial cells

through the inhibition of activation of the NFκB pathway (Cosseau, Devine et al. 2008). It is therefore feasible that the pathogenic streptococci involved in RAT, if present, were able to prevent the up-regulation of AMP gene expression in the tonsil epithelium. However a report, in which the up-regulation of cathelicidin mRNA transcripts in tonsils excised from patients with RAT is described (Song, Hwang et al. 2006), does not support this. The semi-quantitative RT-PCR data provided in their study indicated that LL-37 was expressed at very low levels in tonsils removed from control subjects, and in fact cDNA bands indicative of expression were not visible on their ethidium bromide stained gels. LL-37 transcripts were in contrast identified in all control tonsils analysed in the Newcastle study and moreover peptide was detected in the tonsillar epithelia of control subjects (Ball, Siou et al. 2007). Thus my observations and those of Song, Hwang et al (2006) are difficult to reconcile, but the data reported in this study do not support the up-regulation of AMP gene expression in tonsils excised from RAT patients.

HBD1 is acknowledged classically as being constitutively expressed at epithelial surfaces and, as expected, statistical analyses of the RAT and control tonsil HBD1 expression data did not provide any significant differences between the groups. Indeed previous studies admittedly involving very small subject cohorts, have also reported HBD1 to be constitutively expressed in both control and RAT tonsils (Chae, Lee et al. 2001; Weise, Meyer et al. 2002; Wang, Dong et al. 2004). However the data obtained in my study was interesting with HBD1 expression values indicative, potentially, of high and low expresser subjects within the population (Figure 4.3c). When these data were further analysed according to the gender of the subjects from which the tonsils were taken it became obvious that high and low expressers existed in both male and female groups.

Recently, it has been reported that the expression of HBD1 can be regulated by circadian clock proteins (Sherman and Froy 2008). Thus it is feasible that the higher HBD1 levels observed in the study reflected the time of day a tonsil was excised. However as the majority of tonsils were excised between 8 and 10am this is probably unlikely, but not impossible as some tonsil samples were collected in the late afternoon. It has also been documented that female menstrual status affects the levels of the

antibacterial agent Secretory Leukocyte Protease Inhibitor, (SLPI). This molecule functioning in the innate defences of the body, has been identified in uterine cell secretions, and is increased in premenopausal compared postmenopausal females (Fahey and Wira 2002). Whether HBD1 is similarly affected by hormonal changes has not been reported although in this study elevated HBD1 values were observed in female subjects <10 years old, which dilutes, but does not eliminate the argument for hormones playing significant roles in HBD1 expression.

As described previously comparison of the RAT and control tonsil mean HBD2 levels did not indicate a significant difference in their levels and these data supported the results published in 2003 by (Claeys, de Belder et al. 2003). Again however the Newcastle study identified distinct populations of expressers within the epithelial group (Figure 4.1d), and like HBD1 these populations were found in both the control and RAT tonsil groups, and equally divided between male and female subjects. Reasons for the differences in individual HBD1 and HBD2 gene expression levels remain unknown although it is feasible that single nucleotide polymorphisms, for example in the 5' untranslated regions of the respective genes and affecting gene expression may be responsible.

Children between the ages of six and ten years present most frequently with tonsillitis (Batra, Safaya et al. 2004). Thus the tonsil AMP expression profiles of children <10 years of age and suffering recurrent acute tonsillitis were investigated, and compared to those of similarly aged control children. Statistical analysis of the data indicated that the AMP gene expression profiles of the two groups were similar although it was noted that the sample sizes, between 12 and 17 per group, were below those recommended by the power calculations to show a significant difference between groups. The data also highlighted that within the groups for each AMP were 'high' and 'low' expressers. Further investigation of the origins of these samples provided no obvious patterns e.g. the high HBD1 expressers were not high HBD2 expressers. Thus the tonsil AMP data did not provide an explanation as to why some children are susceptible to RAT compared to others.

It has also been reported in the literature that the proportion of asymptomatic carriers of *S. pyogenes,* known to be a causal factor in RAT, differs between those under and over

45 years of age (Hoffmann 1985). An aim therefore was to investigate whether the AMP expression profiles of the control and RAT groups, further divided according to age i.e. >45 years or < 45 years respectively, differed. However no tonsils from subjects aged >45 years were collected, which prohibited such analyses. Lack of RAT samples from those aged >45 years probably reflected the fact that those with the disease had their tonsils removed at a much earlier age. It would however be of interest to investigate if age itself has an affect on AMP expression and thus host innate defences.

The LEAP-2 gene was chosen for analyses in this study as it encodes a novel AMP about which little is known. In fact LEAP-2 gene expression has been shown in tonsil to produce four transcripts, presumably encoding four different peptides (Ball, Siou et al. 2007). In this study the expression of the 161bp transcript encoding the secreted peptide with antimicrobial activity was studied. LEAP-2 mRNA expression was not found statistically to be significantly different in the epithelial compared to the lymphoid samples. This disagreed with the results of the pilot study which showed differences between mRNA expression in these tissue types (Ball, Siou et al. 2007). However results from immunohistochemical studies, using an antibody specific to LEAP-2 yielded results which agreed with the LEAP-2 mRNA expression study in Figure 4.1 as LEAP-2 immunoreactivity was observed at both the epithelial surface of the tonsil and within the lymphoid tissues (Figure 4.2). However the discrepancy in the results here and in the pilot study may be explained by the immunohistochemical studies not being quantitatively analysed. Another explanation may be that assuming that the other three LEAP-2 transcripts observed in the tonsil tissues following end-point PCR (Ball, Siou et al. 2007) encode intracellular peptides with primary sequences showing identity to that of the secreted LEAP-2 molecule, and that the LEAP-2 antibody detects these peptide forms. Although not proven these data suggest that LEAP-2, as an innate defence molecule, is more atypical than previously thought.

No difference in LEAP-2 expression levels were observed in the RAT compared to the control tonsils (Figure 4.3b). Although it is has been shown, using a zone inhibition assay, that mature LEAP-2 peptide will kill Gram-positive bacteria (Krause, Sillard et al. 2003), it is not known whether LEAP-2 expression can be regulated by such organisms. Indeed to date LEAP-2 gene expression has only been shown to be up-

regulated in avian (Townes, Michailidis et al. 2004), and porcine gut tissues (Sang, Ramanathan et al. 2006) in response to *Salmonella enterica* serovar Typhimurium infection.

Patients were asked to state the length of time prior to their tonsillectomy since their last sore throat and these data were plotted in relation to AMP expression levels (Figure 4.9). No statistically significant differences were seen between the groups, possibly due to small sample numbers, and no trends were evident. However as patients are usually infection free at the time of their tonsillectomy and the patients were self-assessing the reliability of this data must be questioned. In hindsight it would have been more useful if the last clinical diagnosis of tonsillitis had been documented and used.

In summary, this study investigated and compared the levels of LL-37, HBD1, HBD2 and LEAP-2 AMP mRNA expression in over ninety tonsils excised from RAT patients and control subjects. The data indicated that all AMP genes examined were expressed, that considerable variability was detected between the AMP expression levels of individual subjects but that the mean AMP expression levels between the RAT and control groups was not significantly different. These data did not therefore support a defect in the innate immune response involving host AMPs, such as a deficiency in AMP expression at the epithelial surface, as being a cause or contributory factor in an individual's susceptibility to recurrent acute tonsillitis. However this study was conducted using tonsils excised from RAT patients at the time of their surgery when, despite their self diagnosis, they were probably not suffering a streptococcal infection. Thus it could be argued that in order to answer the question of whether RAT is due to failure of the AMPs to up-regulate in response to infection, we need to look at AMP responses in tonsils when actively infected with streptococci.

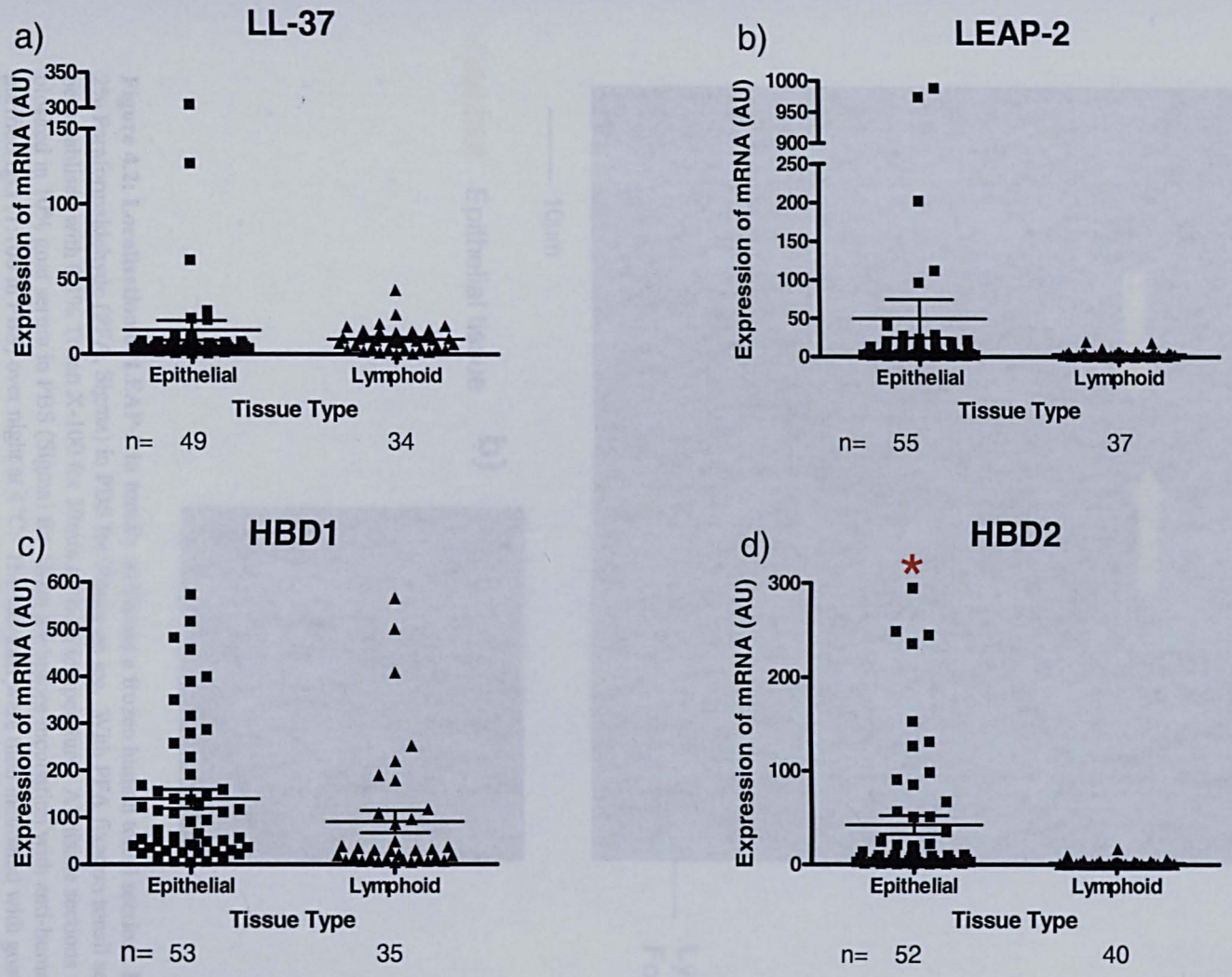

Figure 4.1: Expression of LL-37, LEAP-2, HBD1 and HBD2: mRNA adjusted to GAPDH (AU) in all subjects, classified in terms of epithelial and lymphoid samples. In graphs a), c) and d) all samples outside ± two standard deviations of the mean were omitted. In graph b) all samples have been included as they have an impact on statistical significance (see 4.3). n: numbers of samples analysed. One sample per tonsil collected was assayed in duplicate except for LL-37 which was assayed in quadruplicate. Error bars represent mean values ± SEM. * = $P<0.05$. Statistical analysis was performed with an unpaired T-test.

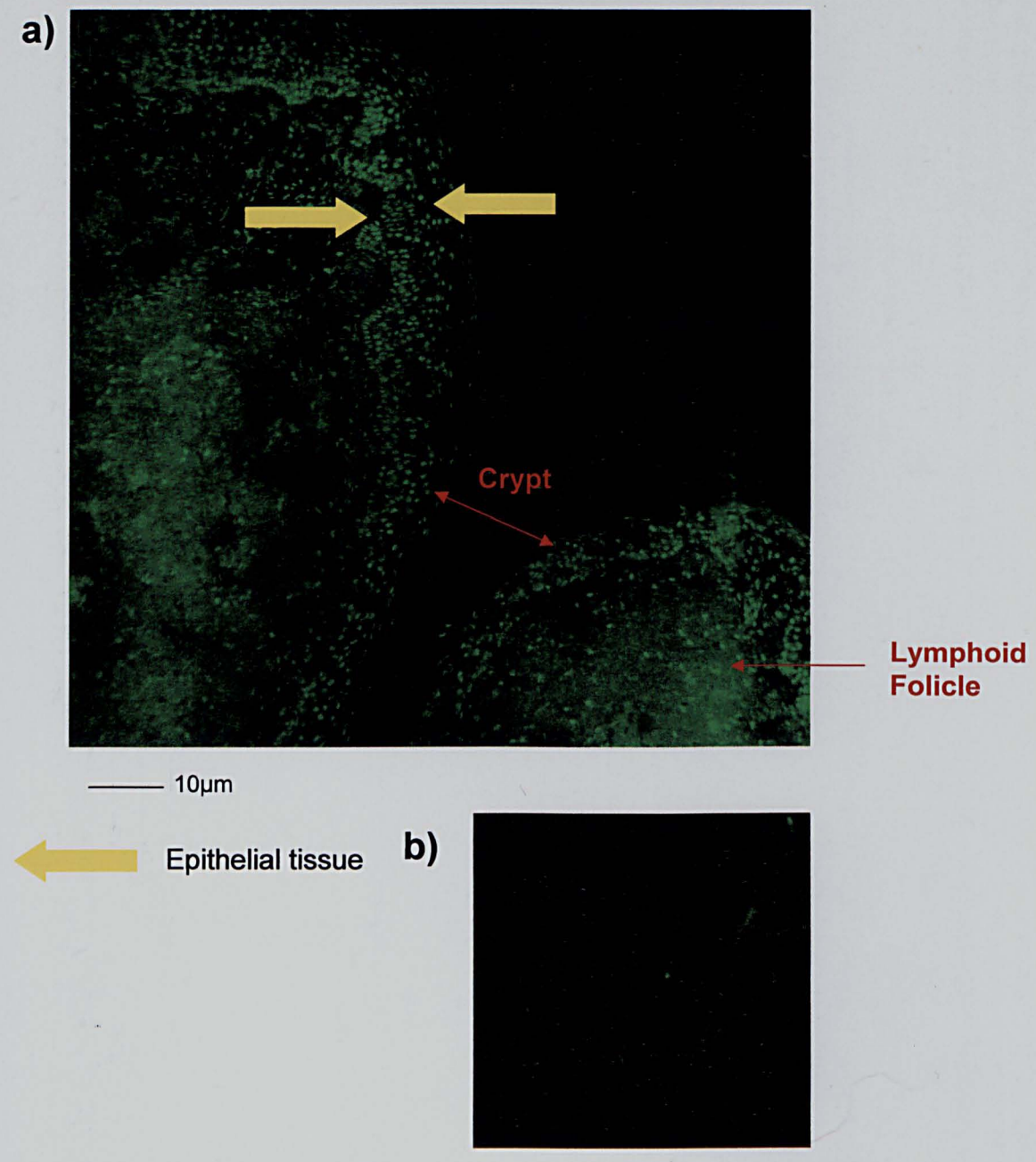

Figure 4.2: Localisation of LEAP-2 in tonsil: a) Shows a frozen human tonsil section. Fixed in 2% Paraformaldehyde (PFA, Sigma) in PBS for 30min on ice. With PFA fixation tonsil section was permeablised with 0.1% Triton X-100 for 30min at room temperature. All tissue sections were blocked in 10% goat serum in PBS (Sigma) for 1h on ice before incubation with anti-human LEAP-2 purified IgG (1:100 in PBS) over night at 4°C. The sections were then incubated with goat anti-rabbit antibody-FITC (Chemicon), 1 : 50 in PBS for 3h before being mounted on slides with Vectashield. LEAP-2 expression is shown in bright green and can be seen to be localised to epithelial surfaces and lymphoid follicles of the tonsil. The tonsil was excised from a RAT patient. The epithelial lined crypt can be observed. **b)** Control without primary antibody.

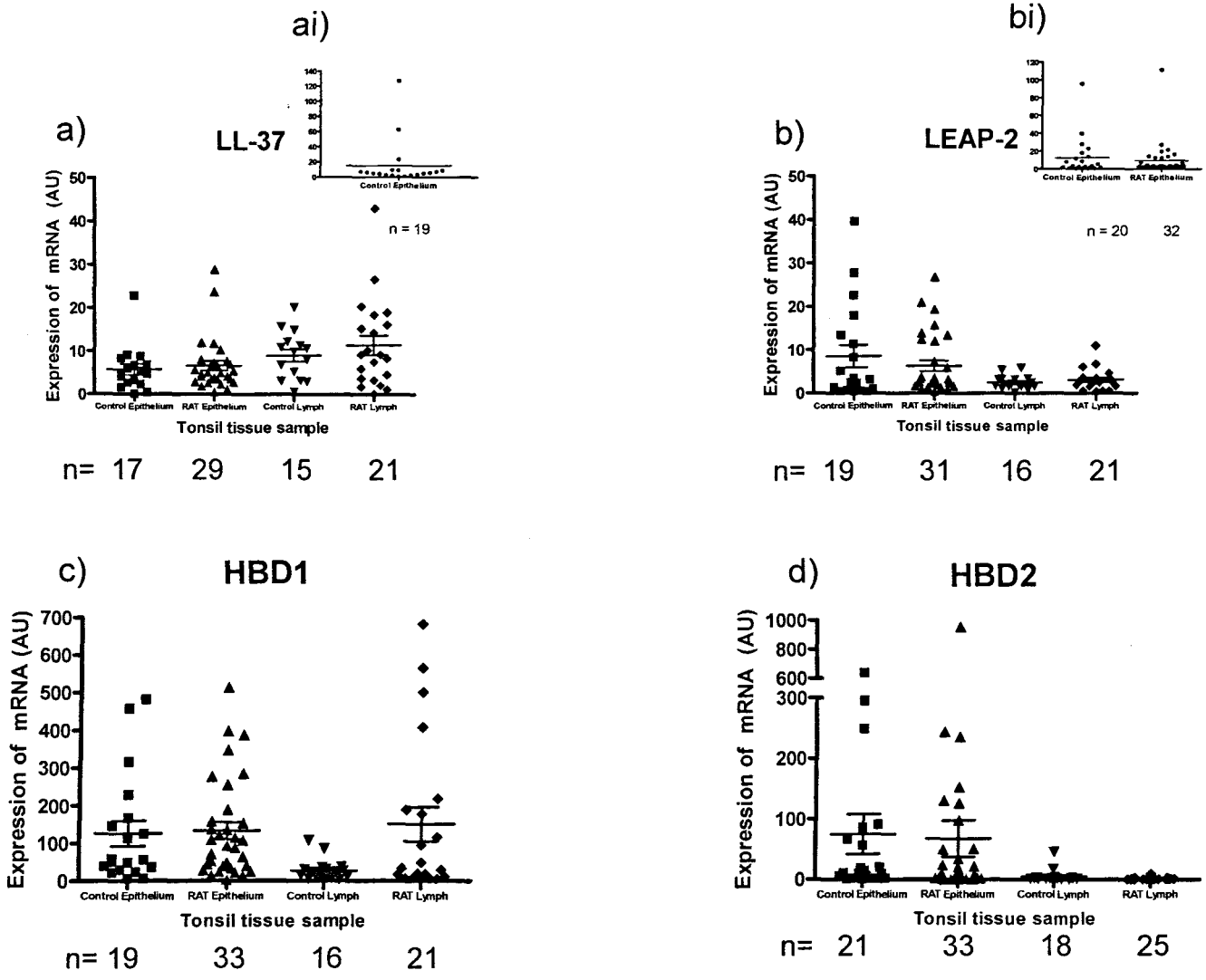

Figure 4.3: Expression of LL-37, LEAP-2, HBD1 and HBD2 mRNA: adjusted to GAPDH (AU) in all subjects, classified in terms of tissue type and disease state. n: number of samples analysed. One sample per tonsil collected was assayed in duplicate except for LL-37 which was assayed in quadruplicate. Inset graphs ai and bi show samples lying outside of the normal range. In graphs a), ai), b), bi) and c) all samples outside of ± two standard deviations of the mean were omitted. In graph d) all samples have been included as they have an impact on statistical significance (see 4.3). Bars represent mean values ± SEM. * = $P<0.05$. Statistical analysis was performed with a one way ANOVA followed by a Bonferroni post-test.

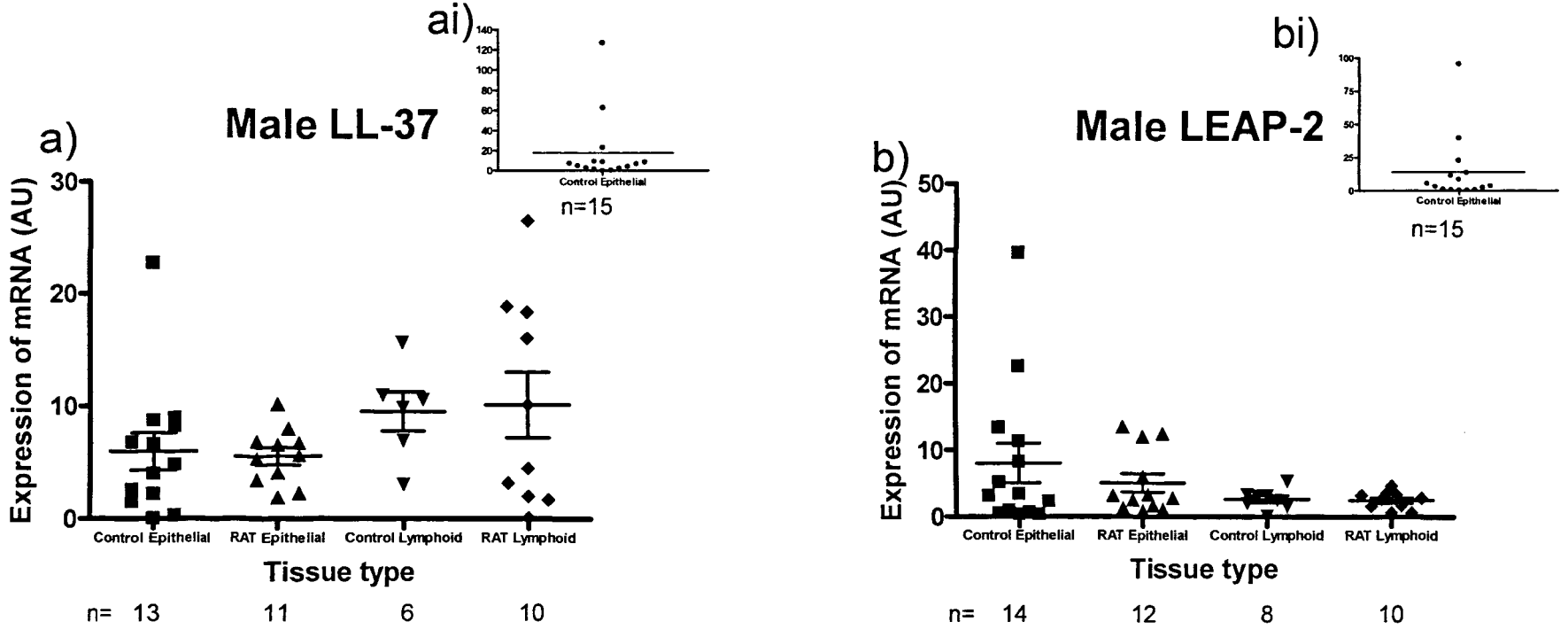

Figure 4.4a-b: Expression of LL-37 and LEAP-2 mRNA: adjusted to GAPDH (AU) in all male subjects, classified in terms of disease state and tissue type. n: number of samples analysed. One sample per tonsil collected was assayed in duplicate except for LL-37 which was assayed in quadruplicate. Inset graphs ai and bi show samples lying outside of the normal range. In all graphs samples outside ± two standard deviations of the mean were omitted. Bars represent mean values ± SEM. Statistical analysis was performed with a one way ANOVA followed by a Bonferroni post-test.

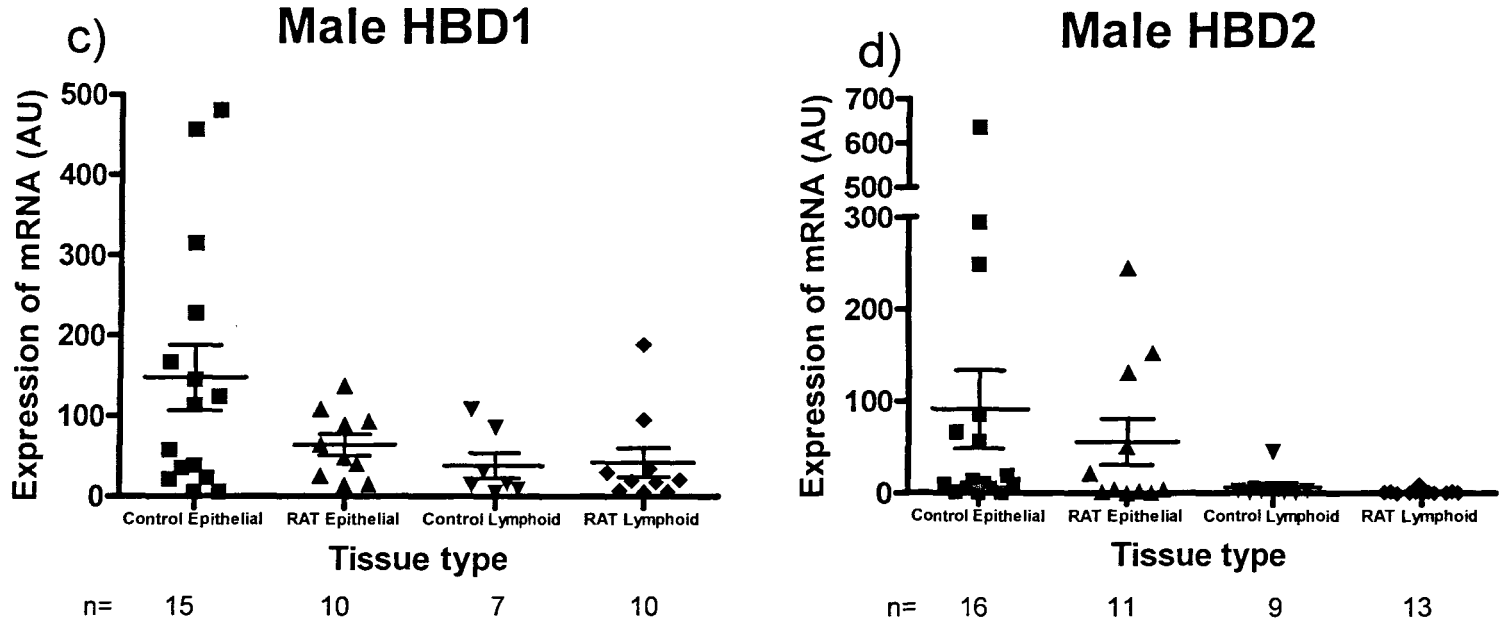

Figure 4.4c-d: Expression of HBD1 and HBD2 mRNA: adjusted to GAPDH (AU) in all male subjects, classified in terms of disease state and tissue type. n: number of tonsil samples analysed. One sample per tonsil collected was assayed in duplicate. Inset graph di shows samples outside of the normal range. In graph c) all samples outside ± two standard deviations of the mean were omitted. In graph d) all samples have been included as they have an impact on statistical significance (see 4.3). Bars represent mean values ± SEM. * = $P<0.05$. Statistical analysis was performed with a one way ANOVA followed by a Bonferroni post-test.

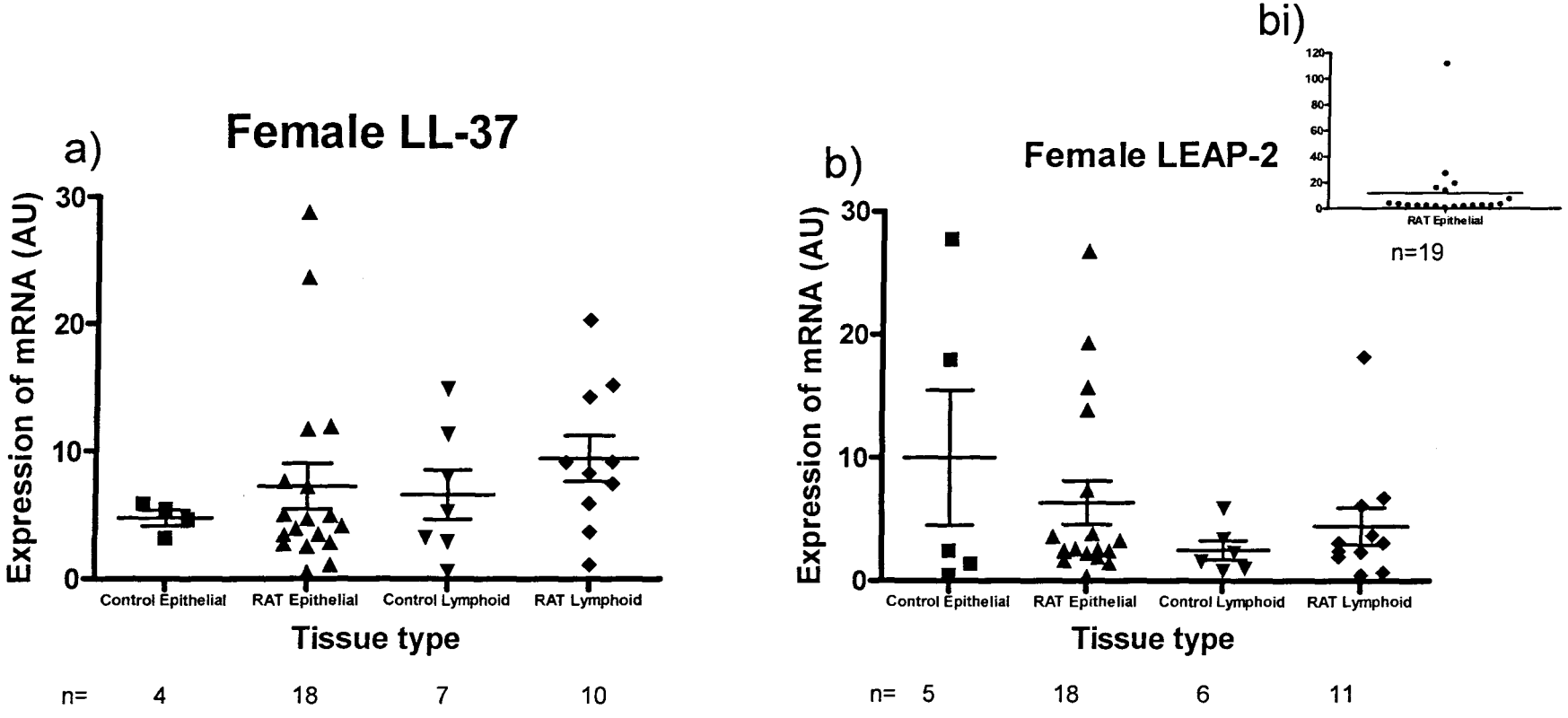

Figure 4.5a-b: Expression of LL-37 and LEAP-2 mRNA: adjusted to GAPDH (AU) in all female subjects, classified in terms of disease state and tissue type. n: numbers of tonsils samples analysed.. One sample per tonsil collected was assayed in duplicate except for LL-37 which was assayed in quadruplicate. Inset graph bi shows samples outside of the normal range. In all graphs all samples outside ± two standard deviations of the mean were omitted. Bars represent mean values ± SEM. Statistical analysis was performed with a one way ANOVA followed by a Bonferroni post-test.

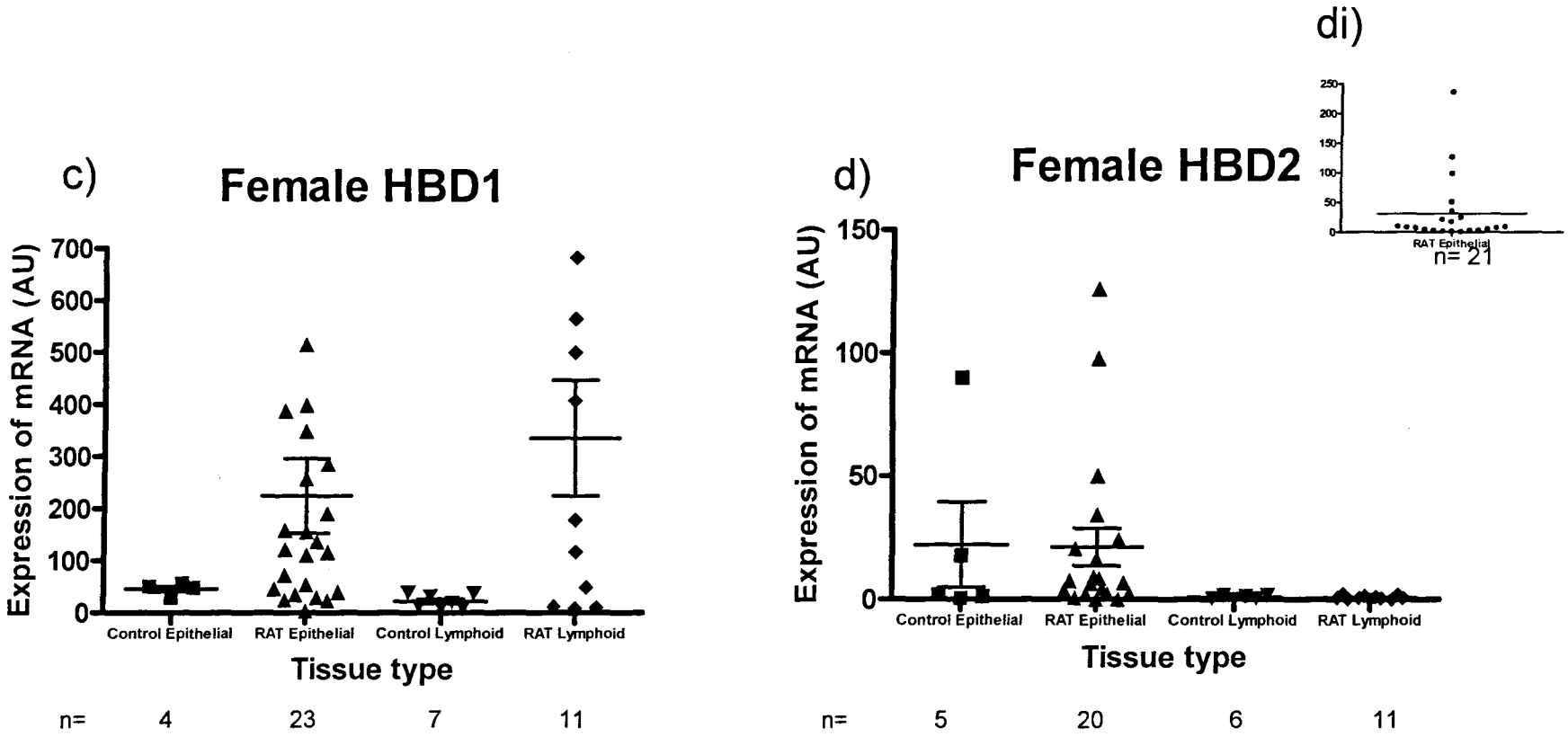

Figure 4.5c-d: Expression of HBD1 and HBD2 mRNA: adjusted to GAPDH (AU) in all female subjects, classified in terms of disease state and tissue type. n: number of tonsils analysed. One sample per tonsil collected was assayed in duplicate. In graph c) all samples have been included as they have an impact on statistical significance (see 4.3). In graphs d) and di) all samples outside ± two standard deviations of the mean were omitted. Bars represent mean values ± SEM. * = $P<0.05$. Statistical analysis was performed with a one way ANOVA followed by a Bonferroni post-test.

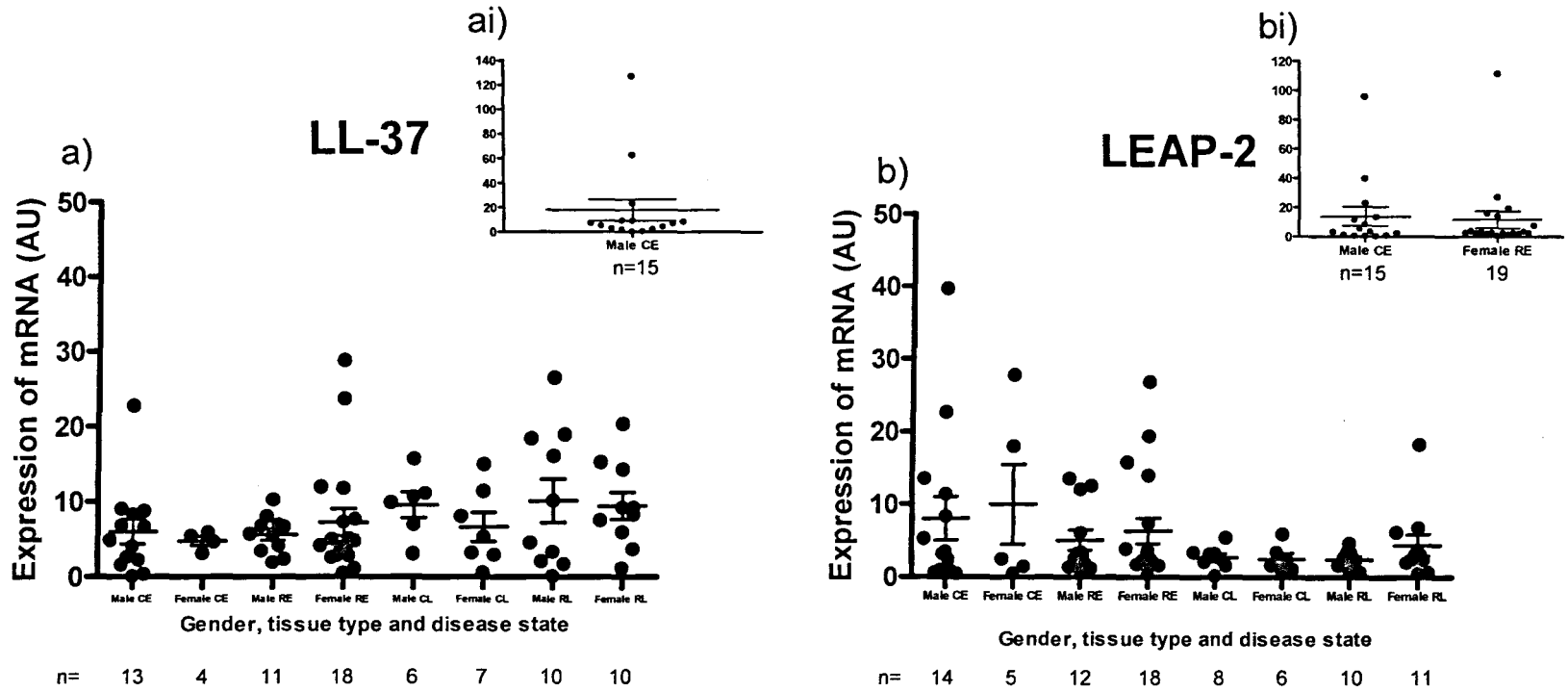

Figure 4.6a-b: Expression of LL-37 and LEAP-2: mRNA adjusted to GAPDH (AU) in all patient subjects, classified in terms of gender. n: number of samples analysed. One sample per tonsil collected was assayed in duplicate except for LL-37 which was assayed in quadruplicate. Inset graphs show samples outside of the normal range. In all graphs all samples outside ± two standard deviations of the mean were omitted. Bars represent mean values ± SEM. CE = control (non-RAT), epithelial samples, RE = RAT, epithelial samples, CL = control (non-RAT), lymphoid samples, RL = RAT, lymphoid samples. Statistical analysis was performed with a one way ANOVA followed by a Bonferroni post-test.

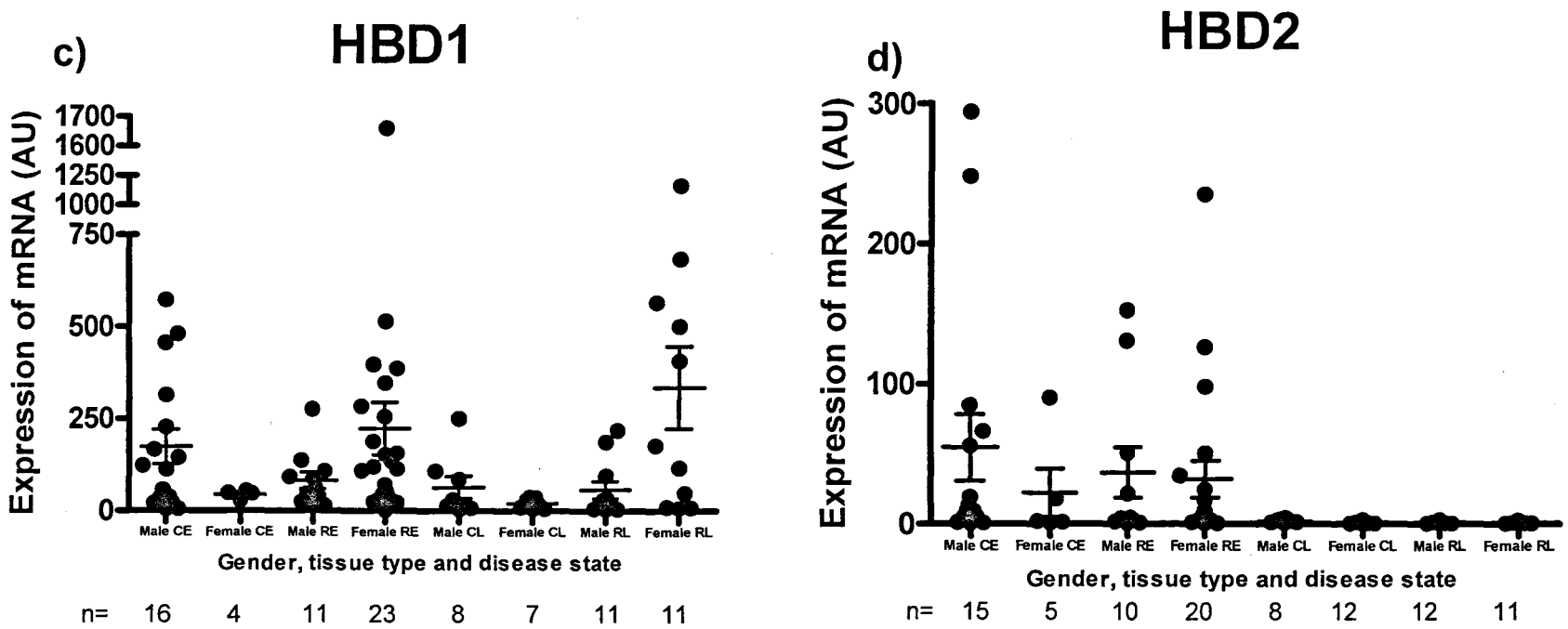

Figure 4.6c-d: Expression of HBD1 and HBD2 mRNA: adjusted to GAPDH (AU) in all patient subjects, classified in terms of gender. n: number of samples analysed. One sample per tonsil collected was assayed in duplicate. In graph c) all samples have been included as they have an impact on statistical significance (see 4.3). In graph d) all samples outside ± two standard deviation of the mean were omitted. Bars represent mean values ± SEM. * = $P<0.05$. CE = control (non-RAT), epithelial samples, RE = RAT, epithelial samples, CL = control (non-RAT), lymphoid samples, RL = RAT, lymphoid samples. Statistical analysis was performed with a one way ANOVA followed by a Bonferroni post-test.

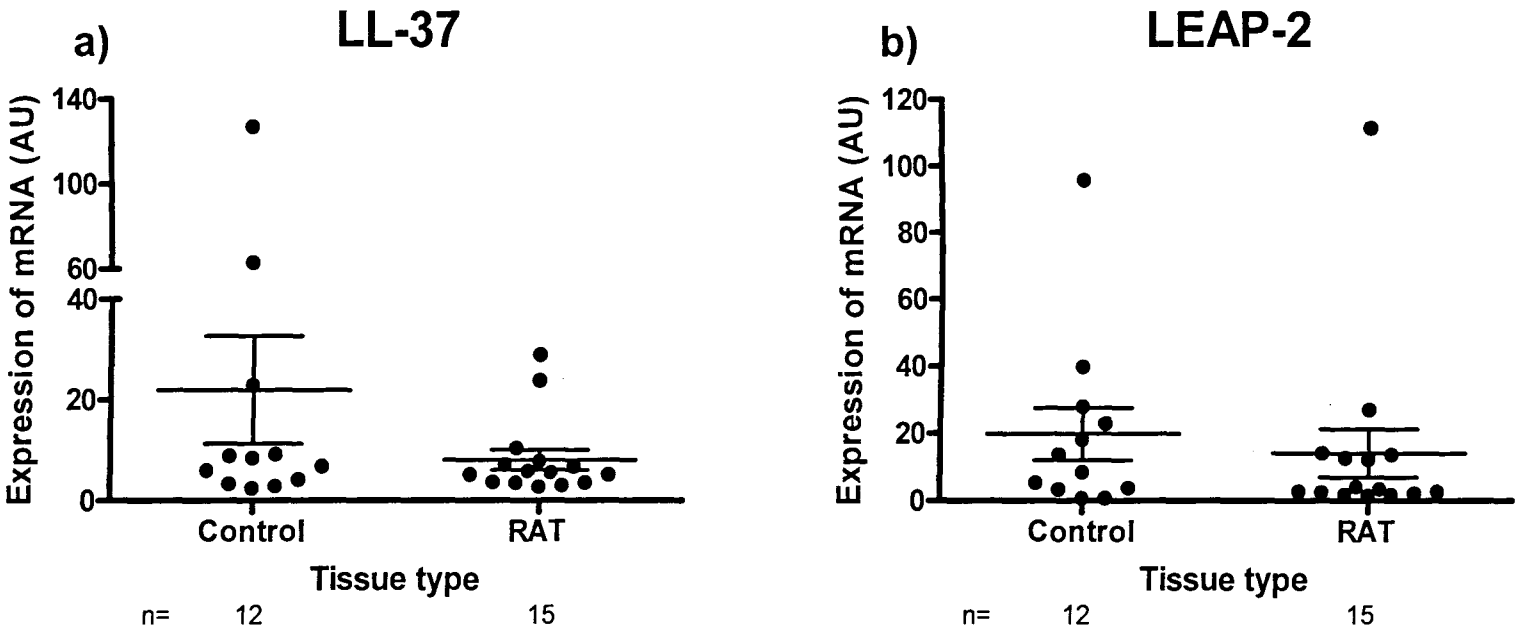

Figure 4.7a-b: Expression of LL-37 and LEAP-2 mRNA: adjusted to GAPDH (AU) in all subjects < ten years old, classified in terms of disease state. n: number of samples analysed. One sample per tonsil collected was assayed in duplicate except for LL-37 which was assayed in quadruplicate. In all graphs all samples outside ± two standard deviations of the mean were omitted. Bars represent mean values ± SEM. Statistical analysis was performed with an unpaired T-test.

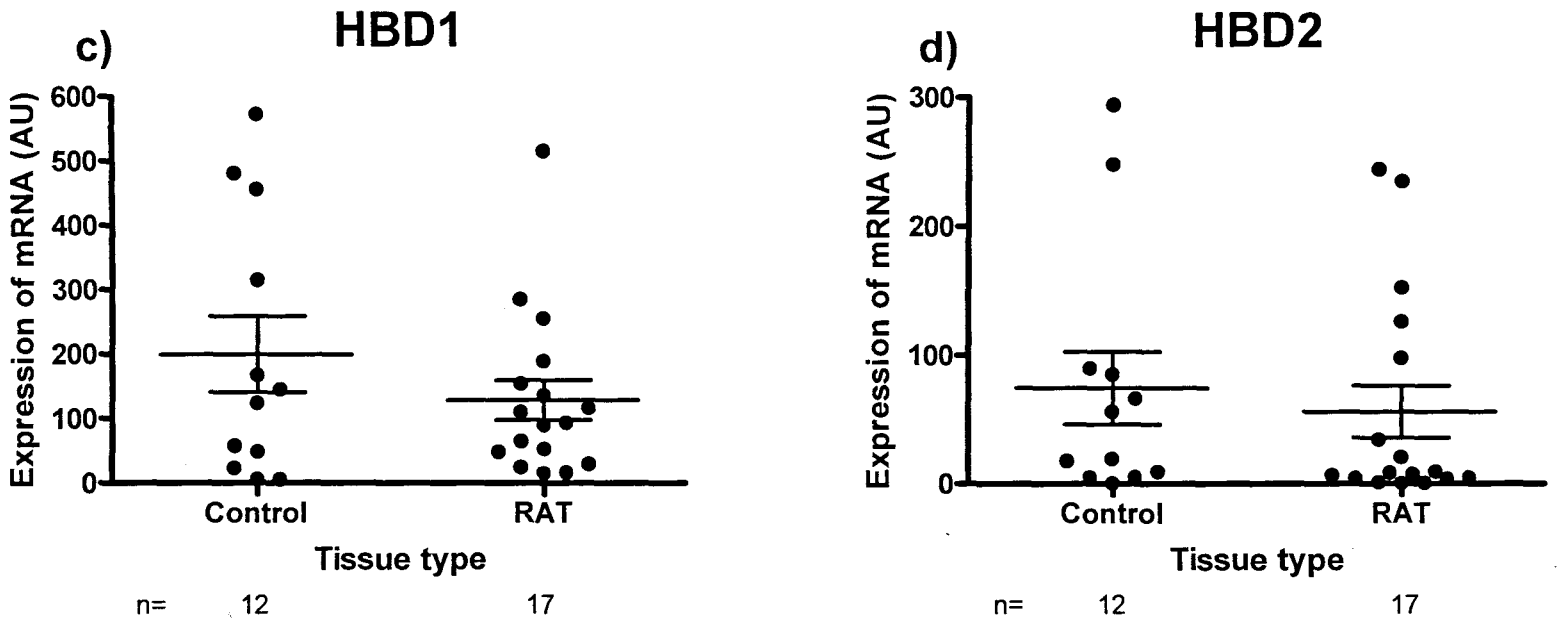

Figure 4.7c-d: Expression of HBD1 and HBD2 mRNA: adjusted to GAPDH (AU) in all subjects < ten years old, classified in terms of disease state. n: number of samples analysed. One sample per tonsil collected was assayed in duplicate. In all graphs all samples outside ± two standard deviations of the mean were omitted. Bars represent mean values ± SEM. Statistical analysis was performed with an unpaired T-test.

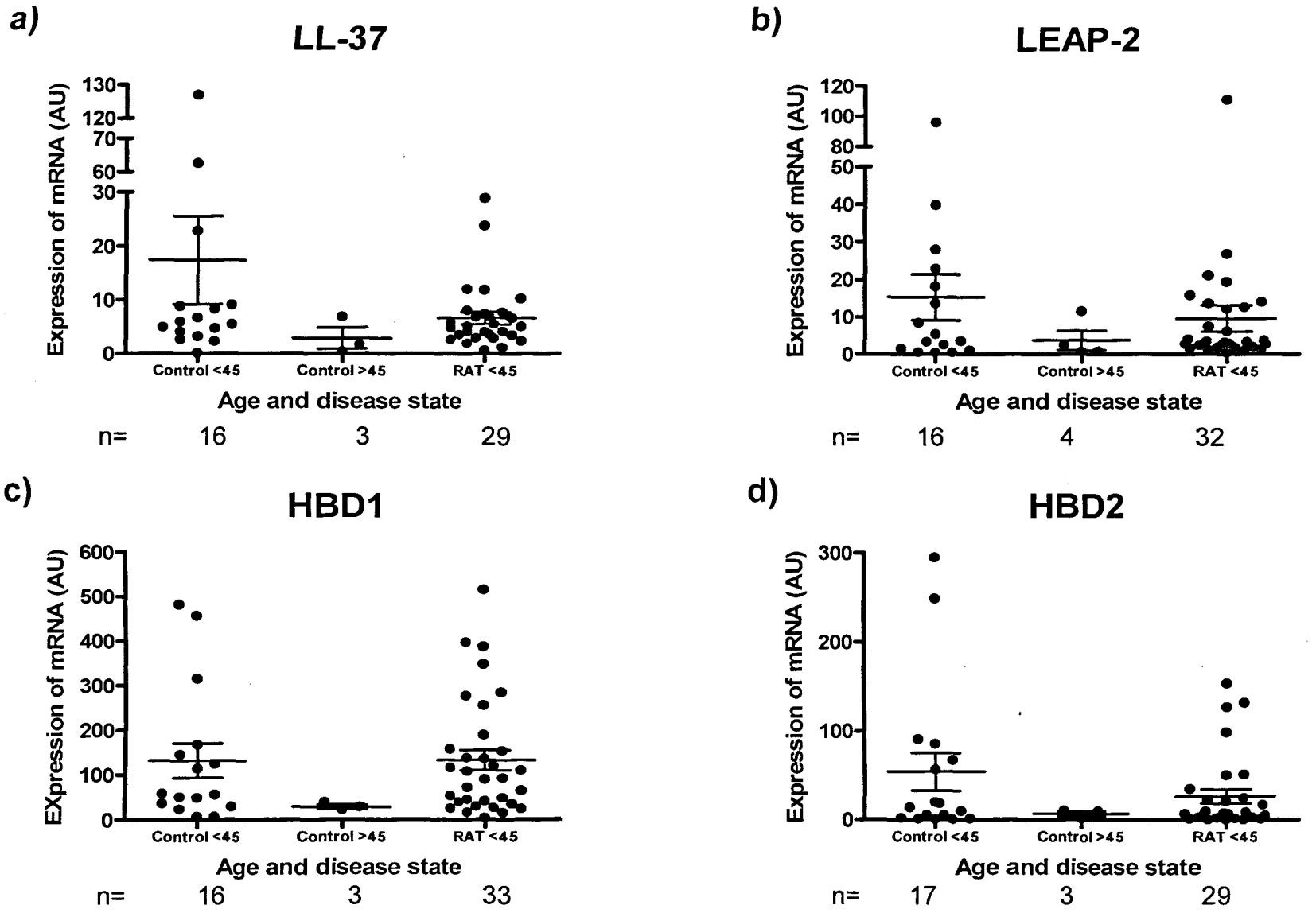

Figure 4.8a-d: Expression of LL-37, LEAP2, HBD1 and HBD2 mRNA: adjusted to GAPDH (AU) in all subjects over and under 45 years of age excluding all samples from subjects ≤10 years old. Samples are classified in terms of disease state. n: number of samples analysed. One sample per tonsil collected was assayed in duplicate except for LL-37 which was assayed in quadruplicate. In all graphs samples outside ± two standard deviations of the mean were omitted. Bars represent mean values ± SEM. Statistical analysis was performed with a one way ANOVA followed by a Bonferroni post-test.

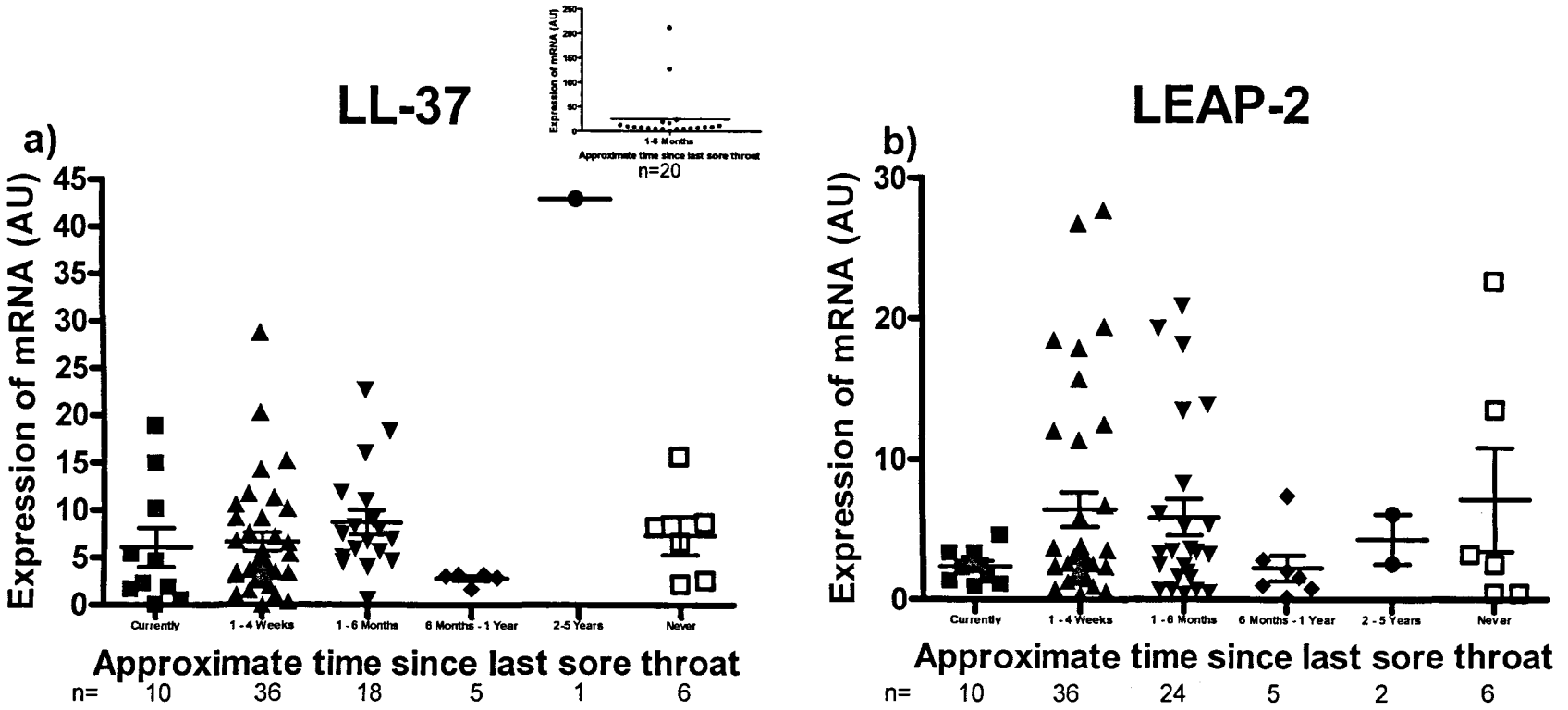

Figure 4.9a-b: Expression of LL-37 and LEAP-2 mRNA: adjusted to GAPDH (AU) in all patient subjects, classified in terms of last sore throat. n :number of samples analysed. One sample per tonsil collected was assayed in duplicate except for LL-37 which was assayed in quadruplicate . In all graphs all samples outside ± two standard deviations of the mean were omitted. Bars represent mean values ± SEM. Statistical analysis was performed with a one way ANOVA followed by a Bonferroni post-test.

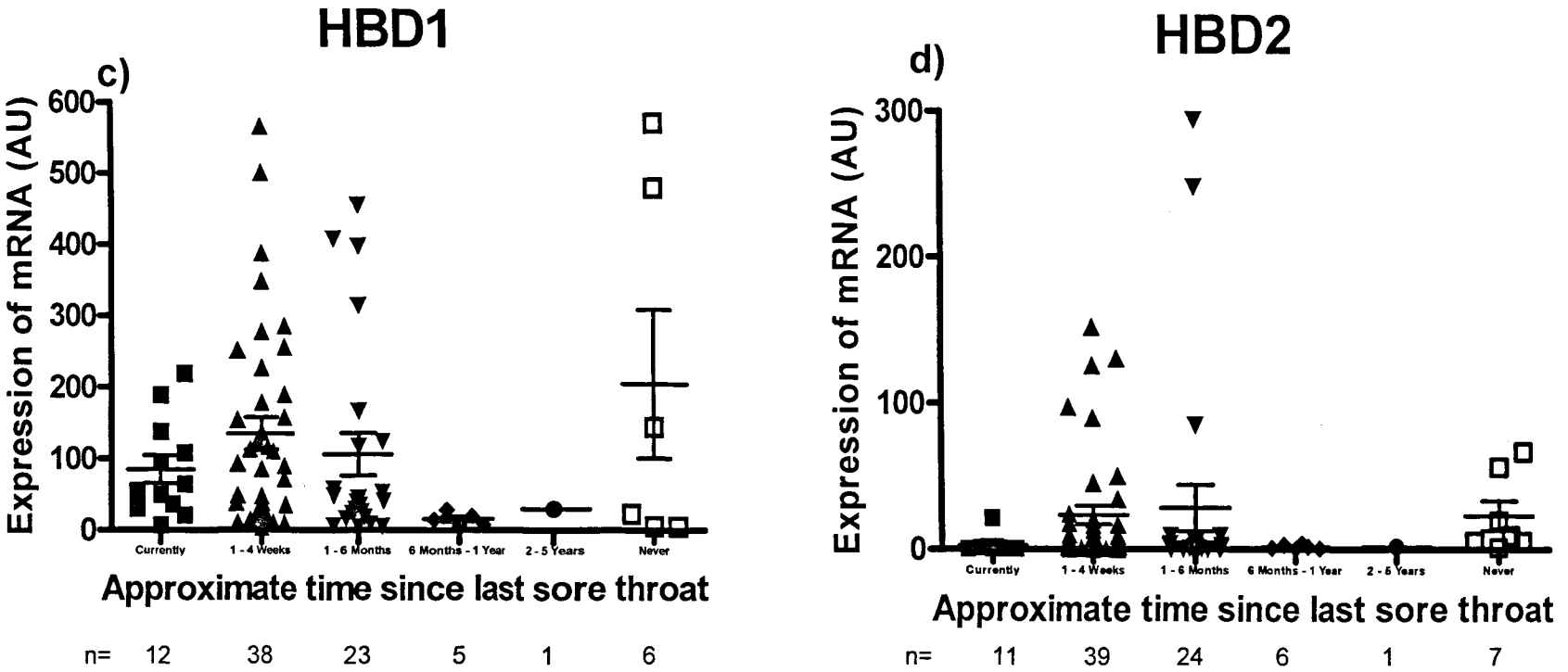

Figure 4.9c-d: Expression of HBD1 and HBD2 mRNA: adjusted to GAPDH (AU) in all patient subjects, classified in terms of last sore throat. n: number of samples analysed. One sample per tonsil collected was assayed in duplicate. In all graphs all samples outside ± two standard deviations of the mean were omitted. Bars represent mean values ± SEM. Statistical analysis was performed with a one way ANOVA followed by a Bonferroni post-test.

Chapter 5

Antimicrobial Peptide Gene Expression in an *In Vitro* HaCaT Cell Model

5.1 Introduction

The results of the previous chapter indicated that human tonsils excised from control (non-RAT) subjects, removed for either apnoea or snoring, and those suffering RAT expressed a broad spectrum of AMPs. While patterns of AMP expression were identified, overall the levels of expression did not appear to be significantly different between the two groups. It is well known that AMPs are induced in host cells in response to microbes (Dorschner, Pestonjamasp et al. 2001; Nizet, Ohtake et al. 2001; Chromek, Slamova et al. 2006; Johansson, Thulin et al. 2008), and thus it could be argued that the RAT patients recruited to the clinical study were, in the main, in the quiescent phase of their disease and thus probably not actively infected with *S. pyogenes*, a major causal factor in the pathology of recurrent acute tonsillitis. To explore this further the direct effects of *S. pyogenes* on the expression of AMP genes in the tonsil epithelium required investigation.

It is neither ethical nor moral to investigate the direct effects of *S. pyogenes* on tonsil epithelium *in vivo* i.e. using human volunteers, thus in this chapter the aim was to identify a suitable *in vitro* system to model the tonsil epithelium and investigate the effects of streptococcal binding on the host AMP response.

The use of an immortalised cell line to model the tonsil epithelium has many advantages; these include performing each independent study in a controlled environment and the simultaneous generation of large numbers of samples, both of which help reduce sample variability. Moreover, the homogeneity of an *in vitro* cell line also ensures that the resulting data relates to one cell type only rather than to a mix of cells as can occur *in vivo*.

In this chapter statistical analysis was performed using either an unpaired T-test or one way ANOVA followed by a Bonferroni post-test, as described in 4.2ii. Here, a one way ANOVA followed by a Dunnett's post-test was also used. This was suggested by the Prism statistics guidelines for tests where each data set is required to be compared to a control (Motulsky 2003).

5.1.1 Aims of Investigation

The aims of the studies described in this chapter were (i) to select an immortalised *in vitro* cell line model that modelled the tonsil epithelium and to describe its AMP expression profile and (ii) to challenge the cells *in vitro* with *S. pyogenes* and to determine the effects of binding and infection on AMP gene expression.

5.2 Consideration of HEp-2 cells as a tonsil model

The HEp-2 cell line (Figure 5.1) was initially considered for this study as these cells exhibit epithelial characteristics and were derived originally from laryngeal cells. It can be argued that the close proximity of the laryngeal cells, in the environment of the pharynx, to the tonsils supports their use as a suitable *in vitro* system to model the tonsil epithelium, and therefore to investigate AMP expression in tonsil in response to a bacterial challenge. Moreover, additional support for the use of this cell line was provided in a preliminary study by Ball (2004), who identified HBD1 and HBD3 mRNA expression in the HEp-2 cells and localised the peptides to the epithelial surface of the cells. It was of concern however that neither the expression of LL-37, HBD2, hepcidin nor LEAP-2 mRNA was detected.

Reanalysis of HEp-2 cell RNA using primers specifically designed to amplify the LL-37, HBD2, hepcidin and LEAP-2 genes using end-point PCR, agarose gel electrophoresis and DNA sequencing confirmed expression of HBD1 and HBD3 (Figure 5.2). LL-37 expression was also detected (Figure 5.3), but only after 40 cycles of PCR (compared to 30 cycles employed by Ball (2004)). A faint cDNA band was detected following amplification of the HEp-2 cell RNA using HBD2 primers (results not shown) but this product was not confirmed by sequencing as the cDNA product could not be cloned successfully. None the less these expression data supported the use of the HEp-2 cell line as a suitable *in vitro* model to investigate AMP gene expression in response to a streptococcal challenge.

However, there were major concerns regarding the actual use of this cell line as a model for tonsil. First information from the cell supplier ATCC (www.atcc.org), described this laryngeal model cell line as being contaminated with HeLa (cervical cancer) cells. Second, significant information suggesting the unsuitability of these cells as a tonsil model was published by our group comparing the binding of *S. pyogenes* to tonsils and HEp-2 cells (Abbot, Smith et al. 2007). This study found that HEp-2 cells were unable to model the tonsillar-streptococcal interactions, and thus were not an appropriate model to investigate host AMP profiles in response to pathogen challenge. However the results of the study by Abbot, Smith et al (2007), suggested that HaCaT cells were an appropriate model as the interactions observed between the cells and *S. pyogenes* mimicked those of the tonsil and the bacterium.

5.3 Consideration of HaCaT cells as a model for tonsil

The HaCaT cell line, an immortalized skin cell-line, was therefore considered as an *in vitro* model for the AMP expression studies. As the AMP expression profile of this cell line was not known, initial experiments focussed on determining the AMP (LL-37, HBD1, HBD2, HBD3, hepcidin and LEAP-2) gene expression profiles and whether such expression could be regulated. For the regulatory studies the HaCaT cells were challenged with bacterial and environmental agents including lipoteichoic acid (LTA), lipopolysaccharide (LPS), phorbol 12-myristate 13-acetate (PMA) and 1,25 dihydroxyvitamin-D3 (D3).

LTA is a Gram-positive cell wall component of particular interest to this study as *S. pyogenes* is a Gram-positive bacterium. In addition LTA has been reported to induce HBD2 expression in human endometrial epithelial cells (King, Fleming et al. 2002). LPS is a Gram-negative cell wall component used to up-regulate antimicrobial peptides directly (MacRedmond, Greene et al. 2005), or indirectly through another immune effecter molecule such as IL-1β (Pioli, Weaver et al. 2006). The environmental component PMA has previously been reported to induce HBD3 and HBD4 expression in human primary keratinocytes, and HBD4 expression in HaCaT cells (Harder, Meyer-

Hoffert et al. 2004). D3 was chosen as it has been shown to up-regulate LL-37 mRNA expression in skin cells (Weber, Heilborn et al. 2005).

5.4 AMP Gene Expression in HaCaT cells Treated with Bacterial and Environmental Agents

5.4.1 End-point PCR studies of AMP mRNA expression in HaCaT cells treated with bacterial and environmental components

End-point PCR analyses of HaCaT cell RNA resulted in the detection of cDNAs supportive of HBD1, HBD2, HBD3, hepcidin and LEAP-2 gene expression (Figures 5.4 & 5.5). However LL-37 expression was found to be very low and often, following the RT-PCR analyses, cDNA bands were not observed (Figure 5.4b lanes 2 & 3).

In view of the latter observations the effects of bacterial and environmental agents on the AMP gene expression patterns were investigated. For these studies the HaCaT cells were cultured to confluency and challenged for up to 22 hours with the appropriate agent. AMP gene expression was determined by semi-quantitative RT-PCR. Essentially, HaCaT cells (1×10^6) were seeded and grown in 12mm diameter wells for 4-5 days at 37°C and 5% CO_2. Once confluent the cells were incubated for three hours in cell growth medium without either FCS or antibiotics, and the appropriate treatment (D3 (Fluka, final concentration 200nM), LTA (from *S. pyogenes*, Sigma final concentration 2μg/ml), LPS (Sigma, final concentration 0.2μg/ml), and PMA (Sigma, final concentration 20μM)) in a total volume of 1ml added before incubation at 37°C in 5% CO_2 for the pre-determined time period. The cells were then washed in PBS and the RNA extracted (Section 2.5.2). The RNA was reverse transcribed and the cDNA analysed using the appropriate primers (described in Chapter 3) and end-point PCR for LEAP-2, LL-37 and GAPDH expression. The samples were analysed for LEAP-2 expression as this gene encodes a novel four cysteine AMP (Krause, Sillard et al. 2003), and for LL-37 expression, as the encoded host peptide is known to interact with streptococci (Dorschner, Pestonjamasp et al. 2001; Nizet, Ohtake et al. 2001; Nyberg, Rasmussen et al. 2004; Johansson, Thulin et al. 2008).

Results of these analyses are shown in Figure 5.4a-c. The data indicated that LTA, LPS, PMA and D3 treatment did not affect LEAP-2 mRNA expression. Similarly LTA, LPS and PMA treatment did not affect LL-37 mRNA expression but the presence of a 500bp cDNA band in response to D3 treatment suggested that the vitamin D metabolite was able to up-regulate LL-37 gene expression.

5.4.2 Treatment of HaCaT cells with 1,25 dihydroxyvitamin-D3

These results indicated that LL-37 gene expression was up-regulated in HaCaT cells in response to D3 (200nM) treatment. To confirm this, the D3 challenge experiments were repeated and in addition the affects of D3 treatment on HBD1, HBD2, HBD3 and hepcidin gene expression were also investigated. For such experiments the HaCaT cells were cultured as previously and incubated with 200nM D3 for up to 22 hours. Post-treatment, the cells were washed, lysed, RNA extracted and, using the appropriate primers, analysed by semi-quantitative end-point PCR. Representative gel data are shown in Figure 5.5. The densitometry data derived from the gels was normalised to GAPDH and plotted as a percentage of control (Figure 5.6).

The semi-quantitative data showed that treatment of HaCaT cells with D3 resulted in a one to two fold increase in LL-37 mRNA expression. In contrast the expression of the HBD1, HBD2, HBD3, hepcidin and LEAP-2 genes did not change in response to the D3 treatment. It is however acknowledged that the data relating to LEAP-2 mRNA expression was from one gel only. It is also acknowledged that the lack of sensitivity of the densitometry and the small sample sizes created large errors, which may have masked small, but potentially important, changes in gene expression. This was particularly evident in relation to the expression of HBD3 where it could be argued that D3 treatment was in fact inhibitory.

None the less these results, detailing the expression of AMP genes and the up-regulation of LL-37 mRNA, in conjunction with those reported by Abbot, Smith et al (2007) supported the use of the HaCaT cell line as an *in vitro* system to model the tonsil epithelium.

5.5 Expression of Antimicrobial Peptides Genes in HaCaT Cells Infected with *S. pyogenes* M1 Serotype

Streptococcus pyogenes is a major bacterial cause of tonsillitis in humans (Brook and Gober 2005), and the focus was now to investigate whether infection of the HaCaT cells with streptococci caused any effects on the expression of the AMP genes. As preliminary experiments using the Gram-positive bacterial cell wall component LTA did not affect either LL-37 or LEAP-2 gene expression (Figure 5.4), the decision was taken to use whole bacteria in all subsequent experiments.

For such experiments 1 x 10^6 HaCaT cells were seeded per 12mm dish and cultured at 37°C and 5% CO_2 for 3-4 days in growth medium until confluent. Infection experiments were performed as described in Section 2.3.3. Essentially, the HaCaT cells were washed and incubated for three hours in medium lacking FCS and antibiotics, and infected with 1 x 10^8 cfu *S. pyogenes* expressing GFP, cultured as described previously (Section 2.3.4) to an OD_{600} of 0.5. The bacterial cells were washed, pelleted and resuspended in normal cell growth media lacking antibiotics and FCS. The HaCaT cells were incubated with the bacteria for an appropriate pre-determined period of time (either 2, 4 or 6 hours) before being washed with PBS, lysed and the RNA extracted. The RNA samples were analysed for LL-37, HBD1, HBD2, HBD3, hepcidin and LEAP-2 gene expression via both semi-quantitative end-point PCR and quantitative real-time PCR. No later time points were investigated as infection periods of greater than six hours were associated with cell death (E. Abbot, personal communication).

A binding control was included in these experiments. This control, described in Section 2.3.5, was used to ensure that the *S. pyogenes* had bound to the HaCaT cells. Essentially, HaCaT cells were grown to confluence on 10mm coverslips and incubated as above with *S. pyogenes.* Following a two hour infection period the cells were fixed and stained, as described in Section 2.3.5, to allow visualisation of both the HaCaT cell morphology and numbers of bound *S. pyogenes* (Figure 5.7).

5.5.1 HaCaT infection at 2, 4 and 6 hours: Semi-quantitative studies

Following infection of the HaCaT cells for 2, 4 and 6 hours respectively, RNA from both control and infected cells was extracted, reverse transcribed and analysed for LL-37, HBD1, HBD2, HBD3, hepcidin and LEAP-2 mRNA expression by end-point PCR. PCR products were separated on 2% agarose gels, the cDNA bands analysed by densitometry and the data normalised via the housekeeping gene GAPDH. Statistical analysis was by one way ANOVA followed, where appropriate, by a Dunnett's post-test.

Results of the LL-37 expression analyses are shown in Figure 5.8a, b & c. As observed previously LL-37 expression in the control (unchallenged) cells was low (Figure 5.8a lanes 2 & 3). Although an increase in HaCaT LL-37 expression was detected in response to D3 treatment (Figure 5.8a, lane 10), no such response was observed when the cells were challenged with *S. pyogenes*. Densitometry analysis confirmed this result as no statistically significant differences in LL-37 expression mRNA were recorded compared to the expression levels in uninfected control cells after 2, 4 or 6 hours of infection with *S. pyogenes* (Figure 5.8c).

The results of HBD1 and HBD2 gene expression analyses are shown in Figures 5.9 and 5.10 respectively. The graphs illustrate a similar pattern of AMP gene expression with reduced levels observed at four to six hours post challenge. In both cases the observed reduction at six hours post infection was statistically significant ($P<0.01$). In contrast no change in HBD3 expression was observed in response to *S. pyogenes* (Figure 5.11).

Figure 5.12 a, b & c shows the results of the hepcidin analyses. No statistically significant differences in gene expression were observed post infection.

The LEAP-2 mRNA expression patterns following *S. pyogenes* infection are shown in Figure 5.13 a & b. No significant differences were observed between the mean LEAP-2 gene expression values recorded at either two, four or six hours of infection respectively.

Figure 5.14 shows the AMP gene expression results following treatment of the HaCaT cells with D3 for two hours. This was included as a positive control for cell responsiveness, and when compared to earlier experiments (Section 5.4.2). The data showed that D3 treatment did not cause an increase in LL-37 expression after two hours, this disagreed with the data shown in 5.4 indicating that D3 caused LL-37 mRNA up-regulation but it must be acknowledged that the two hour incubation here is significantly less than the 22 hour incubation time in the experiment with results in Figure 5.4. D3 also did not affect the expression of the HBD1-3, hepcidin or LEAP-2 genes after two hours of treatment.

Table 5.1: Summary of semi-quantitative PCR data after two, four and six hours of infection with *S. pyogenes* M1 serotype.

AMP mRNA	Semi-quantitative PCR result
LL-37	↔
HBD1	↓ 6 h
HBD2	↓ 6 h
HBD3	↔
Hepcidin	↔
LEAP-2	↔

↔ No statistically significant differences in gene expression compared to control
↓ Statistically significant decrease in gene expression compared to control

The results of the semi-quantitative analyses are summarised in Table 5.1. These results indicated that challenging HaCaT cells with *S. pyogenes* M1 serotype for up to six hours caused a significant reduction in HBD1 and HBD2 gene expression but did not affect LL-37, HBD3, hepcidin or LEAP-2 gene expression. However these data were dependent on the densitometry of a large number of gels which often resulted in large error bars that ultimately reduced the sensitivity of the analyses.

5.5.2 HaCaT infection at 2, 4 and 6 hours: Quantitative studies (Real-time PCR)

The semi-quantitative studies were plagued by large error bars. To try and address this and provide more accurate quantification of the data a more sensitive analysis was

required. Thus real-time PCR, using the assays established in Chapter 3, was employed. For such analyses all target gene values were normalised to the housekeeping gene GAPDH and statistical analyses was performed using a one way ANOVA followed, where appropriate, by a Dunnett's post-test.

The results of the gene expression analyses for LL-37 expression using the real-time methodology are presented in Figure 5.15. These data measures the LL-37 mRNA expression in the HaCaT cells in response to the *S. pyogenes* M1 serotype and D3 treatment. However none of these data were found to be statistically significant. At this point it is worth noting that the level of LL-37 expression in the control cells was found to be low and consequently a high number of cycles (55) were required in the real-time PCR to amplify enough LL-37 PCR product to allow quantification. Although frustrating technically, this result was concomitant with that observed following electrophoresis of the cDNA samples following end-point PCR. However the low levels of LL-37 mRNA expression, as with the semi-quantitative analyses, resulted in large error bars, which again reduced the sensitivity of the statistical analyses.

The results of the real-time PCR analyses for HBD1 expression are shown in Figure 5.16a. These data supported previous observations (Figure 5.9) and indicated a reduction in HBD1 mRNA at four to six hours post streptococcal infection. Statistical analysis confirmed this decrease in mRNA expression to be significant at both four and six hours of infection respectively ($P<0.05$).

Figure 5.16b shows the results of the real-time analyses of HBD2 expression. No statistically significant changes were identified after 6 hours of infection.

The LEAP-2 mRNA real-time expression data are shown in Figure 5.16c, and provided evidence for a statistically significant increase ($P<0.01$), in LEAP-2 mRNA expression after six hours of *S. pyogenes* infection. In fact at six hours of infection the mean (± SEM) LEAP-2 expression value was 195±39% of control indicating an almost two-fold increase in gene expression. In comparison the semi-quantitative PCR data identified no changes between the mRNA levels following infection (Figure 5.13), although as stated previously these latter data were beset by large error bars.

Real-time PCR analyses of the samples were not performed for HBD3 and hepcidin due to technical difficulties, described in Chapter 3, during the development of the real-time PCR assays.

Table 5.2: Summary of quantitative PCR data after two, four and six hours of infection with *S. pyogenes*.

AMP mRNA	Quantitative PCR result
LL-37	↔
HBD1	↓4-6 h
HBD2	↔
LEAP-2	↑6 h

↔ No statistically significant differences in gene expression compared to control
↑ Statistically significantly increase in gene expression compared to control
↓ Statistically significantly decrease in gene expression compared to control

Table 5.2 summarises the results of the quantitative analyses. These results indicated that challenging HaCaT cells with the *S. pyogenes* M1 serotype for up to six hours caused a statistically significant reduction in HBD1 gene expression, a statistically significant increase in LEAP-2 gene expression and no statistically significant changes in LL-37 or HBD2 gene expression compared to the control. These data, with respect to LL-37 and HBD1 gene expression were consistent with that obtained by the semi-quantitative analyses. The HBD2 and the LEAP-2 results were however inconsistent; in the case of the later the real-time data strongly supported a significant increase in LEAP-2 expression (two-fold) six hours following streptococcal infection.

5.5.3 HaCaT infection at 5, 15, 30, 60 minutes of infection with *S. pyogenes*

While these experiments were on-going data was published that showed challenging urinary tract cells with *E. coli* resulted in the up-regulation of LL-37 mRNA after only five minutes of infection (Chromek, Slamova et al. 2006). As the earliest time point investigated in my studies was two hours, shorter time periods (5, 15, 30 and 60 min) in relation to *S. pyogenes* infection were investigated. These experiments were performed as described previously and binding controls were performed at each time point to confirm the *S. pyogenes* had bound to the HaCaT cells. These data are presented in Figure 5.17. While at five minutes very few bacteria had bound to the HaCaT cells the numbers binding did increase with time.

5.5.4 Quantitative studies at 5, 15, 30 and 60 minutes of infection

RNA was collected from the HaCaT cells infected with *S. pyogenes* for 5, 15, 30 and 60 minutes and analysed by quantitative real-time PCR for HBD1, HBD2 and LEAP-2 gene expression. LL-37 analysis of the samples was not undertaken due to the low levels of mRNA expression resulting in sensitivity problems. As previously HBD3 and hepcidin analyses were not undertaken as real-time PCR assays were not available.

The real-time results relating to HBD1, HBD2 and LEAP-2 expression are shown in Figure 5.18a, b & c. These data indicated that infection of the HaCaT cells with *S. pyogenes* did not significantly affect HBD1, HBD2 or LEAP-2 expression at times up to one hour of infection. It was also observed that the standard errors associated with the short infection data were very large.

Table 5.3: Summary of quantitative PCR data after 5, 15, 30 and 60 minutes of infection with *S. pyogenes* M1 serotype.

AMP mRNA	Quantitative PCR result
HBD1	↔
HBD2	↔
LEAP-2	↔

↔ No statistically significant difference in gene expression compared to control.

The results of the quantitative analyses relating to the 'short' infection experiments are summarised in Table 5.3. In summary, when the HaCaT cells were challenged with the *S. pyogenes* M1 serotype for times up to one hour, HBD1, HBD2 and LEAP-2 mRNA expression were not significantly altered compared to control.

5.6 Gene Expression in HaCaT Cells Infected with *S. pyogenes* (Wild-type), M2 Serotype

The *S. pyogenes* M1 serotype binds to cells (HaCaT and tonsil) via pili (Abbot, Smith et al. 2007). Compared to the M1 serotype, the M2 serotype is known to have a large number of pili on its surface (Personal communication W.D. Smith, Newcastle). Thus to determine whether the serotype of *S. pyogenes* affected the AMP mRNA responses in HaCaT cells, the bacterial challenge experiments were repeated using the *S. pyogenes* M2 serotype.

Binding data relating to the *S. pyogenes* M2 serotype experiments are shown in Figure 5.19. Although not quantified very few bacteria were found to bind to the HaCaT cells after 5min, however this number increased with time and was comparable at two hours to that seen previously with the M1 serotype (Figure 5.7). The levels of HBD1, HBD2 and LEAP-2 gene expression in response to binding were analysed by real-time PCR. All the data was normalised to GAPDH and the results were expressed as a percentage of the control. Statistical analysis was performed with a one way ANOVA followed,

where appropriate, by a Dunnett's post-test. LL-37, HBD3 and hepcidin expression were not quantified for reasons described in Section 5.5.2.

5.6.2 Quantitative studies

The results of the *S. pyogenes* M2 serotype challenge experiments are presented in Figure 5.20a-c. Figure 5.20a shows the data relating to the expression of HBD1 mRNA over a range of time points between five minutes and six hours respectively. The standard errors relating to each of the data points were large and statistical analysis of the data revealed no significant changes in HBD1 mRNA expression, indicating that the expression of HBD1 mRNA by the HaCaT cells was not affected by the *S. pyogenes* M2 serotype challenge.

The data relating to HBD2 expression is shown in Figure 5.20b. These data were also affected by large error bars and statistical analysis showed no significant differences between the time points.

Figure 5.20c shows that LEAP-2 mRNA expression levels were significantly reduced at 30 and 60 minutes compared to the control ($P<0.05$), and the mean levels remained low ($\leq$ 50% of control) up to six hours post infection.

Table 5.4: Expression patterns of AMP mRNA with M2 serotype *S. pyogenes*

AMP mRNA	M2 serotype
HBD1	↔
HBD2	↔
LEAP-2	↓ 30 and 60 minutes

↔ No statistically significant differences in gene expression compared to control
↓ Statistically significant decrease in gene expression compared to control

The results of the quantitative analyses relating to the M2 infection experiments are summarised in Table 5.4. In summary, when the HaCaT cells were challenged with the *S. pyogenes* M2 serotype the data suggested no statistically significant changes in HBD1 and HBD2 gene expression. However LEAP-2 gene expression was significantly reduced compared to control after 30 and 60 minutes of infection.

These data suggested that the affects of the M2 serotype on AMP expression in HaCaT cells were not identical to that of the M1 serotype especially with relation to LEAP-2 expression.

5.7 Gene Expression of HBD1 and LEAP-2 in HaCaT Cells Infected with Pili-defective *S. pyogenes* M1 Serotype

Pili are expressed on the surface of S. *pyogenes* and have been reported by this research group to affect the *in vitro* infectivity of this Gram-positive bacterium (Abbot, Smith et al. 2007). Essentially it was found that deletion of the genes encoding pilus-like structures prevents the adhesion of *S. pyogenes* to HaCaT cells and tonsils. To determine the absence of pili on the AMP response of the HaCaT cells to a streptococcal infection, the M1 mutant strains Δ*spy129* and Δ*spy1154* were used in the bacterial challenge experiments. The mutant strain Δ*spy129* lacks the pilus-associated sortase (SrtC1) and fails to synthesise pili, while the Δ*spy1154* mutant lacks pili and various surface binding molecules such as adhesins (Personal communication, W.D. Smith). The wild-type *S. pyogenes* M1 serotype was included in the challenge experiments and acted as the control. Analysis of AMP gene expression was performed at six hours only, as previous data (Figure 5.16) indicated significant changes in AMP gene expression at this time point.

The bacterial binding data relating to these experiments are shown in Figure 5.21. These data confirmed that the *S. pyogenes* (wild-type) M1 serotype bound to the HaCaT cells while, in comparison, the pili-defective mutants did not.

5.7.1 Expression patterns

Following the challenge experiments the RNA collected from the HaCaT cells was analysed by real-time PCR for HBD1 and LEAP-2 expression. As previously, the data

was normalised to GAPDH and expressed as a percentage of control. No HBD2 analysis was performed due to problems with the assay at the time of the investigation.

The results relating to the challenge experiments with the wild-type and mutant M1 strains are presented in Figure 5.22. After six hours of infection with wild type *S. pyogenes,* HBD1 expression (Figure 5.22a) was significantly decreased ($P<0.01$), which agreed with previous results (Figure 5.16a). In addition HBD1 expression was significantly reduced ($P<0.01$), following challenge with both pili-defective mutants i.e. Δ*spy129* and Δ*spy1154*. This indicated that the effects on HBD1 expression were not dependent on the binding of the streptococci to the HaCaT cells.

The data shown in Figure 5.22b showed no statistically significant differences between HaCaT cell expression of LEAP-2 mRNA after six hours of infection with *S. pyogenes* (wild-type) when compared to the control. It was observed that the data relating to the Figure 5.22b control and wild-type results were characterised by large standard errors. When the HaCaT cells were incubated with the pili-defective mutant Δ*spy129* no statistically significant differences were observed. LEAP-2 expression in response to Δ*spy1154* was comparable to the wild-type results.

5.8 Discussion

The results of the clinical study presented in Chapter 4 did not support any statistically significant differences between the AMP expression profiles of tonsils excised and analysed from control subjects and RAT patients. These data therefore favoured the premise that susceptibility to recurrent acute tonsillitis was not due to a defect in the innate immune response involving host AMPs. However the fact that the RAT tonsils analysed in the patient study were excised and analysed during a quiescent phase of the disease, rather than during active infection, may have accounted for the lack of AMP responses observed between the control (non-RAT) and RAT tissues. To explore this further an investigation of tonsil AMP responses during an active streptococcal infection was necessary and this was attempted, initially, using an *in vitro* cell line that modelled the tonsil epithelium.

There is to our knowledge no tonsil-derived cell-line, thus to begin with HEp-2 cells, a laryngeal cell line, was considered for use, as these cells had previously been used by other groups to model the tonsil epithelium (Greco, De Martino et al. 1995; Cheng, Stafslien et al. 2002; Wang, Li et al. 2006). Moreover in a pilot study in Newcastle the AMP profile of the HEp-2 cells revealed HBD1 and HBD3 expression and peptide synthesis, which was comparable to that of the tonsil epithelium, although it was of concern that neither LL-37 nor HBD2 expression was detected (Ball 2004). Further analyses of the HEp-2 cell AMP expression profile using RT-PCR identified LL-37 transcripts, but only by increasing the number of PCR cycles from 30 to 40. Moreover a cDNA band indicative of HBD2 gene expression was observed, but not confirmed due to cloning problems arising from the low amounts of product. Why LL-37 and HBD2 expression specifically should be reduced in this cell line is not known. However the explanation may include the fact that the HEp-2 cells are not homogeneous, but contaminated with cervical cancer derived HeLa cells. The use of the HEp-2 cell line as a model for tonsil was finally vetoed in light of the results of a study in Newcastle (Abbot, Smith et al. 2007), which investigated and compared the interactions of *S. pyogenes*, a bacterium able to infect the oropharynx and skin, with tonsils and epithelial cell lines. In this study the authors reported that the infection of tonsil with *S. pyogenes* was pili-dependant while that of HEp-2 cells was not. These data thus identified an

important difference between the HEp-2 cells, seen classically as modelling the tonsil, and the tonsil *per se*. Interestingly, the study by Abbot, Smith et al (2007), also discounted A549 cells, an alveoli-derived cell line often used as a model for streptococcal interactions (Cue and Cleary 1998), as again *S. pyogenes* binding to the cells was not found to be pili-dependent.

As the nature of the investigations planned in my studies probably depended on the interaction between the eukaryote cells and the streptococci the HEp-2 cell line was deemed unsuitable for subsequent experiments. Abbot, Smith et al (2007), did show however that streptococci bound to human primary keratinocytes and HaCaT cells in a pili-dependent manner. This indicated that the HaCaT cell line could be used as an appropriate *in vitro* model of the tonsil to examine AMP profiles in response to streptococci. The immortalised HaCaT cell line was chosen in preference to primary keratinocytes as it provided a reliable homogenous *in vitro* system that was easy to passage and maintain in culture.

Before the HaCaT cells could be adopted as a model of the tonsil their AMP expression profile required investigation. End-point PCR analyses confirmed HBD1-3, hepcidin, LEAP-2 and LL-37 gene expression, which matched that of the tonsil; however the expression of LL-37 mRNA was found to be low and required 40 cycles of PCR in order to detect a cDNA band indicative of LL-37 transcription. Interestingly in the studies reported by Kim, Kim et al (2005), also using HaCaT cell RNA, the investigators were unable to detect LL-37 expression, although this might be explained by the fact that they used only 35 PCR cycles, rather than 40, in their PCR reaction. Streptococci form part of the normal commensal flora of the mouth, skin, and upper respiratory tract of humans, and considering that the LL-37 peptide is known to interact with streptococci (Dorschner, Pestonjamasp et al. 2001; Nyberg, Rasmussen et al. 2004; Fernie-King, Seilly et al. 2006; Johansson, Thulin et al. 2008), and kill through disruption of the bacterial membrane (Oren, Lerman et al. 1999; Henzler-Wildman, Martinez et al. 2004), it was surprising that LL-37 expression was not easily detectable. However in support it has been reported that LL-37 mRNA expression is very low in healthy skin keratinocytes and increased only following skin injury (Lande, Gregorio et al. 2007). Moreover the AMP LL-37 has been shown to be associated with skin disorders such as psoriasis (Lande, Gregorio et al. 2007) and rosacea (Yamasaki, Di

Nardo et al. 2007) suggesting that elevated LL-37 skin levels can in fact be potentially harmful.

Before using the HaCaT cells as a model in the bacterial challenge experiments it was necessary to confirm that AMP gene expression could be regulated in this system. The active metabolite of vitamin D, D3, has been shown to induce keratinocyte differentiation (Bikle 2004), and previous studies had reported that LL-37 mRNA expression could be up-regulated in keratinocytes and HaCaT cells in response to treatment with D3 (Wang, Nestel et al. 2004; Weber, Heilborn et al. 2005; Schauber, Dorschner et al. 2006). Treatment of the HaCaT cells in this study with 200nM D3 also caused up-regulation of LL-37 expression after 22 hours (Figure 5.4), indicating the sensitivity of our detection system and the suitability of the model. It was probable that this up-regulation was due to the direct effects of D3 on the vitamin D response element (VDRE) situated in the promoter region of the human cathelicidin gene (Wang, Nestel et al. 2004). No comparable effects on LL-37 expression were recorded in response to treatment with LPS, LTA or PMA, with the LPS results supporting previous observations reported by Kim, Kim et al (2005).

Lipoteichoic acid (LTA) is a surface-associated molecule associated with Gram-positive bacteria and the negative results observed following LTA treatment of the HaCaT cells hinted that challenging the cells with streptococci would not affect the AMP expression. However it was known from the studies of Abbot, Smith et al (2007), that infection was associated with the actual binding of the bacteria to the cells thus while the negative result was acknowledged it was decided to continue with the challenge experiments involving whole live bacteria. It was noted that LL-37 expression was shown to be up-regulated in human sinus epithelial cells following treatment with LTA (Nell, Tjabringa et al. 2004). However the concentration of agent and the incubation periods used were not comparative between studies. For example in the studies reported in this thesis the amount of LTA at 2μg/ml was five times less than that in the study of Nell, Tjabringa et al (2004), and the incubation time was 22 hours compared to two weeks.

The initial challenge studies using chemical agents also targeted the LEAP-2 gene. None of the agents appeared to affect LEAP-2 gene expression. This was surprising especially in relation to LPS, as LEAP-2 gene expression in epithelial cells has been

shown to be up-regulated in response to a live *Salmonella* challenge (Townes, Michailidis et al. 2004; Sang, Ramanathan et al. 2006). None-the-less, these interesting *in vitro* results and the lack of literature describing LEAP-2 expression patterns in response to Gram-positive bacteria, supported the continuation of the *in vitro* streptococcal challenge experiments.

All the challenge experiments using the *S. pyogenes* M1 serotype, were performed in media lacking FCS. This media supplement was omitted as it had been suggested that serum can reduce peptide bactericidal activity (Bartlett, McCray et al. 2004). Using a FCS free system thus allowed us the opportunity to measure potential peptide antimicrobial activities, although in fact time constraints meant that such measurements were not made. In all bacterial challenge experiments the binding of the streptococci to the eukaryote cells was checked using GFP labelled bacteria and microscopy. Moreover the initial AMP expression analyses were performed at two hours of infection as previous data (Abbot, Smith et al, 2007) had shown that by this time approximately 10 to 20% of the bacteria added initially were adhering strongly to the cells (100% adherence). Experiments investigating AMP expression at earlier time points (5 to 60min) concomitant with only 10-40% adherence (Abbott, Smith et al, 2007), did not provide any additional insights into the host response, except perhaps for LEAP-2 where an immediate reduction in gene expression was observed (Figure 5.20).

The effects of the streptococcal challenges on AMP gene expression were initially performed using a less reliable semi-quantitative system. These analyses used densitometry to quantify the levels of gene expression, but the variability in the quality of the gels, often resulted in large error bars that ultimately reduced the sensitivity of the analyses. The gene expression of LL-37 was observed to be very low when analysed by this method. Data from the reanalysis of the RNA samples with the more sensitive technique of real-time PCR was also unfortunately plagued by large error bars (again probably due to low gene expression requiring large numbers of cycles) and the expression of LL-37 mRNA was not different to the uninfected control cells to a statistically significant level. The low levels of LL-37 gene expression in fact provided questions over the suitability of the HaCaT cells as a good tonsil model, as LL-37 expression was detected easily in the tonsil RNA samples.

The semi-quantitative analyses did however show statistically significant decreases in HBD1 and HBD2 mRNA expression after six hours of infection with the *S. pyogenes* M1 serotype. HBD1 results were mirrored by the real-time data and were interesting as classically HBD1 is recognised as being constitutively expressed in tissues, including skin and those of the oral cavity (Mathews, Jia et al. 1999; Ali, Falconer et al. 2001; Wang, Dong et al. 2004; Kimball, Nittayananta et al. 2006; Schroder and Harder 2006). Regulated expression has however been reported, for example increased HBD1 expression was shown in HCT-116 cells, in response to albumin and amino acids (Sherman, Chapnik et al. 2006), and in cultured human mesangial cells maintained in high glucose (Malik and Al-Kafaji 2007). Interestingly a loss of HBD1 has been documented, but in renal cell carcinomas and prostate cancers and explained by either promoter polymorphisms and/or deletion of the gene residing on the short arm of chromosome 8 (Donald, Sun et al. 2003; Sun, Arnold et al. 2006). Inhibition of HBD2 gene expression in response to the streptococcal challenge was also atypical as the literature generally favours the induction of HBD2 gene expression in response to potential pathogens (Pivarcsi, Nagy et al. 2005; Mendez-Samperio, Alba et al. 2007). However down-regulation of HBD2 has been reported in cultured keratinocytes in response to stress, namely heat shock (Bick, Poindexter et al. 2004). Similarly a decrease in cathelin-related AMP (CRAMP) and mouse beta-defensin 3, the closest murine homologue of HBD2, was reported in the skin of female hairless mice in response to psychological stress (Aberg, Radek et al. 2007). Moreover this down-regulation of AMP gene expression was associated with the increased susceptibility of the mice to *Streptococcus* infection and proposed to function through the increased production of endogenous glucocorticoids.

HBD3 is an inducible peptide (Harder, Bartels et al. 2001) shown to have antimicrobial activity (MIC/LC_{90} of 12μg/ml) against *S. pyogenes* (Dhople, Krukemeyer et al. 2006) as well as other potentially pathogenic oral strains (Song 2008). It was therefore interesting that the expression data from the semi-quantitative studies indicated that the streptococcal infection of the HaCaT cells did not affect HBD3 gene transcription (Figure 5.11), although it was recognised that the results were beset by large error bars and thus lacked sensitivity. It was therefore disappointing that the results could not be verified by real-time PCR due to problems with the assay. However no induction of HBD3 gene expression was observed in response to the mouth commensal

Streptococcus gordonii (Ji, Kim et al. 2007) although in contrast a substantial eight-fold increase in expression was reported in oral epithelial cells in response to *Candida albicans* (Feng, Jiang et al. 2005).

The hepcidin peptide is known to be strongly induced during infections and inflammation, causing intracellular iron sequestration, reduced plasma iron levels which in turn limits the amounts of iron available to invading micro-organisms (Vyoral and Petrak 2005). In addition the peptide has intrinsic antimicrobial activity. Thus the statistical result indicating that hepcidin (*HAMP*) gene expression was not significantly different to that of the control after four and six hours of *S. pyogenes* M1 infection was surprising. However interpretation of the semi-quantitative hepcidin expression data was complicated by the large error bars, which in conjunction with the lack of a real-time assay system meant that these data were not authenticated. While the liver is the major site of hepcidin production other tissues and cells are known to express the gene and recently a TLR4 dependent increase in *HAMP* gene expression was reported in macrophages and neutrophils in response to an infection with *S. pyogenes* (Peyssonnaux, Zinkernagel et al. 2006), again presumably to limit the availability of iron to the invading micro-organisms. To date the roles of the hepcidin peptide in the skin are not known and thus the mechanisms and consequent effects of gene down-regulation are conjecture, but the loss of hepcidin can only result in a more successful pathogen.

The LEAP-2 gene encodes a peptide with antimicrobial activity against Gram-positive bacteria (Krause, Sillard et al. 2003) Semi-quantitative analyses of LEAP-2 gene expression following challenge of the HaCaT cells with the streptococci suggested that the LEAP-2 gene was not regulated in response to the bacterial challenge and these data concurred with the results of the LTA challenge. However this result was contradicted by the more sensitive real-time assay data that indicated the gene to be up-regulated. There is little information published in relation to LEAP-2 expression in cells in response to a bacterial challenge, although two mammalian studies involving the Gram-negative organism *S. enterica* serovar Typhimurium rather than a Gram-positive bacterium, support the up-regulation of the LEAP-2 gene in response to a microbial assault (Townes, Michailidis et al. 2004; Sang, Ramanathan et al. 2006).

Overall the HaCaT data showed that HBD1 gene expression were down-regulated, whereas LEAP-2 was up-regulated, in response to the *S. pyogenes* challenge. It also showed that LL-37 and HBD2 gene expression was not changed to a statistically significant level under the conditions in these tests. These data indicated that the *S. pyogenes* M1 serotype was able to modulate defensin gene expression but the mechanisms by which the organism achieved this are not known. It is acknowledged that the β-defensin genes are activated through TLR signalling pathways; in keratinocytes these include the NF-κB and mitogen activated protein kinase pathways although different organisms appear to trigger distinct signalling cascades (Chung and Dale 2004; Joly, Organ et al. 2005; Schauber, Dorschner et al. 2006; Mendez-Samperio, Alba et al. 2007; Wehkamp, Schauber et al. 2007). Also studies in HaCaT cells have described the expression of TLR1, TLR2, TLR3, TLR4, TLR5 and TLR10 in this immortalized cell line (Pivarcsi, Koreck et al. 2004; Kollisch, Kalali et al. 2005). These studies have considered the effects the expression of these receptors may have on the immune responses of this cell line. The study by Pivarcsi, Koreck et al, 2004 described how the expression of TLRs 2 and 4 mRNA increase with the differentiation state of HaCaT cells. The work by Kollisch, Kalali et al, 2005 used LPS to induce TLR4 expression in HaCaT cells, suggesting that bacterial components such as LPS may trigger a TLR related response in this cell line. It thus appears that *S. pyogenes* interferes with these signalling systems and disrupts the host AMP response. The molecular mechanisms regulating LL-37 expression are poorly described but computational analysis of the hCAP18 promoter has identified a number of potential transcription factor binding sites, including Sp1, PU-1 and C/EBP amongst others, indicative of complex regulatory systems (Elloumi and Holland 2008). To date nothing is known of the signalling systems regulating LEAP-2 expression although the 5' flanking sequence of the chicken gene is characterised by a potential NF-κB binding site (Lynn, Lloyd et al. 2003; Townes, Michailidis et al. 2004). The data from the challenge experiments suggested that LEAP-2 expression was up-regulated in the streptococcal challenged HaCaT cells indicative of increased transcription, peptide synthesis and a host innate response. However as no peptide levels were measured it cannot be discounted that the *S. pyogenes* blocked mRNA translation and thus peptide synthesis.

Both the M1 and M2 serotypes of *S. pyogenes* have been identified in the throat (Tyrrell, Lovgren et al. 2002). The initial bacterial challenge experiments in this study

were performed using the M1 serotype as it had been well characterised and was known to bind HaCaT cells in a pili-dependant manner (Abbot, Smith et al. 2007). To investigate whether the host AMP response was affected by the *S. pyogenes* serotype the challenge experiments were repeated but using the M2 serotype, which has increased numbers of pili. Binding of the M2 serotype to the HaCaT cells, although subjective, appeared comparable to that of M1. HBD1 and HBD2 gene expression profiles were different to what was observed in M1 infections as no difference was seen in expression compared to the uninfected control cells after a total of 6 hours of infection. The LEAP-2 expression profile was also different in that no significant up-regulation of gene expression was detected. Because nothing is known of the signalling systems regulating LEAP-2 expression it is difficult to explain or indeed comment on this novel result, but the two serotypes will probably provide useful tools for future studies investigating the pathways controlling LEAP-2 expression.

The choice of the HaCaT cells for use in the *in vitro* experiments investigating AMP gene expression was directed by the fact that the cells bound *S. pyogenes* and modelled the tonsil. Once the AMP expression patterns in relation to streptococcal binding were determined the experiments were repeated but using the pili-defective mutants Δ*spy129* and Δ*spy1154*, that were unable to bind to the HaCaT cells (Figure 5.21). These experiments, performed to determine whether streptococcal binding was necessary to elicit an AMP response, indicated that the reduction in HBD1 mRNA expression following the streptococcal challenge was in fact pili-independent. Moreover as Δ*spy1154* also lacked surface proteins such as adhesins, it was also deduced that such proteins were not involved in regulating HBD1 gene expression. The LEAP-2 expression data was complicated by the large error bars associated with the control and wild-type columns and no statistically significant differences were observed between uninfected control cells and both wild-type and mutant streptococci. The identity of the streptococcal factor or factors responsible for initiating the changes in HBD1 mRNA expression is not known, but it is possible that secreted molecules, for example SIC or streptococcal specific proteases play a role.

In summary, HaCaT cells were adopted as an *in vitro* model of the tonsil to investigate the effects of *S. pyogenes* M1 and M2 serotypes on host AMP gene responses. This cell line was selected specifically as previous investigations had shown it to model tonsil-

streptococcal interactions. The quantitative real-time expression data suggested that in response to the *S. pyogenes* M1 serotype HBD1 gene expression were decreased, HBD2 and LL-37 gene expression was unchanged and that of LEAP-2 was induced. The results of challenge experiments performed using pili-defective mutants also suggested that such changes in the host response occurred in the absence of streptococcal binding. The mechanisms by which *S. pyogenes* causes such effects are not known but the HaCaT cells provide a good model for such studies. HaCaT cells are not however derived from tonsil. Thus to further investigate streptococcal–tonsil AMP responses it was decided to utilise the *ex vivo* tonsil model developed by Abbot, Smith et al (2007).

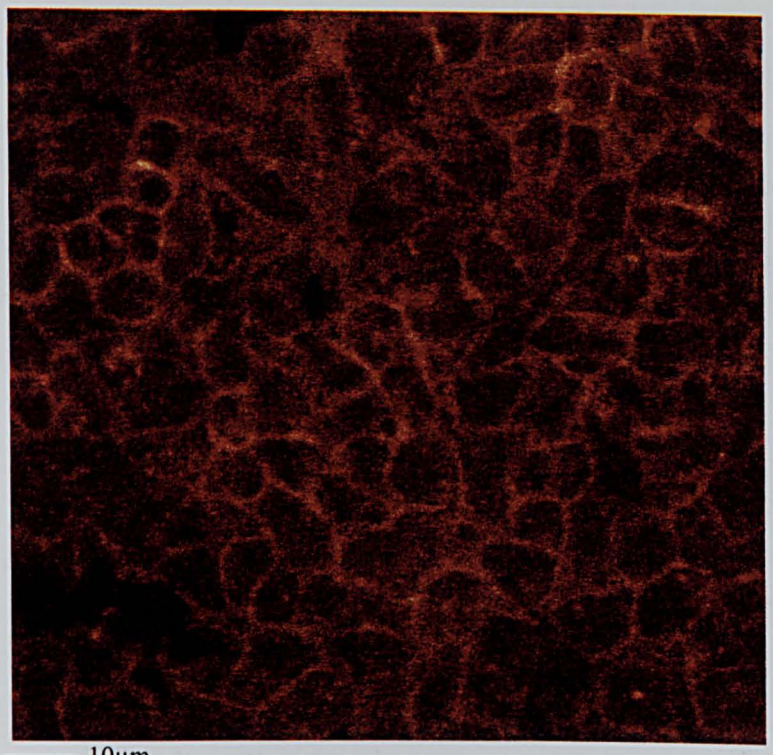

Figure 5.1: HEp-2 cells: x100 Magnification. Cell membrane is stained with Phalloidin-Rhodamine, an actin stain (shown in red). The cells show the typical appearance of a monolayer of epithelial cells.

a)

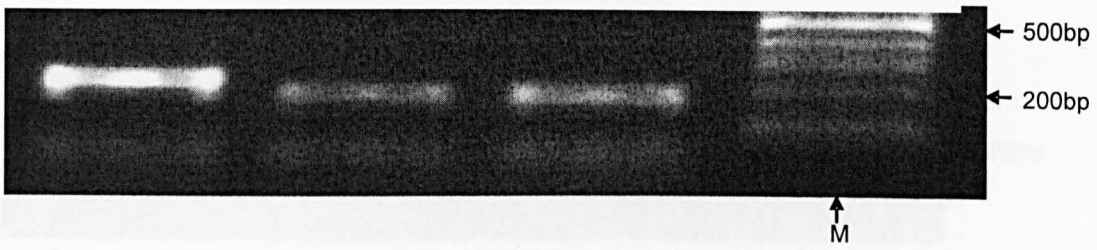

b)

```
Query: 5   caacactctcgtcatgtttcanggtttttatttctttcttcggcagcattttcggccacg 64
           ||||||||||||||||||| ||||||||||||||||||||||||||||||||||||||
Sbjct: 449 caacactctcgtcatgtttcagggtttttatttctttcttcggcagcattttcggccacg 390

Query: 65  cgtcgagcacttgccgatctgttcctcctttggaaggcagctgagcacagcacaccggcc 124
           ||||||||||||||||||||||||||||||||||||||||||||||||||||||||||||
Sbjct: 389 cgtcgagcacttgccgatctgttcctcctttggaaggcagctgagcacagcacaccggcc 330

Query: 125 gcctctgactctgcaataatatttctgtaatgtgtttatgattcctccatgaccaggaac 184
           |||||||||||||||||||||||||||||||||||||||||||||||||||| |||||
Sbjct: 329 gcctctgactctgcaataatatttctgtaatgtgtttatgattcctccatgacctggaac 270

Query: 185 a 185
           |
Sbjct: 269 a 269
```

Figure 5.2: a) Agarose gel results showing PCR products amplified from cDNA reverse transcribed from HEp-2 cell RNA with HBD3 (lane 1) and HBD1 (lane 2-3) specific primers. (Product size is approximately 200bp for HBD1 and 180bp for HBD3). M: Size marker (lane 4). **b)** Sequence analysis performed by BLAST (http://www.ncbi.nlm.nih.gov/blast/Blast.cgi) matched the cloned HBD3 product (query) to the Genbank sequence (sbjct) for HBD3 with 98% identity.

a)

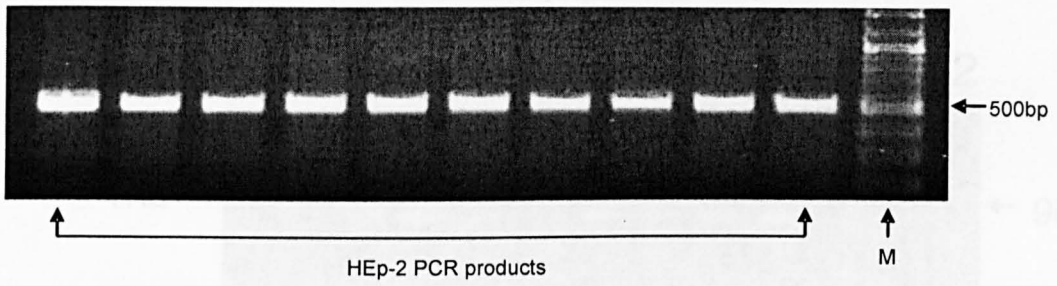

b)

```
Query: 1   gccactccctggggcggtggtcactggtgctcctgctgctgggcctggtgatgcctctgg 60
           ||||||||||||||||||||||||||||||||||||||||||||||||||||||||||||
Sbjct: 20  gccactccctggggcggtggtcactggtgctcctgctgctgggcctggtgatgcctctgg 79

Query: 61  ccatcattgcccaggtcctcagctacaaggaagctgtgcttcgtgctatagatggcatca 120
           ||||||||||||||||||||||||||||||||||||||||||||||||||||||||||||
Sbjct: 80  ccatcattgcccaggtcctcagctacaaggaagctgtgcttcgtgctatagatggcatca 139

Query: 121 accagcggtcctcggatgctaacctctaccgcctcctggacctggaccccaggcccacga 180
           ||||||||||||||||||||||||||||||||||||||||||||||||||||||||||||
Sbjct: 140 accagcggtcctcggatgctaacctctaccgcctcctggacctggaccccaggcccacga 199

Query: 181 tggatggggacccagacacgccaaagcctgtgagcttcacagtgaaggagacagtgtgcc 240
           ||||||||||||||||||||||||||||||||||||||||||||||||||||||||||||
Sbjct: 200 tggatggggacccagacacgccaaagcctgtgagcttcacagtgaaggagacagtgtgcc 259

Query: 241 ccaggacgacacagcagtcaccagaggattgtgacttcaagaaggacgggctggtgaagc 300
           ||||||||||||||||||||||||||||||||||||||||||||||||||||||||||||
Sbjct: 260 ccaggacgacacagcagtcaccagaggattgtgacttcaagaaggacgggctggtgaagc 319

Query: 301 ggtgtatggggacagtgaccctcaaccaggccaggggctcctttgacatcagttgtgata 360
           ||||||||||||||||||||||||||||||||||||||||||||||||||||||||||||
Sbjct: 320 ggtgtatggggacagtgaccctcaaccaggccaggggctcctttgacatcagttgtgat- 378

Query: 361 aaggataacaagaagatttgccctgctgggtgatttctttcccggaaatctaaagagaag 420
           |||||||||||| |||||||||||||||||||||||  ||||||||||||||||||||
Sbjct: 379 aaggataacaag-agatttgccctgctgggtgatttctt--ccggaaatctaaagagaag 435

Query: 421 attggcaaa 429
           |||||||||
Sbjct: 436 attggcaaa 444
```

Figure 5.3: a) Agarose gel results showing PCR products amplified from cDNA reverse transcribed from 10 HEp-2 cell samples with LL-37 specific primers (product size is approximately 500bp). M: size marker. **b)** Sequence analysis performed by BLAST (http://www.ncbi.nlm.nih.gov/blast/Blast.cgi) matched the cloned sequence (query) to the Genbank sequence (sbjct: subject) for LL-37.

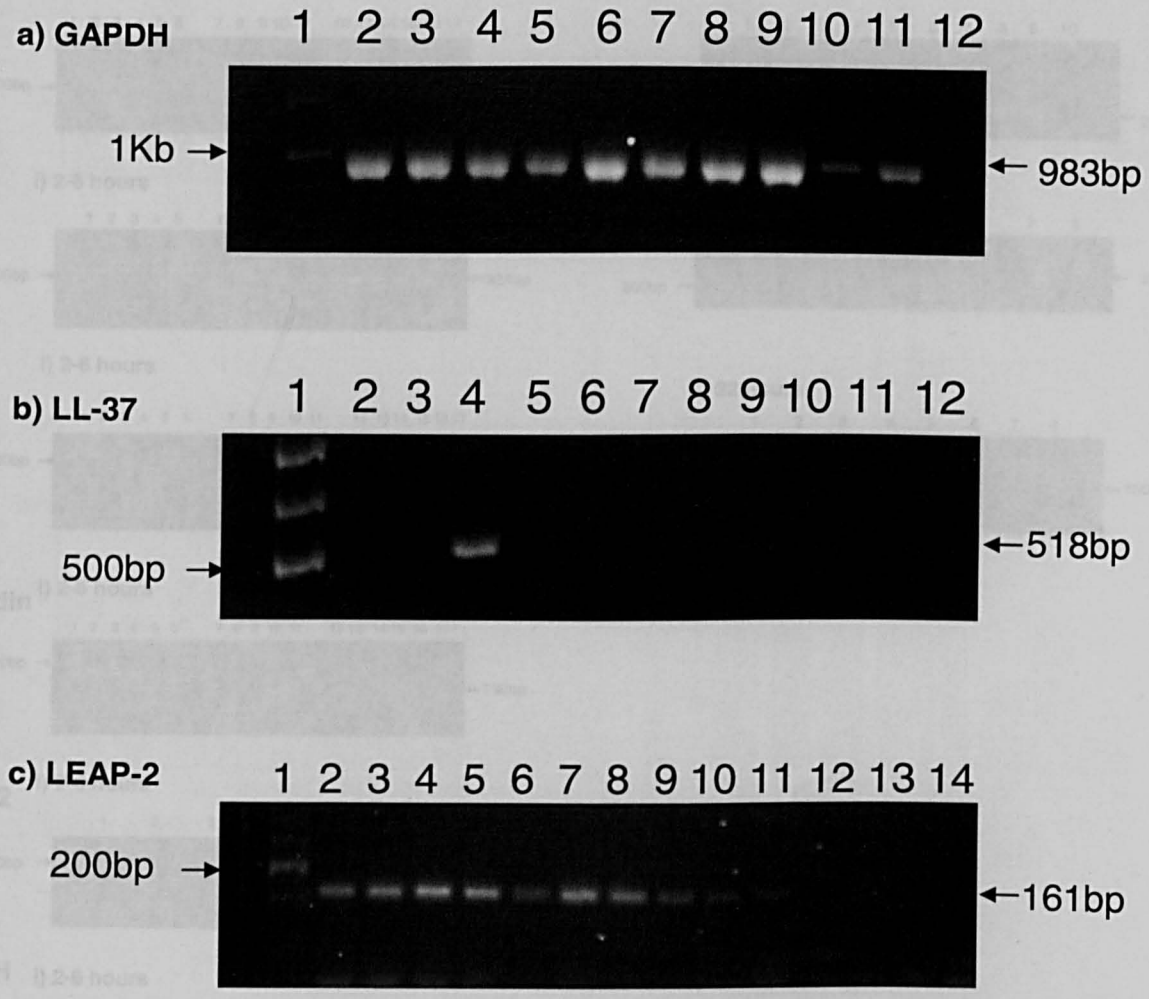

Figure 5.4 GAPDH, LL-37, LEAP-2 expression in HaCaT cells: Agarose gel results showing RT-PCR products amplified with GAPDH, LL-37 and LEAP-2 specific primers.
a) GAPDH PCR products: 1: Size marker; 2 & 3: untreated control cells; 4: cells treated with 1,25 dihydroxyvitamin-D3; 5: cells treated with LTA; 6 & 7: cells treated with LPS; 8 & 9: cells treated with PMA; 10 & 11: cells treated with a combination of all treatment agents; 12: no template control.
b)LL-37 PCR products: 1: Size marker; 2 & 3: untreated control cells; 4: cells treated with 1,25 dihydroxyvitamin-D3 (a PCR product at approximately 500bp can be observed); 5 & 6: cells treated with PMA; 7 & 8: cells treated with LPS; 9 & 10: cells treated with a combination of all treatment agents; 11: cells treated with LTA; 12: no template control.
c) LEAP-2 PCR products: 1: Size marker, 2 & 3: untreated control cells; 4: cells treated with 1,25 dihydroxyvitamin-D3; 5 & 6: cells treated with LPS; 7 & 8: cells treated with PMA; 9: cells treated with LTA; 10 & 11: cells treated with a combination of all treatment agents, 12 & 13: negative control no reverse transcriptase); 14: negative control (no template).
Gels were performed once. Each test treatment was performed 1-2 times.

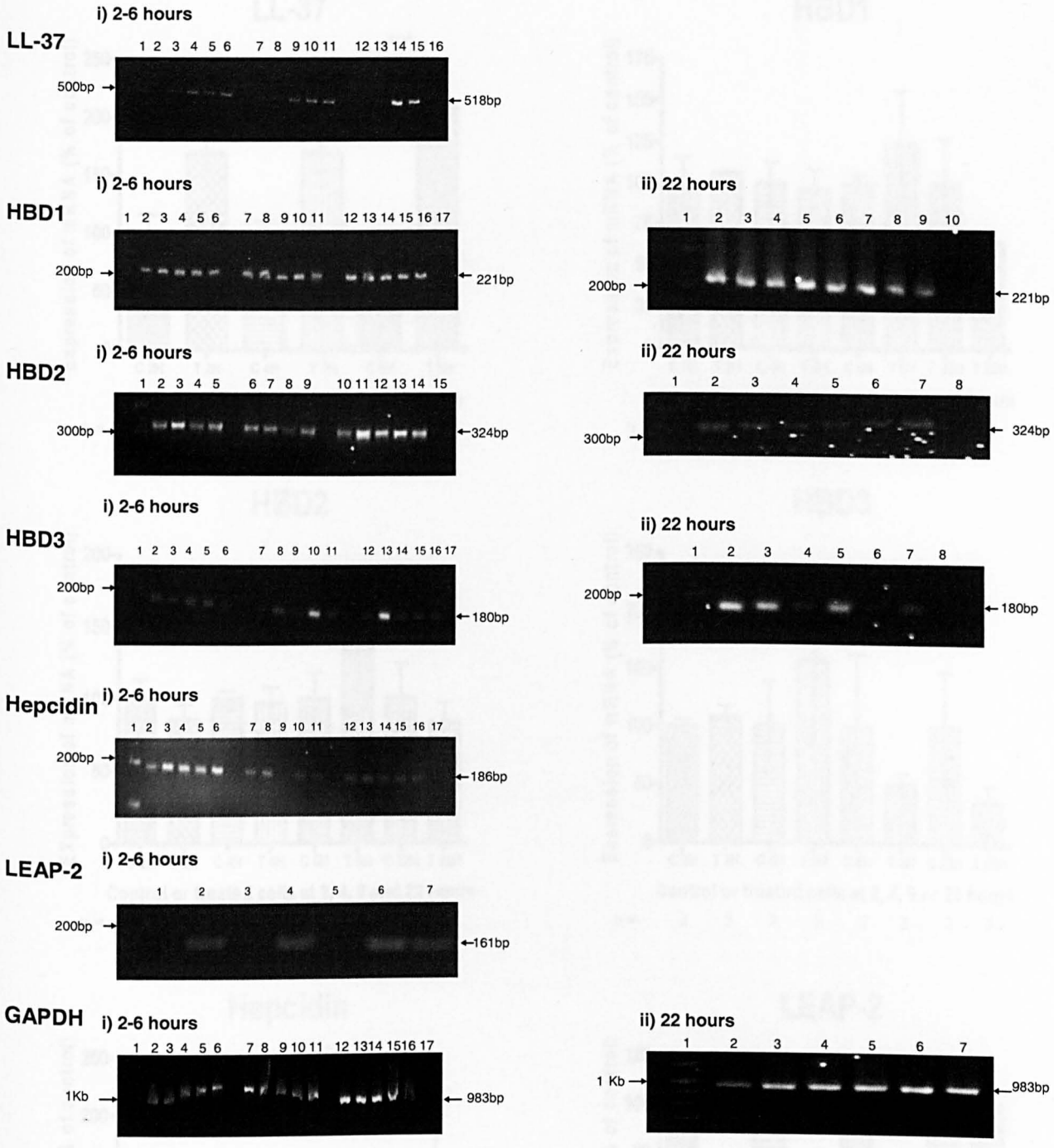

Figure 5.5: Representative RT-PCR results following challenge of HaCaT cells with D3. For all gels lane 1 is a size marker.

LL-37 (518bp): i) 2-3: 2 hour, control cells; 4-6: 2 hour, treated cells; 7-8: 4 hour, control cells; 9-11: 4 hour, treated cells; 12-13: 6 hour, control cells; 14-15: 6 hour, treated cells; 16: no template control.

HBD1 (221bp): i) 2-3: 2 hour, control cells; 4-6: 2 hour, treated cells; 7-8: 4 hour, control cells; 9-11: 4 hour, treated cells; 12-13: 6 hour, control cells; 14-16: 6 hour, treated cells; 17: no template control. **ii)** 2-4: 22 hour, control cells; 5-7: 22 hour, treated cells.

HBD2 (324bp): i) 2-4: 22 hour, control cells; 5-7: 22 hour, treated cells; 8-9: HaCaT cells treated with 1, 25 dihydroxyvitamin-D3 from a previous experiment; 10: no template control. **ii)** 2-4: 22 hour, control cells; 5-7: 22 hour, treated cells; 8: no template control.

HBD3 (180bp): i) 2-3: 2 hour, control cells; 4-6: 2 hour, treated cells; 7-8: 4 hour, control cells; 9-11: 4 hour, treated cells; 12-13: 6 hour, control cells; 14-16: 6 hour, treated cells; 17: no template control. **ii)** 2-4: 22 hour, control cells; 5-7: 22 hour, treated cells; 8: no template control .

Hepcidin (186bp): i) 2-3: 2 hour, control cells; 4-6: 2 hour, treated cells; 7-8: 4 hour, control cells; 9-10: 4 hour, treated cells; 11-12: 6 hour, control cells; 13-15: 6 hour, treated cells; 16: no template control.

LEAP-2 (161bp) i) 2: 2 hour, control cells; 3: 2 hour, treated cells; 4: 4 hour, control cells; 5: 4 hour, treated cells; 6: 6 hours, control cells; 7: 6 hours, treated cells.

GAPDH (983bp): i) 2-3: 2 hour, control cells; 4-6: 2 hour, treated cells; 7-8: 4 hour, control cells; 9-11: 4 hour, treated cells; 12-13: 6 hour, control cells; 14-16: 6 hour, treated cells; 17: no template control. **ii)** 2-4: 22 hour, control cells; 5-7: 22 hour, treated cells.

Gels were performed once. Each test was performed 2-3 times except for LEAP-2 samples for which treatment was performed only on one sample.

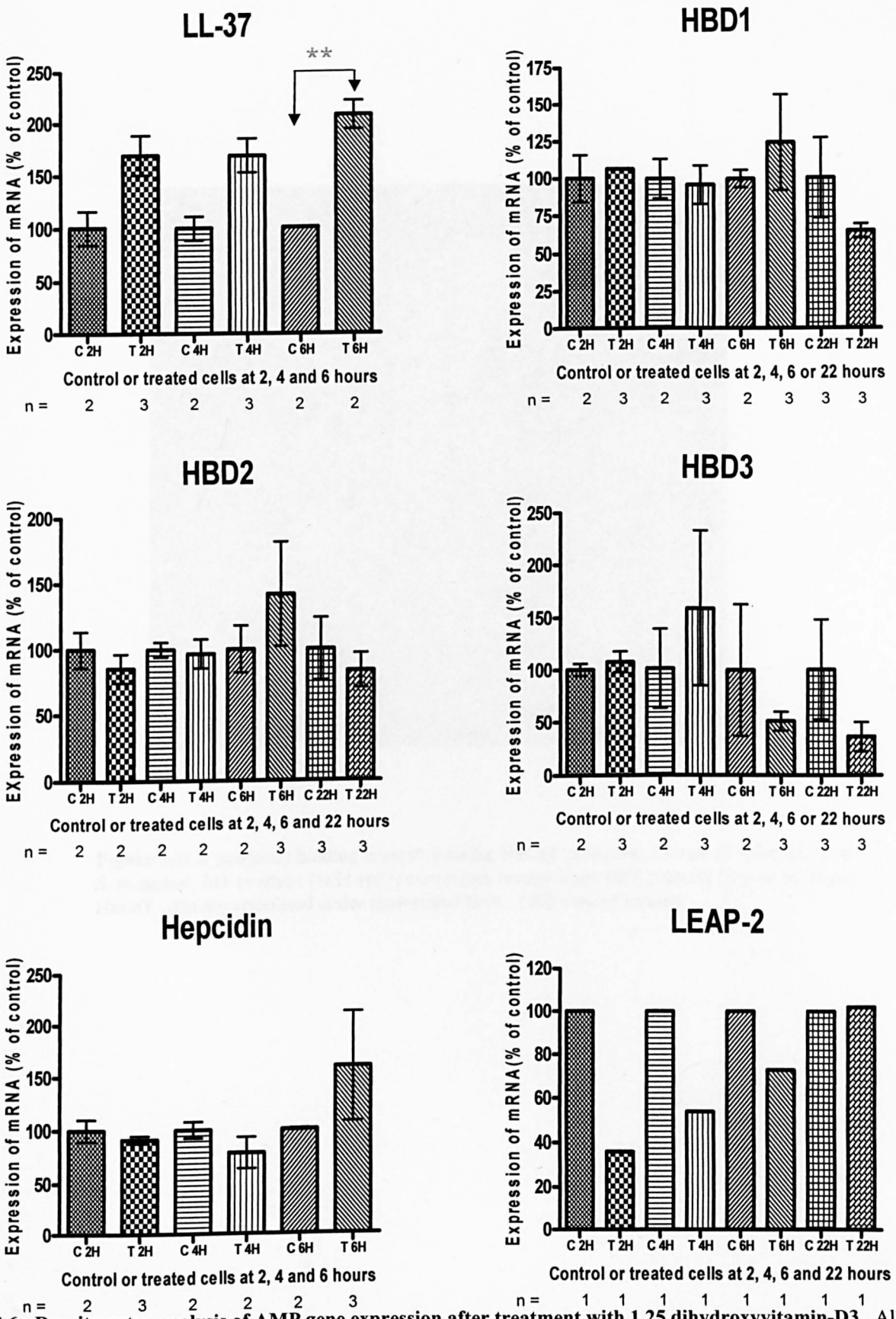

Figure 5.6: Densitometry analysis of AMP gene expression after treatment with 1,25 dihydroxyvitamin-D3. All data normalised to GAPDH and expressed as a percentage of control. All values represent mean ± SEM. Statistical analysis was performed with one way ANOVA followed by a Bonferroni post-test. ** = P<0.01. n: number of samples analysed. Analysis of each gel was performed once.

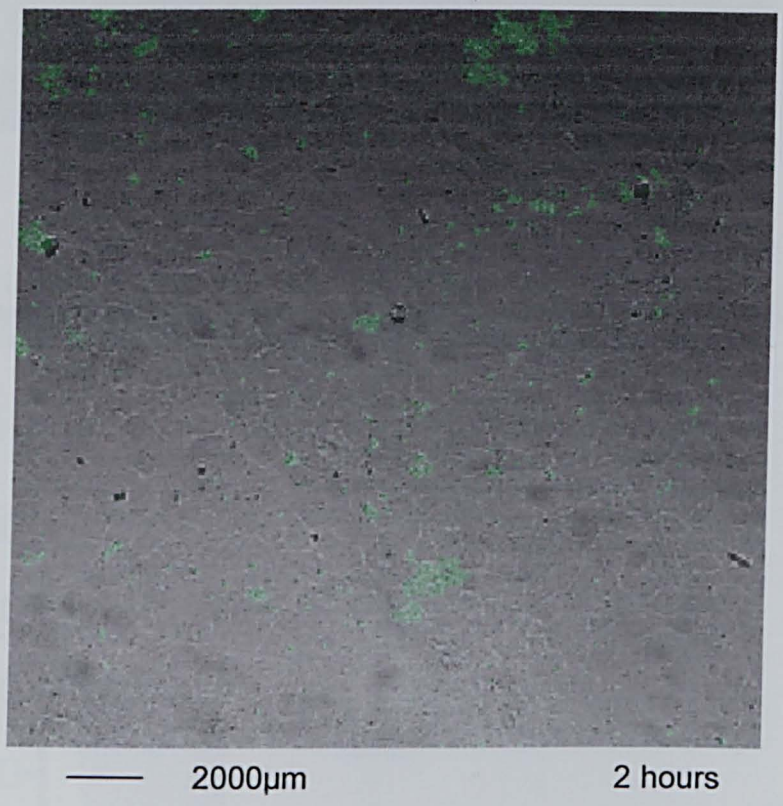

Figure 5.7: *S. pyogenes* binding control showing HaCaT cells after 2 hours of infection with *S. pyogenes*, M1 serotype (wild-type) expressing recombinant GFP plasmid (shown in green). HaCaT cells are visualised under transmitted light. (x20 magnification).

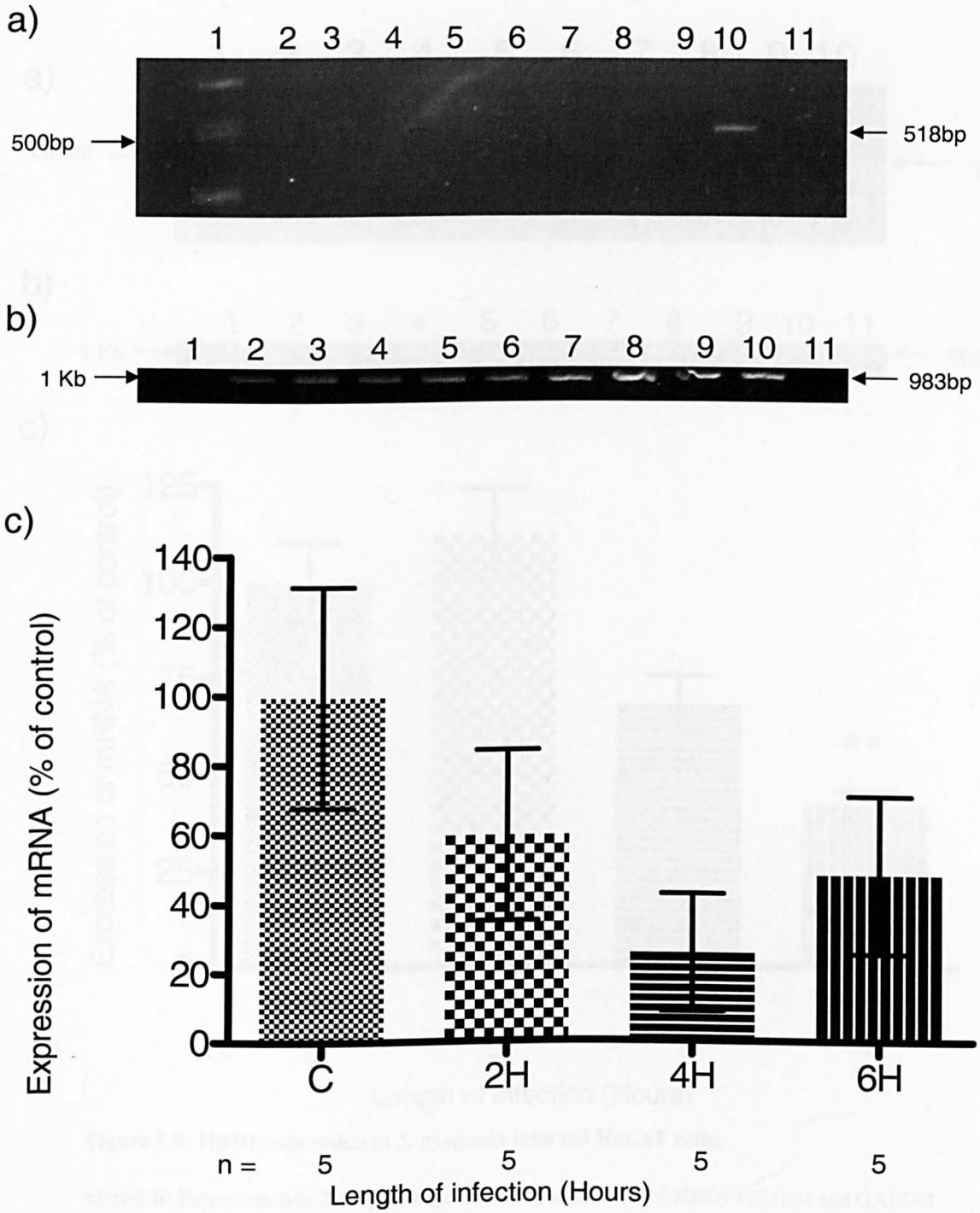

Figure 5.8: LL-37 expression in *S. pyogenes* infected HaCaT cells:

a) & b) Representative 2% agarose gel showing separation of LL-37 (518bp) and GAPDH (983bp) PCR products generated from DNA template which was reverse transcribed from RNA extracted from control HaCaT cells, HaCaT cells infected with *S. pyogenes*, M1 serotype and HaCaT cells treated with D3. 1: Size marker; 2-3: uninfected control cells; 4-5: HaCaT cells infected with *S. pyogenes* for 2H; 6-7: HaCaT cells infected for 4H; 8-9: cells infected for 6H; 10: cells treated with D3 for 2H; 11: no template control.

c) Graph shows data from densitometry analysis from the gels, normalised to GAPDH and expressed as a percentage of control. All values represent mean ± SEM.

Statistical analysis was performed by one way ANOVA followed by a Dunnett's Post-test.

Gels were performed once, 5 biological repeats were performed per infection time point.

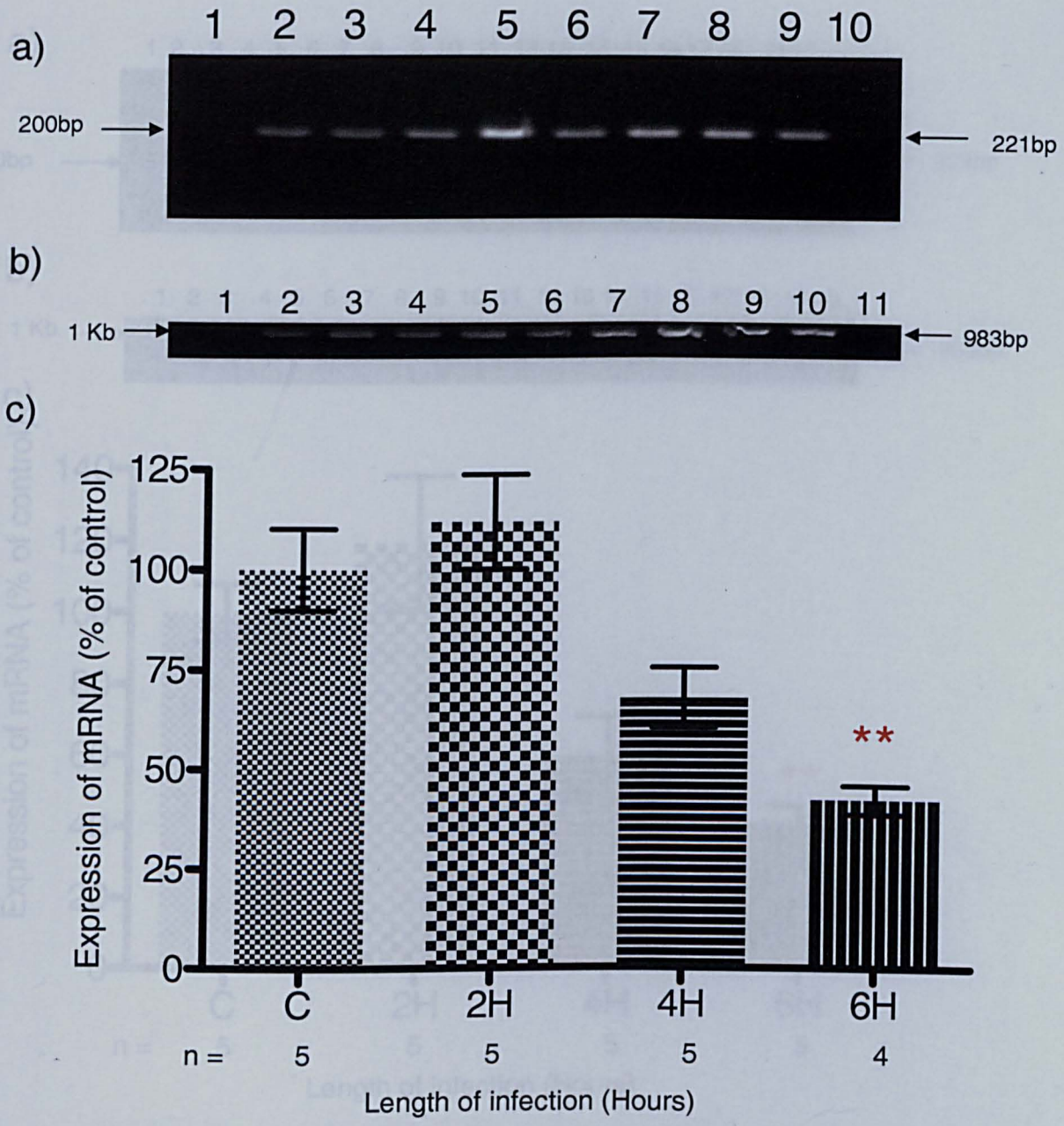

Figure 5.9: HBD1 expression in *S. pyogenes* infected HaCaT cells:

a) and b) Representative 2% agarose gel showing separation of HBD1 (221bp) and GAPDH (983bp) PCR products generated from DNA template which was reverse transcribed from RNA extracted from control HaCaT cells, HaCaT cells infected with *S. pyogenes*, M1 serotype and HaCaT cells treated with D3. 1: Size marker; 2-3: uninfected control cells; 4-5: HaCaT cells infected with *S. pyogenes* for 2H; 6-7: HaCaT cells infected for 4H; 8: cells infected for 6H; 9: cells treated with D3 for 2H; 10: no template control.
b) 1: Size marker; 2-3: uninfected control cells; 4-5: HaCaT cells infected with *S. pyogenes* for 2H; 6-7: HaCaT cells infected for 4H; 8-9: cells infected for 6H, 10: cells treated with D3 for 2H.
c) Graph shows data from densitometry analysis from the gels, normalised to GAPDH and expressed as a percentage of control. All values represent mean ± SEM. ** = $P<0.01$

Statistical analysis was performed by one way ANOVA followed by a Dunnett's Post-test. Gels were performed once, 4-5 biological repeats were performed per infection time point.

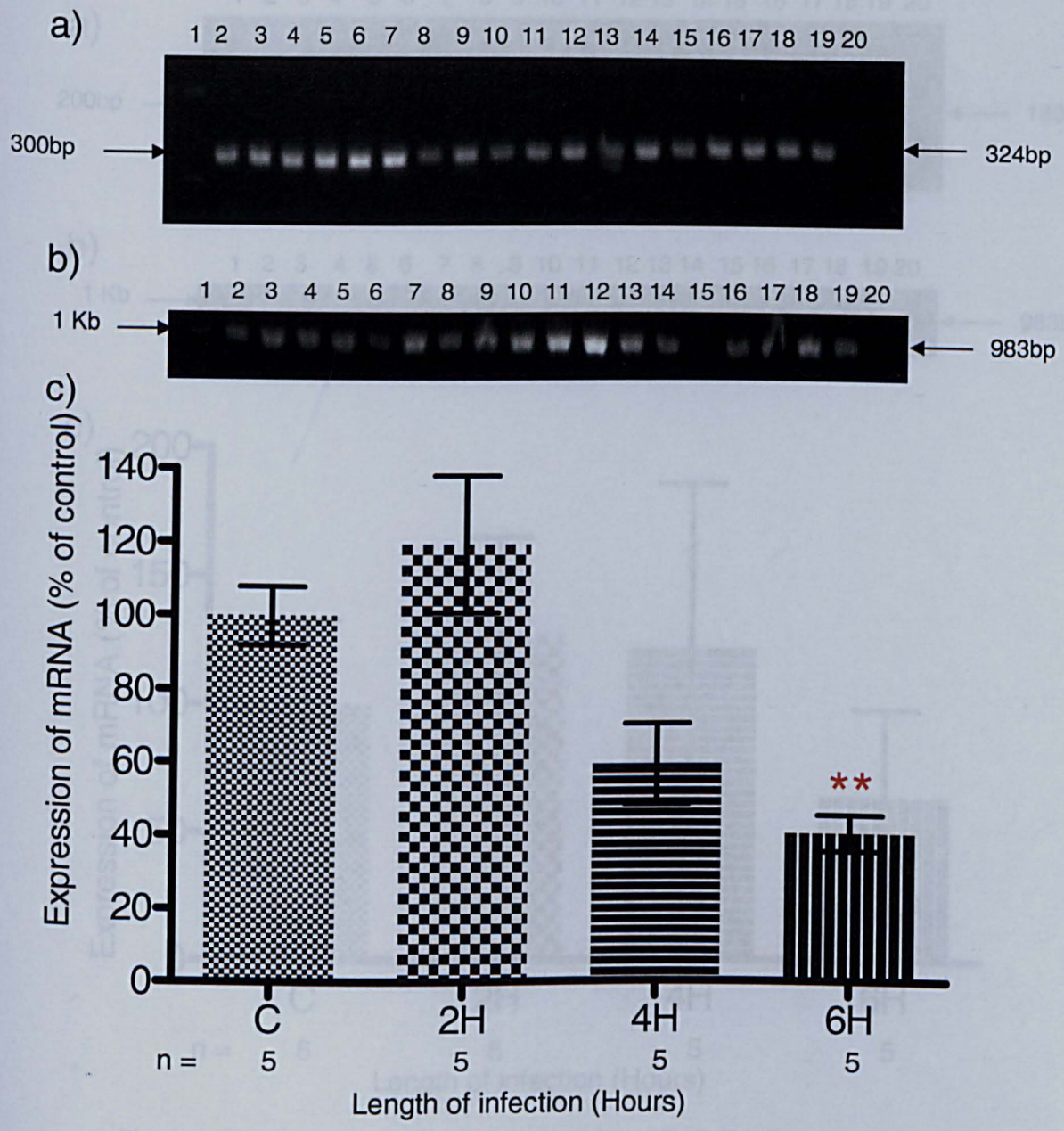

Figure 5.10: HBD2 expression in *S. pyogenes* infected HaCaT cells:
a) & b) Representative 2% agarose gel showing separation of HBD2 (324bp) and GAPDH (983bp) PCR products generated from DNA template which was reverse transcribed from RNA extracted from control HaCaT cells, HaCaT cells infected with *S. pyogenes*, M1 serotype and HaCaT cells treated with D3. 1: Size marker; 2-4: uninfected control cells; 5-7: HaCaT cells infected with *S. pyogenes* for 2H; 8-10: HaCaT cells infected for 4H; 11-13: HaCaT cells infected for 6 H; 14-16: HaCaT cells infected and treated with D3 for 2H; 17-19: HaCaT cells treated with D3 for 2H; 20: no template control.
c) Graph shows data from densitometry analysis from the gels, normalised to GAPDH and expressed as a percentage of control. All values represent mean ± SEM. ** = $P<0.01$

Statistical analysis was performed by one way ANOVA followed by a Dunnett's Post-test.
Gel a) was performed once, gel b) was performed 3 times. 5 biological repeats were performed per infection time point.

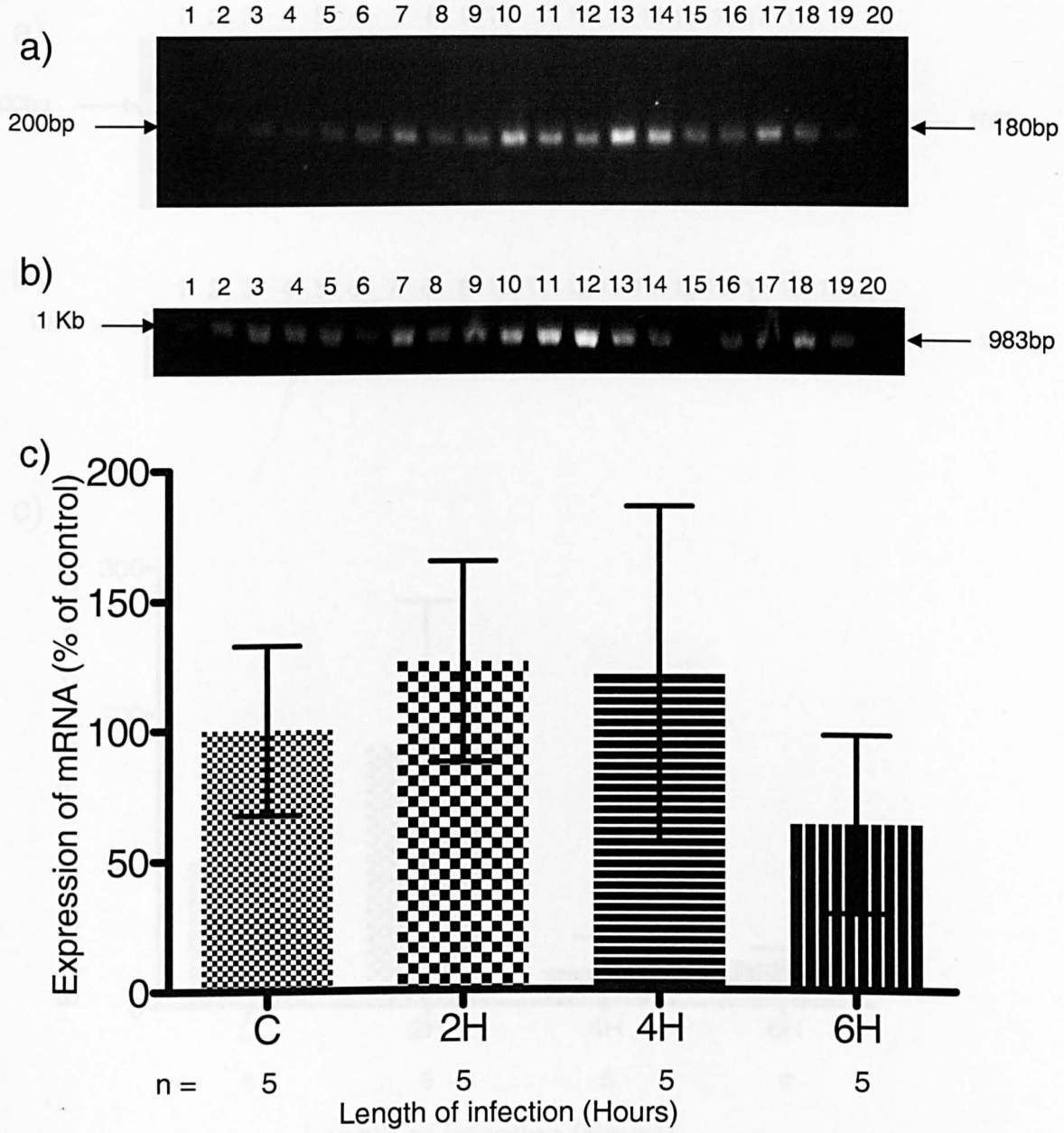

Figure 5.11: HBD3 expression in *S. pyogenes* infected HaCaT cells:

a) & b) Representative 2% agarose gel showing separation of HBD3 (180bp) and GAPDH (983bp) PCR products generated from DNA template which was reverse transcribed from RNA extracted from control HaCaT cells, HaCaT cells infected with *S. pyogenes*, M1 serotype and HaCaT cells treated with D3. 1: Size marker; 2-4: uninfected control cells; 5-7: HaCaT cells infected with *S. pyogenes* for 2H; 8-10: HaCaT cells infected for 4H; 11-13: HaCaT cells infected for 6 H; 14-16: HaCaT cells infected and treated with D3 for 2H; 17-19: HaCaT cells treated with D3 for 2H; 20: no template control.
196
c) Graph shows data from densitometry analysis from the gels, normalised to GAPDH and expressed as a percentage of control. All values represent mean ± SEM.

Statistical analysis was performed by one way ANOVA followed by a Dunnett's Post-test.
Gel a) was performed once, gel b) was performed 3times. 5 biological repeats were performed per infection time point.

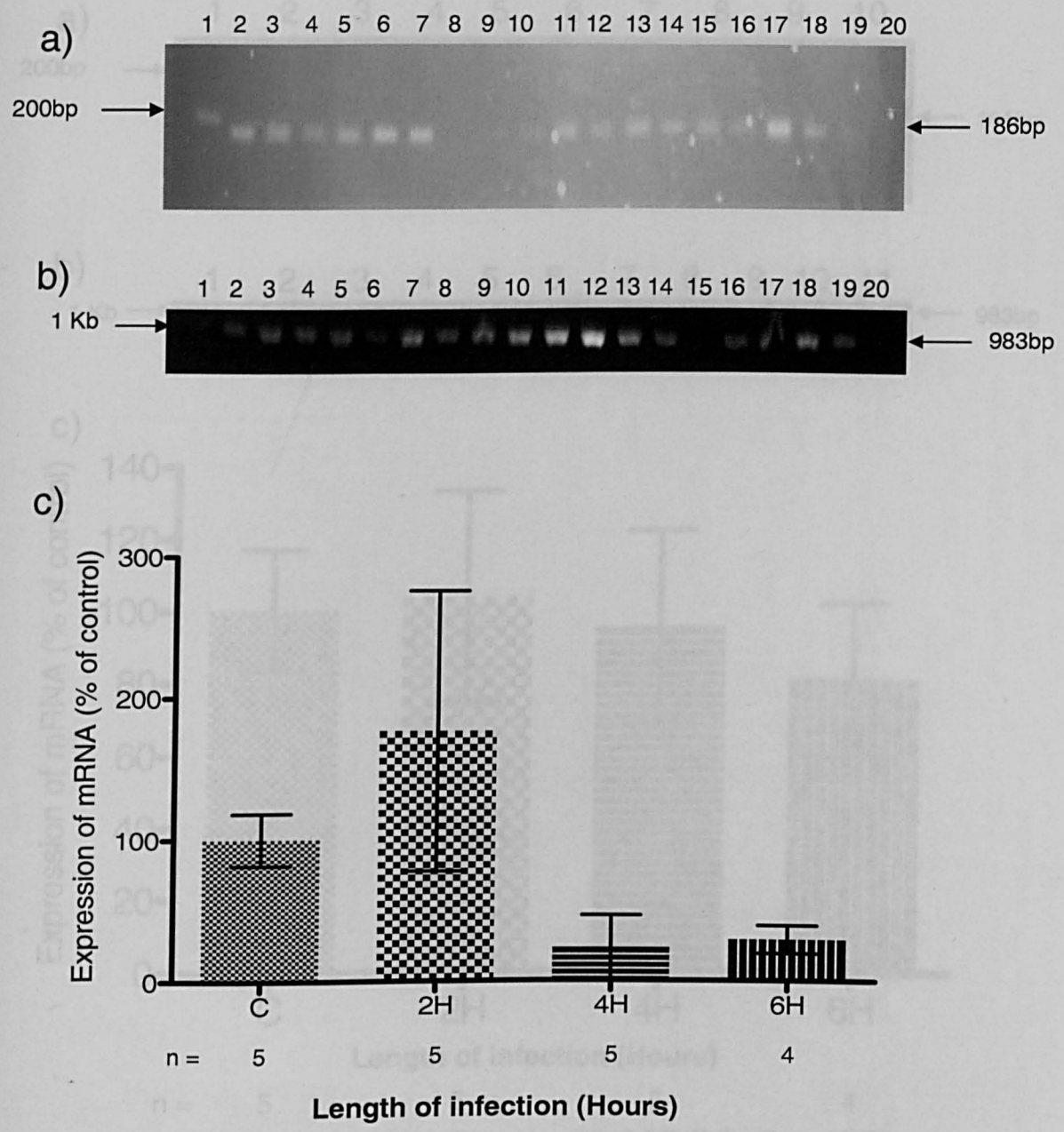

Figure 5.12: Hepcidin expression in *S. pyogenes* infected HaCaT cells:

a) & b) Representative 2% agarose gel showing separation of Hepcidin (186bp) and GAPDH (983bp) PCR products generated from DNA template which was reverse transcribed from RNA extracted from control HaCaT cells, HaCaT cells infected with *S. pyogenes*, M1 serotype and HaCaT cells treated with D3. 1: Size marker; 2-4: uninfected control cells; 5-7: HaCaT cells infected with *S. pyogenes* for 2H; 8-10: HaCaT cells infected for 4H; 11-13: HaCaT cells infected for 6 H; 14-16: HaCaT cells infected and treated with D3 for 2H; 17-19: HaCaT cells treated with D3 for 2H; 20: no template control.
c) Graph shows data from densitometry analysis from the gels, normalised to GAPDH and expressed as a percentage of control. All values represent mean ± SEM.

Statistical analysis was performed by one way ANOVA followed by a Dunnett's Post-test.
Gel a) was performed once, gel b) was performed 3 times. 4-5 biological repeats were performed per infection time point.

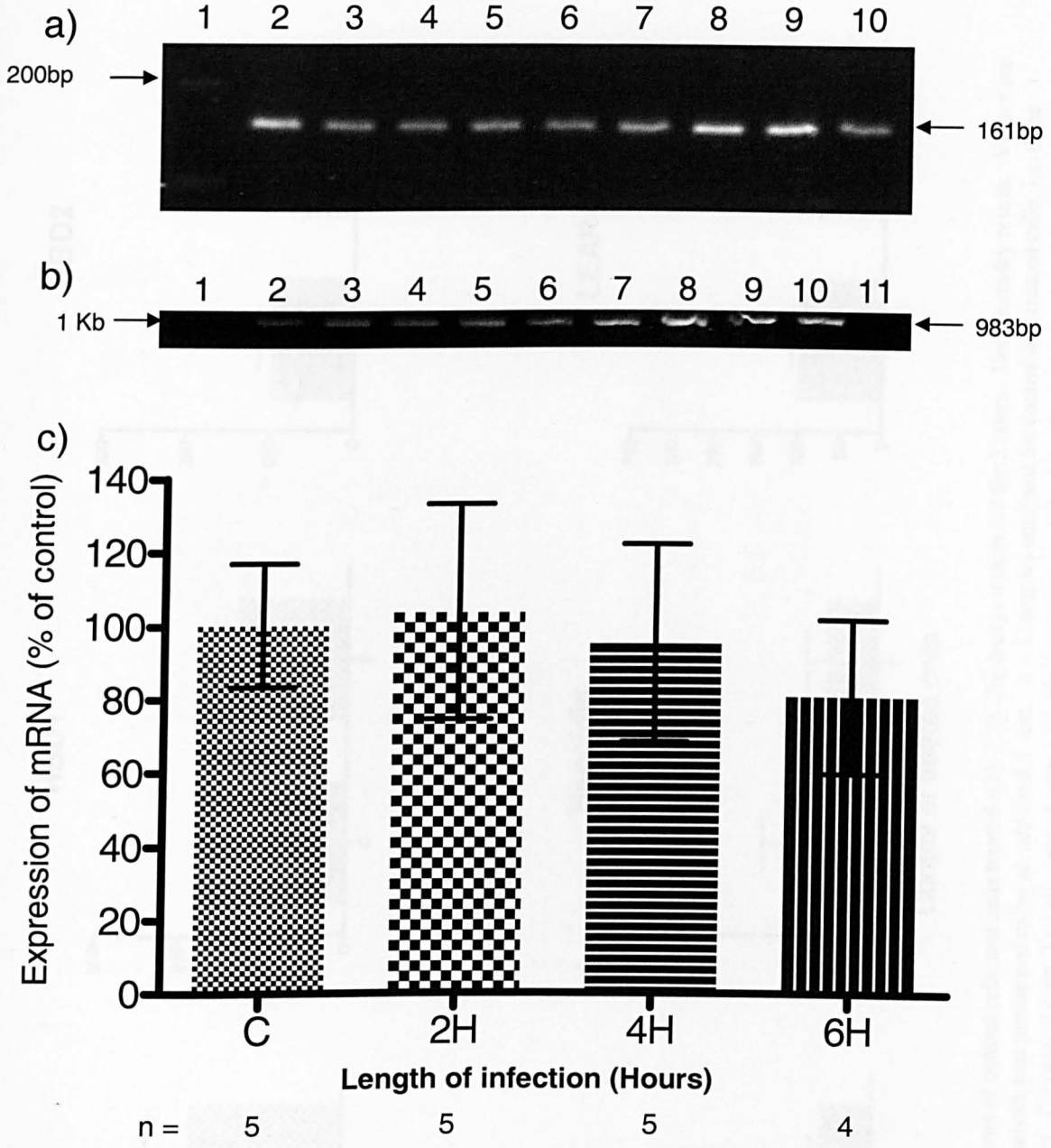

Figure 5.13: LEAP-2 expression in *S. pyogenes* infected HaCaT cells:

a) & b) Representative 2% agarose gel showing separation of LEAP-2 (161bp) and GAPDH (983bp) PCR products generated from DNA template which was reverse transcribed from RNA extracted from control HaCaT cells, HaCaT cells infected with *S. pyogenes*, M1 serotype and HaCaT cells treated with D3. 1: Size marker; 2-3: uninfected control cells; 4-5: HaCaT cells infected with *S. pyogenes* for 2H; 6-7: HaCaT cells infected for 4H; 8-9: cells infected for 6H; 10: cells treated with D3 for 2H.
b) 1: Size marker; 2-3: uninfected control cells; 4-5: HaCaT cells infected with *S. pyogenes* for 2H; 6-7: HaCaT cells infected for 4H; 8-9: cells infected for 6H; 10: cells treated with D3 for 2H; 11: no template control
c) Graph shows data from densitometry analysis from the gels, normalised to GAPDH and expressed as a percentage of control. All values represent mean ± SEM.

Statistical analysis was performed by one way ANOVA followed by a Dunnett's Post-test. Gels were performed once, 4-5 biological repeats were performed per infection time point.

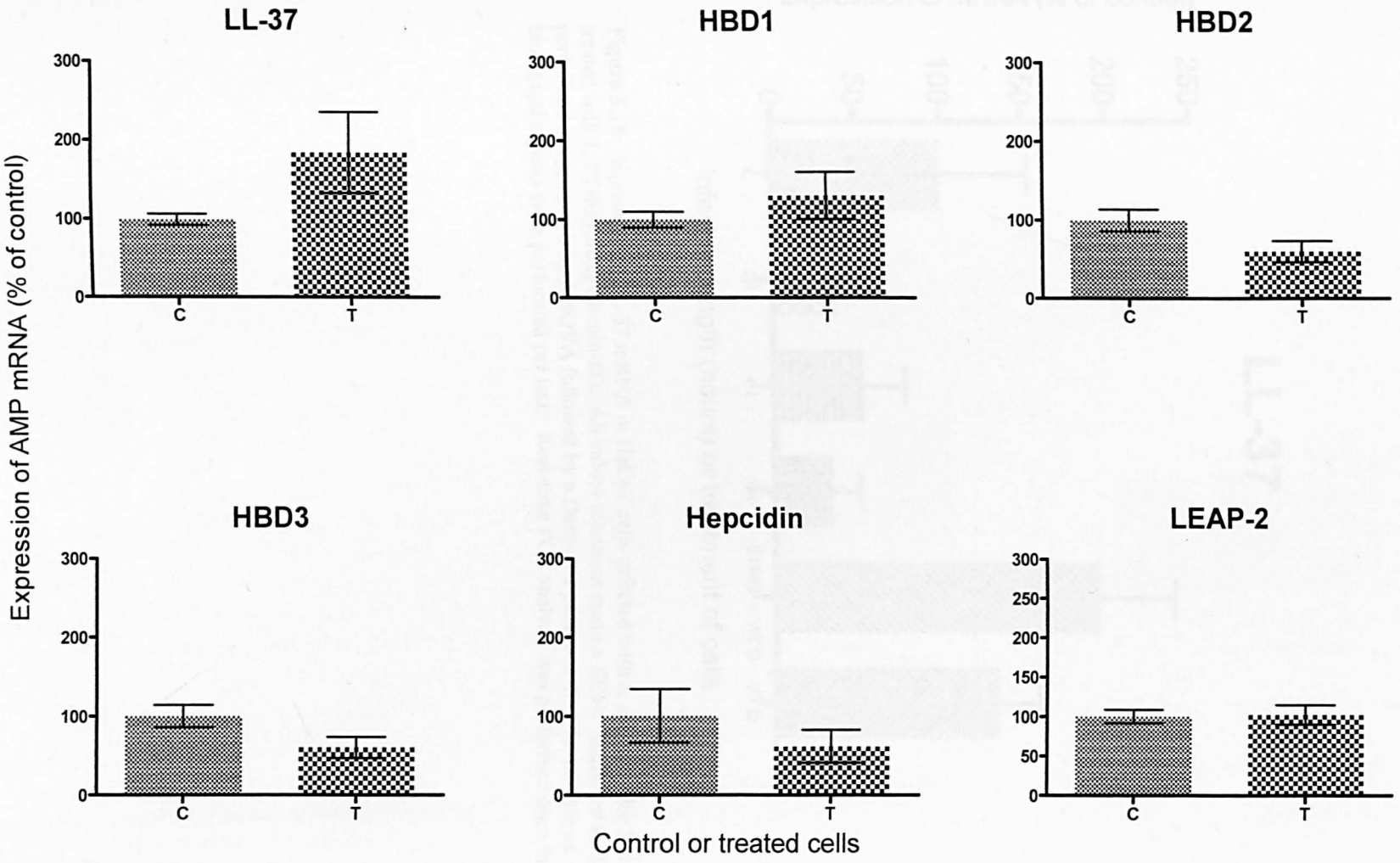

Figure 5.14: AMP gene expression patterns of control cells and cells treated with 1,25 dihydroxyvitamin-D3 for 2 hours. Densitometry results. Values are expressed as % of control. Statistical analysis was performed using an unpaired T-test. n = 3 samples analysed for control and treated cells, i.e. three biological repeats were performed per test. C= control cells, T= cells treated with 1,25 dihydroxyvitamin-D3. All values represent mean ± SEM.

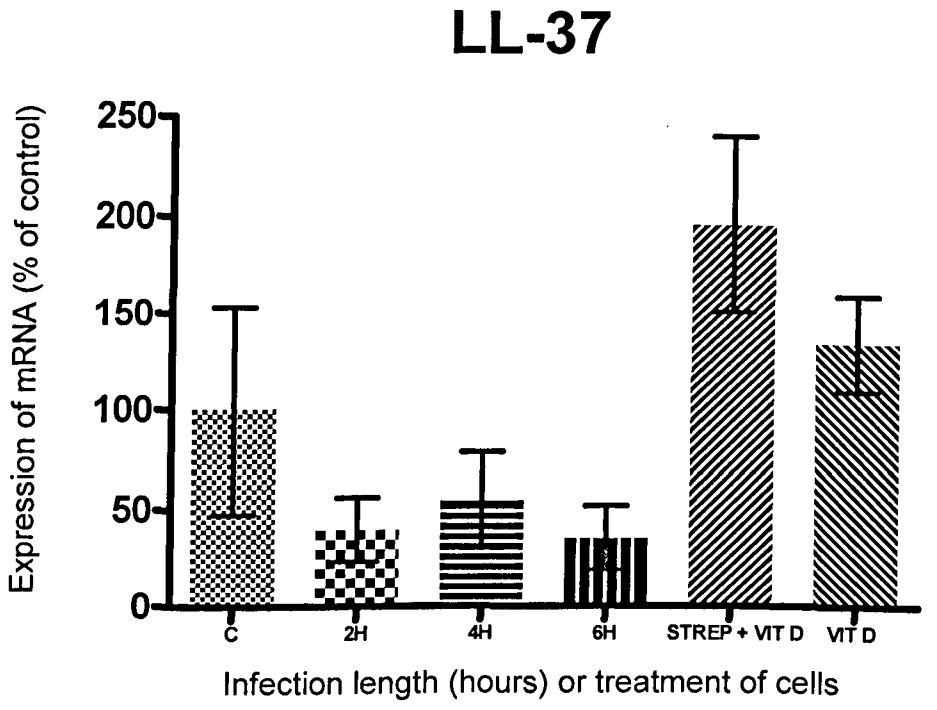

Figure 5.15: Expression of LL-37 mRNA in HaCaT cells infected with *S. pyogenes* for 2, 4 and 6 hours and treated with 1, 25 dihydroxyvitamin-D3. All values represent mean ± SEM. Statistical analysis was performed using a one way ANOVA followed by a Dunnett's post-test. n=3 for all groups, i.e. three biological repeats were performed per test. Real-time PCR analysis was performed once in quadruplicate.

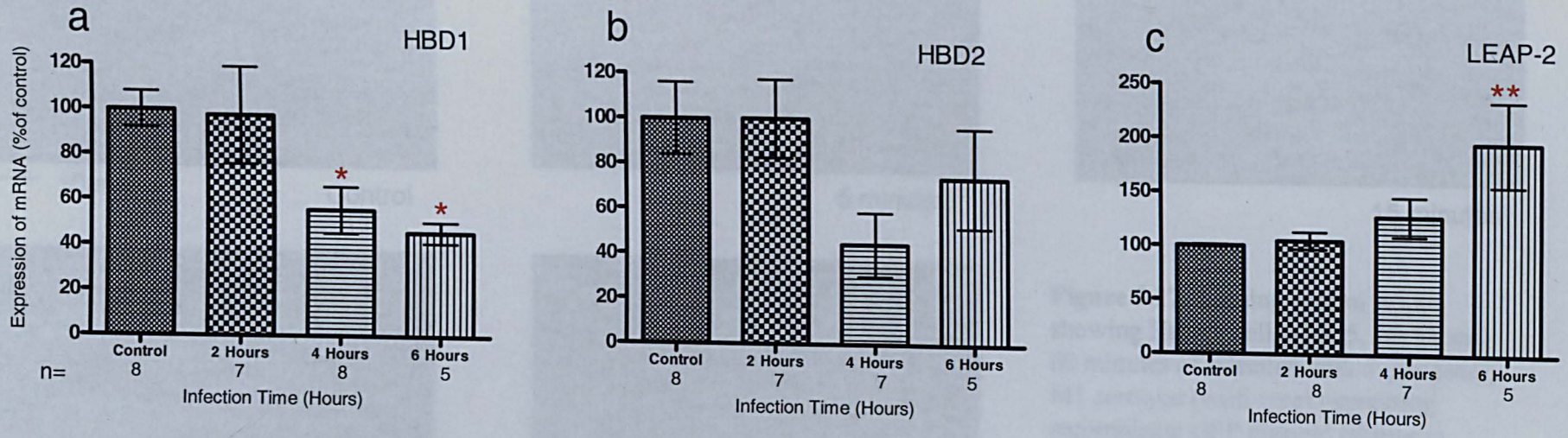

Figure 5.16: Expression of HBD1, HBD2 and LEAP-2 mRNA in HaCaT cells infected for 2, 4 and 6 hours with *S. pyogenes*, M1 serotype (wild-type). Real-time PCR results are normalised to GAPDH and expressed as a percentage of control. All values represent mean ± SEM. Statistical analysis was performed by one way ANOVA followed by a Dunnett's post-test. * = P<0.05 compared to control, ** = P<0.01 compared to control. n: number of samples analysed, i.e. 5-8 biological repeats were used per test. Real-time PCR analysis was performed once in duplicate.

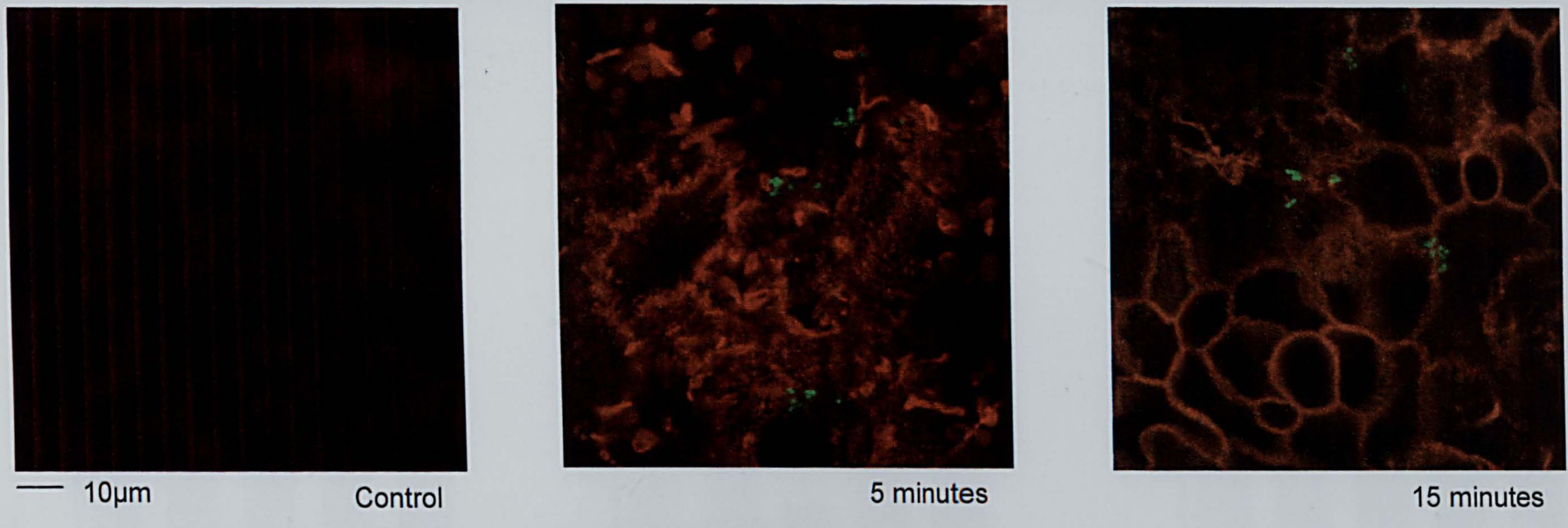

Figure 5.17: Binding control results showing HaCaT cells after 5, 15, 30 and 60 minutes of infection with *S. pyogenes*, M1 serotype (wild-type) expressing recombinant GFP plasmid (shown in green). HaCaT cells have been incubated with Phalloidin-TRITC (shown in red). Images are representative of images obtained each time an experiment was performed. Images are x100 magnification.

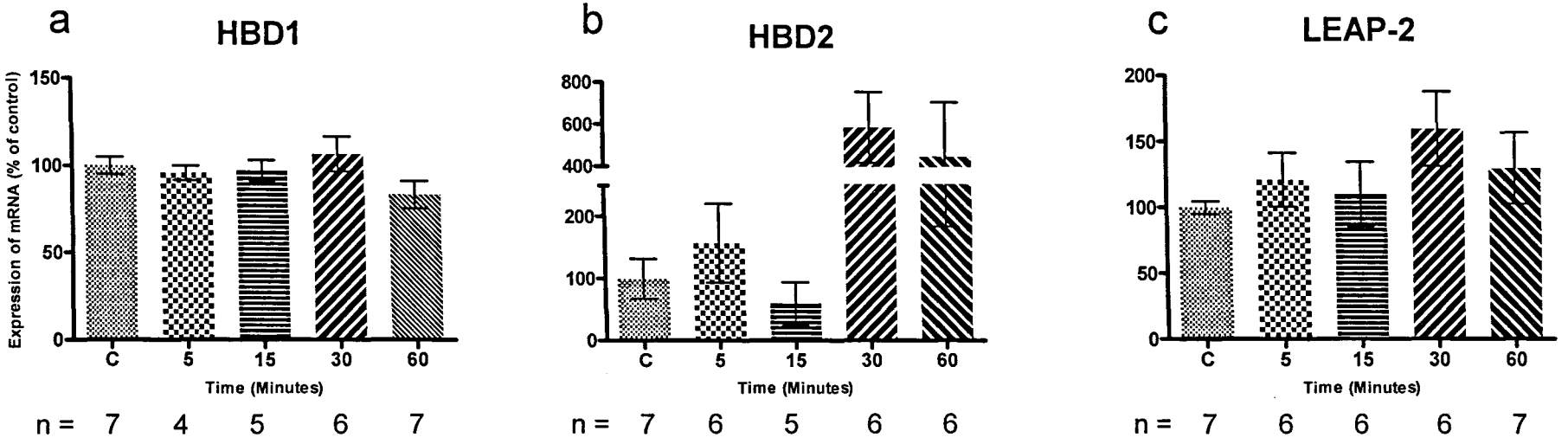

Figure 5.18: Real-time PCR results showing expression of HBD1, HBD2 and LEAP-2 mRNA in HaCaT cells infected with *S. pyogenes*, M1 serotype (wild-type) for 5, 15, 30 and 60 minutes. Results were normalised to GAPDH and expressed as a percentage of control. All values represent mean ± SEM. Statistical analysis was performed by one way ANOVA followed by Dunnett's post-tests. n: number of samples analysed, i.e. between 4-7 biological repeats were performed per test. Real-time PCR analysis was performed once in duplicate.

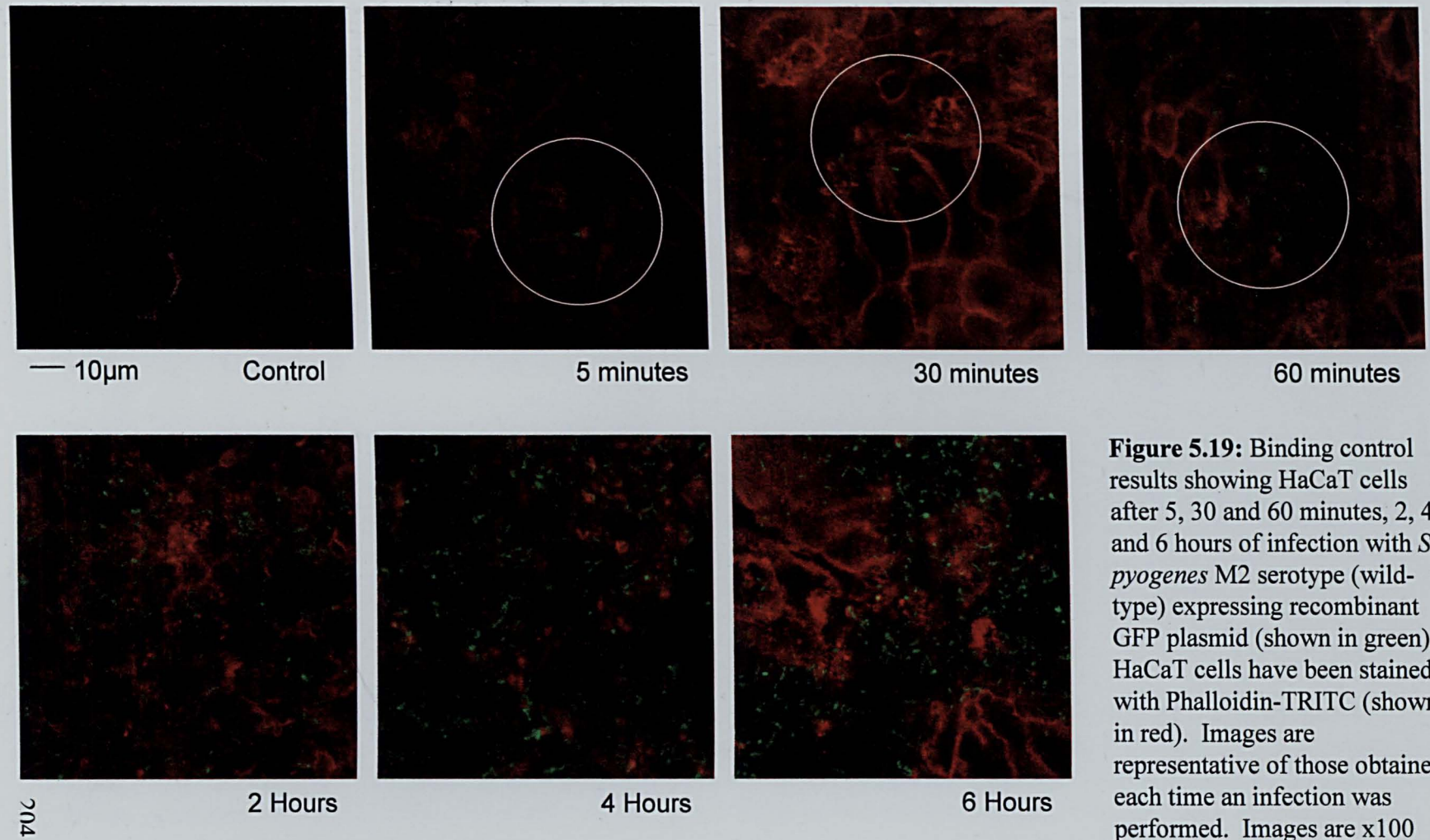

Figure 5.19: Binding control results showing HaCaT cells after 5, 30 and 60 minutes, 2, 4 and 6 hours of infection with *S. pyogenes* M2 serotype (wild-type) expressing recombinant GFP plasmid (shown in green). HaCaT cells have been stained with Phalloidin-TRITC (shown in red). Images are representative of those obtained each time an infection was performed. Images are x100 magnification.

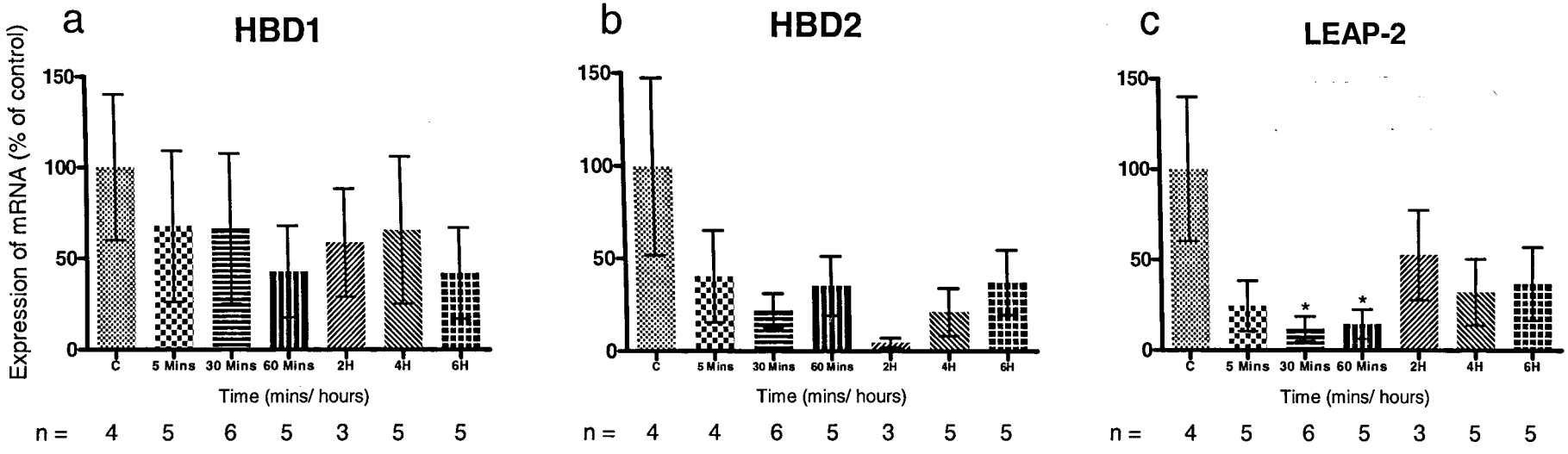

Figure 5.20: Real-time PCR data showing expression of HBD1, HBD2 and LEAP-2 in HaCaT cells infected with *S. pyogenes* M2 serotype (wild-type). Data was normalised to GAPDH and expressed as a percentage of control. All values represent mean ± SEM. * = P<0.05 compared to control. Statistical analysis was performed using a one way ANOVA followed by a Dunnetts post-test. n: number of samples analysed as shown on graphs, i.e. between 3-6 biological repeats were performed in each test. Replicates are from two challenge experiments. Real-time PCR analysis was performed once, in duplicate.

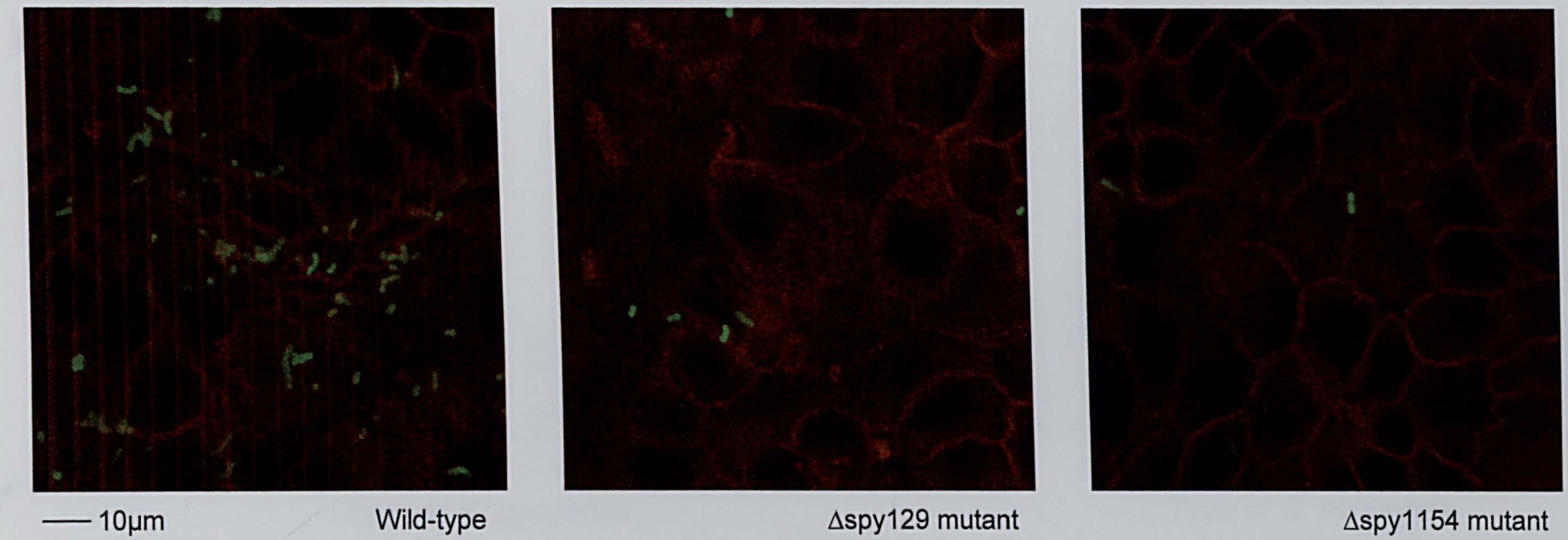

Figure 5.21: Binding control results showing HaCaT cells after 6 hours of infection with *S. pyogenes* M1 serotype wild-type and pili-defective mutants Δspy129 and Δspy1154 expressing recombinant GFP plasmid (shown in green). HaCaT cells have been stained with Phalloidin-TRITC (shown in red). Images are representative of those obtained each time an infection was performed. Images are x100 magnification.

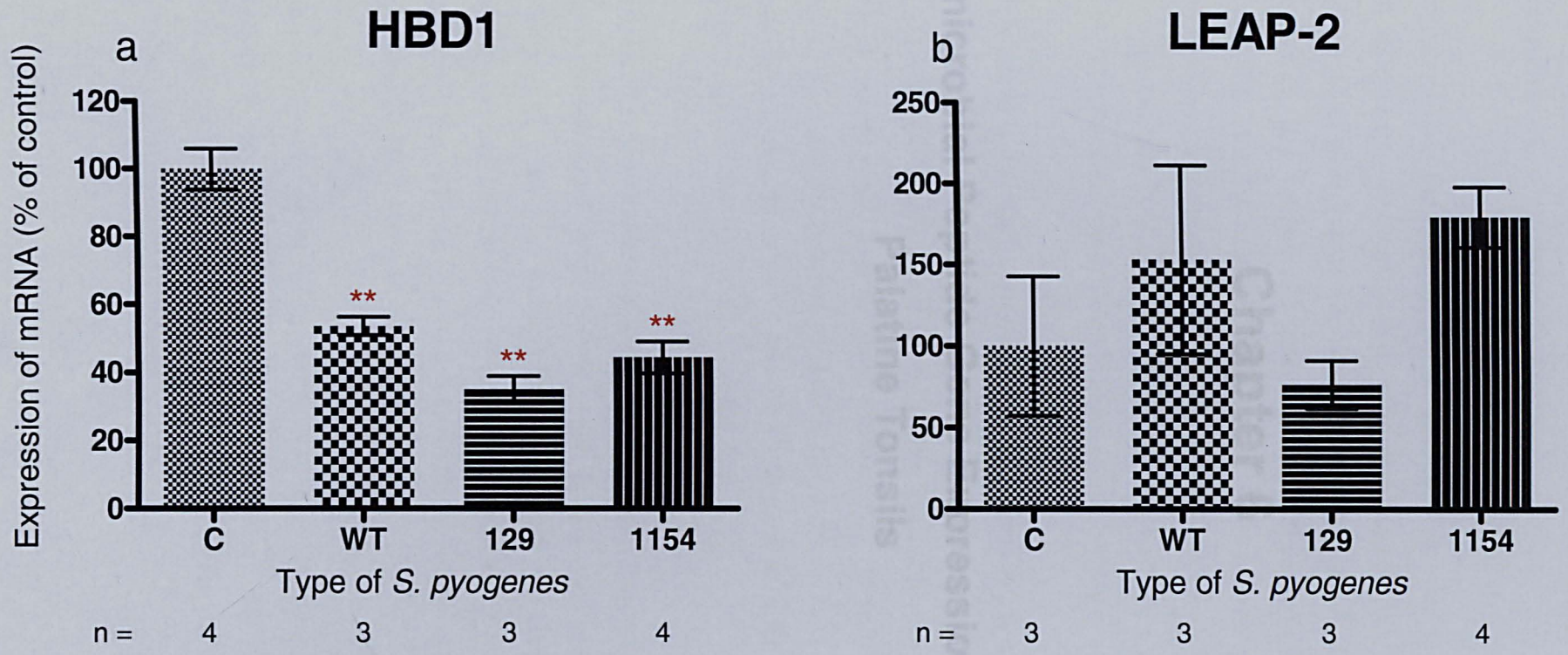

Figure 5.22: Real-time PCR results for a six hour incubation of HaCaT cell with control cells (C), and the *S. pyogenes* M1 strain, wild-type (wt) and pili-defective mutants Δspy129 (129) and Δspy1154 (1154). Data was normalised to GAPDH and expressed as a percentage of control. All values represent mean ± SEM. ** = P<0.01 compared to control. Statistical analysis was performed using one way ANOVA followed by a Dunnett's post-test. n: number of samples analysed, i.e. between 3-4 biological repeats were performed for each test. Real-time PCR analysis was performed once in duplicate.

Chapter 6

Antimicrobial Peptide Gene Expression in Human Palatine Tonsils

6.1 Introduction

In the previous chapter the immortalised HaCaT cell line, used as an *in vitro* model of the tonsil epithelium, was challenged with streptococci and the effects of such challenges on AMP gene expression examined by real-time PCR. The resultant data suggested that *in vitro,* streptococci were able to affect HaCaT AMP gene expression patterns, with LL-37, HBD1 and HBD2 gene expression reduced and LEAP-2 gene expression increased in response to a *S. pyogenes* M1 serotype challenge. These data therefore suggested that the *S. pyogenes* M1 serotype, a causal agent in tonsillitis, can modulate and consequently evade the host innate AMP response.

It is acknowledged that HaCaT cells are not tonsil derived but if similar effects were to occur in the tonsil *per se* then it may in part help explain the pathogenicity of the *S. pyogenes* M1 serotype in recurrent acute tonsillitis. Thus it was proposed to investigate the effects of streptococci on AMP gene expression in human palatine tonsils, and specifically to compare the patterns of AMP gene expression in tonsils excised from control (non-RAT) subjects and RAT patients challenged with the *S. pyogenes* M1 and M2 serotypes.

To facilitate such investigations the tonsil *ex vivo* model, developed and optimised by the group in Newcastle to study streptococcal binding and infection, was adopted (Abbot, Smith et al. 2007). In this model system freshly isolated samples of human palatine tonsil were cultured on filter supports with the apical surface partly exposed to the atmosphere. This technique allowed the conditions within the airways, where the tonsils are situated, to be mimicked.

Thus the aims of this part of the study were to use this *ex vivo* tonsil model, reproducing the environment of the pharynx, to investigate and compare the effects of *S. pyogenes* M1 and M2 challenges on the AMP gene expression patterns in human tonsils excised from control (non-RAT) subjects and RAT patients.

6.2 AMP Gene Expression in Human Tonsils Treated With Environmental Agents

The quantitative antimicrobial peptide gene expression data relating to tonsils removed from control (non-RAT) subjects and RAT patients was presented in Chapter 4. In the Chapter 4 study the RNA used in the analyses was extracted from large segments of either epithelial or lymphoid tissue, however in this study the tonsil sections used in the *ex vivo* model were only 3 x 3mm in size and predominantly epithelial tissue. Thus the initial experiments were performed to demonstrate that the AMP gene expression profiles of such small amounts of tonsil material could be determined, and to investigate if potential changes in gene expression could be detected. For the latter experiments the same reagents as described previously i.e. D3, LTA, LPS and PMA were used.

The challenge experiments were performed as described in Section 2.2.4. Briefly fresh human tonsils were dissected into 3 x 3mm sections and incubated apical side up for three hours in a tissue culture dish containing tonsil media with gentamicin (200μg ml^{-1}), to kill any bacteria on the tonsil surface. The tonsil samples were washed in PBS to remove any residual antibiotics before being placed apical side up in the upper chamber of a Transwell culture insert (0.4μm pore size). Medium without antibiotics was added to the lower chamber of the Transwell, thus immersing basolateral surfaces of the tonsil, but leaving the apical surface exposed to the atmosphere. Challenge reagents (D3 (200nM), LTA (from *S. pyogenes*, 2μg/ml), LPS (0.2μg/ml) and PMA (20μM)) were added directly to the exposed apical surface of the tonsil. Following incubation for a pre-determined time period, total RNA was isolated from each of the tonsil sections, DNase treated, reverse transcribed into cDNA and analysed as appropriate by real-time PCR.

The challenge experiments were performed using seven different tonsils, two from control (non-RAT) subjects and five from RAT patients. As observed previously (Chapter 4), the levels of AMP gene expression between tonsils could be very variable and thus to improve accuracy two to four replicates of each sample were analysed by real-time PCR. As previously all target gene expression values were normalised to the house-keeping gene GAPDH. Statistical analyses were performed using one way

ANOVA followed by Bonferroni post-tests used as described in 4.2ii or paired T-tests, a statistical test which is suitable for samples before and after treatment, as advised in the Prism statistics guide (Motulsky 2003).

The results of the D3 , LTA, LPS and PMA challenge experiments are shown in Figures 6.1- 6.4, and these data confirmed that AMP gene expression could be detected and quantified in the small tonsil tissue sections used in the *ex vivo* model system.

The data relating to LL-37 gene expression is presented in Figure 6.1. Within the control (non-RAT) tonsil group none of the treatments had a statistically significant effect on gene expression. Moreover in relation to the PMA data, which was associated with a large SEM, it was noted that one LL-37 expression value in particular was at variance being 5-6 times greater than the four other values in the group. Statistical analyses of the data relating to the tonsils from RAT patients indicated none of the treatments had a significant effect on LL-37 gene expression although again the data was variable and characterised particularly by four values indicative of very high LL-37 mRNA expression.

Analyses of the HBD1 data within the control (non-RAT) and RAT groups (Figure 6.2) identified no statistically significant differences between gene expression in the unchallenged and challenged tonsil samples. Moreover the expression patterns identified in relation to the control (non-RAT) and RAT samples analysed for HBD2 (Figure 6.3) and LEAP-2 (Figure 6.4) expression were similar and not statistically significant.

Overall these data indicated that AMP gene expression in the tonsil sections could be quantified, but that treatment of tonsils from either control (non-RAT) subjects or RAT patients with D3, LTA, LPS or PMA did not affect AMP gene expression significantly.

As noted previously the levels of AMP gene expression within a particular challenge experiment were often quite variable. As the challenge studies used tonsils from a number of individuals it was feasible that such variability was linked to the responses of individual tonsils.

To consider this further the data was re-plotted in bar charts, focussing on the expression data relating to individual tonsil samples and their responses to treatment with the agents i.e. D3, LTA, LPS or PMA. These data are presented in Figures 6.5-8. It can be determined from statistical analysis of the data represented in this way that once again no statistically significant differences were seen between control (untreated) tonsil samples and those samples which had been incubated with any of the treatment agents. Although it is acknowledged that the data was constrained by the numbers of tonsils analysed e.g. only two control tonsils were used and by the low numbers of samples of each tonsil analysed, i.e. in many cases there was only one gene expression value per individual tonsil.

None the less these data did support the use of the *ex vivo* model to investigate and compare the effects of a streptococcal challenge on the expression of the AMP genes in tonsils excised from control (non-RAT) subjects and RAT patients. However it was recognized that for the results to have significance, the numbers of tonsils could not be limiting and that for each tonsil more than one section per challenge was required. Moreover the use of the *ex vivo* model allowed the effects *S. pyogenes* on tonsil AMP expression patterns to be investigated directly.

6.3 Expression of Antimicrobial Peptide Genes in Human Tonsils Infected with *S. pyogenes* M1 Serotype (Wild-type)

In the HaCaT - *S. pyogenes* challenge experiments, the down-regulation of HBD1 mRNA, and the up-regulation of LEAP-2 mRNA were observed after four to six hours of streptococcal infection. Thus in the following experiments the tonsil samples were incubated with *S. pyogenes* M1 for two, four and six hours respectively. The *S. pyogenes* (2×10^7 cfu), were added directly to the exposed apical surface of the tonsil. Importantly at each time point the experiments included both control (non-infected) and infected tonsil samples. In addition samples from each tonsil were used as binding controls. These controls were always sampled following two hours of incubation with *S. pyogenes* and provided confirmation that the bacteria had bound successfully to the tonsil.

For the bacterial challenge experiments tonsil sections from a total of 13 tonsils, three control (non-RAT) (TA-C) and ten RAT (TA-J), were used. In all experiments bacteria bound to the tonsil sections indicative of a streptococcal infection (Figure 6.9).

6.3.1 Real-time PCR data: all samples

The tonsil samples were analysed for LL-37, HBD1, HBD2 and LEAP-2 gene expression by real-time PCR. All data was normalised to GAPDH and expressed as a percentage of control. Statistical analysis was performed using a paired T-test as described in 6.2 or a one way ANOVA followed, where appropriate, by Bonferroni post-tests as described in 4.2ii. It should be noted that the sample size for some time points was small, because only three control (non-RAT) tonsils were used in these experiments.

The LL-37 expression data following streptococcal infection of the tonsils from control (non-RAT) subjects and RAT patients is presented in Figure 6.10. The mean data relating to both the control (non-RAT) and RAT tonsils was indicative of no statistically significant changes in LL-37 mRNA expression levels following two, four or six hours of incubation with *S. pyogenes.*

Figure 6.11 shows the HBD1 expression data. In the control (non-RAT) tonsils a statistically significant ($P<0.01$) difference was identified between the mean HBD1 expression in the non-challenged and the two hour *S. pyogenes* infected tonsil samples. In fact the mean data suggested a three-fold increase in HBD1 expression. A comparable increase was not observed in the RAT tonsils. No differences in HBD1 gene expression were detected at either four or six hours of infection respectively in either the control (non-RAT) or RAT tonsil tissue sections.

The HBD2 mRNA expression data is presented in Figure 6.12. After four hours of infection respectively, the mean data relating to the control (non-RAT) tonsils suggested a reduction in HBD2 expression to 58±14 and 23±7% of control values which was

statistically significant ($P<0.05$). Differences between control tissues and infected tissues were however not statistically significant at either two or six hours.

HBD2 expression levels of the RAT tonsil sections exhibited no statistically significant differences after either two or four hours of infection respectively, although the latter time-point was skewed by two data points indicative of very high HBD2 mRNA expression, which related to one particular tonsil (sample TA; Figure 6.16).

Figure 6.13 illustrates the data relating to the effects of a *S. pyogenes* M1 serotype infection on LEAP-2 expression in tissue sections from control (non-RAT) and RAT tonsils. In both control (non-RAT) and RAT tonsils no differences were suggested between control and infected samples at each time point and this was confirmed statistically.

These data were re-plotted in a bar chart format to show the response of individual tonsils (Figures 6.14-6.17). Once again no statistically significant differences can be observed between the control tonsil samples and the infected tonsil samples in both the control (non-RAT) and RAT tonsils. It can be observed that the data again, as with the experiment involving the treatments (Figures 6.5-6.8) illustrates the problems associated with using limited numbers of tonsil samples, and the variable responses of the individual tonsils. For example the HBD2 response of RAT tonsil TA to the streptococcal challenge (Figure 6.16 HBD2 RAT 4h), was very high compared to the values of the six other tonsil samples. Similarly the LEAP-2 expression pattern of RAT tonsil sample TD was contradictory when compared to those of other RAT tonsils (Figure 6.17).

Overall AMP expression patterns of control (non-RAT) and RAT tonsils in response to a *S. pyogenes* M1 challenge were identified and these are summarised in Table 6.1.

Table 6.1: Expression of AMPs in control (non-RAT) and RAT tonsils after 2, 4 and 6 hours of infection with *S. pyogenes*.

	Control			RAT	
	2h	4h	6h	2h	4h
LL-37	↔	↔	↔	↔	↔
HBD1	↑	↔	↔	↔	↔
HBD2	↔	↓	↔	↔	↔
LEAP-2	↔	↔	↔	↔	↔

↔ No statistically significant difference in gene expression compared to control

↓ Statistically significant decrease in gene expression compared to control

↑ Statistically significant increase in gene expression compared to control

6.4 Expression of Antimicrobial Peptide Genes in Human Tonsils Infected with *S. pyogenes* M2 Serotype (Wild-type)

As described previously the *S. pyogenes* M2 serotype, also known to be involved in the pathology of recurrent acute tonsillitis, is characterised by increased numbers of surface pili. In Chapter 5, it was shown that challenging the HaCaT cell line with the two different serotypes did not appear to affect the AMP expression profiles of the cells, except for LEAP-2, where the mean expression data showed a significant increase in LEAP-2 expression in response to the M1 serotype but not in response to the M2 serotype (Figure 5.20). Challenging the control (non-RAT) tonsils with the M1 serotype also supported an increase in LEAP-2 expression at two hours post infection. Thus to determine and compare the effects of the *S. pyogenes* M2 serotype on tonsil AMP expression patterns, and specifically LEAP-2 expression, the bacterial challenge experiments were repeated using the *ex vivo* model and the *S. pyogenes* M2 serotype.

This investigation used four control (non-RAT) tonsils. Each tonsil tissue sample was incubated with the *S. pyogenes* M2 serotype (2×10^7 cfu), for either two or four hours respectively and, as previously, unchallenged control samples were included at each time-point. Quantification of expression was performed using the real-time PCR assays, target gene expression normalised to GAPDH and expressed as a percentage of

control. Statistical analysis was performed by one way ANOVA and followed by a Bonferroni post-test where appropriate.

Tissue sections from each tonsil were also used as binding controls. These controls were sampled following two hours of incubation with the *S. pyogenes* M2 serotype and provided confirmation that the bacteria had bound successfully to the tonsil. The data confirming binding of the *S. pyogenes* M2 serotype to each of the four tonsils (M2TC1-4) is presented in Figure 6.18. In all cases GFP-tagged bacteria (green) adhered to the tonsil section (red) indicative of infection.

6.4.1 Real-time PCR- all samples

The results of the quantitative AMP mRNA expression analyses are shown in Figures 6.19 and 6.20 respectively.

The LL-37 expression data following *S. pyogenes* M2 infection of the tonsils excised from control (non-RAT) subjects is presented in Figure 6.19a, and the mean data was indicative of no changes in LL-37 mRNA levels following either two or four hours of incubation with the bacteria. The data was however compromised by the small number of values at each time point, especially in relation to the four hour control (non-RAT) samples challenged with streptococci, and the variability of the data.

Figure 6.19b shows the LEAP-2 expression data. Again no significant changes were identified in LEAP-2 expression following the *S. pyogenes* M2 serotype challenge and no obvious trends were observed.

The HBD1 and HBD2 mRNA expression data are presented in Figures 6.20a and b respectively. No significant changes were identified in the expression of either gene following the *S. pyogenes* M2 serotype challenge. However the mean AMP gene expression values in response to the *S. pyogenes* M2 serotype challenge were often associated with large SEM bars. This variability was evident when the expression data from the individual tonsils was presented in a bar chart format (Figures 6.21-6.24). For

example at two hours the LL-37 gene expression value relating to tonsil M2TC1 in response to the streptococcal challenge (<20% control) was at odds with those observed for tonsils M2TC2 and M2TC3 (~100%) respectively (Figure 2.21). Similarly at two hours the HBD2 mRNA expression data (Figure 6.23) relating to tonsils M2TC1 and MCTC2 (<5% control) were reduced compared to that recorded for tonsil M2TC3 (>150%).

6.5 Discussion

In Chapter 5 HaCaT cells were adopted as an *in vitro* model of the tonsil to investigate the effects of *S. pyogenes* M1 and M2 serotypes on host AMP gene responses. The quantitative real-time expression data suggested that in response to the *S. pyogenes* M1 serotype HBD1 gene expression were decreased. As described previously HaCaT cells are not derived from tonsil. However if, for example, such patterns were observed in the tonsils of RAT patients but not control (non-RAT) subjects then it could explain the susceptibility of the former to infection and recurrent acute tonsillitis. Thus to further investigate streptococcal–tonsil AMP responses it was decided to utilise the *ex vivo* tonsil model developed by Abbot, Smith et al (2007). This model was developed originally by the group in Newcastle to explore *S. pyogenes* M1–tonsil binding interactions and it has the distinct advantage of utilising tonsil material directly. Moreover the model involves sectioning each tonsil which provides, potentially, large numbers of samples although in practise the number of sections was actually constrained by the size of the tonsil and the amount of intact surface epithelia. A major disadvantage was that the tissue sections were not homogeneous.

Experiments in which the HaCaT cells were challenged with D3, resulted in the up-regulation of LL-37 gene expression. When the D3 challenge was repeated using the *ex vivo* model no statistically significant changes in LL-37 gene expression were observed in tonsil sections from either control (non-RAT) subjects or RAT patients. Similarly treatment with LTA, LPS and PMA did not significantly affect the AMP gene expression profiles of the tonsils. It is known that vitamin D, synthesised in skin, is able to regulate immune defences (Liu, Stenger et al. 2006; Zasloff 2006). Indeed the active vitamin D metabolite, D3, has been shown to up-regulate cathelicidin gene expression in macrophages exposed to *Mycobacterium tuberculosis*, but interestingly to down-regulate the transcription of the pro-inflammatory mediators IFNγ and TNFα (Martineau, Wilkinson et al. 2007). Moreover Vitamin D deficiency in humans has been associated with reduced innate immune function and it has been proposed that antibiotic treatments of infections should be accompanied by Vitamin D supplementation (Zasloff 2007).

The mechanisms by which D3 could potentially down-regulate LL-37 gene expression are not known. Moreover the regulation of the cathelicidin gene is still poorly characterised, but it is of interest that regions mediating gene repression have been identified within the hCAP18 gene promoter (Elloumi and Holland 2008). Interestingly the commensal *S. salivarius* K12, known to protect the host against pathogens causing throat infections, ensures its survival in the mouth, by down-regulating inflammatory responses and thus the innate immune response, by inhibition of the NF-κB pathway (Cosseau, Devine et al. 2008).

The incidence of tonsillitis within the population indicates that *S. pyogenes* is a successful pathogen. It is known to overcome host innate defences, including cationic AMPs, through the synthesis of proteins including SIC (Frick, Akesson et al. 2003); SpeB (Schmidtchen, Frick et al. 2002) and GRAB (Nyberg, Rasmussen et al. 2004), which can inactivate the host defence peptides. Indeed of these SIC, is known to bind to and inhibit LL-37 as well as HBD1-3 activities (Fernie-King, Seilly et al. 2006). In addition there is evidence that SIC is taken up by human epithelial cells causing cell flattening and loss of the microvilli (Hoe, Ireland et al. 2002), which presumably damages the epithelial barrier and further weakens the host antimicrobial defences.

The results of the *S. pyogenes* M1 challenge study showed a statistically significant difference in the HBD1 AMP gene expression profiles of tonsils excised from control (non-RAT) subjects, with the levels of HBD1 expression increased in the control tonsils in response to the streptococcal infection after two hours. There was also a statistically significant reduction in HBD2 expression in the control (non-RAT) tonsils (Figure 6.12) following four hours of infection, which supports the ability of *S. pyogenes* to weaken the tonsil AMP epithelial defences. Moreover as HBD2 is also known to bind to CCR6 and induce the chemotaxis of either memory T-cells or immature dendritic cells (Yang, Chertov et al. 1999), its reduced synthesis in the tonsil would presumably cause a delay in the signalling to, and recruitment of, antigen presenting cells (APC). Again *in vivo* this would favour the survival of the streptococci.

It was of note that the fall in HBD2 gene expression in the tonsils in response to the *S. pyogenes* M1 challenge was also observed in the HaCaT cells. Taken together these

data support, potentially, *S. pyogenes* targeting the mechanisms regulating tonsil HBD2 gene expression. The tonsil is known to express an array of TLR genes (1-10) (Lesmeister, Bothwell et al. 2006), and it is presumed that HBD2 gene expression in the tonsil is activated through a TLR2 mediated mechanism, which in keratinocytes has been shown to involve P38, JUNK, ERK and NF-κB signalling pathways (Chung and Dale 2004). The mechanism by which *S. pyogenes* switches off HBD2 gene expression is not known but potentially involves disruption of one of the signalling pathways. To investigate whether the effects of streptococci on HBD2 gene expression were actually mediated through a TLR2 signalling pathway it would be interesting to repeat the tonsil challenge experiments in the presence of TLR2 antibody.

The skin and tonsils are two major sites of streptococcal infection and both have been shown to express the HBD3 gene (Harder, Bartels et al. 2001; Ball, Siou et al. 2007). This suggests that HBD3 may be particularly effective in the defence of the host against streptococci, and thus it was disappointing that no HBD3 mRNA expression data was available in this study. Recently it has been reported that the capacity of keratinocytes to kill *Staphylococcus aureus* is dependent on the constitutive synthesis of HBD3 (Kisich, Howell et al. 2007). With this in mind, and the fact that, the RNA samples arising from the tonsil challenge studies are still available, it would be of interest to analyse these samples for patterns of HBD3 gene expression.

The *S. pyogenes* M2 challenge results were disappointing and did not reveal any statistically significant differences in AMP gene expression patterns between the two sets of tonsils. Moreover the numbers of tonsils, and thus tonsil sections, used were small and it was difficult to detect potential patterns. In addition the small numbers further emphasised the variability of the data.

Indeed the results of the studies described in this Chapter were characterised by large standard errors caused by the variability in AMP expression values measured between individual tonsils, and between sections derived from individual tonsils. This variability was caused by very elevated or low expression values, and combined with the low sample numbers probably masked potential changes in the AMP expression patterns. The reasons for the variable data are not known, but the tonsils used in the studies were

all from different individuals and as such the data is comparable to that observed in the clinical study reported in Chapter 4.

Quantification of AMP expression was performed using the real-time PCR assays developed in Chapter 3. Although these assays were a common factor between the studies described in Chapter 4 and here in Chapter 6 respectively, the observed variability was not due to either intra- or inter-assay errors as each sample was assayed in duplicate (sometimes quadruplicate), and test standards were included in all analyses. One possibility for the variability between the tonsil sections was due to each epithelial section having a different amount of lymphoid tissue attached to it as a result of the dissection i.e. the samples were not homogeneous. As such it could be argued that the AMP expression data was biased by the proportion of epithelial and lymphoid tissue. However the results of the study presented in Chapter 4, did not support this as the epithelial and lymphoid tissues appeared to express AMPs at a similar levels within the control (non-RAT) and RAT groups. None the less the effects of either necrotic or scarred tissue on the AMP expression data, or perhaps the presence of a lymphoid follicle on the AMP expression levels could not be excluded entirely. The length of time from the excision of a tonsil to dissection was also considered as influencing AMP gene expression, but this was unlikely as all the tonsils were immersed in tonsil medium within one hour of excision.

It is acknowledged that the surgery to excise the tonsils, the dissection of the epithelium from the tonsils and the sectioning of the tonsil *per se* may have caused inflammatory responses that affected the expression of the AMP genes. While it has been reported that the APC derived cytokines IL-12, IL-23 and IL-27 enhance HBD2 secretion and mRNA expression in keratinocytes functioning through NF-κB, STAT3 and STAT1 signalling pathways (Kanda and Watanabe 2008), the effects of other inflammatory factors on AMP gene expression are not known. For this reason it could be argued that the *ex vivo* model, while mimicking the moisture lined airways where the tonsils are situated, and an excellent model for investigating the mechanisms by which streptococci bind to tonsil, was not as ideal for studying the tonsil AMP responses resulting from such binding. However, a superior tonsil model has yet to be reported.

Following challenge of the control (non-RAT) and RAT tonsil sections with *S. pyogenes*, a statistically significant increase in HBD1 gene expression and a decrease in HBD2 gene expression were observed in the control (non-RAT) tonsils. No comparable statistically significant changes were identified in the RAT tonsils although there was the suggestion of a reduction in HBD2 expression. These data therefore highlight differences between the AMP expression profiles of the control (non-RAT) and RAT tonsils in response to a *S. pyogenes* M1 challenge. Although speculative these data indicate that the RAT tonsils were less able to respond to the *S. pyogenes* challenge, which may in part help to explain the susceptibility of RAT patients to infection.

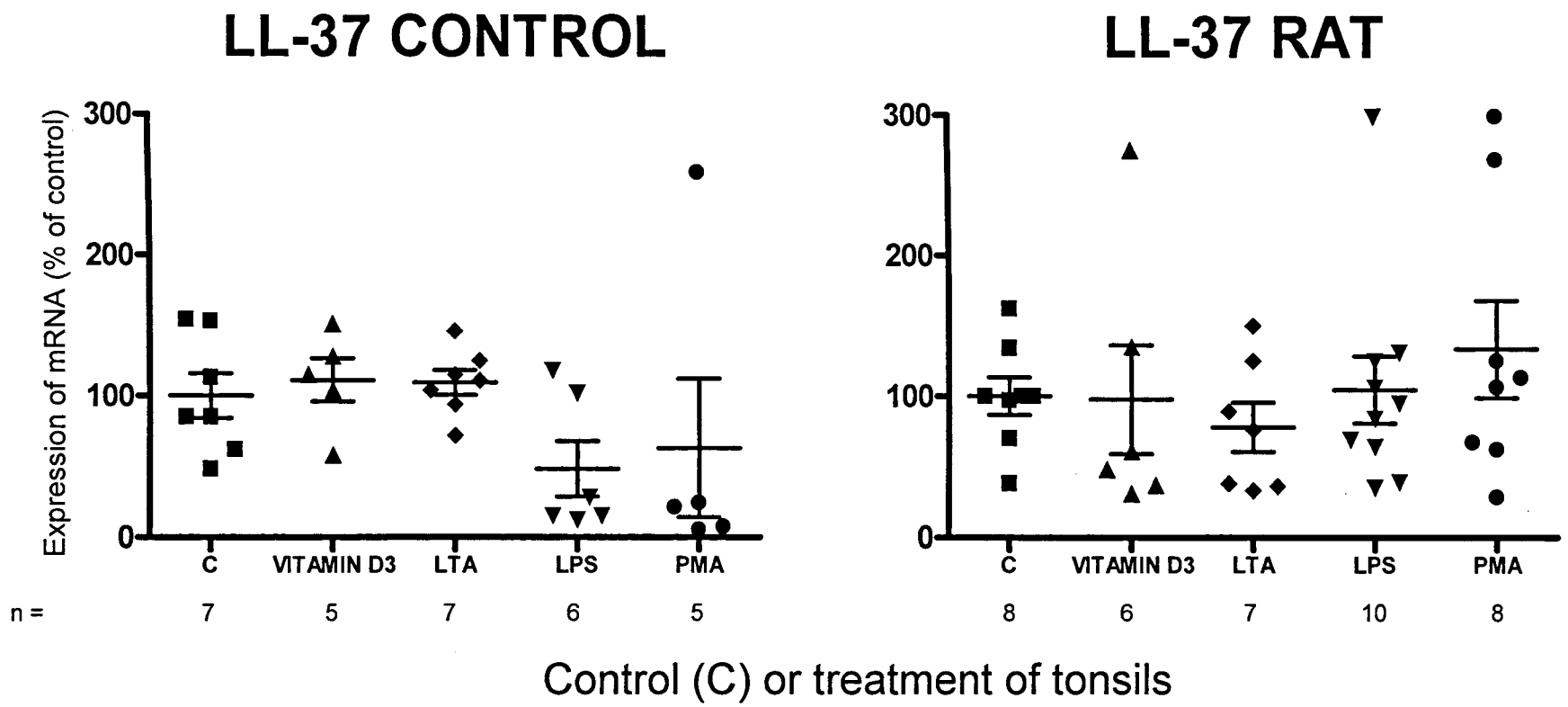

Figure 6.1: LL-37 Gene Expression: Real-time PCR data showing LL-37 mRNA expression in human tonsil sections incubated for two hours with D3 (VITAMIN D3), LTA, LPS and PMA using the *ex vivo* tonsil model. Data is normalised to GAPDH and expressed as a percentage of control. All values represent mean ± SEM. n: number of tonsil sections analysed in total from 2 control (non-RAT) and 5 RAT tonsils. Statistical analysis was performed by one way ANOVA followed by a Bonferroni post-test. Real-time PCR assays were performed once, each sample was assayed in quadruplicate.

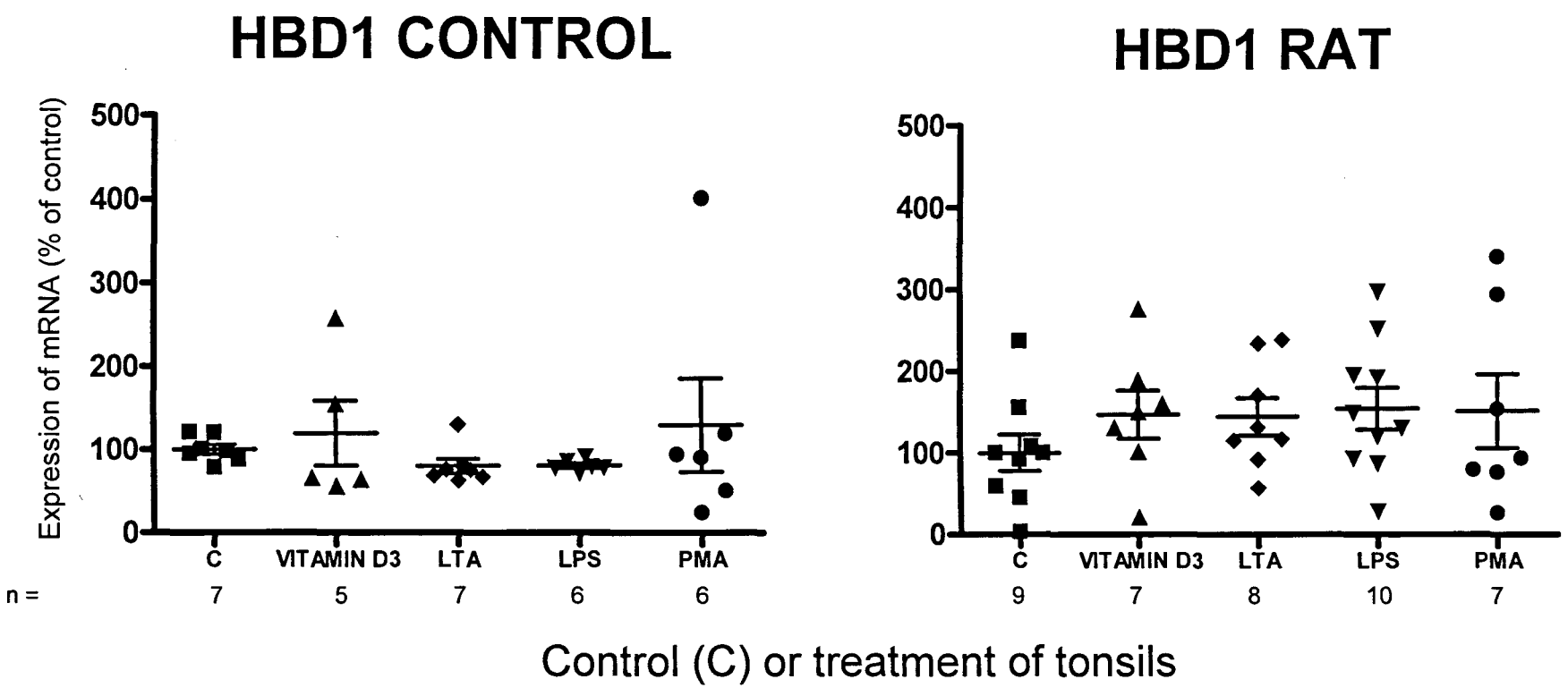

Figure 6.2: HBD1 Gene Expression: Real-time PCR data showing HBD1 mRNA expression in human tonsil tissue sections incubated for two hours with D3 (VITAMIN D3), LTA, LPS and PMA using the *ex vivo* tonsil model. *Data is normalised to GAPDH and expressed as a percentage of control. All values represent* mean ± SEM. n: number of tonsil sections analysed in total from two control (non-RAT) and 5 RAT tonsils. *Statistical analysis was performed by a one way* ANOVA followed by a Bonferroni post-test. *Real-time PCR analysis was performed once, each sample was assayed in duplicate.*

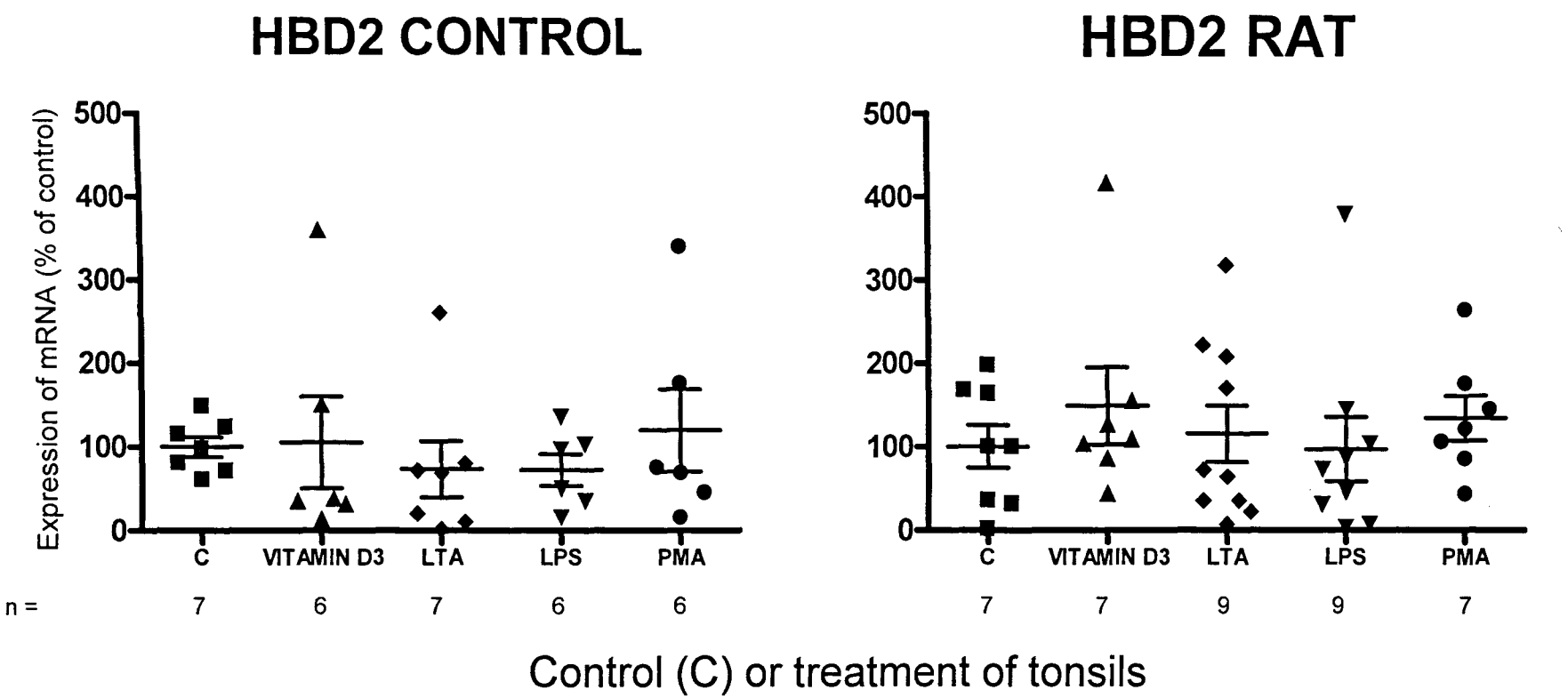

Figure 6.3: HBD2 Gene Expression: Real-time PCR data showing HBD2 mRNA expression in human tonsil tissue sections incubated for two hours with D3 (VITAMIN D3), LTA, LPS and PMA using the *ex vivo* tonsil model. Data is normalised to GAPDH and expressed as a percentage of control. All values represent mean ± SEM. n: number of tonsil sections analysed in total from two control (non-RAT) and 5 RAT tonsils. Statistical analysis was performed by a one way ANOVA followed by a Bonferroni post-test. Real-time PCR analysis was performed once, each sample was assayed in duplicate.

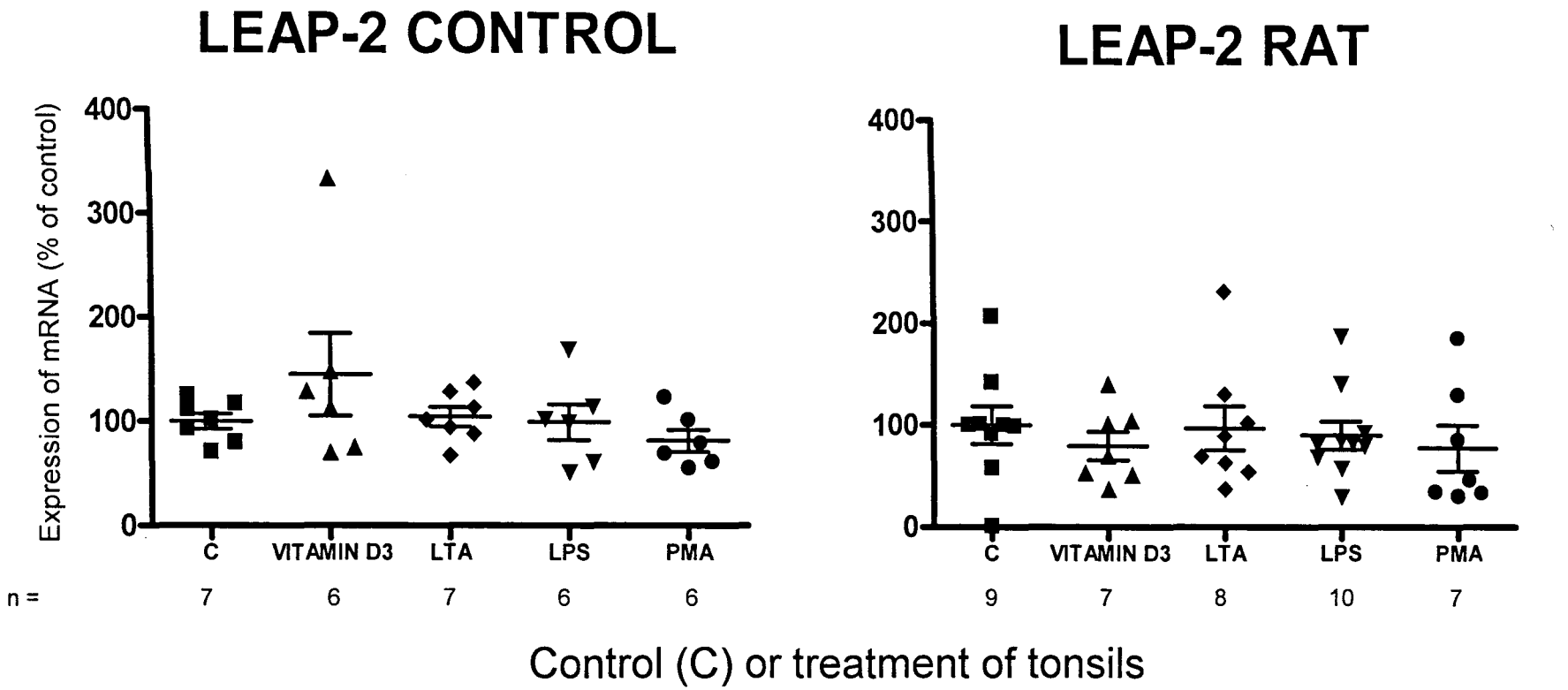

Figure 6.4: LEAP-2 Gene Expression: Real-time PCR data showing LEAP-2 mRNA expression in human tonsil tissue sections incubated for two hours with D3 (VITAMIN D3), LTA, LPS and PMA using the *ex vivo* tonsil model. Data is normalised to GAPDH and expressed as a percentage of control. All values represent mean ± SEM. n: number of tonsil sections are analysed in total from two control (non-RAT) and 5 RAT tonsils. Statistical analysis was performed by a one way ANOVA followed by a Bonferroni post-test. Real-time PCR analysis was performed once each sample was assayed in duplicate.

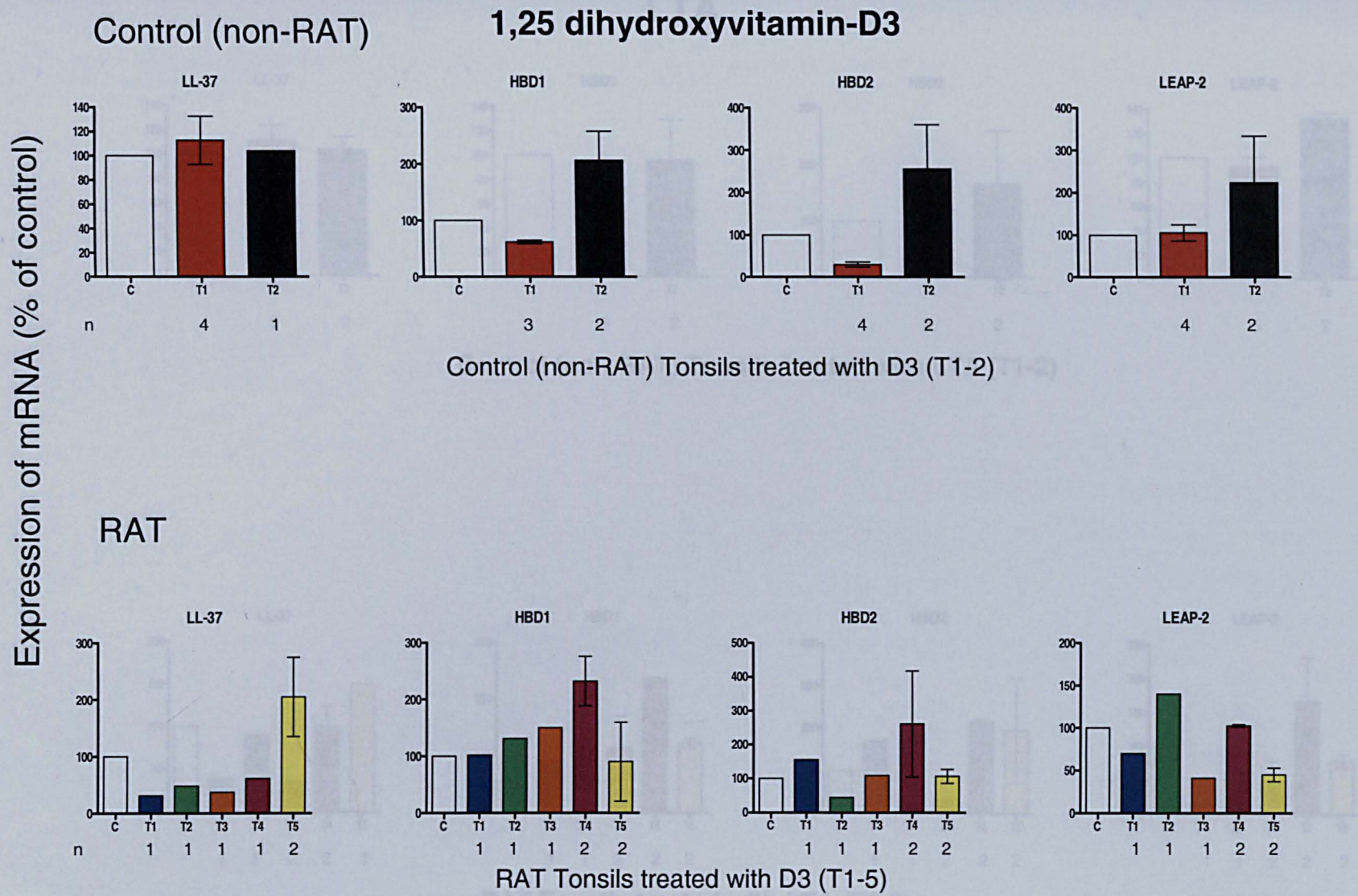

Figure 6.5: 1,25 dihydroxyvitamin-D3: Real-time PCR data showing LL-37, HBD1, HBD2 and LEAP-2 mRNA expression in individual human tonsils incubated for 2 hours with D3 using the *ex vivo* model. Data represents two control (non-RAT) tonsils and five RAT tonsils. n: number of samples analysed per tonsil. Each coloured bar represents an individual tonsil (2 for control T1-T2, 5 for RAT T1-T5). C = untreated control tonsils. Bars represent SEM. Statistical analysis was performed by a one way ANOVA followed by a Bonferroni post-test. Real-time PCR analysis was performed once, each sample was assayed in duplicate except for LL-37 which was assayed in quadruplicate.

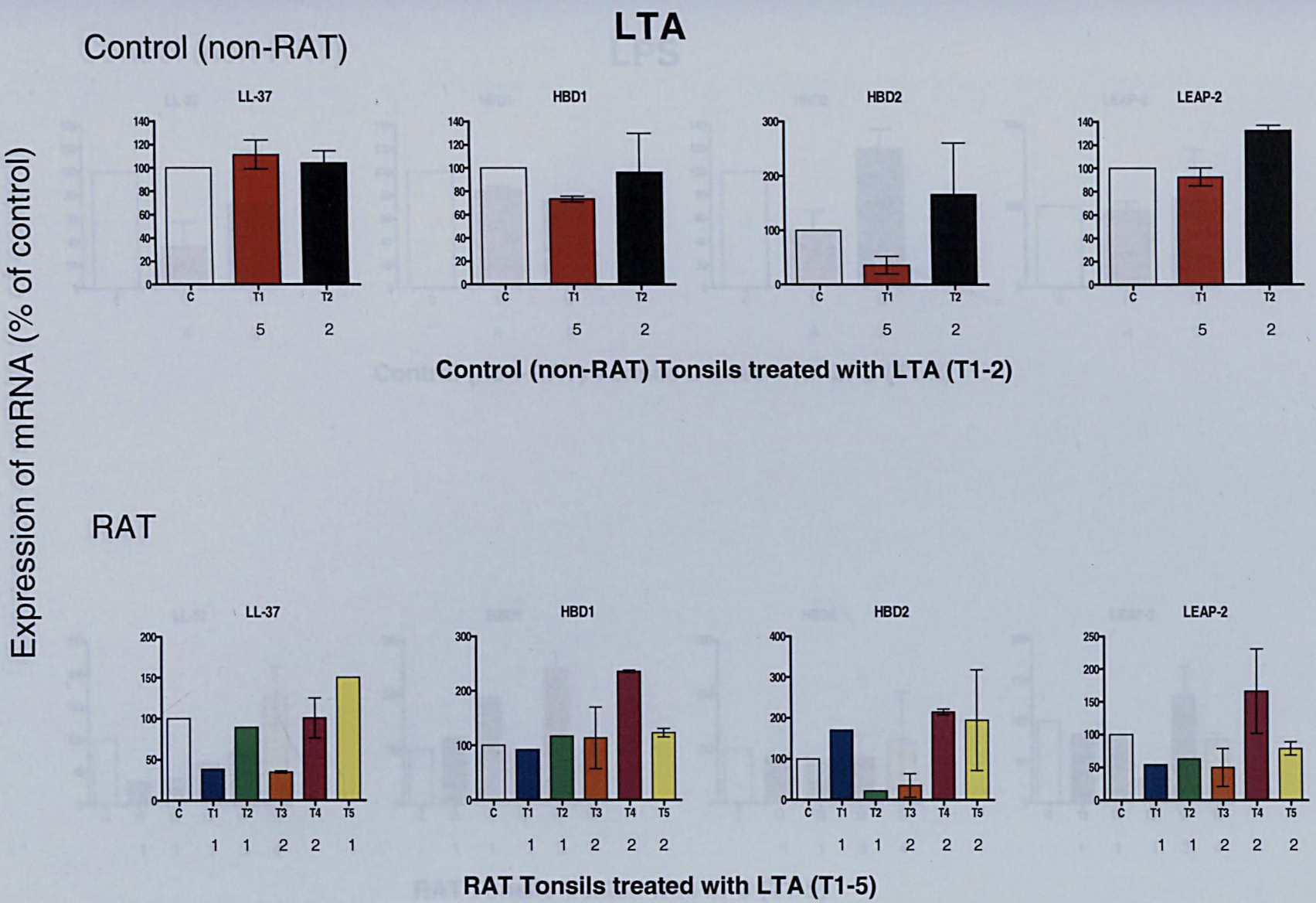

Figure 6.6: LTA: Real-time PCR data showing LL-37, HBD1, HBD2 and LEAP-2 mRNA expression in individual human tonsils incubated for 2 hours with LTA using the *ex vivo* model. Data represents two control (non-RAT) tonsils and five RAT tonsils. n: is number of samples analysed per tonsil. C = untreated control tonsils. Bars represent SEM. Statistical analysis was performed by one way ANOVA followed by a Bonferroni post-test. Real-time PCR analysis was performed once, each sample was assayed in duplicate except for LL-37 which was assayed in quadruplicate.

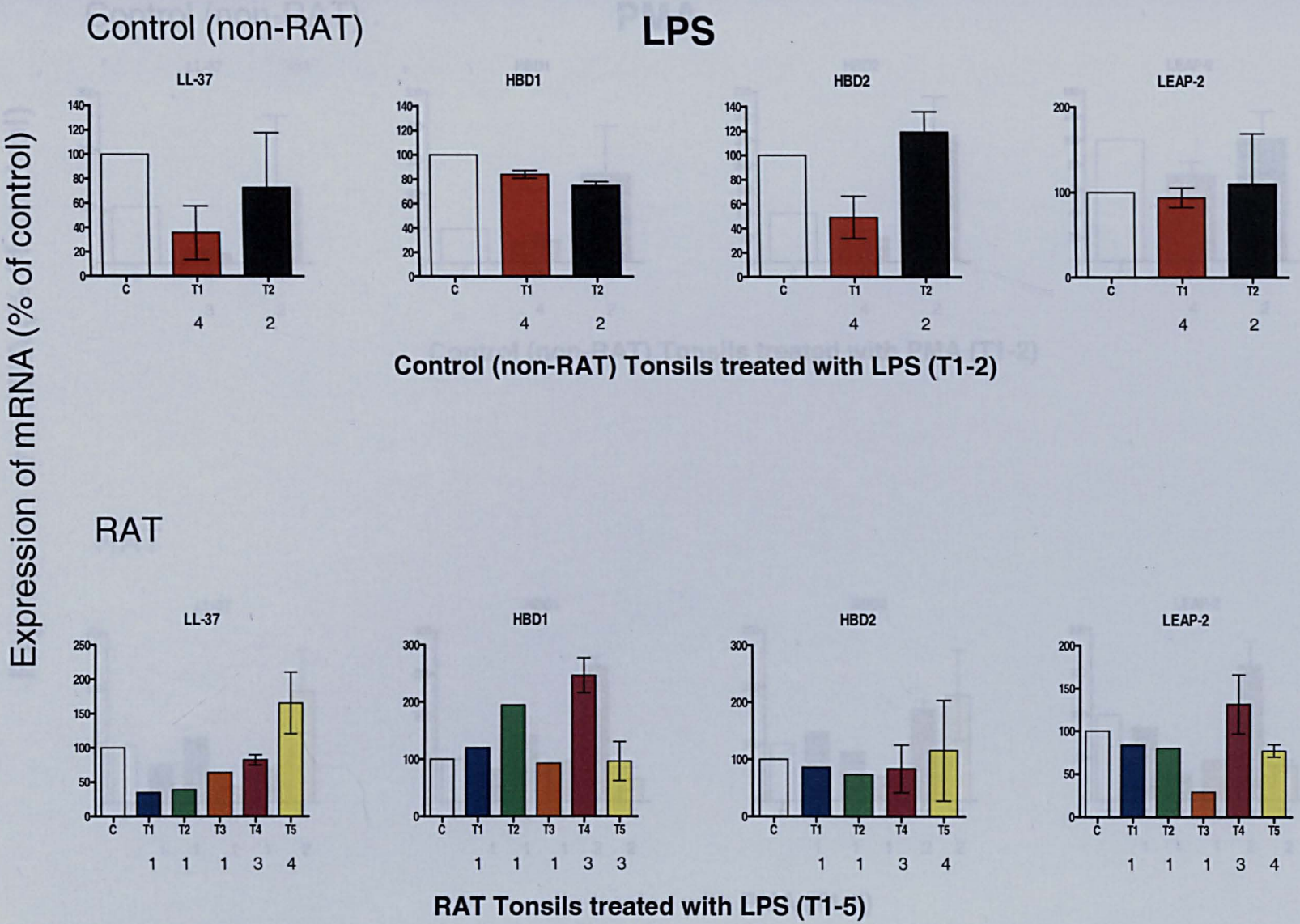

Figure 6.7: LPS: Real-time PCR data showing LL-37, HBD1, HBD2 and LEAP-2 mRNA expression in individual human tonsils incubated for 2 hours with LPS using the *ex vivo* model. Data represents two control (non-RAT) tonsils and five RAT tonsils. n: is number of samples analysed per tonsil. C = untreated control tonsils. Bars represent SEM. Statistical analysis was performed by a one way ANOVA followed by a Bonferroni post-test. Real-time PCR analysis was performed once, each sample was assayed in duplicate except for LL-37 which was assayed in quadruplicate.

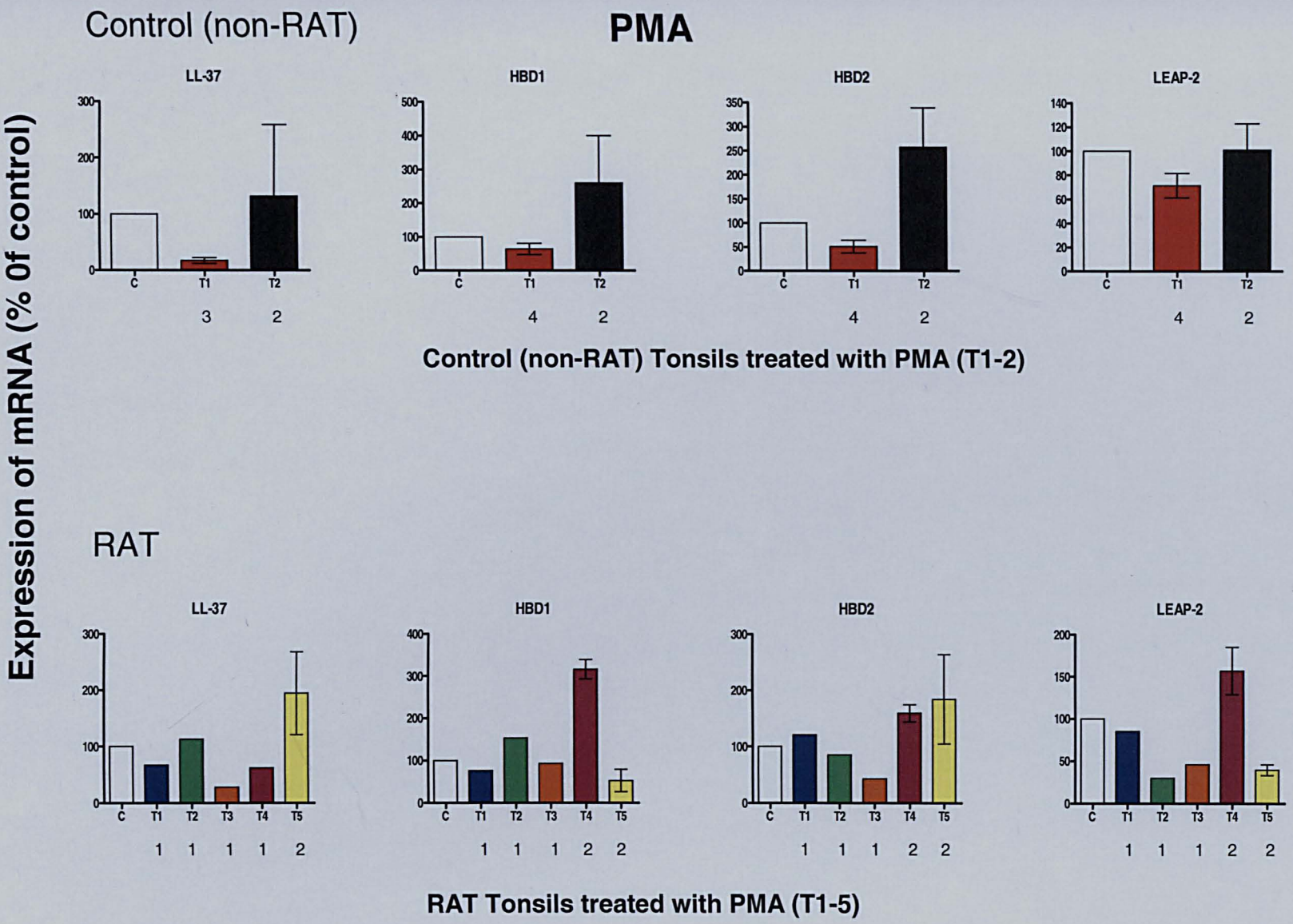

Figure 6.8: PMA: Real-time PCR data showing LL-37, HBD1, HBD2 and LEAP-2 mRNA expression in individual human tonsils incubated for 2 hours with PMA using the *ex vivo* model. Data represents two control (non-RAT) tonsils and five RAT tonsils. n: is number of samples analysed per tonsil. C = untreated control tonsils. Bars represent SEM. Statistical analysis was performed by a one way ANOVA followed by a Bonferroni post-test. Real-time PCR analysis was performed once, each sample was assayed in duplicate except for LL-37 which was assayed in quadruplicate.

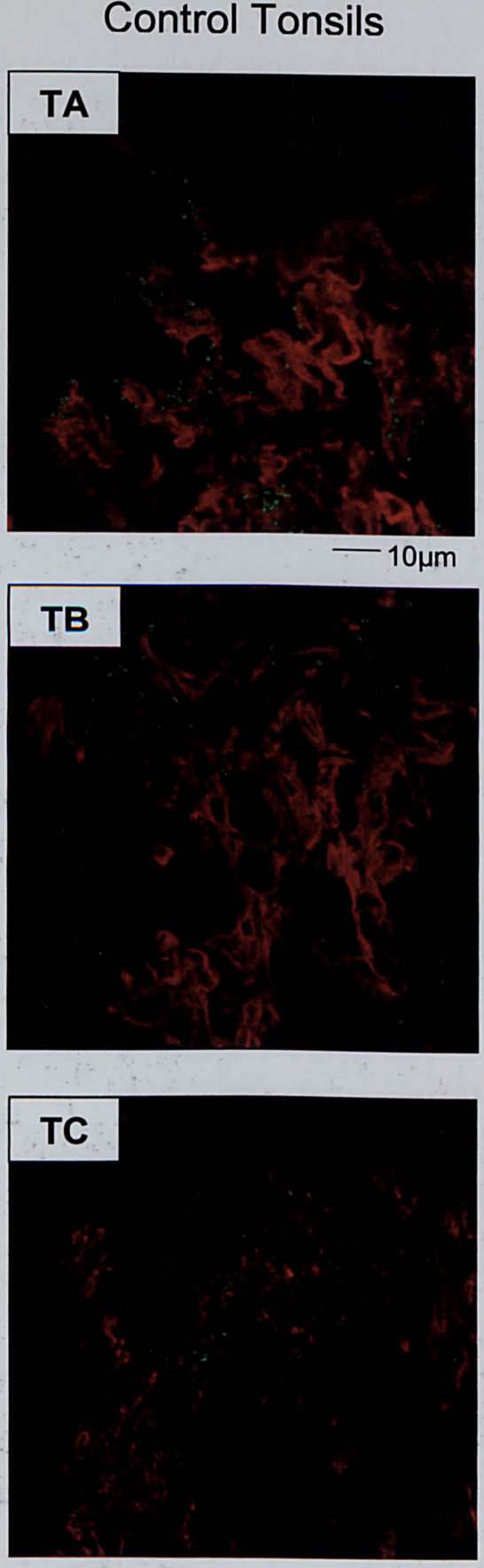

Figure 6.9: Binding control results showing control (non-RAT TA-C) and RAT tonsil (TA-J) tissue after two hours of infection with *S. pyogenes* M1 serotype expressing recombinant GFP plasmid (shown in green). Tonsil tissue has been stained with Cytokeratin-14 (shown in red). Images are x100 magnification.

RAT Tonsils

— 10µm

TA

TB

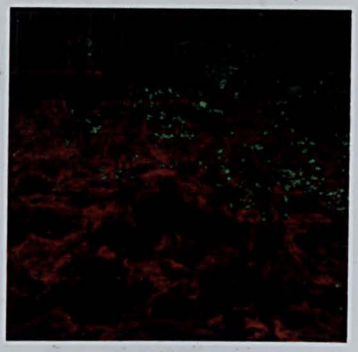

TC

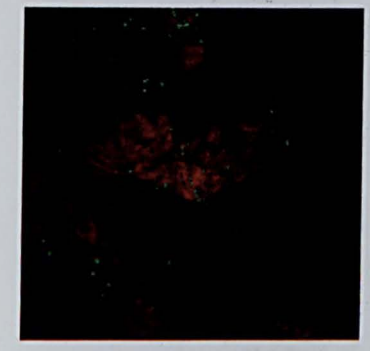

TD

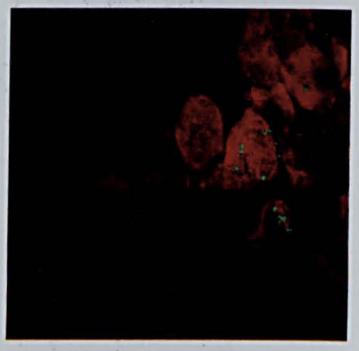

TE

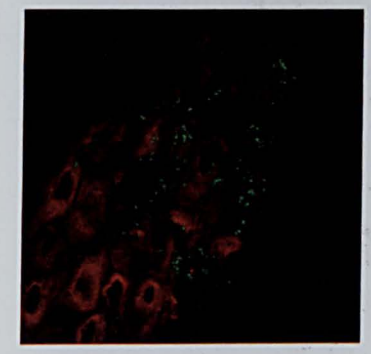

TF

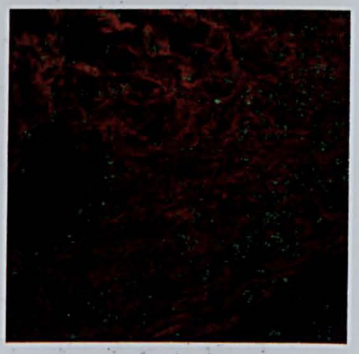

TG

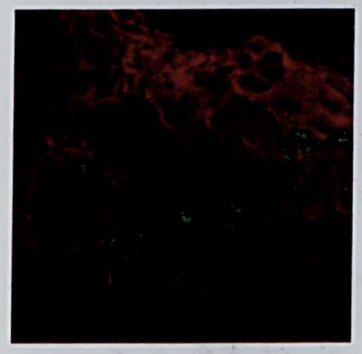

TH

TI

TJ

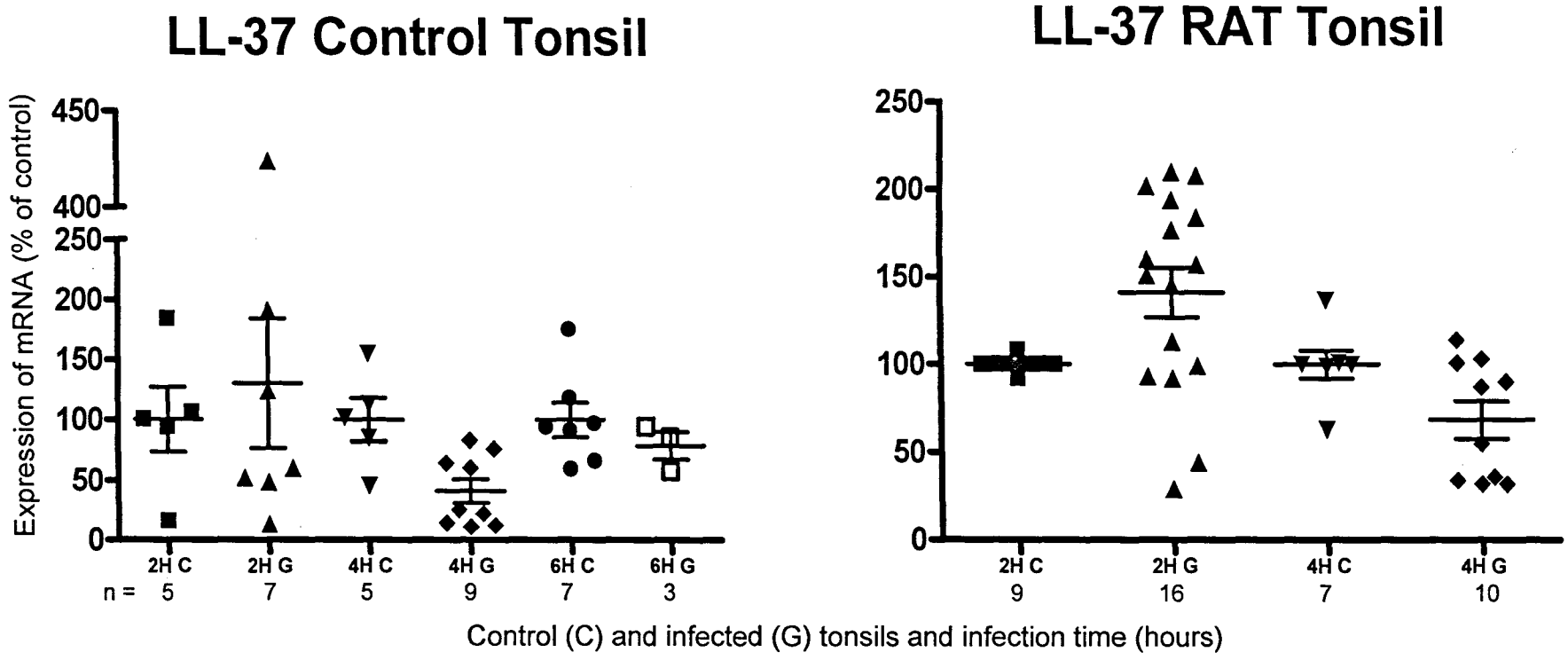

Figure 6.10: LL-37 Gene Expression: Real-time PCR data showing LL-37 mRNA expression in human tonsil incubated for two, four and six hours with *S. pyogenes* M1 serotype using the *ex vivo* tonsil model. Tonsils were incubated with medium (C) or medium containing Group A *Streptococcus* (G). Data was normalised to GAPDH and expressed as a percentage of control. All values represent mean ± SEM. n: number of tonsil sections analysed in total from 3 control (non-RAT) and 10 RAT tonsils. Statistical analysis was performed by one way ANOVA followed by a Bonferroni post-test. Real-time PCR analysis was performed once, each sample was assayed in quadruplicate.

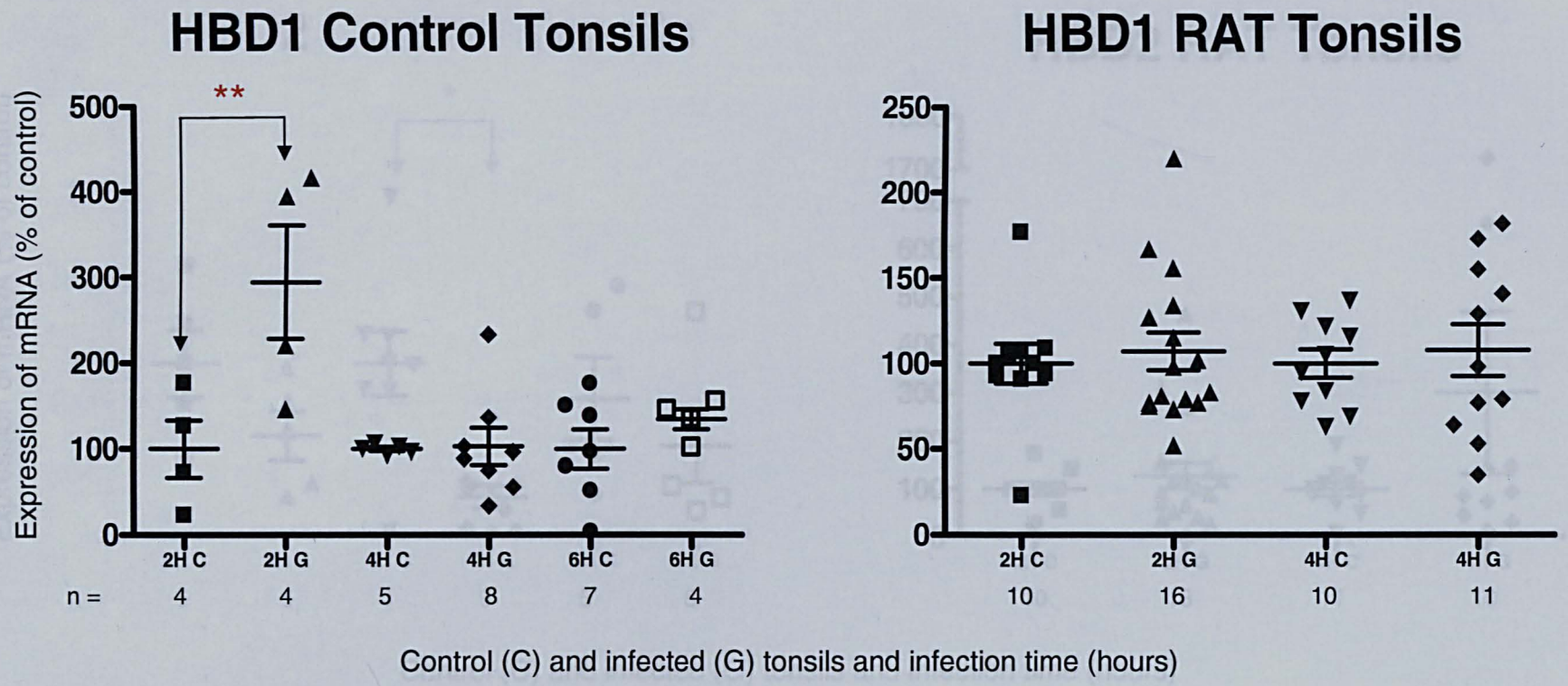

Figure 6.11: HBD1 Gene Expression: Real-time PCR data showing HBD1 mRNA expression in human tonsil incubated for two, four and six hours with *S. pyogenes* M1 serotype using the *ex vivo* tonsil model. Tonsils were incubated with normal tonsil medium (C) or with medium containing Group A *Streptococcus* (G) . Data was normalised to GAPDH and expressed as a percentage of control. All values represent mean ± SEM. n: number of tonsil sections analysed in total from 3 control (non-RAT) and 10 RAT tonsils. Statistical analysis was performed by a one way ANOVA followed by a Bonferroni post-test. ** = P< 0.01. Real-time PCR analysis was performed once, each sample was assayed in duplicate.

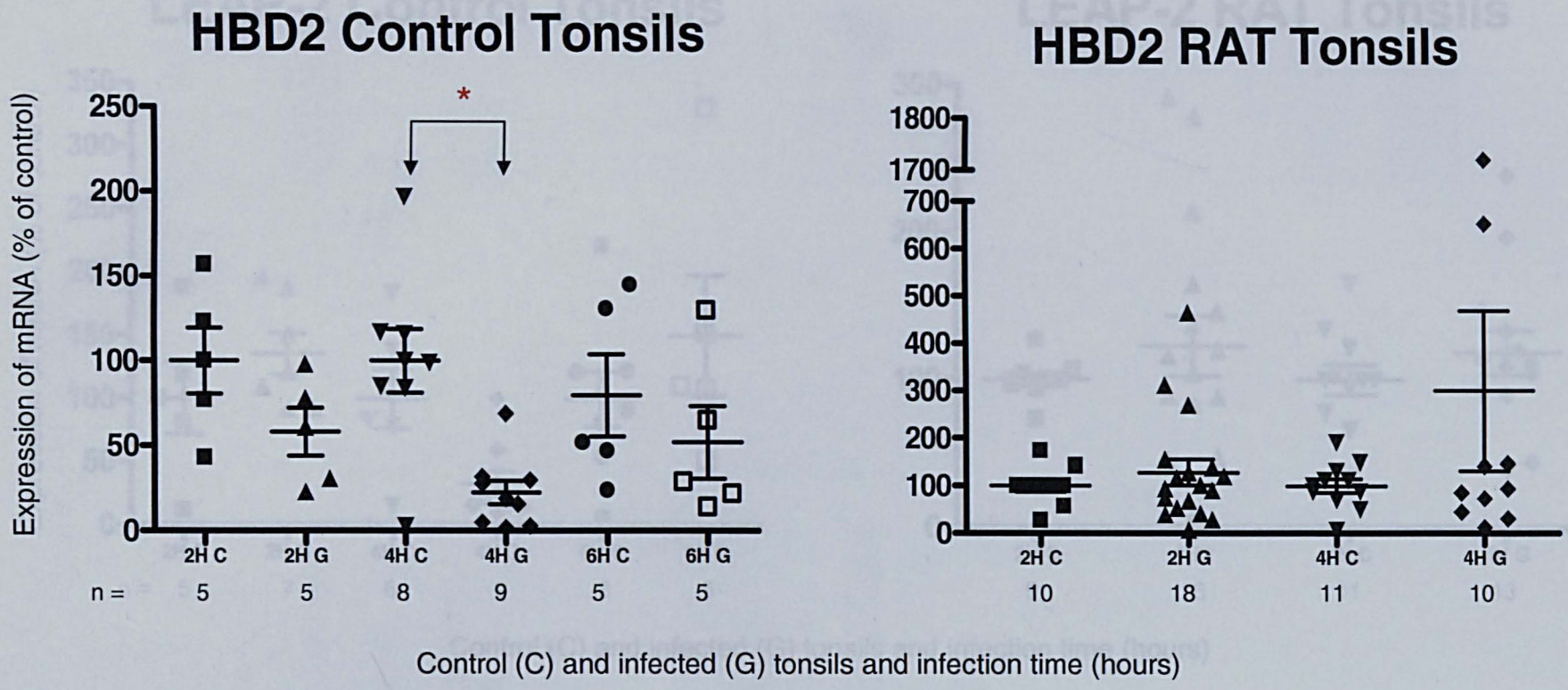

Figure 6.12: HBD2 Gene Expression: Real-time PCR data showing HBD2 mRNA expression in human tonsil incubated for two, four and six hours with *S. pyogenes* M1 serotype using the *ex vivo* tonsil model. Tonsils were incubated with normal tonsil medium (C) or with medium containing Group A *Streptococcus* (G). Data was normalised to GAPDH and expressed as a percentage of control. All values represent mean ± SEM. n = number of tonsil sections analysed in total from 3 control (non-RAT) and ten RAT tonsils. Statistical analysis was performed using a one way ANOVA followed by a Bonferroni post-test. * $P<0.05$. Real-time PCR analysis was performed once, each sample was assayed in duplicate.

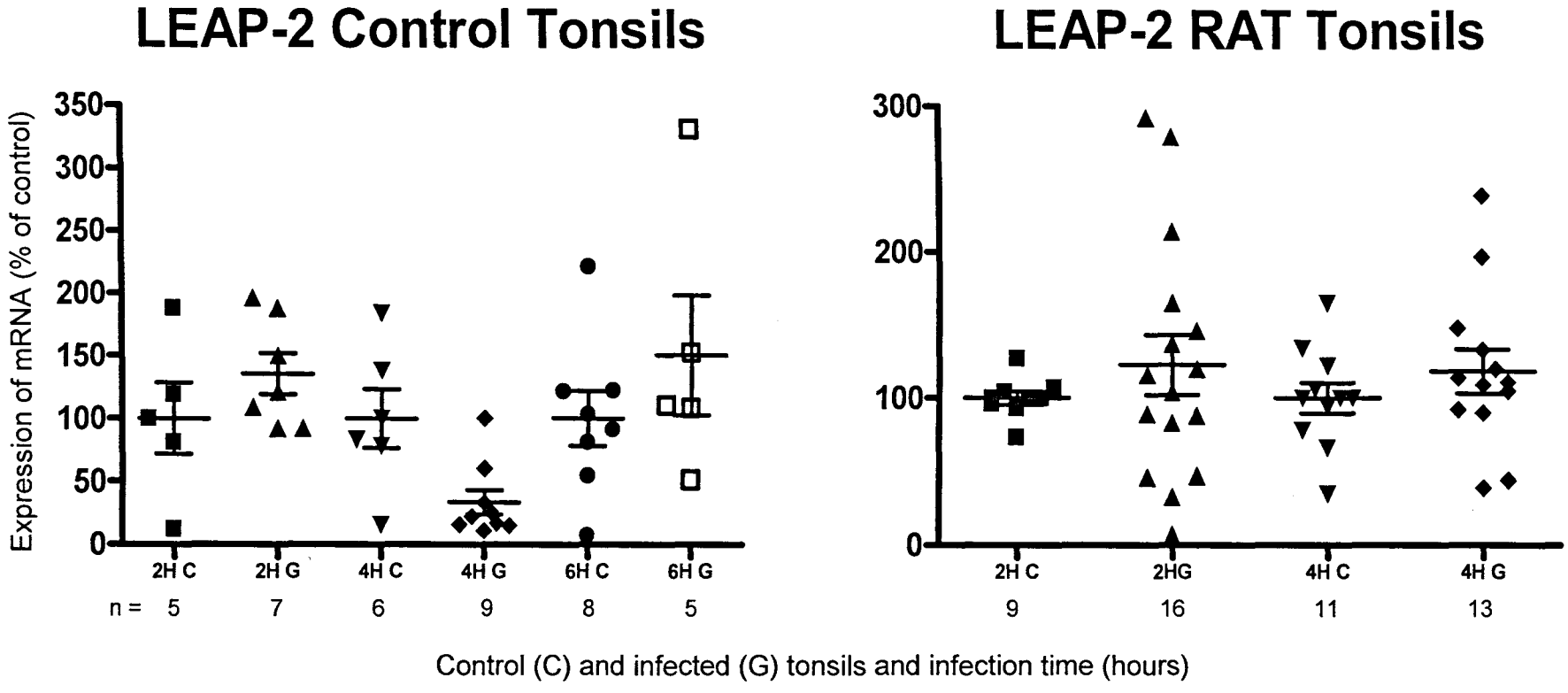

Figure 6.13: LEAP-2 Gene Expression: Real-time PCR data showing LEAP-2 mRNA expression in human tonsil incubated for two, four and six hours with *S. pyogenes* M1 serotype using the *ex vivo* tonsil model. Tonsils were incubated with normal tonsil medium (C) or with medium containing Group A *Streptococcus* (G) . Data was normalised to GAPDH and expressed as a percentage of control. All values represent mean ± SEM. n = number of tonsil sections analysed in total from two (non-RAT) and ten RAT tonsils. Statistical analysis was performed by a one way ANOVA followed by a Bonferroni post-test. Real-time PCR analysis was performed once, each sample was assayed in duplicate.

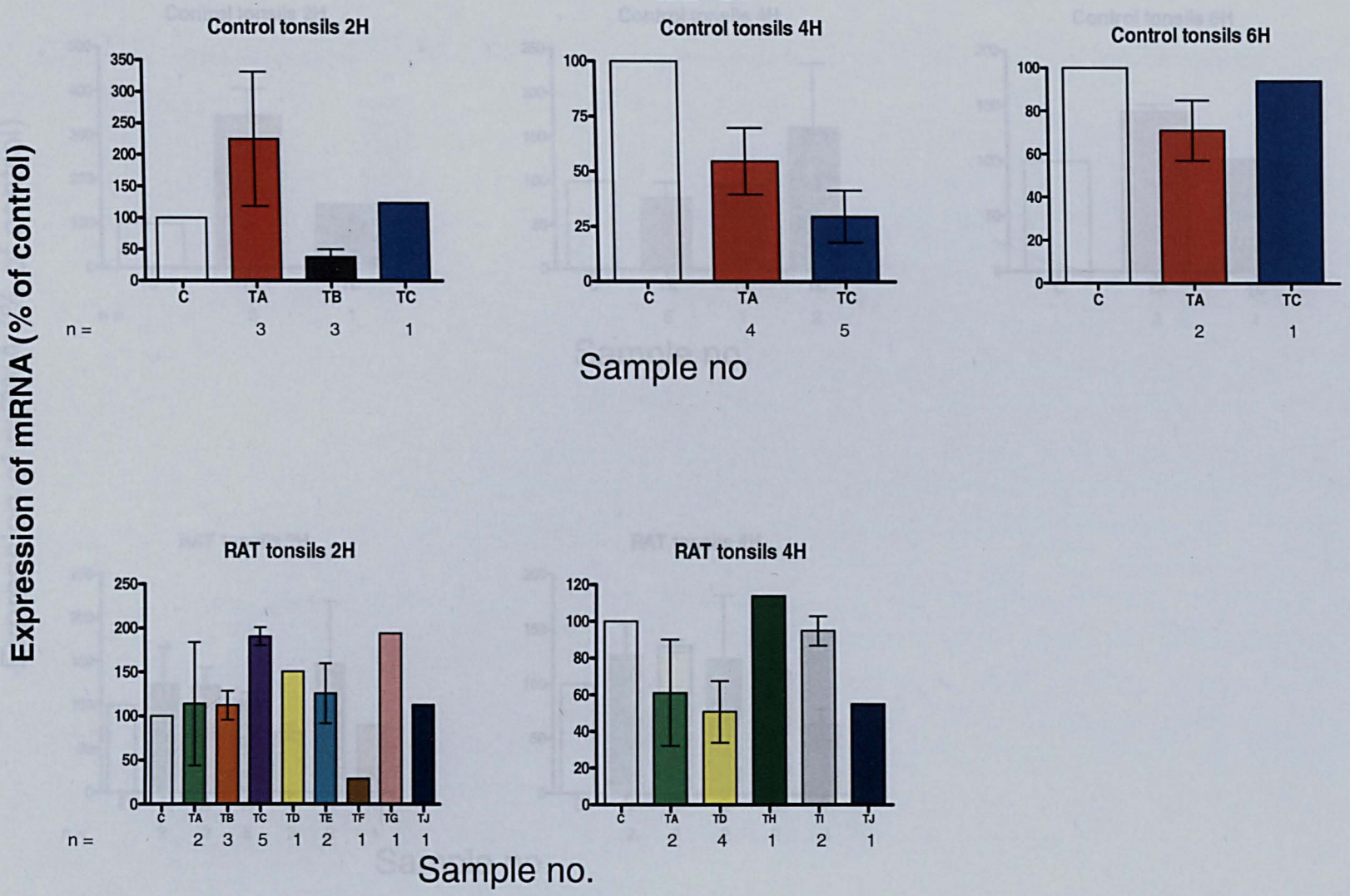

Figure 6.14: LL-37 Gene Expression: Real-time PCR data showing LL-37 mRNA expression in human tonsil incubated for two, four and six hours with *S. pyogenes* M1 serotype using the *ex vivo* model. Control samples were incubated in normal tonsil media (C) and all tonsils (TA-J) were infected with *S. pyogenes.* Data was normalised to GAPDH and expressed as a percentage of control. n = number of samples analysed in total from 3 control (non-RAT) and ten RAT tonsils. Statistical analysis was performed by a one way ANOVA followed by a Bonferroni post-test. All values represent mean ±SEM. Real-time PCR analysis was performed once, each sample was assayed in quadruplicate.

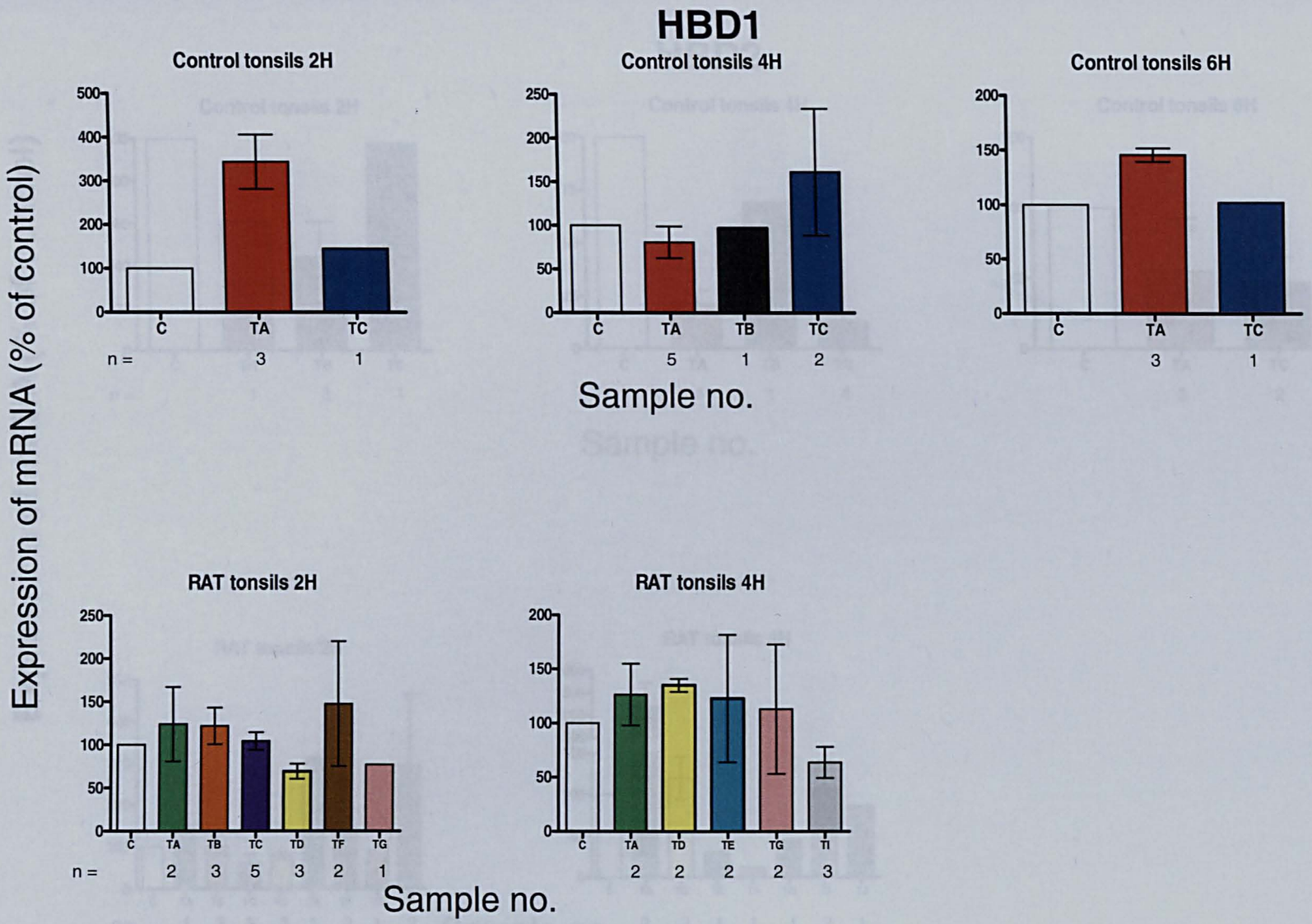

Figure 6.15: HBD1 Gene Expression: Real-time PCR data showing HBD1 mRNA expression in human tonsil incubated for two, four and six hours with *S. pyogenes* M1 serotype using the *ex vivo* model. Control samples were incubated in normal tonsil media (C) and all tonsils (TA-J) were infected with *S. pyogenes*. Data was normalised to GAPDH and expressed as a percentage of control. n = number of samples analysed in total from 3 control (non-RAT) and ten RAT tonsils. Statistical analysis was performed by a one way ANOVA followed by a Bonferroni post-test. All values represent mean ±SEM. Real-time PCR analysis was performed once, each sample was assayed in duplicate.

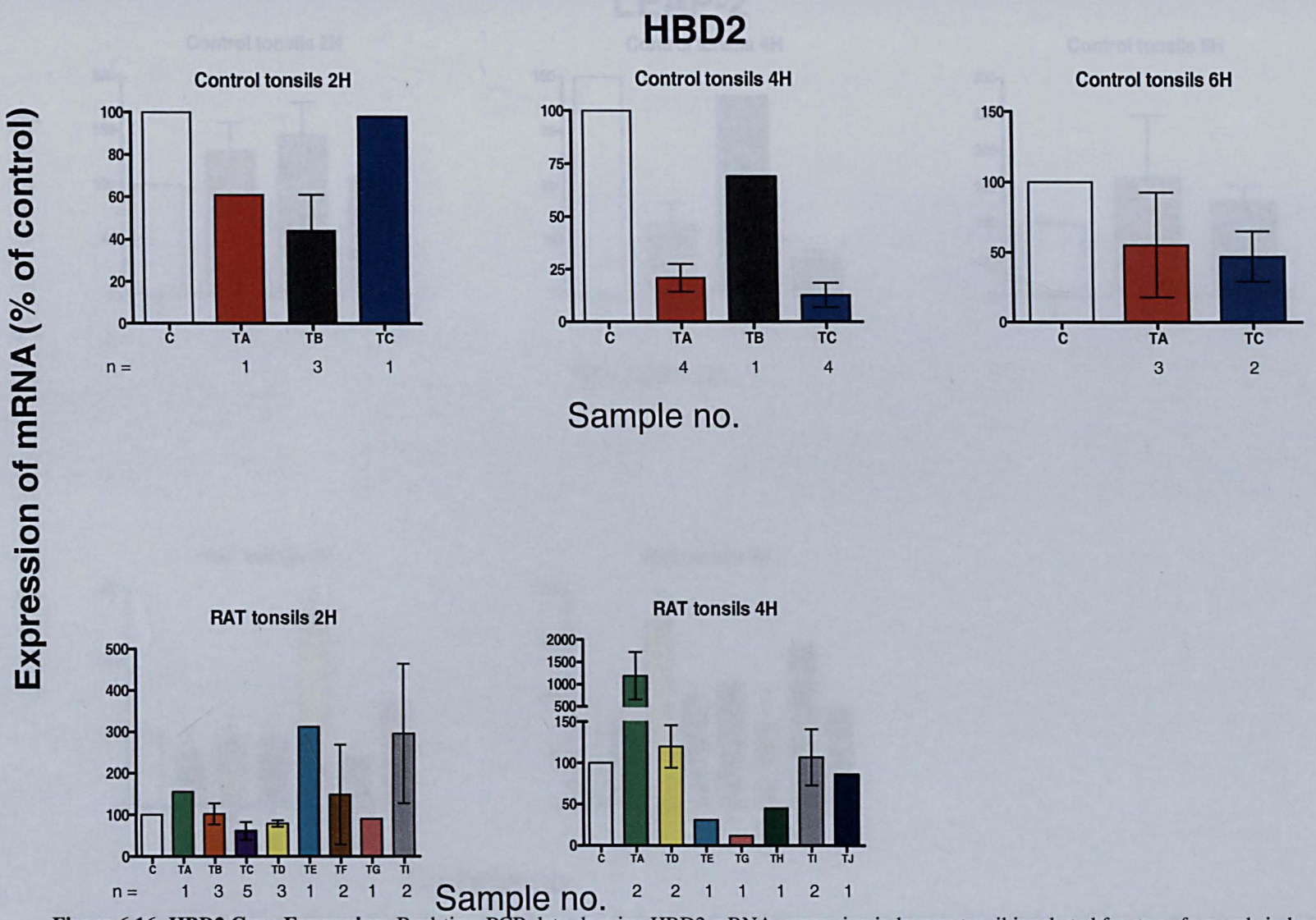

Figure 6.16: HBD2 Gene Expression: Real-time PCR data showing HBD2 mRNA expression in human tonsil incubated for two, four and six hours with *S. pyogenes* M1 serotype using the *ex vivo* model. Control samples were incubated in normal tonsil media (C) and all tonsils (TA-J) were infected with *S. pyogenes*. Data was normalised to GAPDH and expressed as a percentage of control. n = number of samples analysed in total from 3 control (non-RAT) and ten RAT tonsils. Statistical analysis was performed by a one way ANOVA followed by a Bonferroni post-test. All values represent mean ±SEM. Real-time PCR analysis was performed once, each sample was assayed in duplicate.

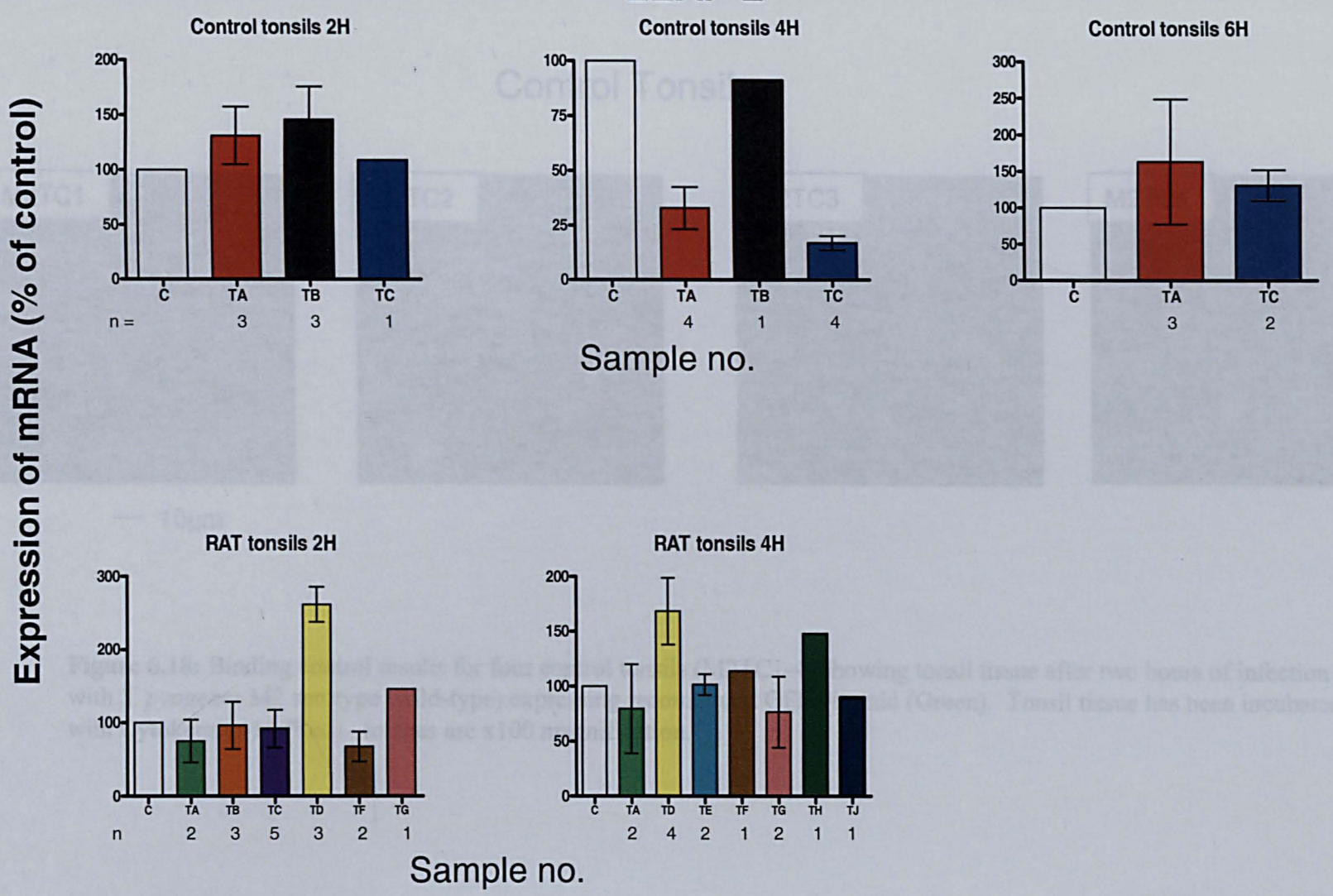

Figure 6.17: LEAP-2 Gene Expression: Real-time PCR data showing LEAP-2 mRNA expression in human tonsil incubated for two, four and six hours with *S. pyogenes* M1 serotype using the *ex vivo* model. Control samples were incubated in normal tonsil media (C) and all tonsils (TA-J) were infected with *S. pyogenes*. Data was normalised to GAPDH and expressed as a percentage of control. n = number of samples analysed in total from 3 control (non-RAT) and ten RAT tonsils. Statistical analysis was performed by a one way ANOVA followed by a Bonferroni post-test. All values represent mean ±SEM. Real-time PCR analysis was performed once, each sample was assayed in duplicate.

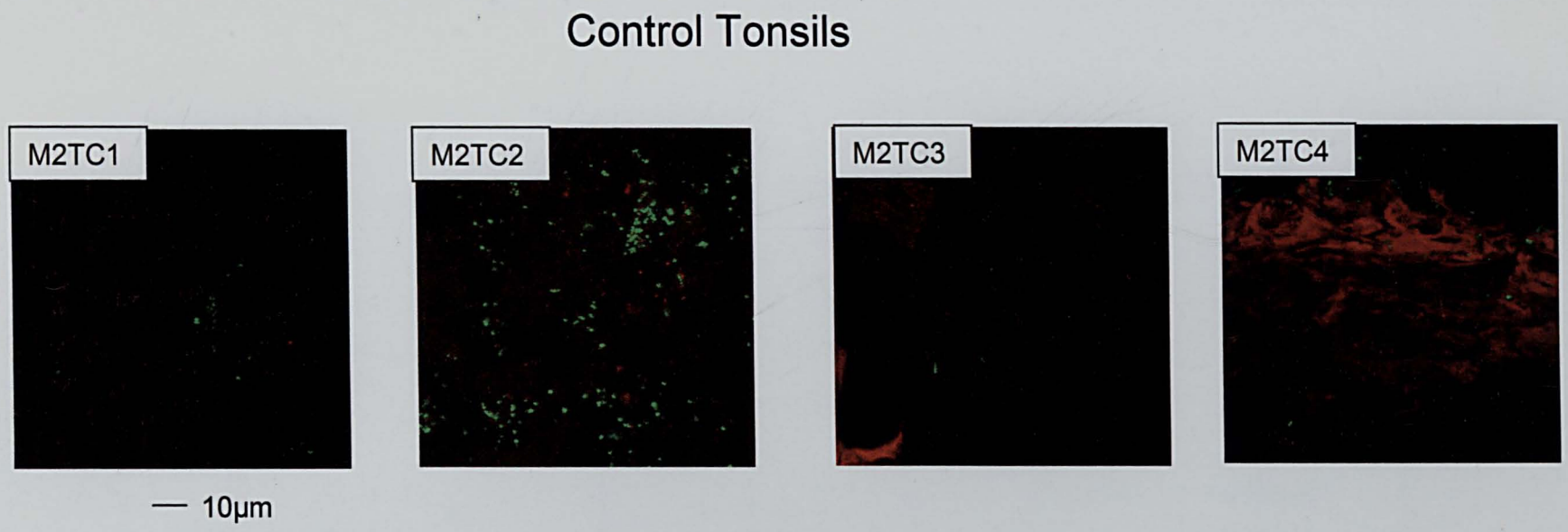

Figure 6.18: Binding control results for four control tonsils (M2TC1-4) showing tonsil tissue after two hours of infection with *S. pyogenes* M2 serotype (wild-type) expressing recombinant GFP plasmid (Green). Tonsil tissue has been incubated with Cytokeratin-14 (Red). Images are x100 magnification.

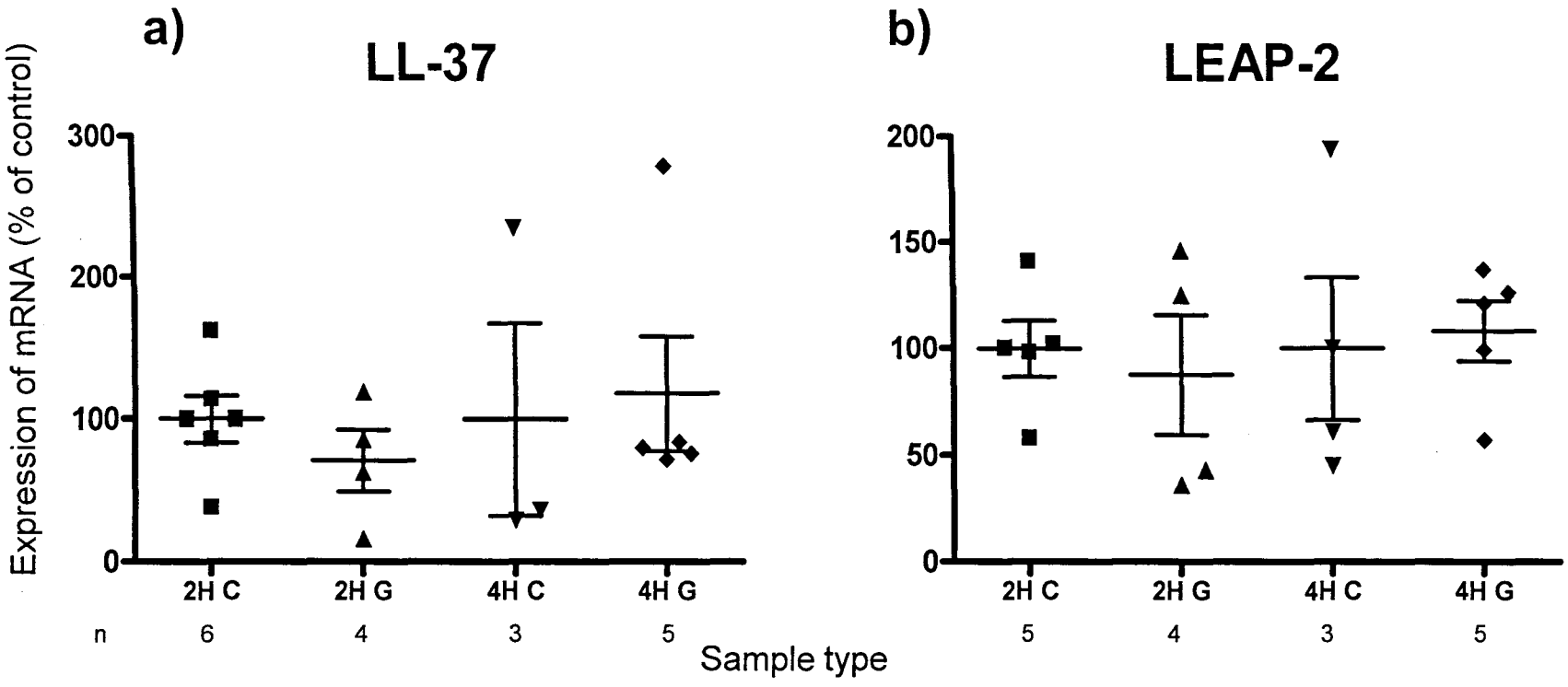

Figure 6.19: LL-37 Gene Expression: Real-time PCR data showing (a) LL-37 and (b) LEAP-2 mRNA expression in all human tonsils incubated for 2 and 4 hours with *S. pyogenes*, M2 serotype (wild-type) using the *ex vivo* tonsil model. Expression is shown in control (C) and cells infected with Group A *Streptococcus* (G) for 2 (2H) or 4 (4H) hours. Data is normalised to GAPDH and expressed as a percentage of control. n = number of tonsil sections analysed from a total of 4 control (non-RAT) tonsils. Statistical analysis was performed by a one way ANOVA followed by a Bonferroni post-test. All values represent mean ± SEM. Real-time PCR analysis was performed once, each samples was assayed in duplicate except for LL-37 which was assayed in quadruplicate .

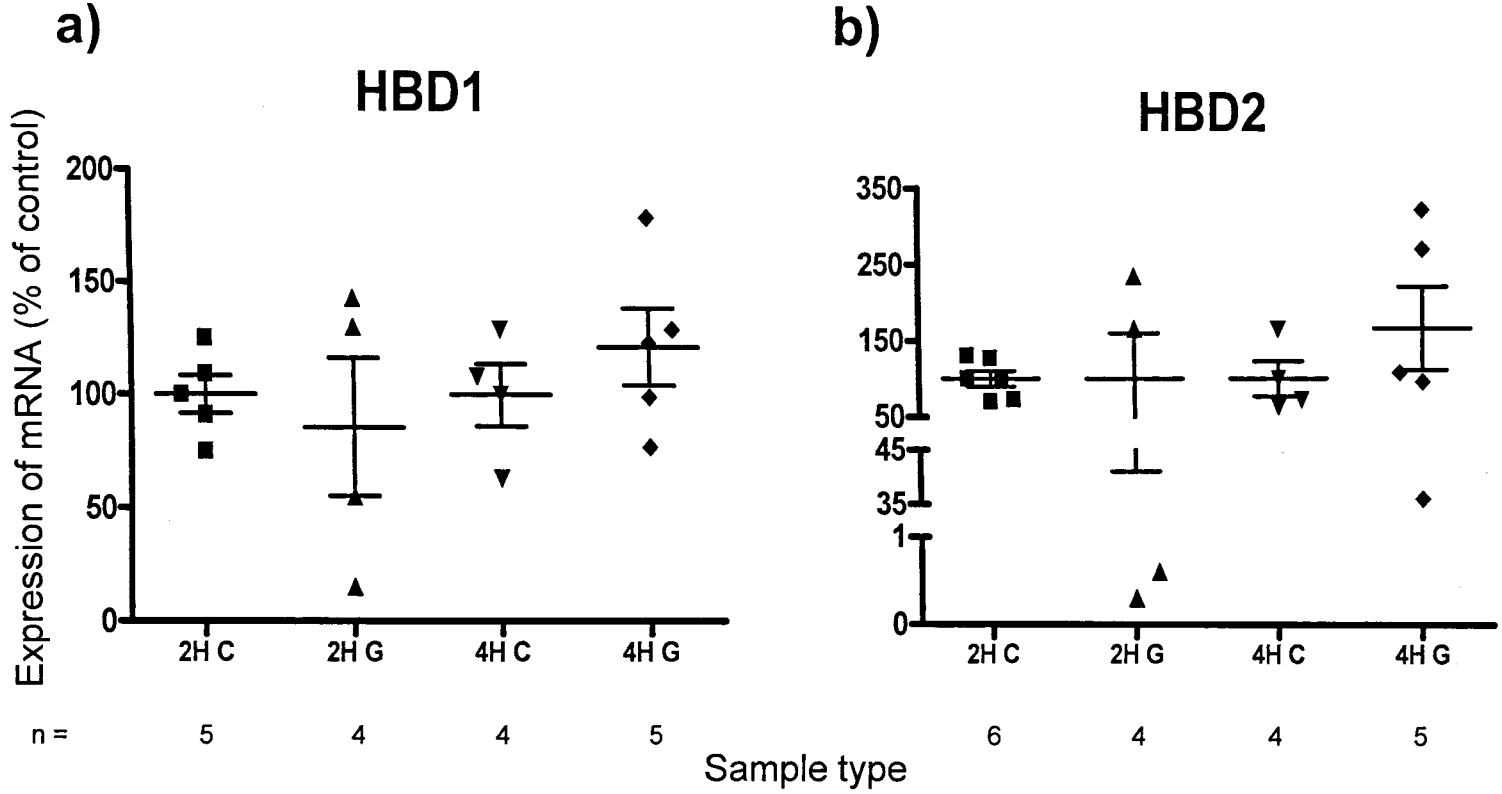

Figure 6.20 : Real-time PCR data showing (a) HBD1 and (b) HBD2 mRNA expression in all human tonsils incubated for 2 and 4 hours (2H and 4H) with *S. pyogenes* M2 serotype (wild-type) using the *ex vivo* tonsil model. Expression is shown in control (C) and cells infected with Group A *Streptococcus* (G). Data is normalised to GAPDH and expressed as a percentage of control. n= number of tonsil sections analysed in total from 4 control (non-RAT) tonsils. Statistical analysis was performed by a one way ANOVA followed by a Bonferroni post-test. All values represent mean ± SEM. Real-time PCR analysis was performed once. Each sample was assayed in duplicate.

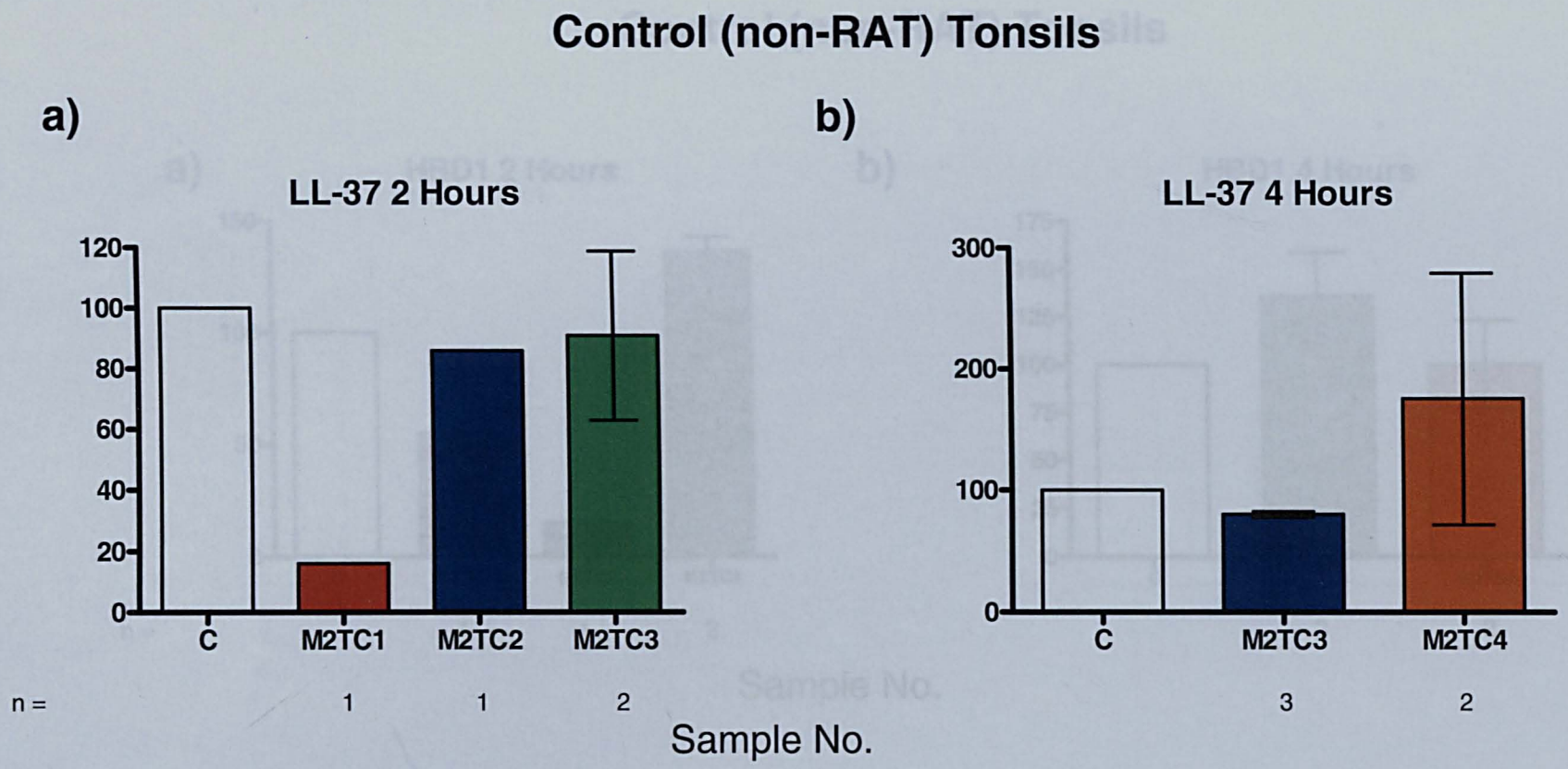

Figure 6.21: LL-37 Gene Expression: Real-time PCR data showing LL-37 mRNA expression in human tonsil incubated for (a) two and (b) four hours with *S. pyogenes* M2 serotype using the *ex vivo* model. Control samples were incubated in normal tonsil media (C) and all tonsils (M2TC1-4) were infected with *S. pyogenes*. Data was normalised to GAPDH and expressed as a percentage of control. n = number of samples analysed in total from 4 control (non-RAT) tonsils. Statistical analysis was performed by a one way ANOVA followed by a Bonferroni post-test. All values represent mean ±SEM where appropriate. Real-time PCR analysis was performed once, each sample was assayed in quadruplicate.

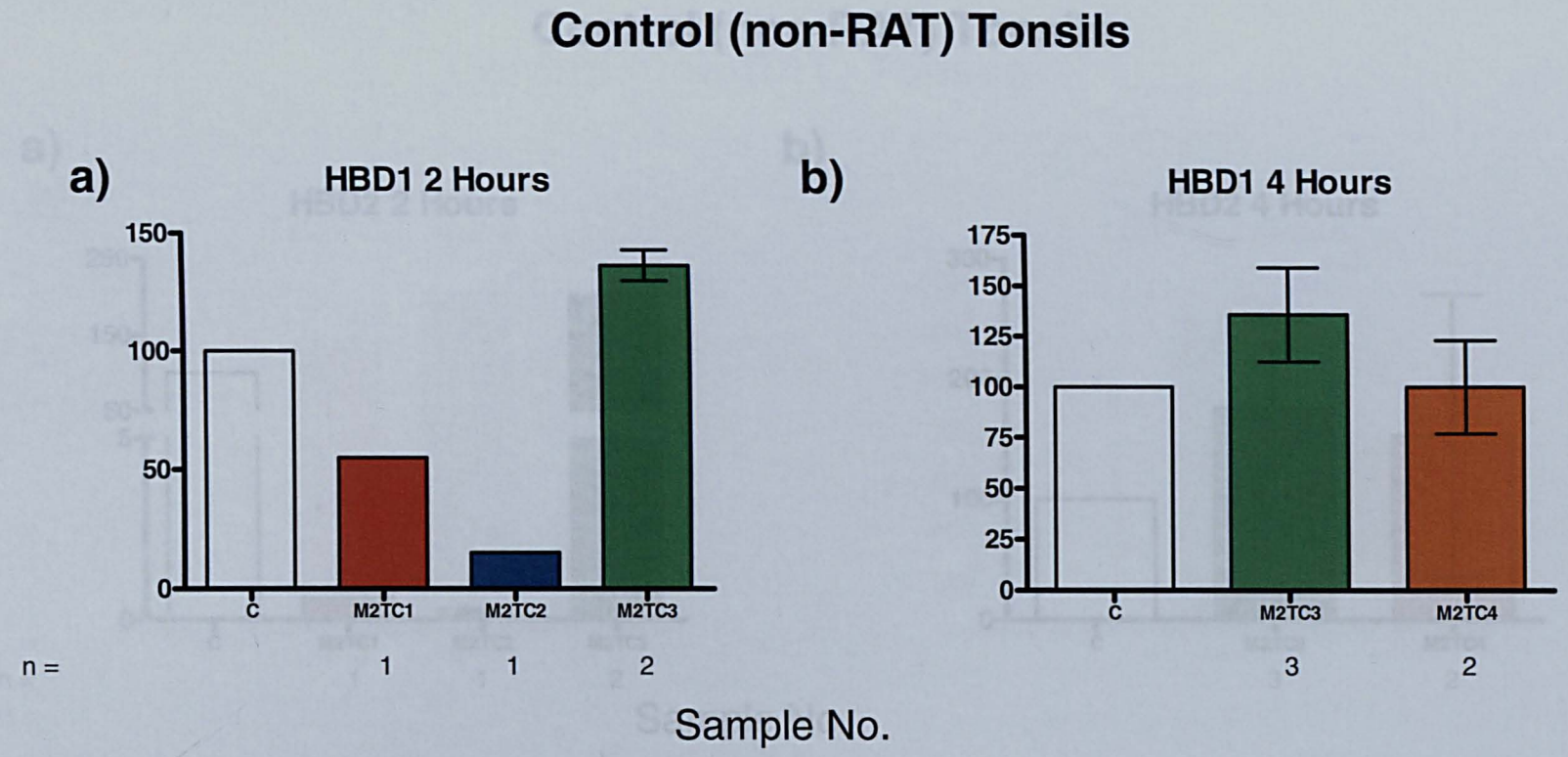

Figure 6.22: HBD1 Gene Expression: Real-time PCR data showing HBD1 mRNA expression in human tonsil incubated for (a) two and (b) four hours with *S. pyogenes* M2 serotype using the *ex vivo* model. Control samples were incubated in normal tonsil media (C) and all tonsils (M2TC1-4) were infected with *S. pyogenes*. Data was normalised to GAPDH and expressed as a percentage of control. n = number of samples analysed in total from 4 control (non-RAT) tonsils. Statistical analysis was performed by one way ANOVA followed by a Bonferroni post-test. All values represent mean ±SEM where appropriate. Real-time PCR analysis was performed once, each sample was assayed in duplicate.

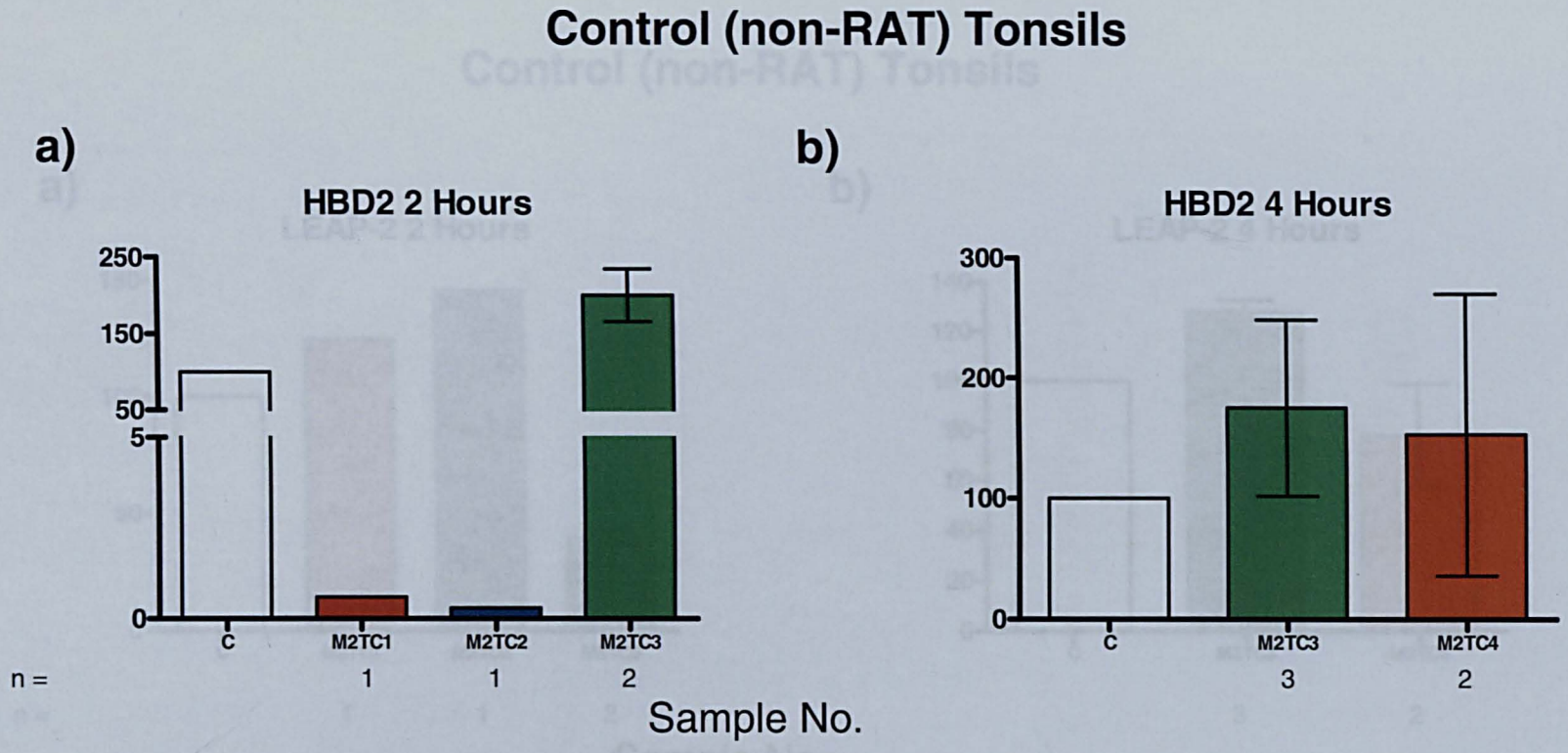

Figure 6.23: HBD2 Gene Expression: Real-time PCR data showing HBD2 mRNA expression in human tonsil incubated for (a) two and (b) four hours with *S. pyogenes* M2 serotype using the *ex vivo* model. Control samples were incubated in normal tonsil media (C) and all tonsils (M2TC1-4) were infected with *S. pyogenes*. Data was normalised to GAPDH and expressed as a percentage of control. n = number of samples analysed in total from 4 control (non-RAT) tonsils. Statistical analysis was performed by a one way ANOVA followed by a Bonferroni post-test. All values represent mean ± SEM where appropriate. Real-time PCR analysis was performed once, each sample was assayed in duplicate.

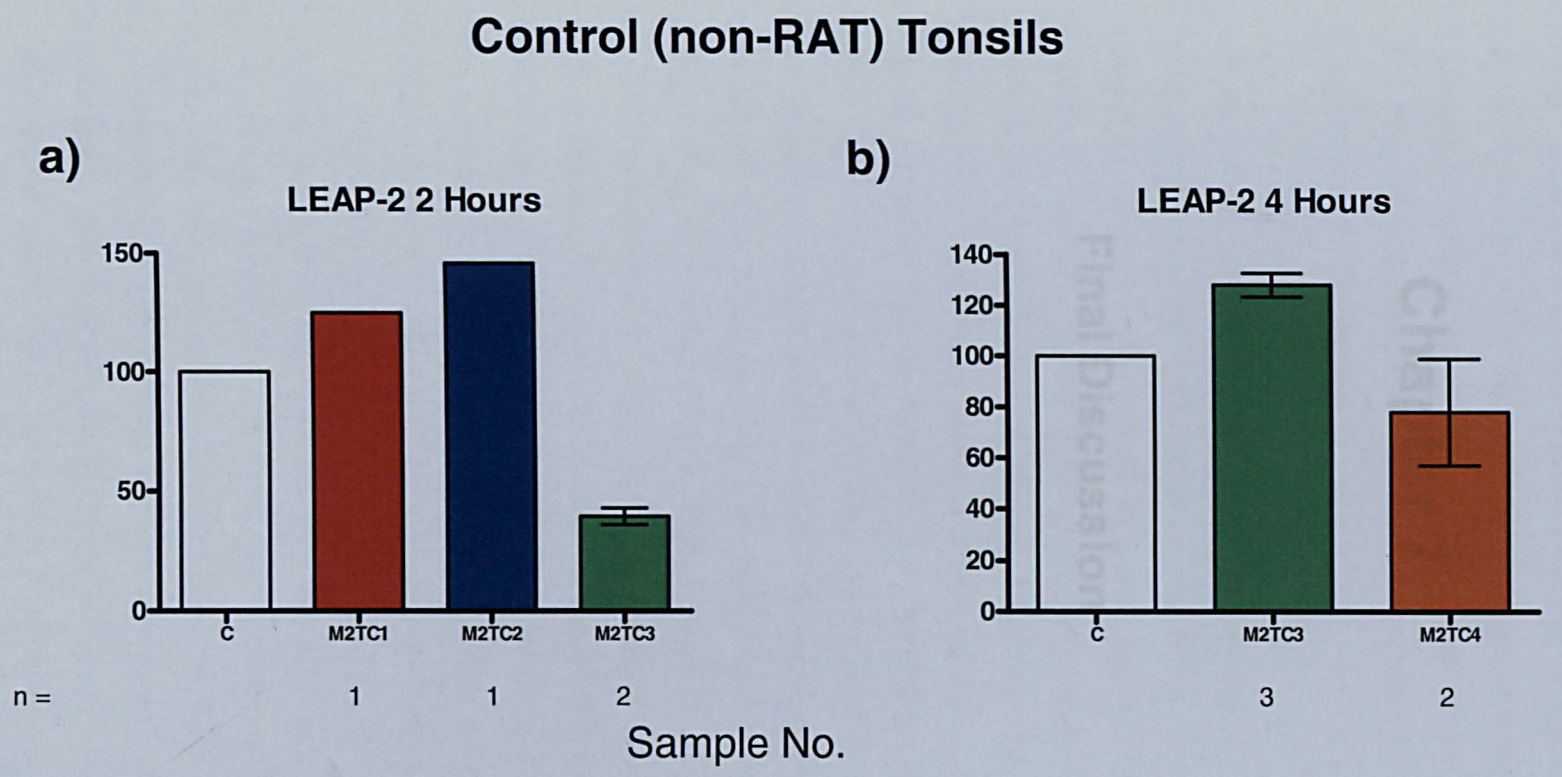

Figure 6.24: LEAP-2 Gene Expression: Real-time PCR data showing LEAP-2 mRNA expression in human tonsil incubated for (a) two and (b) four hours with *S. pyogenes* M2 serotype using the *ex vivo* model. Control samples were incubated in normal tonsil media (C) and all tonsils (M2TC1-4) were infected with *S. pyogenes*. Data was normalised to GAPDH and expressed as a percentage of control. n = number of samples analysed in a total of 4 control (non-RAT) tonsils. Statistical analysis was performed by one way ANOVA followed by a Bonforroni post-test. All values represent mean ± SEM where appropriate. Real-time PCR analysis was performed once, each sample was assayed in duplicate.

Chapter 7

Final Discussion

Humans are constantly exposed to an array of micro-organisms, some of which are innocuous but others can cause infection and death. Therefore the ability of the host to sense pathogenic microbes and to respond appropriately to control infection is pivotal to survival. Indeed delayed detection and killing of pathogens contributes to overwhelming infections, inflated systemic responses, tissue damage and in many cases organ dysfunction. A better understanding of the disease process may therefore be achieved by studying and comparing the immune response of subjects either susceptible or resistant to specific diseases.

The innate immune system has evolved as the first line of defence against invading pathogens. It plays a critical role in destroying pathogens by not only pinpointing the location of a potential infection, instigating the host challenge but also signalling to the adaptive immune response. The recognition of potential pathogenic micro-organisms is through receptors on eukaryote cells that recognise conserved pathogen-associated molecular patterns shared by different classes of micro-organisms. One consequence of the triggering of such receptors is the production of host defence peptides of which cationic antimicrobial peptides (AMPs) are part. These small, structurally diverse, molecules function as the body's 'natural antibiotics,' displaying broad spectrum antimicrobial activity against a range of microbes including Gram-positive and negative bacteria. Their cationic charge targets them specifically to microbes and their hydrophobicity allows them to integrate into the microbial membrane causing depolarisation and death. This killing mechanism ensures that microbes are killed rapidly, thus preventing the onset of infection. Moreover these molecules have evolved to play a role in mediating inflammation through the stimulation of chemotaxis and wound repair (Bowdish, Davidson et al. 2006).

The human palatine tonsils play important roles in host immunity and provide a barrier against invading pathogens. However the Gram-positive bacterium, *Streptococcus pyogenes* often penetrates these defences resulting in the disease tonsillitis, in which sufferers present with swollen and painful palatine tonsils. Moreover the infection is often recurrent. Despite tonsillitis being relatively common, the immunological factors that allow this infection to perpetuate remain obscure, and in particular the roles of the AMPs in tonsillitis are not well documented. Thus the results of the studies presented in this thesis were designed to test the hypothesis that

a defect in the innate immune response involving host AMPs, is a cause or contributory factor to recurrent acute tonsillitis (RAT).

To address this, the first study, AMP gene expression patterns in palatine tonsils excised from patients undergoing tonsillectomy for RAT to those of control subjects whose tonsils were excised for conditions such as snoring were compared (Chapter 4). It was the largest investigation of its kind to date and used over ninety tonsils. The data indicated that all the AMP genes examined i.e. LL-37, HBD1, HBD2 and LEAP-2, were expressed, but disappointingly that the mean AMP expression levels between the RAT and control groups were not statistically different. However considerable variability was detected between the AMP expression levels of individual subjects and as the AMP expression data was pooled this meant that any patterns relating to actual individuals were lost.

Allelic variants of genes involved in the innate response have been shown to influence an individual's susceptibility to infection (Hill 2001). In the future it would be of interest to take each individual RAT and control tonsil, and to examine and compare the LL-37, HBD1, HBD2 and LEAP-2 AMP profiles. This, possibly, would allow patterns between individuals in the RAT and control groups to be revealed e.g. a group of RAT patients may present with reduced HBD2 and LL-37 gene expression but HBD1 and LEAP-2 mRNA levels comparable to those of the control. If so this may indicate, potentially, the synergistic activities of peptides in protecting against a *S. pyogenes* infection. The real-time assay to quantify HBD3 gene expression was at the time of these analyses not working efficiently. As HBD3 has been shown to have streptococcal killing activities (Harder, Bartels et al. 2001), it would be valuable to have the HBD3 gene expression data, however as RNA samples from each of the tonsils are available this is still feasible.

In addition it would be practical to genotype the patient samples to explore potential single nucleotide polymorphisms (SNPs) in the AMP genes and their promoters that might increase the susceptibility of certain individuals to RAT. In humans it is also known that polymorphisms in the TLRs, which attenuate receptor signalling, can also enhance the risk of infection (Bochud, Hawn et al. 2003). As mentioned previously the RNA samples from each of the RAT and control tonsils are still available so it

would also be valuable to analyse the TLR gene expression patterns, particularly those relating to TLR2 and TLR4, in these samples. Again in future analyses it would be beneficial to genotype for TLR polymorphisms and establish whether populations with increased susceptibility to RAT are characterised particularly by specific polymorphisms in genes encoding molecules involved in the innate immune response.

It could be argued that the patient study, as presented, was flawed as it was conducted using tonsils excised from RAT patients at the time of their surgery when they were probably not suffering a streptococcal infection. Thus at this time it might be predicted that no differences in AMP gene expression between RAT and control tonsils would be revealed. Therefore, to answer the question of whether RAT was due to a failure of the AMP genes to up-regulate expression in response to infection, an *in vitro* model was adopted. The HaCaT cell model was selected as interactions observed between the HaCaT cells and *S. pyogenes* mimicked those of the tonsil and the bacterium (Abbot, Smith et al, 2007). Moreover it was found that the HaCaT AMP expression profile was similar to tonsil, although characteristically of keratinocyte derived cells, the LL-37 gene expression levels were very low.

The results of the experiments using this model cell line, described in Chapter 5, indicated that HBD1 gene expression was reduced following a *S. pyogenes* challenge, suggesting that the pathogen was inhibiting or down-regulating AMP gene expression. The mechanisms by which this occurred is not known but investigations to unravel the signalling pathways would naturally be the next stage for this work. Such analyses could be performed using either chemical and/or immunological inhibitors of components of known signalling pathways. This work could be carried out in a model cell line first, therefore only one cell type would be encountered initially making results clearer to analyse.

Previous observations have indicated that pili are necessary for *S. pyogenes* to bind to tonsils. The studies reported in this thesis with the pili-defective mutants indicated that binding and colonisation is not necessary for an antimicrobial peptide response to take place and that it is the proximity of the streptococci to the cells that causes an immune response rather than direct binding through pili. This is exciting and it

suggests that additional investigations using such mutants are essential to explore this further.

The HaCaT cells, although an appropriate model for the *in vitro* studies, were not derived from tonsil. To further investigate streptococcal–tonsil AMP responses the *ex vivo* tonsil model developed here in Newcastle was used (Abbot, Smith et al. 2007). The data from these studies described in Chapter 6, highlighted differences between the AMP expression profiles of the control (non-RAT) and RAT tonsils in response to a *S. pyogenes* M1 challenge. Although speculative these data suggested that the RAT tonsils were less able to respond to the *S. pyogenes* challenge, which may in part help to explain the susceptibility of RAT patients to infection. However the data was very variable and raised questions as to whether the model, as is, provided a good enough *in vitro* system for studying the tonsil AMP responses in response to streptococci. The reasons for the variability have already been discussed in Chapter 6, and include the fact that the AMP expression data between actual individuals is very different. Thus as the model does allow the responses of actual tonsil tissue to be studied in response to a live streptococcal infection, and as a superior tonsil model has not been reported, it can be argued that it provides a unique, and suitable system for our investigations. However in future it is possible that primary or indeed immortalised tonsil derived cell lines will be established to facilitate such investigations.

In the studies reported in Chapter 6, only AMP gene expression profiles were examined. However AMPs are only a part of the tonsil innate defences and do not work in isolation. As RNA from the streptococcal challenge experiments is stored it would be possible to analyse the nucleic acid material for other immune responses, for example, using the Applied Biosystems TaqMan immune array. This array includes 96 gene targets associated with the immune response and inflammation, and profiling the data from RAT and control tonsils may allow the recognition of unique transcripts encoding proteins playing key roles in the tonsil defence pathways.

It is acknowledged that gene expression relates only to what is happening at a molecular level. However the results of previous studies in Newcastle (Ball, Siou et al, 2007), using tonsil sections and immunohistochemical analyses suggested that the amounts of the HBD1 and 3, and LL-37 peptide were reduced in the tonsils of RAT

patients compared to control subjects. Thus potential future investigations should also aim to quantify actual peptide concentrations either through ELISA and/or immunohistochemistry.

The studies reported in this thesis have focused specifically on *S. pyogenes*. Using the *ex vivo* model it would also be of interest to challenge the tonsils with other potential oral pathogens and investigate the innate responses. This in turn may allow us a better understanding of the disease process operating in recurrent acute tonsillitis.

Chapter 8

References

Abbot, E. L., W. D. Smith, et al. (2007). "Pili mediate specific adhesion of Streptococcus pyogenes to human tonsil and skin." Cell Microbiol **9**(7): 1822-33.
Aberg, K. M., K. A. Radek, et al. (2007). "Psychological stress downregulates epidermal antimicrobial peptide expression and increases severity of cutaneous infections in mice." J Clin Invest **117**(11): 3339-49.
Agerberth, B., H. Gunne, et al. (1995). "FALL-39, a putative human peptide antibiotic, is cysteine-free and expressed in bone marrow and testis." Proc Natl Acad Sci U S A **92**(1): 195-9.
Akesson, P., A. G. Sjoholm, et al. (1996). "Protein SIC, a novel extracellular protein of Streptococcus pyogenes interfering with complement function." J Biol Chem **271**(2): 1081-8.
Ali, R. S., A. Falconer, et al. (2001). "Expression of the peptide antibiotics human beta defensin-1 and human beta defensin-2 in normal human skin." J Invest Dermatol **117**(1): 106-11.
Bajaj-Elliott, M., P. Fedeli, et al. (2002). "Modulation of host antimicrobial peptide (beta-defensins 1 and 2) expression during gastritis." Gut **51**(3): 356-61.
Ball, S. L. (2004). Antimicrobial Peptides In Human Tonsils. ICAMB, Newcastle University. **M. PHIL.**
Ball, S. L., G. P. Siou, et al. (2007). "Expression and immunolocalisation of antimicrobial peptides within human palatine tonsils." J Laryngol Otol **121**(10): 973-8.
Bals, R. (2000). "Epithelial antimicrobial peptides in host defense against infection." Respir Res **1**(3): 141-50.
Bals, R., X. Wang, et al. (1998). "The peptide antibiotic LL-37/hCAP-18 is expressed in epithelia of the human lung where it has broad antimicrobial activity at the airway surface." Proc Natl Acad Sci U S A **95**(16): 9541-6.
Banchereau, J., F. Briere, et al. (1994). "Molecular control of B lymphocyte growth and differentiation." Stem Cells **12**(3): 278-88.
Barlow, P. G., Y. Li, et al. (2006). "The human cationic host defense peptide LL-37 mediates contrasting effects on apoptotic pathways in different primary cells of the innate immune system." J Leukoc Biol **80**(3): 509-20.
Bartlett, K. H., P. B. McCray, Jr., et al. (2004). "Reduction in the bactericidal activity of selected cathelicidin peptides by bovine calf serum or exogenous endotoxin." Int J Antimicrob Agents **23**(6): 606-12.
Batra, K., A. Safaya, et al. (2004). "Sore throat - a review of presentation and etiology " Indian Journal of Otolaryngology and Head and Neck Surgery **56**(1): 14-20.
Beachey, E. H. and I. Ofek (1976). "Epithelial cell binding of group A streptococci by lipoteichoic acid on fimbriae denuded of M protein." J Exp Med **143**(4): 759-71.
Beall, B., R. Facklam, et al. (1996). "Sequencing emm-specific PCR products for routine and accurate typing of group A streptococci." J Clin Microbiol **34**(4): 953-8.
Bensch, K. W., M. Raida, et al. (1995). "hBD-1: a novel beta-defensin from human plasma." FEBS Lett **368**(2): 331-5.
Beres, S. B., G. L. Sylva, et al. (2002). "Genome sequence of a serotype M3 strain of group A Streptococcus: phage-encoded toxins, the high-virulence phenotype, and clone emergence." Proc Natl Acad Sci U S A **99**(15): 10078-83.
Bick, R. J., B. J. Poindexter, et al. (2004). "Effects of cytokines and heat shock on defensin levels of cultured keratinocytes." Burns **30**(4): 329-33.

Bikle, D. D. (2004). "Vitamin D regulated keratinocyte differentiation." J Cell Biochem **92**(3): 436-44.
Bochud, P., T. Hawn, et al. (2003). "Cutting edge: a toll-like receptor 2 polymorphism that is associated with lepromatous leprosy is unable to mediate mycobacterial signaling." J Immunol **170**(7): 3451-4.
Boman, H. G., B. Agerberth, et al. (1993). "Mechanisms of action on Escherichia coli of cecropin P1 and PR-39, two antibacterial peptides from pig intestine." Infect Immun **61**(7): 2978-84.
Bonass, W. A., A. S. High, et al. (1999). "Expression of beta-defensin genes by human salivary glands." Oral Microbiol Immunol **14**(6): 371-4.
Boukamp, P., R. T. Petrussevska, et al. (1988). "Normal keratinization in a spontaneously immortalized aneuploid human keratinocyte cell line." J Cell Biol **106**(3): 761-71.
Bowdish, D., D. Davidson, et al. (2006). "Immunomodulatory properties of defensins and cathelicidins." Curr Top Microbiol Immunol **306**: 27-66.
Brachtel, E. F., M. Washiyama, et al. (1996). "Differences in the germinal centres of palatine tonsils and lymph nodes." Scand J Immunol **43**(3): 239-47.
Brodsky, L., L. Moore, et al. (1988). "The immunology of tonsils in children: the effect of bacterial load on the presence of B- and T-cell subsets." Laryngoscope **98**(1): 93-8.
Brogden, K. A. (2005). "Antimicrobial peptides: pore formers or metabolic inhibitors in bacteria?" Nat Rev Microbiol **3**(3): 238-50.
Brook, I. and A. E. Gober (2005). "Treatment of non-streptococcal tonsillitis with metronidazole." Int J Pediatr Otorhinolaryngol **69**(1): 65-8.
Caldas, M. P., E. G. Neves, et al. (2007). "Tonsillolith--report of an unusual case." Br Dent J **202**(5): 265-7.
Cebra, J. J., S. B. Periwal, et al. (1998). "Development and maintenance of the gut-associated lymphoid tissue (GALT): the roles of enteric bacteria and viruses." Dev Immunol **6**(1-2): 13-8.
Chae, S. W., S. H. Lee, et al. (2001). "Expression of human beta-defensin 1 mRNA in human palatine tonsil." Acta Otolaryngol **121**(3): 414-8.
Chang, C. I., Y. A. Zhang, et al. (2006). "Two cathelicidin genes are present in both rainbow trout (Oncorhynchus mykiss) and atlantic salmon (Salmo salar)." Antimicrob Agents Chemother **50**(1): 185-95.
Chen, C. I., S. Schaller-Bals, et al. (2004). "Beta-defensins and LL-37 in bronchoalveolar lavage fluid of patients with cystic fibrosis." J Cyst Fibros **3**(1): 45-50.
Chromek, M., Z. Slamova, et al. (2006). "The antimicrobial peptide cathelicidin protects the urinary tract against invasive bacterial infection." Nat Med **12**(6): 636-41.
Chronnell, C. M., L. R. Ghali, et al. (2001). "Human beta defensin-1 and -2 expression in human pilosebaceous units: upregulation in acne vulgaris lesions." J Invest Dermatol **117**(5): 1120-5.
Chung, W. O. and B. A. Dale (2004). "Innate immune response of oral and foreskin keratinocytes: utilization of different signaling pathways by various bacterial species." Infect Immun **72**(1): 352-8.

Claeys, S., T. de Belder, et al. (2003). "Human beta-defensins and toll-like receptors in the upper airway." Allergy **58**(8): 748-53.
Cleary, P. P., J. Handley, et al. (1992). "Similarity between the group B and A streptococcal C5a peptidase genes." Infect Immun **60**(10): 4239-44.
Collin, M. and A. Olsen (2001). "EndoS, a novel secreted protein from Streptococcus pyogenes with endoglycosidase activity on human IgG." Embo J **20**(12): 3046-55.
Cook, D. N., D. S. Pisetsky, et al. (2004). "Toll-like receptors in the pathogenesis of human disease." Nat Immunol **5**(10): 975-9.
Cosseau, C., D. A. Devine, et al. (2008). "The commensal Streptococcus salivarius K12 downregulates the innate immune responses of human epithelial cells and promotes host-microbe homeostasis." Infect Immun **76**(9): 4163-75.
Courtney, H. S., Y. Li, et al. (1994). "Cloning, sequencing, and expression of a fibronectin/fibrinogen-binding protein from group A streptococci." Infect Immun **62**(9): 3937-46.
Cowland, J. B., A. H. Johnsen, et al. (1995). "hCAP-18, a cathelin/pro-bactenecin-like protein of human neutrophil specific granules." FEBS Lett **368**(1): 173-6.
Cue, D., H. Lam, et al. (2001). "Genetic dissection of the Streptococcus pyogenes M1 protein: regions involved in fibronectin binding and intracellular invasion." Microb Pathog **31**(5): 231-42.
Cunningham, M. W. (2000). "Pathogenesis of group A streptococcal infections." Clin Microbiol Rev **13**(3): 470-511.
Dale, B. A. and L. P. Fredericks (2005). "Antimicrobial peptides in the oral environment: expression and function in health and disease." Curr Issues Mol Biol **7**(2): 119-33.
Davidson, D. J., A. J. Currie, et al. (2004). "The cationic antimicrobial peptide LL-37 modulates dendritic cell differentiation and dendritic cell-induced T cell polarization." J Immunol **172**(2): 1146-56.
DeAngelis, P. L., J. Papaconstantinou, et al. (1993). "Isolation of a Streptococcus pyogenes gene locus that directs hyaluronan biosynthesis in acapsular mutants and in heterologous bacteria." J Biol Chem **268**(20): 14568-71.
Devine, D. A. and C. Cosseau (2008). "Host defense peptides in the oral cavity." Adv Appl Microbiol **63**: 281-322.
Devine, D. A. and R. E. W. Hancock, Eds. (2004). Mammalian Host Defense Peptides, Cambridge University Press.
Dhople, V., A. Krukemeyer, et al. (2006). "The human beta-defensin-3, an antibacterial peptide with multiple biological functions." Biochim Biophys Acta **1758**(9): 1499-512.
Di Nardo, A., K. Yamasaki, et al. (2008). "Mast cell cathelicidin antimicrobial peptide prevents invasive group A Streptococcus infection of the skin." J Immunol **180**(11): 7565-73.
Discolo, C. M., D. H. Darrow, et al. (2003). "Infectious indications for tonsillectomy." Pediatr Clin North Am **50**(2): 445-58.
Donald, C. D., C. Q. Sun, et al. (2003). "Cancer-specific loss of beta-defensin 1 in renal and prostatic carcinomas." Lab Invest **83**(4): 501-5.

Dorschner, R. A., V. K. Pestonjamasp, et al. (2001). "Cutaneous injury induces the release of cathelicidin anti-microbial peptides active against group A Streptococcus." J Invest Dermatol **117**(1): 91-7.
Durr, U. H., U. S. Sudheendra, et al. (2006). "LL-37, the only human member of the cathelicidin family of antimicrobial peptides." Biochim Biophys Acta **1758**(9): 1408-25.
Ebenfelt, A., L. E. Ericson, et al. (1998). "Acute pharyngotonsillitis is an infection restricted to the crypt and surface secretion." Acta Otolaryngol **118**(2): 264-71.
Ebenfelt, A. and C. Lundberg (1996). "Cellular defence in surface secretion in acute pharyngotonsillitis." Acta Otolaryngol **116**(1): 97-103.
Ellen, R. P. and R. J. Gibbons (1972). "M protein-associated adherence of Streptococcus pyogenes to epithelial surfaces: prerequisite for virulence." Infect Immun **5**(5): 826-30.
Elloumi, H. Z. and S. M. Holland (2008). "Complex regulation of human cathelicidin gene expression: novel splice variants and 5'UTR negative regulatory element." Mol Immunol **45**(1): 204-17.
England, R. J., D. R. Strachan, et al. (1997). "Streptococcal tonsillitis and its association with psoriasis: a review." Clin Otolaryngol Allied Sci **22**(6): 532-5.
Fahey, J. V. and C. R. Wira (2002). "Effect of menstrual status on antibacterial activity and secretory leukocyte protease inhibitor production by human uterine epithelial cells in culture." J Infect Dis **185**(11): 1606-13.
Fahlgren, A., S. Hammarstrom, et al. (2004). "beta-Defensin-3 and -4 in intestinal epithelial cells display increased mRNA expression in ulcerative colitis." Clin Exp Immunol **137**(2): 379-85.
Falla, T. J., D. N. Karunaratne, et al. (1996). "Mode of action of the antimicrobial peptide indolicidin." J Biol Chem **271**(32): 19298-303.
Fanning, A., Y. Volkov, et al. (2005). "CD44 cross-linking induces protein kinase C-regulated migration of human T lymphocytes." Int Immunol **17**(4): 449-58.
Fast, D. J., P. M. Schlievert, et al. (1989). "Toxic shock syndrome-associated staphylococcal and streptococcal pyrogenic toxins are potent inducers of tumor necrosis factor production." Infect Immun **57**(1): 291-4.
Feng, Z., B. Jiang, et al. (2005). "Human beta-defensins: differential activity against candidal species and regulation by Candida albicans." J Dent Res **84**(5): 445-50.
Fernie-King, B. A., D. J. Seilly, et al. (2004). "The interaction of streptococcal inhibitor of complement (SIC) and its proteolytic fragments with the human beta defensins." Immunology **111**(4): 444-52.
Fernie-King, B. A., D. J. Seilly, et al. (2006). "Inhibition of antimicrobial peptides by group A streptococci: SIC and DRS." Biochem Soc Trans **34**(Pt 2): 273-5.
Ferretti, J. J., W. M. McShan, et al. (2001). "Complete genome sequence of an M1 strain of Streptococcus pyogenes." Proc Natl Acad Sci U S A **98**(8): 4658-63.
Fischetti, V. A. (1989). "Streptococcal M protein: molecular design and biological behavior." Clin Microbiol Rev **2**(3): 285-314.
Fontaine, M. C., J. J. Lee, et al. (2003). "Combined contributions of streptolysin O and streptolysin S to virulence of serotype M5 Streptococcus pyogenes strain Manfredo." Infect Immun **71**(7): 3857-65.

Frick, I. M., P. Akesson, et al. (2003). "SIC, a secreted protein of Streptococcus pyogenes that inactivates antibacterial peptides." J Biol Chem **278**(19): 16561-6.
Frohm, M., B. Agerberth, et al. (1997). "The expression of the gene coding for the antibacterial peptide LL-37 is induced in human keratinocytes during inflammatory disorders." J Biol Chem **272**(24): 15258-63.
Froy, O. (2005). "Regulation of mammalian defensin expression by Toll-like receptor-dependent and independent signalling pathways." Cell Microbiol **7**(10): 1387-97.
Gabay, J. E., J. M. Heiple, et al. (1986). "Subcellular location and properties of bactericidal factors from human neutrophils." J Exp Med **164**(5): 1407-21.
Galioto, N. J. (2008). "Peritonsillar abscess." Am Fam Physician **77**(2): 199-202.
Ganz, T. (2007). "Molecular control of iron transport." J Am Soc Nephrol **18**(2): 394-400.
Garcia, J. R., F. Jaumann, et al. (2001). "Identification of a novel, multifunctional beta-defensin (human beta-defensin 3) with specific antimicrobial activity. Its interaction with plasma membranes of Xenopus oocytes and the induction of macrophage chemoattraction." Cell Tissue Res **306**(2): 257-64.
Gennaro, R. and M. Zanetti (2000). "Structural features and biological activities of the cathelicidin-derived antimicrobial peptides." Biopolymers **55**(1): 31-49.
Gentle, A., F. Anastasopoulos, et al. (2001). "High-resolution semi-quantitative real-time PCR without the use of a standard curve." Biotechniques **31**(3): 502, 504-6, 508.
Gerard, G. F. and D. P. Grandgenett (1975). "Purification and characterization of the DNA polymerase and RNase H activities in Moloney murine sarcoma-leukemia virus." J Virol **15**(4): 785-97.
Greco, R., L. De Martino, et al. (1995). "Invasion of cultured human cells by Streptococcus pyogenes." Res Microbiol **146**(7): 551-60.
Gudmundsson, G. H., K. P. Magnusson, et al. (1995). "Structure of the gene for porcine peptide antibiotic PR-39, a cathelin gene family member: comparative mapping of the locus for the human peptide antibiotic FALL-39." Proc Natl Acad Sci U S A **92**(15): 7085-9.
Gul, M., E. Okur, et al. (2007). "The comparison of tonsillar surface and core cultures in recurrent tonsillitis." Am J Otolaryngol **28**(3): 173-6.
Guzman, C. A., S. R. Talay, et al. (1999). "Protective immune response against Streptococcus pyogenes in mice after intranasal vaccination with the fibronectin-binding protein SfbI." J Infect Dis **179**(4): 901-6.
Habermann, E. (1972). "Bee and wasp venoms." Science **177**(46): 314-22.
Hackett, S. P. and D. L. Stevens (1992). "Streptococcal toxic shock syndrome: synthesis of tumor necrosis factor and interleukin-1 by monocytes stimulated with pyrogenic exotoxin A and streptolysin O." J Infect Dis **165**(5): 879-85.
Hancock, R. E. (1997). "Peptide antibiotics." Lancet **349**(9049): 418-22.
Hancock, R. E. and D. S. Chapple (1999). "Peptide antibiotics." Antimicrob Agents Chemother **43**(6): 1317-23.
Hancock, R. E. and M. G. Scott (2000). "The role of antimicrobial peptides in animal defenses." Proc Natl Acad Sci U S A **97**(16): 8856-61.
Hansen, M. C., R. J. Palmer, Jr., et al. (2001). "Assessment of GFP fluorescence in cells of Streptococcus gordonii under conditions of low pH and low oxygen concentration." Microbiology **147**(Pt 5): 1383-91.

Harder, J., J. Bartels, et al. (1997). "A peptide antibiotic from human skin." Nature **387**(6636): 861.
Harder, J., J. Bartels, et al. (2001). "Isolation and characterization of human beta - defensin-3, a novel human inducible peptide antibiotic." J Biol Chem **276**(8): 5707-13.
Harder, J., U. Meyer-Hoffert, et al. (2004). "Differential gene induction of human beta-defensins (hBD-1, -2, -3, and -4) in keratinocytes is inhibited by retinoic acid." J Invest Dermatol **123**(3): 522-9.
Hauser, A. and P. M. Schlievert (1990). "Nucleotide sequence of the Streptococcal pyrogenic Exotoxin type B gene and relationship between the toxin and the Streptococcal proteinase precursor." J. Bacteriol **172**(8): 4536-42.
Hedman, K., A. Vaheri, et al. (1978). "External fibronectin of cultured human fibroblasts is predominantly a matrix protein." J Cell Biol **76**(3): 748-60.
Heilborn, J. D., M. F. Nilsson, et al. (2005). "Antimicrobial protein hCAP18/LL-37 is highly expressed in breast cancer and is a putative growth factor for epithelial cells." Int J Cancer **114**(5): 713-9.
Henzler-Wildman, K. A., G. V. Martinez, et al. (2004). "Perturbation of the hydrophobic core of lipid bilayers by the human antimicrobial peptide LL-37." Biochemistry **43**(26): 8459-69.
Hill, A. (2001). "The genomics of human infectious disease suseptibility." Annu Rev Genomics Hum Genet **2**: 373-400.
Hoe, N. P., R. M. Ireland, et al. (2002). "Insight into the molecular basis of pathogen abundance: group A Streptococcus inhibitor of complement inhibits bacterial adherence and internalization into human cells." Proc Natl Acad Sci U S A **99**(11): 7646-51.
Hoffmann, S. (1985). "The throat carrier rate of group A and other beta hemolytic streptococci among patients in general practice." Acta Pathol Microbiol Immunol Scand [B] **93**(5): 347-51.
Hollox, E. J., J. A. Armour, et al. (2003). "Extensive normal copy number variation of a beta-defensin antimicrobial-gene cluster." Am J Hum Genet **73**(3): 591-600.
Horstmann, R. D., H. J. Sievertsen, et al. (1988). "Antiphagocytic activity of streptococcal M protein: selective binding of complement control protein factor H." Proc Natl Acad Sci U S A **85**(5): 1657-61.
Howie, A. J. (1980). "Scanning and transmission electron microscopy on the epithelium of human palatine tonsils." J Pathol **130**(2): 91-8.
Huang, H. W., F. Y. Chen, et al. (2004). "Molecular mechanism of Peptide-induced pores in membranes." Phys Rev Lett **92**(19): 198304.
Huggett, J., K. Dheda, et al. (2005). "Real-time RT-PCR normalisation; strategies and considerations." Genes Immun **6**(4): 279-84.
Hunter, H. N., D. B. Fulton, et al. (2002). "The solution structure of human hepcidin, a peptide hormone with antimicrobial activity that is involved in iron uptake and hereditary hemochromatosis." J Biol Chem **277**(40): 37597-603.
Huttner, K. M. and C. L. Bevins (1999). "Antimicrobial peptides as mediators of epithelial host defense." Pediatr Res **45**(6): 785-94.
Izadpanah, A. and R. L. Gallo (2005). "Antimicrobial peptides." J Am Acad Dermatol **52**(3 Pt 1): 381-90; quiz 391-2.

Jelinek, R. and S. Kolusheva (2005). "Membrane interactions of host-defense peptides studied in model systems." Curr Protein Pept Sci **6**(1): 103-14.
Ji, S., Y. Kim, et al. (2007). "Innate immune responses of gingival epithelial cells to nonperiodontopathic and periodontopathic bacteria." J Periodontal Res **42**(6): 503-10.
Jia, H. P., B. C. Schutte, et al. (2001). "Discovery of new human beta-defensins using a genomics-based approach." Gene **263**(1-2): 211-8.
Jin, T., M. Bokarewa, et al. (2004). "Staphylococcus aureus resists human defensins by production of staphylokinase, a novel bacterial evasion mechanism." J Immunol **172**(2): 1169-76.
Johansson, L., P. Thulin, et al. (2008). "Cathelicidin LL-37 in severe Streptococcus pyogenes soft tissue infections in humans." Infect Immun **76**(8): 3399-404.
Joly, S., C. C. Organ, et al. (2005). "Correlation between beta-defensin expression and induction profiles in gingival keratinocytes." Mol Immunol **42**(9): 1073-84.
Kanda, N. and S. Watanabe (2008). "IL-12, IL-23, and IL-27 enhance human beta-defensin-2 production in human keratinocytes." Eur J Immunol **38**(5): 1287-96.
Kapur, V., S. Topouzis, et al. (1993). "A conserved Streptococcus pyogenes extracellular cysteine protease cleaves human fibronectin and degrades vitronectin." Microb Pathog **15**(5): 327-46.
Kielmovitch, I. H., G. Keleti, et al. (1989). "Microbiology of obstructive tonsillar hypertrophy and recurrent tonsillitis." Arch Otolaryngol Head Neck Surg **115**(6): 721-4.
Kim, J. E., B. J. Kim, et al. (2005). "Expression and modulation of LL-37 in normal human keratinocytes, HaCaT cells, and inflammatory skin diseases." J Korean Med Sci **20**(4): 649-54.
Kimball, J. R., W. Nittayananta, et al. (2006). "Antimicrobial barrier of an in vitro oral epithelial model." Arch Oral Biol **51**(9): 775-83.
King, A. E., D. C. Fleming, et al. (2002). "Regulation of natural antibiotic expression by inflammatory mediators and mimics of infection in human endometrial epithelial cells." Mol Hum Reprod **8**(4): 341-9.
Kisich, K. O., M. D. Howell, et al. (2007). "The constitutive capacity of human keratinocytes to kill Staphylococcus aureus is dependent on beta-defensin 3." J Invest Dermatol **127**(10): 2368-80.
Koczulla, A. R. and R. Bals (2003). "Antimicrobial peptides: current status and therapeutic potential." Drugs **63**(4): 389-406.
Kollisch, G., B. N. Kalali, et al. (2005). "Various members of the Toll-like receptor family contribute to the innate immune response of human epidermal keratinocytes." Immunology **114**(4): 531-41.
Koo, S. P., M. R. Yeaman, et al. (1997). "The cytoplasmic membrane is a primary target for the staphylocidal action of thrombin-induced platelet microbicidal protein." Infect Immun **65**(11): 4795-800.
Krause, A., S. Neitz, et al. (2000). "LEAP-1, a novel highly disulfide-bonded human peptide, exhibits antimicrobial activity." FEBS Lett **480**(2-3): 147-50.
Krause, A., R. Sillard, et al. (2003). "Isolation and biochemical characterization of LEAP-2, a novel blood peptide expressed in the liver." Protein Sci **12**(1): 143-52.

Krisanaprakornkit, S., A. Weinberg, et al. (1998). "Expression of the peptide antibiotic human beta-defensin 1 in cultured gingival epithelial cells and gingival tissue." Infect Immun **66**(9): 4222-8.
Kusser, W. (2006). "Use of self-quenched, fluorogenic LUX primers for gene expression profiling." Methods Mol Biol **335**: 115-33.
Lande, R., J. Gregorio, et al. (2007). "Plasmacytoid dendritic cells sense self-DNA coupled with antimicrobial peptide." Nature **449**(7162): 564-9.
Larionov, A., A. Krause, et al. (2005). "A standard curve based method for relative real time PCR data processing." BMC Bioinformatics **6**: 62.
Larrick, J. W., M. Hirata, et al. (1995). "Human CAP18: a novel antimicrobial lipopolysaccharide-binding protein." Infect Immun **63**(4): 1291-7.
Lauer, P., C. D. Rinaudo, et al. (2005). "Genome analysis reveals pili in Group B Streptococcus." Science **309**(5731): 105.
Lee, P. H., T. Ohtake, et al. (2005). "Expression of an additional cathelicidin antimicrobial peptide protects against bacterial skin infection." Proc Natl Acad Sci U S A **102**(10): 3750-5.
Lehrer, R. I. and T. Ganz (2002). "Defensins of vertebrate animals." Curr Opin Immunol **14**(1): 96-102.
Lesmeister, M. J., M. R. Bothwell, et al. (2006). "Toll-like receptor expression in the human nasopharyngeal tonsil (adenoid) and palantine tonsils: a preliminary report." Int J Pediatr Otorhinolaryngol **70**(6): 987-92.
Li, L. (2004). "Regulation of innate immunity signaling and its connection with human diseases." Curr Drug Targets Inflamm Allergy **3**(1): 81-6.
Lilja, M., J. Silvola, et al. (1999). "SIgA- and IgG-coated Streptococcus pyogenes on the tonsillar surfaces during acute tonsillitis." Acta Otolaryngol **119**(6): 718-23.
Little, P. and I. Williamson (1996). "Sore throat management in general practice." Fam Pract **13**(3): 317-21.
Liu, P. T., S. Stenger, et al. (2006). "Toll-like receptor triggering of a vitamin D-mediated human antimicrobial response." Science **311**(5768): 1770-3.
Liu, W. and D. A. Saint (2002). "A new quantitative method of real time reverse transcription polymerase chain reaction assay based on simulation of polymerase chain reaction kinetics." Anal Biochem **302**(1): 52-9.
Livak, K. J. and T. D. Schmittgen (2001). "Analysis of relative gene expression data using real-time quantitative PCR and the 2(-Delta Delta C(T)) Method." Methods **25**(4): 402-8.
Llewelyn, M. and J. Cohen (2002). "Superantigens: microbial agents that corrupt immunity." Lancet Infect Dis **2**(3): 156-62.
Lu, X., Z. Kurago, et al. (2006). "Effects of polymicrobial communities on host immunity and response." FEMS Microbiol Lett **265**(2): 141-50.
Lukomski, S., N. P. Hoe, et al. (2000). "Nonpolar inactivation of the hypervariable streptococcal inhibitor of complement gene (sic) in serotype M1 Streptococcus pyogenes significantly decreases mouse mucosal colonization." Infect Immun **68**(2): 535-42.
Lynn, D. J., A. T. Lloyd, et al. (2003). "In silico identification of components of the Toll-like receptor (TLR) signaling pathway in clustered chicken expressed sequence tags (ESTs)." Vet Immunol Immunopathol **93**(3-4): 177-84.

MacRedmond, R., C. Greene, et al. (2005). "Respiratory epithelial cells require Toll-like receptor 4 for induction of human beta-defensin 2 by lipopolysaccharide." Respir Res **6**: 116.
Maier, V. H., K. V. Dorn, et al. (2008). "Characterisation of cathelicidin gene family members in divergent fish species." Mol Immunol **45**(14): 3723-30.
Malik, A. N. and G. Al-Kafaji (2007). "Glucose regulation of beta-defensin-1 mRNA in human renal cells." Biochem Biophys Res Commun **353**(2): 318-23.
Martineau, A. R., R. J. Wilkinson, et al. (2007). "A single dose of vitamin D enhances immunity to mycobacteria." Am J Respir Crit Care Med **176**(2): 208-13.
Mathews, M., H. P. Jia, et al. (1999). "Production of beta-defensin antimicrobial peptides by the oral mucosa and salivary glands." Infect Immun **67**(6): 2740-5.
Matsuzaki, K. (1999). "Why and how are peptide-lipid interactions utilized for self-defense? Magainins and tachyplesins as archetypes." Biochim Biophys Acta **1462**(1-2): 1-10.
Mendez-Samperio, P., L. Alba, et al. (2007). "Mycobacterium bovis-mediated induction of human beta-defensin-2 in epithelial cells is controlled by intracellular calcium and p38MAPK." J Infect **54**(5): 469-74.
Menendez, A. and B. Finlay (2007). "Defensins in the immunology of bacterial infections." Curr Opin Immunol **19**(4): 385-91.
Mora, M., G. Bensi, et al. (2005). "Group A Streptococcus produce pilus-like structures containing protective antigens and Lancefield T antigens." Proc Natl Acad Sci U S A **102**(43): 15641-6.
Motulsky, H. (2003). GraphPad Prism Statistics Guide. Version 4, GraphPad Prism Statistics Guide.
Muller, P. Y., H. Janovjak, et al. (2002). "Processing of gene expression data generated by quantitative real-time RT-PCR." Biotechniques **32**(6): 1372-4, 1376, 1378-9.
Murakami, M., T. Ohtake, et al. (2002). "Cathelicidin anti-microbial peptide expression in sweat, an innate defense system for the skin." J Invest Dermatol **119**(5): 1090-5.
Navarre, W. W. and O. Schneewind (1999). "Surface proteins of gram-positive bacteria and mechanisms of their targeting to the cell wall envelope." Microbiol Mol Biol Rev **63**(1): 174-229.
Nave, H., A. Gebert, et al. (2001). "Morphology and immunology of the human palatine tonsil." Anatomy & Embryology **204**(5): 367-73.
Nealon, T. J., E. H. Beachey, et al. (1986). "Release of fibronectin-lipoteichoic acid complexes from group A streptococci with penicillin." Infect Immun **51**(2): 529-35.
Nell, M. J., G. S. Tjabringa, et al. (2004). "Bacterial products increase expression of the human cathelicidin hCAP-18/LL-37 in cultured human sinus epithelial cells." FEMS Immunol Med Microbiol **42**(2): 225-31.
Nicolas, G., M. Bennoun, et al. (2001). "Lack of hepcidin gene expression and severe tissue iron overload in upstream stimulatory factor 2 (USF2) knockout mice." Proc Natl Acad Sci U S A **98**(15): 8780-5.
Niyonsaba, F., K. Iwabuchi, et al. (2002). "A cathelicidin family of human antibacterial peptide LL-37 induces mast cell chemotaxis." Immunology **106**(1): 20-6.
Niyonsaba, F., A. Someya, et al. (2001). "Evaluation of the effects of peptide antibiotics human beta-defensins-1/-2 and LL-37 on histamine release and prostaglandin D(2) production from mast cells." Eur J Immunol **31**(4): 1066-75.

Niyonsaba, F., H. Ushio, et al. (2005). "The human beta-defensins (-1, -2, -3, -4) and cathelicidin LL-37 induce IL-18 secretion through p38 and ERK MAPK activation in primary human keratinocytes." J Immunol **175**(3): 1776-84.

Niyonsaba, F., H. Ushio, et al. (2007). "Antimicrobial peptides human beta-defensins stimulate epidermal keratinocyte migration, proliferation and production of proinflammatory cytokines and chemokines." J Invest Dermatol **127**(3): 594-604.

Nizet, V., T. Ohtake, et al. (2001). "Innate antimicrobial peptide protects the skin from invasive bacterial infection." Nature **414**(6862): 454-7.

Nokso-Koivisto, J., T. Hovi, et al. (2006). "Viral upper respiratory tract infections in young children with emphasis on acute otitis media." Int J Pediatr Otorhinolaryngol **70**(8): 1333-42.

Norrby-Teglund, A., M. Norgren, et al. (1994). "Similar cytokine induction profiles of a novel streptococcal exotoxin, MF, and pyrogenic exotoxins A and B." Infect Immun **62**(9): 3731-8.

Nyberg, P., M. Rasmussen, et al. (2004). "alpha2-Macroglobulin-proteinase complexes protect Streptococcus pyogenes from killing by the antimicrobial peptide LL-37." J Biol Chem **279**(51): 52820-3.

Ofek, I., W. A. Simpson, et al. (1982). "Formation of molecular complexes between a structurally defined M protein and acylated or deacylated lipoteichoic acid of Streptococcus pyogenes." J Bacteriol **149**(2): 426-33.

Ofek, I., E. Whitnack, et al. (1983). "Hydrophobic interactions of group A streptococci with hexadecane droplets." J Bacteriol **154**(1): 139-45.

Ogushi, K., A. Wada, et al. (2001). "Salmonella enteritidis FliC (flagella filament protein) induces human beta-defensin-2 mRNA production by Caco-2 cells." J Biol Chem **276**(32): 30521-6.

Okumura, K., A. Itoh, et al. (2004). "C-terminal domain of human CAP18 antimicrobial peptide induces apoptosis in oral squamous cell carcinoma SAS-H1 cells." Cancer Lett **212**(2): 185-94.

Oppenheim, F. G., T. Xu, et al. (1988). "Histatins, a novel family of histidine-rich proteins in human parotid secretion. Isolation, characterization, primary structure, and fungistatic effects on Candida albicans." J Biol Chem **263**(16): 7472-7.

Oren, Z., J. C. Lerman, et al. (1999). "Structure and organization of the human antimicrobial peptide LL-37 in phospholipid membranes: relevance to the molecular basis for its non-cell-selective activity." Biochem J **341 (Pt 3)**: 501-13.

Oren, Z. and Y. Shai (1998). "Mode of action of linear amphipathic alpha-helical antimicrobial peptides." Biopolymers **47**(6): 451-63.

Osterlund, A. and L. Engstrand (1997). "An intracellular sanctuary for Streptococcus pyogenes in human tonsillar epithelium--studies of asymptomatic carriers and in vitro cultured biopsies." Acta Otolaryngol **117**(6): 883-8.

Otvos, L., Jr. (2000). "Antibacterial peptides isolated from insects." J Pept Sci **6**(10): 497-511.

Palmer, M. (2001). "The family of thiol-activated, cholesterol-binding cytolysins." Toxicon **39**(11): 1681-9.

Palmer, M., I. Vulicevic, et al. (1998). "Streptolysin O: a proposed model of allosteric interaction between a pore-forming protein and its target lipid bilayer." Biochemistry **37**(8): 2378-83.

Park, C. H., E. V. Valore, et al. (2001). "Hepcidin, a urinary antimicrobial peptide synthesized in the liver." J Biol Chem **276**(11): 7806-10.
Pazgier, M., D. M. Hoover, et al. (2006). "Human beta-defensins." Cell Mol Life Sci **63**(11): 1294-313.
Peirson, S. N., J. N. Butler, et al. (2003). "Experimental validation of novel and conventional approaches to quantitative real-time PCR data analysis." Nucleic Acids Res **31**(14): e73.
Perry, M. and A. Whyte (1998). "Immunology of the tonsils." Immunol Today **19**(9): 414-21.
Perry, M. E. (1994). "The specialised structure of crypt epithelium in the human palatine tonsil and its functional significance." J Anat **185 (Pt 1)**: 111-27.
Peschel, A. (2002). "How do bacteria resist human antimicrobial peptides?" Trends Microbiol **10**(4): 179-86.
Peyssonnaux, C., A. S. Zinkernagel, et al. (2006). "TLR4-dependent hepcidin expression by myeloid cells in response to bacterial pathogens." Blood **107**(9): 3727-32.
Pfaffl, M. W. (2001). "A new mathematical model for relative quantification in real-time RT-PCR." Nucleic Acids Res **29**(9): e45.
Pioli, P. A., L. K. Weaver, et al. (2006). "Lipopolysaccharide-induced IL-1 beta production by human uterine macrophages up-regulates uterine epithelial cell expression of human beta-defensin 2." J Immunol **176**(11): 6647-55.
Pivarcsi, A., A. Koreck, et al. (2004). "Differentiation-regulated expression of Toll-like receptors 2 and 4 in HaCaT keratinocytes." Arch Dermatol Res **296**(3): 120-4.
Pivarcsi, A., I. Nagy, et al. (2005). "Microbial compounds induce the expression of pro-inflammatory cytokines, chemokines and human beta-defensin-2 in vaginal epithelial cells." Microbes Infect **7**(9-10): 1117-27.
Porter, E. M., E. van Dam, et al. (1997). "Broad-spectrum antimicrobial activity of human intestinal defensin 5." Infect Immun **65**(6): 2396-401.
Proft, T. and J. D. Fraser (2007). "Streptococcal superantigens." Chem Immunol Allergy **93**: 1-23.
Proud, D., S. P. Sanders, et al. (2004). "Human rhinovirus infection induces airway epithelial cell production of human beta-defensin 2 both in vitro and in vivo." J Immunol **172**(7): 4637-45.
Putsep, K., G. Carlsson, et al. (2002). "Deficiency of antibacterial peptides in patients with morbus Kostmann: an observation study." Lancet **360**(9340): 1144-9.
Putto, A. (1987). "Febrile exudative tonsillitis: viral or streptococcal?" Pediatrics **80**(1): 6-12.
Rapaport, D. and Y. Shai (1992). "Aggregation and organization of pardaxin in phospholipid membranes. A fluorescence energy transfer study." J Biol Chem **267**(10): 6502-9.
Rivas-Santiago, B., R. Hernandez-Pando, et al. (2008). "Expression of cathelicidin LL-37 during Mycobacterium tuberculosis infection in human alveolar macrophages, monocytes, neutrophils, and epithelial cells." Infect Immun **76**(3): 935-41.
Rivera, S., E. Nemeth, et al. (2005). "Synthetic hepcidin causes rapid dose-dependent hypoferremia and is concentrated in ferroportin-containing organs." Blood **106**(6): 2196-2199.

Roetto, A., G. Papanikolaou, et al. (2003). "Mutant antimicrobial peptide hepcidin is associated with severe juvenile hemochromatosis." Nat Genet **33**(1): 21-2.
Rosenfeld, R. M. and R. P. Green (1990). "Tonsillectomy and adenoidectomy: changing trends." Ann Otol Rhinol Laryngol **99**(3 Pt 1): 187-91.
Russell, H. H. and S. Sriskandan (2008). "Superantigens SPEA and SMEZ do not affect secretome expression in Streptococcus pyogenes." Microb Pathog **44**(6): 537-43.
Ryan, P. A., V. Pancholi, et al. (2001). "Group A streptococci bind to mucin and human pharyngeal cells through sialic acid-containing receptors." Infect Immun **69**(12): 7402-12.
Sang, Y., B. Ramanathan, et al. (2006). "Porcine liver-expressed antimicrobial peptides, hepcidin and LEAP-2: cloning and induction by bacterial infection." Dev Comp Immunol **30**(4): 357-66.
Sawaki, K., N. Mizukawa, et al. (2002). "High concentration of beta-defensin-2 in oral squamous cell carcinoma." Anticancer Res **22**(4): 2103-7.
Schaller-Bals, S., A. Schulze, et al. (2002). "Increased levels of antimicrobial peptides in tracheal aspirates of newborn infants during infection." Am J Respir Crit Care Med **165**(7): 992-5.
Schauber, J., R. A. Dorschner, et al. (2006). "Control of the innate epithelial antimicrobial response is cell-type specific and dependent on relevant microenvironmental stimuli." Immunology **118**(4): 509-19.
Schmidt, K. H. and T. Wadstrom (1990). "A secreted receptor related to M1 protein of Streptococcus pyogenes binds to fibrinogen, IgG, and albumin." Zentralbl Bakteriol **273**(2): 216-28.
Schmidtchen, A., I. M. Frick, et al. (2002). "Proteinases of common pathogenic bacteria degrade and inactivate the antibacterial peptide LL-37." Mol Microbiol **46**(1): 157-68.
Schneider, J. J., A. Unholzer, et al. (2005). "Human defensins." J Mol Med **83**(8): 587-95.
Schroder, J. M. (1999). "Epithelial peptide antibiotics." Biochem Pharmacol **57**(2): 121-34.
Schroder, J. M. and J. Harder (2006). "Antimicrobial skin peptides and proteins." Cell Mol Life Sci **63**(4): 469-86.
Scott, M. G., D. J. Davidson, et al. (2002). "The human antimicrobial peptide LL-37 is a multifunctional modulator of innate immune responses." J Immunol **169**(7): 3883-91.
Semple, C. A., M. Rolfe, et al. (2003). "Duplication and selection in the evolution of primate beta-defensin genes." Genome Biol **4**(5): R31.
Sherman, H., N. Chapnik, et al. (2006). "Albumin and amino acids upregulate the expression of human beta-defensin 1." Mol Immunol **43**(10): 1617-23.
Sherman, H. and O. Froy (2008). "Expression of human beta-defensin 1 is regulated via c-Myc and the biological clock." Mol Immunol **45**(11): 3163-7.
Shiba, H., Y. Mouri, et al. (2003). "Macrophage inflammatory protein-3alpha and beta-defensin-2 stimulate dentin sialophosphoprotein gene expression in human pulp cells." Biochem Biophys Res Commun **306**(4): 867-71.

Shinzato, T., K. Abe, et al. (2008). "Serum pro-hepcidin level and iron homeostasis in japanese dialysis patients with erythropoietin (EPO)-resistant anemia." Med Sci Monit **14**(9): CR431-7.
SIGN (1999). SIGN Publication: Management of Sore Throat and Indications for Tonsillectomy. Scottish Intercollegiate Guidelines Network.
Smith, W. D. (2004). A Functional Genomic Analysis of Group A Streptococcal Virulence Factors. ICAMB. Newcastle upon Tyne, Newcastle University. **PhD**.
Smoot, J. C., K. D. Barbian, et al. (2002). "Genome sequence and comparative microarray analysis of serotype M18 group A Streptococcus strains associated with acute rheumatic fever outbreaks." Proc Natl Acad Sci U S A **99**(7): 4668-73.
Song, J. J., K. S. Hwang, et al. (2006). "Expression of cathelicidin in recurrent throat infection." Int J Pediatr Otorhinolaryngol **70**(3): 487-92.
Song, W. (2008). "In vitro bactericidal activity of recombinant human beta-defensin-3 against pathogenic bacterial strains in human tooth root canal." Int J Antimicrob Agents **In press**.
Sorensen, O., K. Arnljots, et al. (1997). "The human antibacterial cathelicidin, hCAP-18, is synthesized in myelocytes and metamyelocytes and localized to specific granules in neutrophils." Blood **90**(7): 2796-803.
Sorensen, O., J. B. Cowland, et al. (1997). "An ELISA for hCAP-18, the cathelicidin present in human neutrophils and plasma." J Immunol Methods **206**(1-2): 53-9.
Sorensen, O. E., P. Follin, et al. (2001). "Human cathelicidin, hCAP-18, is processed to the antimicrobial peptide LL-37 by extracellular cleavage with proteinase 3." Blood **97**(12): 3951-9.
Steinstraesser, L., A. Ring, et al. (2006). "The human host defense peptide LL37/hCAP accelerates angiogenesis in PEGT/PBT biopolymers." Ann Plast Surg **56**(1): 93-8.
Stenfors, L. E., H. M. Bye, et al. (2003). "Noticeable differences in bacterial defence on tonsillar surfaces between bacteria-induced and virus-induced acute tonsillitis." Int J Pediatr Otorhinolaryngol **67**(10): 1075-82.
Sun, C. Q., R. Arnold, et al. (2006). "Human beta-defensin-1, a potential chromosome 8p tumor suppressor: control of transcription and induction of apoptosis in renal cell carcinoma." Cancer Res **66**(17): 8542-9.
Suvorov, A. N. and J. J. Ferretti (1996). "Physical and genetic chromosomal map of an M type 1 strain of Streptococcus pyogenes." J Bacteriol **178**(18): 5546-9.
Tao, R., R. J. Jurevic, et al. (2005). "Salivary antimicrobial peptide expression and dental caries experience in children." Antimicrob Agents Chemother **49**(9): 3883-8.
Taviloglu, K., N. Cabioglu, et al. (2005). "Idiopathic necrotizing fasciitis: risk factors and strategies for management." Am Surg **71**(4): 315-20.
Theodore, T. S. and G. B. Calandra (1981). "Streptolysin S activation by lipoteichoic acid." Infect Immun **33**(1): 326-8.
Tjabringa, G. S., J. Aarbiou, et al. (2003). "The antimicrobial peptide LL-37 activates innate immunity at the airway epithelial surface by transactivation of the epidermal growth factor receptor." J Immunol **171**(12): 6690-6.
Ton-That, H. and O. Schneewind (2003). "Assembly of pili on the surface of Corynebacterium diphtheriae." Mol Microbiol **50**(4): 1429-38.

Toppel, A. W., M. Rasmussen, et al. (2003). "Contribution of protein G-related alpha2-macroglobulin-binding protein to bacterial virulence in a mouse skin model of group A streptococcal infection." J Infect Dis **187**(11): 1694-703.
Townes, C. L., G. Michailidis, et al. (2004). "Induction of cationic chicken liver-expressed antimicrobial peptide 2 in response to Salmonella enterica infection." Infect Immun **72**(12): 6987-93.
Tschernig, T. and R. Pabst (2000). "Bronchus-associated lymphoid tissue (BALT) is not present in the normal adult lung but in different diseases." Pathobiology **68**(1): 1-8.
Tyrrell, G. J., M. Lovgren, et al. (2002). "M types of group a streptococcal isolates submitted to the National Centre for Streptococcus (Canada) from 1993 to 1999." J Clin Microbiol **40**(12): 4466-71.
Uehara, A. and H. Takada (2008). "Synergism between TLRs and NOD1/2 in oral epithelial cells." J Dent Res **87**(7): 682-6.
Van Den Akker, E. H., A. W. Hoes, et al. (2004). "Large international differences in (adeno)tonsillectomy rates." Clin Otolaryngol Allied Sci **29**(2): 161-4.
van Dijk, A., E. J. Veldhuizen, et al. (2008). "Avian defensins." Vet Immunol Immunopathol **124**(1-2): 1-18.
Varoga, D., T. Pufe, et al. (2005). "Human beta-defensin 3 mediates tissue remodeling processes in articular cartilage by increasing levels of metalloproteinases and reducing levels of their endogenous inhibitors." Arthritis Rheum **52**(6): 1736-45.
Verga Falzacappa, M. V. and M. U. Muckenthaler (2005). "Hepcidin: iron-hormone and anti-microbial peptide." Gene **364**: 37-44.
Viatte, L., J. C. Lesbordes-Brion, et al. (2005). "Deregulation of proteins involved in iron metabolism in hepcidin-deficient mice." Blood **105**(12): 4861-4.
von Gaudecker, B. and H. K. Muller-Hermelink (1982). "The development of the human tonsilla palatina." Cell Tissue Res **224**(3): 579-600.
von Pawel-Rammingen, U., B. P. Johansson, et al. (2002). "IdeS, a novel streptococcal cysteine proteinase with unique specificity for immunoglobulin G." Embo J **21**(7): 1607-15.
Voss, E., J. Wehkamp, et al. (2006). "NOD2/CARD15 mediates induction of the antimicrobial peptide human beta-defensin-2." J Biol Chem **281**(4): 2005-11.
Vyoral, D. and J. Petrak (2005). "Hepcidin: a direct link between iron metabolism and immunity." Int J Biochem Cell Biol **37**(9): 1768-73.
Wang, B., S. Li, et al. (2006). "Streptococcal modulation of cellular invasion via TGF-beta1 signaling." Proc Natl Acad Sci U S A **103**(7): 2380-5.
Wang, C., Z. Dong, et al. (2004). "[Expression of human beta-defensin in palatine tonsil]." Lin Chuang Er Bi Yan Hou Ke Za Zhi **18**(3): 129-31.
Wang, T. T., F. P. Nestel, et al. (2004). "Cutting edge: 1,25-dihydroxyvitamin D3 is a direct inducer of antimicrobial peptide gene expression." J Immunol **173**(5): 2909-12.
Wannamaker, L. W. (1958). "The differentiation of three distinct desoxyribonucleases of group A Streptococci." J Exp Med **107**(6): 797-812.
Warnke, P. H., I. N. Springer, et al. (2006). "Innate immunity in human bone." Bone **38**(3): 400-8.

Weber, G., J. D. Heilborn, et al. (2005). "Vitamin D induces the antimicrobial protein hCAP18 in human skin." J Invest Dermatol **124**(5): 1080-2.
Wehkamp, J., J. Schauber, et al. (2007). "Defensins and cathelicidins in gastrointestinal infections." Curr Opin Gastroenterol **23**(1): 32-8.
Weise, J. B., J. E. Meyer, et al. (2002). "A newly discovered function of palatine tonsils in immune defence: the expression of defensins." Otolaryngol Pol **56**(4): 409-13.
Wong, J. H., L. Xia, et al. (2007). "A review of defensins of diverse origins." Curr Protein Pept Sci **8**(5): 446-59.
Wu, H. and P. M. Fives-Taylor (2001). "Molecular strategies for fimbrial expression and assembly." Crit Rev Oral Biol Med **12**(2): 101-15.
Xiao, Y., Y. Cai, et al. (2006). "Identification and functional characterization of three chicken cathelicidins with potent antimicrobial activity." J Biol Chem **281**(5): 2858-67.
Yamaji, S., P. Sharp, et al. (2004). "Inhibition of iron transport across human intestinal epithelial cells by hepcidin." Blood **104**(7): 2178-80.
Yamasaki, K., A. Di Nardo, et al. (2007). "Increased serine protease activity and cathelicidin promotes skin inflammation in rosacea." Nat Med **13**(8): 975-80.
Yang, D., O. Chertov, et al. (1999). "Beta-defensins: linking innate and adaptive immunity through dendritic and T cell CCR6." Science **286**(5439): 525-8.
Yang, D., O. Chertov, et al. (2001). "Participation of mammalian defensins and cathelicidins in anti-microbial immunity: receptors and activities of human defensins and cathelicidin (LL-37)." J Leukoc Biol **69**(5): 691-7.
Yeaman, G. R., P. M. Guyre, et al. (1997). "Unique CD8+ T cell-rich lymphoid aggregates in human uterine endometrium." J Leukoc Biol **61**(4): 427-35.
Yeaman, M. R., A. S. Bayer, et al. (1998). "Platelet microbicidal proteins and neutrophil defensin disrupt the Staphylococcus aureus cytoplasmic membrane by distinct mechanisms of action." J Clin Invest **101**(1): 178-87.
Zanetti, M., G. Del Sal, et al. (1993). "The cDNA of the neutrophil antibiotic Bac5 predicts a pro-sequence homologous to a cysteine proteinase inhibitor that is common to other neutrophil antibiotics." J Biol Chem **268**(1): 522-6.
Zanetti, M., R. Gennaro, et al. (1995). "Cathelicidins: a novel protein family with a common proregion and a variable C-terminal antimicrobial domain." FEBS Lett **374**(1): 1-5.
Zasloff, M. (2002). "Antimicrobial peptides of multicellular organisms." Nature **415**(6870): 389-95.
Zasloff, M. (2006). "Defending the epithelium." Nat Med **12**(6): 607-8.
Zasloff, M. (2007). "Antimicrobial peptides, innate immunity, and the normally sterile urinary tract." J Am Soc Nephrol **18**(11): 2810-6.
Zeya, H. I. and J. K. Spitznagel (1966 (a)). "Cationic proteins of polymorphonuclear leukocyte lysosomes. I. Resolution of antibacterial and enzymatic activities." J Bacteriol **91**(2): 750-4.
Zeya, H. I. and J. K. Spitznagel (1966 (b)). "Cationic proteins of polymorphonuclear leukocyte lysosomes. II. Composition, properties, and mechanism of antibacterial action." J Bacteriol **91**(2): 755-62.

Zhang, L., P. Dhillon, et al. (2000). "Interactions of bacterial cationic peptide antibiotics with outer and cytoplasmic membranes of Pseudomonas aeruginosa." Antimicrob Agents Chemother **44**(12): 3317-21.

Zhang, P. C., Y. T. Pang, et al. (2003). "Comparison of histology between recurrent tonsillitis and tonsillar hypertrophy." Clin Otolaryngol Allied Sci **28**(3): 235-9.

Zhao, C., I. Wang, et al. (1996). "Widespread expression of beta-defensin hBD-1 in human secretory glands and epithelial cells." FEBS Lett **396**(2-3): 319-22.

The Newcastle upon Tyne Hospitals NHS
NHS Trust

UNIVERSITY OF NEWCASTLE

University of Newcastle
The Medical School
Newcastle upon Tyne NE2 4HH

The Freeman Hospital
High Heaton
Newcastle upon Tyne
NE7 7DN

Tel: 0191 233 6161
Fax: 0191 213 1968

Study title

Molecular determinants of streptococcal regulation of antimicrobial peptide expression in human tonsils

The study is concerned with bacterial infection of the tonsils and its prevention by the immune system.

Dear participant

You are being invited to take part in a research study. Before you decide to take part, it is important that you understand why the research is being done, and what it will involve. Please take time to read the following information carefully and discuss it with others if you wish. Ask me if there is anything that is not clear or if you would like more information. Take time to decide whether or not you wish to take part.

Thank you for reading this.

What is the purpose of this study?
We are researching how Streptococcus (the main bacterial cause of tonsillitis) attaches to the tonsil and considering how the body's immune defences cope with the invasion of these bacteria by producing naturally occurring antimicrobial peptides – a bit like the body's own 'antibiotic'.

This study is a continuation of a previously successful study in this area and will continue over the next few years.

Why have I been chosen?
You have been selected because you are undergoing tonsillectomy. Although the study is concerned with recurrent acute tonsillitis you do not have to be a sufferer to take part. If you are undergoing tonsillectomy for other reasons your tonsils will be used as examples of normal tonsils in the study. Thus patients both affected or unaffected by tonsillitis who are undergoing tonsillectomy will be invited to take part in this study.

Do I have to take part?
It is up to you to decide whether or not to take part. If you do decide to take part you will be given this information sheet to keep and be asked to sign a consent form. If you decide to take part you are still free to withdraw at any time and without giving a reason. A decision to withdraw at any time, or a decision not to take part, will not affect the standard of care you receive.

What do I have to do? You will have to fill in the questionnaire (some basic information about why you are having a tonsillectomy). It should take no more than 5 minutes. The information on this form will be strictly anonymous; your answers will be linked to your clinical sample by only a study number. Your name, address, hospital number are **not** required. Please ask if you need help to fill in the form.

What is the drug or procedure that is being tested? This study is not testing any drug or procedure.

What are the alternatives for diagnosis or treatment? This study does not involve any diagnosis or treatment.

What are the side effects of any treatment when taking part? No treatment is being given.

What are the possible side effects and risks of taking part? There are no side effects or risks of taking part.

What are the possible benefits of taking part? There are no benefits to you personally from taking part in this study. However your tonsils would be very useful to us in achieving our long term goal of understanding how the tonsils and the immune system cope with recurrent acute tonsillitis. We hope as a result to help other patients with similar trouble in the future.

Will my taking part in this study be kept confidential?
All information which is collected about you will be kept strictly confidential. Any information about you that leaves the hospital will not contain your name, address, hospital number or any other means of identifying you. As previously mentioned, your questionnaire will be linked to the clinical sample only by an anonymous number.

What will happen to the results of the research study? The results will be published in a scientific journal. Participants' names will not be used.

Who is organising and funding the study? This study is being organised and carried out by the Institute for Cell and Molecular Biosciences at the University of Newcastle upon Tyne and the Department of Ear nose and Throat Surgery at the Freeman Hospital, Newcastle upon Tyne. The project is funded by the Medical Research Council.

Who has reviewed the study?
This study has been reviewed by the Newcastle and North Tyneside Local Research Ethics Committees (4th October 2004).

Contact for further information
If you have any questions or concerns about this study, please do not hesitate to contact:

Janet A Wilson
Prof. Otolaryngology Head Neck Surgery

Freeman Hospital
Newcastle upon Tyne
NE7 7DN
UK

Telephone: (44) 191 223 1086
Fax: (44) 191 223 1246

E-mail: J.A.Wilson@ncl.ac.uk
NHS email: Janet.Wilson@nuth.nhs.uk

Thank you for your time.

Yours sincerely

Stephanie Bell BSc (Hons).

The Newcastle upon Tyne Hospitals NHS
NHS Trust

UNIVERSITY OF NEWCASTLE

University of Newcastle
The Medical School
Newcastle upon Tyne NE2 4HH

The Freeman Hospital
High Heaton
Newcastle upon Tyne
NE7 7DN

Tel: 0191 233 6161
Fax: 0191 213 1968

Title of study:

Molecular determinants of streptococcal regulation of antimicrobial peptide expression in human tonsils

The study is concerned with bacterial interactions with tonsils and protection against tonsillitis by the immune system.

Name of researcher:

Miss Stephanie Bell BSc (Hons.)

Please initial box

1. I confirm that I have read and understand the information sheet dated March 05 for the above study and have had the opportunity to ask questions. ☐

2. I understand that my participation is voluntary and that I am free to withdraw at any time, without giving any reason, and without my medical care or legal rights being affected. ☐

3. I understand that sections of any of my medical notes may be looked at by responsible individuals from the hospital or from regulatory authorities where it is relevant to my taking part in research. I give permission for these individuals to have access to my medical records. ☐

4. I agree to take part in the above study. ☐

5. I **am not / am** involved in any other study. ..... ☐
(other study details - if known)

Name of patient	date	signature
Name of person taking consent (if different from researcher)	date	signature
Name of researcher	date	signature

1 for patient; 1 for researcher; 1 to be kept with hospital notes

APPENDIX B

Molecular determinants of streptococcal regulation of antimicrobial peptide expression in human tonsils

The study is concerned with bacterial tonsil infection and its prevention by the immune system.

Please answer the following questions:

SECTION A

Age: (please state in months if under four years).....

Sex: Male ☐ Female ☐

Why are you/your child undergoing tonsillectomy?
Recurrent Acute Tonsillitis ☐
Snoring ☐
OSAS (Obstructive Sleep Apnoea Syndrome) ☐
Other Reason ☐ (Please State) .....

Do you/Does your child regularly have sore throats? Yes ☐ No ☐

When approximately was the last one? .....

If you/your child has ever had tonsillitis please proceed to section B
If not please proceed to section C

SECTION B

When did you/your child last have tonsillitis? .....

How often do you/your child get tonsillitis?.....

How long does it usually last?.....

SECTION C

Have you/your child had a peritonsillar abscess? (quinsy) Yes ☐ No ☐

Have you/your child recently taken antibiotics?
Yes ☐ No ☐
For tonsillitis / sore throat ☐
Other ☐

Have you/your child lost much time from work/school due to this condition?
Yes ☐ No ☐
If yes please indicate approximately how much: .....

N.B. THIS FORM TO BE KEPT WITH TONSIL SAMPLES COLLECTED FROM THEATRE